Development, characterisation, and testing of CNS deliverable TRAIL-receptor agonists for the treatment of Glioblastoma (GBM)

Von der Fakultät Energie-, Verfahrens- und Biotechnik

der Universität Stuttgart zur Erlangung der Würde eines

Doktors der Naturwissenschaften (Dr. rer. nat.)

genehmigte Abhandlung

Vorgelegt von

Nivetha Krishna Moorthy

aus Madurai, Indien

Hauptberichter: Professor Dr. Markus Morrison

Mitberichter: Associate Professor Dr. Brona Murphy

Tag der mündlichen Prüfung: 28.07.2022

Institut für Zellbiologie und Immunologie

Universität Stuttgart

2022

Für meine Familie

Erklärung

Hiermit erkläre ich, dass die vorliegende Arbeit von mir persönlich ohne unrechtmäßige Hilfe angefertigt wurde. Verwendete Daten, Grafiken und Informationen, die nicht von mir stammen wurden entsprechend gekennzeichnet.

Declaration

I hereby declare that this thesis was prepared by myself without illegal help. Where information has been derived from other sources, I confirm that this has been acknowledged and cited in the thesis.

Nivetha Krishna Moorthy

Stuttgart, 16.03.2022

Table of contents

List of abbreviations

aa. amino acid

AIC. *5-aminoimidazole-4-carboxamide*

AMT. *adsorptive-mediated transcytosis*

APAF1. *apoptotic peptidase-activating factor 1*

Bad. Bcl-2 associated death promoter

BAX. BCL-2 associated X protein

BBB. *blood brain barrier*

BCL2. *B-cell lymphoma 2*

BCL-W. BCL-2-like protein 2

BCL-XL. anti-apoptotic B-cell lymphoma-extra-large protein

BER. *base-excision repair*

Bid. BH3-interacting domain death agonist

Bmf. Bcl-2 modifying factor

BOK. BCL-2 related ovarian killer

CARD. *caspase recruiting domain*

cFLIP. *cellular FLICE-like inhibitory protein*

$cFLIP_L$. *cFLIP long*

cIAP1. cellular IAP1

CMT. *carrier-mediated transport*

CRD. cysteine-rich domains

CT. *computed tomography*

CTLA-4. *cytotoxic T-lymphocyte antigen*

DED. *death effector domain*

DISC. *death inducing signalling complex*

EGFR. *epidermal growth factor receptor*

EST. *expressed sequence tag*

FADD. *FAS-associated death domain*

FasL. *Fas ligand*

GABRA. *gamma-aminobutyric acid type A receptor alpha1*

GPI. *glycosylphosphatidylinositol*

GY. *gray*

His. *poly-Histidine tag*

hTERT. *high frequency of telomerase reverse transcriptase*

IAPs. inhibitor of apoptosis

IDH1. *isocitrate dehydrogenase 1*

IFNs. *type I interferons*

JAMs. *junctional adhesion molecules*

LOH. *loss of heterozygosity*

LPS. *lipopolysaccharide*

MCL-1. myeloid cell leukaemia 1

MMR. *mismatch repair*

MOMP. mitochondrial outer membrane permeabilization

MRI. *magnetic resonance imaging*

MTIC. *monomethyl triazene 5-(3-methyltriazen-1-yl)- imidazole-4-carboxamide*

NEFL. *neurofilament light polypeptide*

NF1. *neurofibromatosis type 1*

NK. *natural killer*

PD-1. *programmed cell death protein*

PDGFA. *platelet-derived growth factor A*

PDGFRα. platelet-derived growth factor receptor alpha

PD-L1. *programmed cell death ligand 1*

PNS. *peripheral nervous system*

PS. *phosphotidylserine*

PTEN. *phosphatase and tensin homolog gene*

Puma. p53-upregulated modulator of apoptosis

RB. *retinoblastoma*

RTK. *receptor tyrosine kinase*

S1P. *sphingosine-1-phosphate*

scTRAIL. *single chain TRAIL*

SLC12A5. *solute carrier family 12 members 5*

Smac. second mitochondria-derived activator of caspases

tBID. truncated Bid

TCGA. *the cancer genome atlas*

TJ. *tights junctions*

TMZ. *temozolomide*

TNF. *tumour necrosis factor*

TNFR1. *TNF receptor 1*

TRAIL. *TNF-related apoptosis-inducing ligand*

TRAILR. TRAIL receptor

XIAP. X-chromosome-linked IAP

Abstract

Glioblastoma (GBM) is a grade IV glioma, which is the most malignant and aggressive form of glioma. It accounts for 80% of the primary malignant brain tumours with a median survival time of just ~14 months. Therefore, GBM is presented as a highly challenging tumour and continuous efforts are required to find innovative and more effective treatment options. Tumour Necrosis Factor Related Apoptosis Inducing Ligand (TRAIL)-based therapeutics potently induce apoptosis in cancer cells, including GBM cells, by binding and activating TRAIL receptors (TRAIL-R1 and R2). However, the blood-brain barrier (BBB) is a major obstacle for these biologics to enter the central nervous system (CNS). The BBB is mainly made up of tightly connected endothelial cells and therefore the penetration of large biologics into the CNS is generally controlled and prevented by the presence of the BBB, with approximately 0.1% of injected antibody doses reaching the brain parenchyma. Receptor-mediated transcytosis is a mode of transport capable of carrying large proteins and lipoproteins across the BBB. Therefore, in this research work, studies were performed to investigate if antibody-based fusion proteins that combine the apoptosis-inducing TRAIL with transcytosis-inducing angiopep-2 could be developed.

It was observed that the addition of the ANG2 moiety does not interfere with the potent apoptosis induction of TRAIL and these hexavalent TRAIL-receptor agonists demonstrated robust cytotoxicity against GBM cells. TRAIL receptor quantification demonstrated that the BBB cells do indeed express TRAIL receptors although in significantly reduced amounts compared to cancer cells. In cytotoxicity studies, BBB cells remained highly resistant to this fusion protein in response to clinically relevant doses of TRAIL-receptor agonists. Binding studies indicated that ANG2 is active in these constructs, however, control peptides and TRAIL-blocking experiments demonstrated that TRAIL-ANG2 fusion construct binding to BBB cells is mainly TRAIL-mediated. TRAIL-agonists bind cells effectively at sub-nanomolar concentrations, whereas angiopep-2 binds its target Lrp1 with an affinity of 313 nM. As a result of the binding studies and the difference in affinity, it was hypothesized that low TRAIL receptor expression on BBB endothelial cells may interfere with efficient transport of TRAIL-ANG2 fusion proteins, which was indeed observed by transwell transport

studies. However, ANG2-mediated transport can be restored by blocking the TRAIL moieties in the fusion proteins. Overall, this study showed that TRAIL-ANG2 fusion proteins are highly potent in inducing apoptosis in GBM cells, but it requires TRAIL-R masking or other innovative strategies to achieve efficient CNS-transport and utilize them for the treatment of GBM.

Zusammenfassung

Das Glioblastom (GBM) ist ein Gliom vierten Grades, welches die bösartigste, aggressivste und mit einem Anteil von 80 % auch die häufigste Ausprägung dieser Art von Gehirntumoren darstellt. Da Patienten nach Diagnose nur durchschnittlich 14 Monate überleben, bedarf es kontinuierlicher Anstrengungen, um neue, wirksamere Behandlungsmethoden zu etablieren. TRAIL (*Tumour Necrosis Factor Related Apoptosis Inducing Ligand*) -basierte Therapeutika induzieren Apoptose in Krebszellen unterschiedlichsten Ursprungs, einschließlich GBM, durch Bindung und Aktivierung von TRAIL-Rezeptoren (TRAIL-R1 und R2). Ein Hindernis bei der Behandlung von Gehirntumoren ist allerdings die, aus eng miteinander verbundenen Endothelzellen aufgebaute Blut-Hirn-Schranke (BHS), welche den Eintritt der meisten größeren Moleküle in das zentrale Nervensystem (ZNS) verhindert. Zum Beispiel erreichen nur 0,1 % einer verabreichten Antikörperdosis tatsächlich das Hirnparenchym. Die rezeptorvermittelte Transzytose ist ein Transportmechanismus, mit dem größere Proteine und Lipoproteine dennoch über die BHS transportiert werden können. Daher wurde in dieser Arbeit untersucht, ob Antikörper-basierte Fusionsproteine entwickelt werden können, die einerseits das Apoptose-induzierende TRAIL beinhalten, andererseits aber auch Angiopep-2 (ANG2), welches den Transport über die BHS erlaubt.

Hierbei wurde festgestellt, dass das hergestellte Antikörper-basierte Fusionsprotein *in vitro* zytotoxisch auf GBM Zellen wirkte, was bedeutet, dass ANG2 den TRAIL Anteil nicht darin behindert, Apoptose auszulösen. Die Quantifizierung von TRAIL-Rezeptoren zeigte außerdem, dass Zellen der BHS diese durchaus exprimieren, allerdings in deutlich geringeren Mengen als die untersuchten Krebszellen. Damit übereinstimmend waren die Zellen der BHS im Gegensatz zu den Krebszellen auch relativ resistent gegenüber der Induktion von Zelltod durch klinisch relevante Dosen von TRAIL-Rezeptor Agonisten. Bindungsstudien deuten des Weiteren darauf hin, dass ANG2 in den generierten Konstrukten aktiv ist. Kontrollpeptide und TRAIL-blockierende Experimente zeigten jedoch, dass die Bindung des TRAIL-ANG2-Fusionskonstruktes an BHS-Zellen hauptsächlich durch TRAIL und nicht durch ANG2 vermittelt wurde. Während die Bindung von TRAIL-Rezeptor Agonisten an die auf

Zellen exprimierenden TRAIL-Rezeptoren auch bei niedrigen, sub-nanomolaren Konzentrationen des Proteins relativ stark ist, bindet ANG2 nur schwach an seinen Rezeptor Lrp1 (Affinität: 313 nM). Aufgrund der Ergebnisse der durchgeführten Bindungsstudien, sowie des beschriebenen Affinitätsunterschiedes wurde vermutet, dass die geringe TRAIL-Rezeptor Expression auf BHS-Endothelzellen den effizienten Transport von TRAIL-ANG2-Fusionsproteinen beeinträchtigt, was tatsächlich später durch Transwell-Transportstudien bestätigt werden konnte. Eine Möglichkeit, den Transport über die BHS zu verbessern, wäre den TRAIL-Anteil zu blockieren und damit nur eine Bindung von ANG2 an Lrp1 zu erlauben.

Insgesamt wurde in dieser Studie gezeigt, dass TRAIL-ANG2-Fusionsproteine generiert werden können, die Apoptose in GBM Zellen auslösen. Um solche Konstrukte allerdings erfolgreich in der Behandlung von GBM einzusetzen, muss auch der Transport über die BHS gewährleistet werden, was im Falle des in dieser Arbeit generierten Fusionsproteins, zum Beispiel durch TRAIL-Rezeptor Maskierung, erreicht werden könnte.

Introduction

1.1 Glioblastoma (GBM)

Gliomas are tumours of glial cell origin and they account for approximately 80% of the primary malignant brain tumours and 27% of all CNS tumours (Ostrom et al., 2015; Schwartzbaum et al., 2006). Based on the glial cell origin, glioma is classified majorly into astrocytic, oligodendroglial, ependymal and mixed neuronal-glial tumours (Louis et al., 2007, 2016). The World Health Organisation (WHO) classifies glioma from grade I to IV based on the increasing malignancy level determined by histological information and molecular parameters (Louis et al., 2007, 2016, 2021).

Glioblastoma (GBM), a grade IV astrocytoma (Kleihues et al., 2002; Louis et al., 2007), is the most prevalent and deadly form of primary cancer of the central nervous system (CNS) with the rate of incidence of 3.22 cases per 100 000 people (Ostrom et al., 2019). The term Glioblastoma multiforme was first coined by Mallory in 1914, however, it was commonly named as spongioblastoma multiforme until 1926, when Bailey and Cushing reintroduced the term glioblastoma from the idea that they originate from primitive precursors of glial cells, glioblasts. GBM is considered as one of the most challenging malignancies worldwide due to their extreme proliferative nature, diffusive infiltration, recurrence after resection and heterogeneity (Jovčevska et al., 2013).

1.1.1 Epidemiology and classification

According to Central Brain Tumour Registry of the United States (CBTRUS) data, GBM has the highest number of cases with 12,900 and 13,140 cases registered in 2019 and 2020, respectively. The GBM incidence is higher in men than in women (Thakkar et al., 2014; Urbańska et al., 2014) and in the 2012-2016 report, the incidence ratio was 1.58:1 (male: female) (Ostrom et al., 2019). GBM is more prevalent in the age group of 75 to 84 years with a median age of diagnosis of 64 years (Ostrom et al., 2019; Thakkar et al., 2014).

GBM is classified into primary and secondary glioblastoma. The difference between primary and secondary GBM was first identified by the German neuropathologist Hans-Joachim Scherer (Peiffer & Kleihues, 1999). He mentioned in his writing that “From a biological and clinical point of view, the secondary glioblastomas developing in

astrocytomas must be distinguished from ‘primary’ glioblastomas. They are probably responsible for most of the glioblastomas of long clinical duration”. Primary GBM arises de novo from glial cells and accounts for 90% of the GBM cases (Kleihues & Ohgaki, 1999; Ohgaki & Kleihues, 2013; Louis et al., 2016). Secondary GBM arises from low grade astrocytoma, corresponding to 10% of the GBM cases (Ohgaki & Kleihues, 2007) and it tends to have better prognosis in comparison to the primary GBM.

Primary and secondary GBM are phenotypically non-differentiable, however, there are genetic and molecular changes that result in the alteration of different signalling pathways leading to GBM growth, proliferation and transformation (Dunn et al., 2012). Primary GBM is characterised by overexpression of epidermal growth factor receptor (EGFR), mutation of phosphatase and tensin homolog gene (PTEN), loss of heterozygosity (LOH) of chromosome 10q (Fujisawa et al., 2000; Knobbe et al., 2002), deletion of the p16 gene, and high frequency of telomerase reverse transcriptase (hTERT) promoter mutations (Ohgaki & Kleihues, 2007; Killela et al., 2013). Secondary GBM is characterised by deregulation of TP53 gene (Watanabe et al., 1996; Y. Zhang et al., 2018), mutations in alpha thalassemia X-linked intellectual disability (ATRX) (X.-Y. Liu et al., 2012), overexpression of platelet-derived growth factor A and platelet-derived growth factor receptor alpha (PDGFA/PDGFRα), and loss of heterozygosity (LOH) of chromosome 19q (Ohgaki & Kleihues, 2007, 2013; Cloughesy et al., 2014).

Transcription-based classification of GBM has been focused on for years for better diagnosis and treatment of GBM. In 2001, Rickman and colleagues studied the gene expression status between 21 GBM and 19 pilocytic astrocytoma samples. Based on oligonucleotide microarrays, they analysed approximately 6800 genes and found 360 genes that differentiated GBM and pilocytic astrocytoma (Rickman et al., 2001). Later in 2003, Nutt et al., combined gene expression profiling and computational methodology of class prediction to distinguish sub-groups of gliomas. The 21 samples they analysed included 14 GBM and 7 anaplastic oligodendroglioma. Of all the samples, the prediction model was able to classify 18 samples that correlated more with the clinical outcomes than with standard pathology (Nutt et al., 2003). In 2006, Phillips et al., described the first molecular classification of GBM, they performed a cutting-edge study by using a set of 35 genes for the hierarchical clustering of GBM subtypes. They classified GBM into proneural, proliferative and mesenchymal subtypes. Proliferative and mesenchymal subtypes are associated with poor survival

due to their high proliferative and angiogenic features (H. S. Phillips et al., 2006). However, a study from Verhaak et al. in 2010 gave deeper insights on molecular subtypes with bulk tumours and individual tumour cells data. This group performed the study with a 850 gene signature (210 gene per class) using a broader dataset of 173 GBM samples obtained from the cancer genome atlas (TCGA) (Verhaak et al., 2010) and classified GBM into four subtypes: classical, mesenchymal, proneural and neural. The classical subtype is associated with high level EGFR amplification, which was seen in 97% of the classical subtypes. Surprisingly, classical subtype lacked the TP53 mutation, which is the most commonly seen mutation in GBM (Y. Zhang et al., 2018). The mesenchymal subtype is characterised by high amount of neurofibromatosis type 1 (NF1), which is observed commonly in GBM (Philpott et al., 2017). The aggressive treatment reduced the mortality significantly in this subtype. The proneural subtype is characterised by mutation in platelet-derived growth factor alpha (PDGFRA). As characterised by Phillips et al. (H. S. Phillips et al., 2006), this subtype included high expression of OLIG2 genes. The neural subtype included neural markers, such as synaptotagmin YT1 (SYT1), solute carrier family 12 members 5 (SLC12A5), gamma-aminobutyric acid type A receptor alpha1 (GABRA) and neurofilament light polypeptide (NEFL) (Verhaak et al., 2010).

1.1.2 Current GBM standard of care

GBM is diagnosed at the median age of 65 years (Chakrabarti et al., 2005; Ostrom et al., 2019). The common symptoms include headache, nausea, vomiting, focal neurological deficits, and patients show varied symptoms based on the tumour locality. The standard methods used to diagnose GBM are magnetic resonance imaging (MRI) (Ellingson et al., 2017) and computed tomography (CT) with or without the contrast agent, gadolinium. However, for an effective treatment plan using histology and molecular features, it is highly recommended to perform tissue diagnosis before the surgery (Weller et al., 2021). As the location of the tumour makes the microsurgical tissue acquisition difficult, a stereotactic biopsy is recommended (McGirt et al., 2003; Eigenbrod et al., 2014). First-line treatment for GBM is maximal surgical resection and its main goal is to remove as much of the tumour as possible. Complete surgical removal of GBM depends on the location of the tumour, as it can lead to compromising

neurological function (Wilson et al., 2014). Therefore, there are many techniques currently used for safer and low-risk surgical resection, such as awake craniotomy, fluorescent-guided resection with 5-aminolevulinic acid, MRI, diffusion tensor imaging and ultrasonography (Hervey-Jumper & Berger, 2016; Stummer et al., 2006). A post-operative MRI must be performed to validate the surgical resection efficiency and to prepare a follow-up treatment plan (Tan et al., 2020). According to Stupp protocol, the current standard of care, after surgery, patients should be treated with the combination of radiotherapy (RT) and temozolomide (TMZ) (Stupp et al., 2005).

TMZ, an orally available alkylating agent of the imidazotetrazine class, functions by inducing DNA methylation in cancerous cells. Due to its small size of 194 Da and lipophilic nature, TMZ can cross the blood-brain barrier (BBB) and reach the tumour site for the treatment of GBM. Upon oral administration and absorption, TMZ is hydrolysed into monomethyl triazene 5-(3-methyltriazen-1-yl)- imidazole-4-carboxamide (MTIC). MTIC is later degraded into 5-aminoimidazole-4-carboxamide (AIC), which methylates DNA at N^7 position of guanine (N^7-MeG), N^3 position of adenine (N^3-MeA) and O^6 position guanine (O^6-MeG) residues (Denny et al., 1994). The TMZ-induced methylation in Guanine (N7-MeG) is about 70% and in Adenine (N3-MeA) is about 9%, however, these methylations are repaired by base-excision repair (BER) mechanism. 6% of TMZ-induced methylation at O6-MeG is the main mechanism of action of TMZ (J. Zhang et al., 2012). The DNA mismatch repair (MMR) enzyme's repair mechanism on O6-MeG results in long-lived nicks in DNA, which leads to initiation of apoptosis. In 2005, Stupp and colleagues demonstrated that radiotherapy plus TMZ increased the survival time from 12 months to approximately 14 months (Stupp et al., 2005).

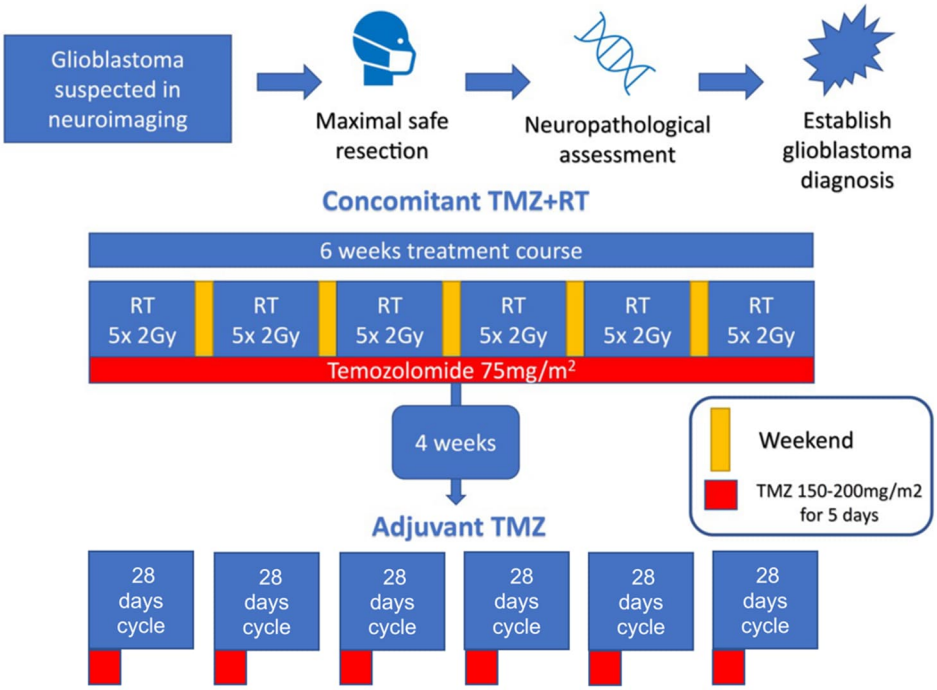

Figure 1: Stupp protocol. Newly diagnosed GBM patients initially undergo surgical resection to remove the tumour as much as possible. After resection, patients receive concomitant TMZ and RT for 6 weeks, followed by 4-week break. Then, the patients receive up to 6 cycles of adjuvant TMZ every 28 days. Figure obtained from (Batistella et al., 2021). TMZ: Temozolomide; RT: Radiotherapy; Gy: Gray.

The radiotherapy includes fractionated focal irradiation and the patients receive an overall dose of 60 Gray (GY) at a daily dose of 2 Gy per fraction, given 5 days per week over a period of 6 weeks. For concomitant chemotherapy, patients receive TMZ at a daily dose of 75 mg/m^2, given 7 days per week along with RT. After a 4-week break from radio-chemotherapy, patients receive up to 6 cycles of adjuvant TMZ for 5 days repeated every 28 days. The starting dose of adjuvant TMZ is 150 mg/m^2 and is eventually increased to 200 mg/m^2 in the second cycle (Figure 1) (Stupp et al., 2005, 2009). The O^6-methylguanine-DNA methyltransferase (MGMT) promoter methylation has been considered a prognostic marker for GBM. MGMT functions by antagonizing the cytotoxic effects of TMZ by removing the alkyl groups at the O6 position of the guanine. Studies have also shown that patients with methylated MGMT promoter benefitted from the TMZ treatment with increased overall survival (Donson et al., 2007; Hegi et al., 2005). However, it has been shown that the TMZ resistance is not only based on MGMT status but also on multiple processes (Egaña et al., 2020; S. Y. Lee, 2016).

Despite the current standard of care treatment of surgery followed by concomitant radiotherapy and chemotherapy, outcomes for GBM patients are extremely poor with a median survival of ~14 months (Koshy et al., 2012; Tran & Rosenthal, 2010). The standard of care for GBM has not changed or improved since 2005. Besides poor survival rate, GBM patients also suffer from recurrence and poor prognosis, which are the underlying problems to be addressed. Currently, GBM is considered a highly malignant tumour with no effective treatments, therefore, new treatment strategies are required.

1.1.3 Potential targets and developments for the treatment of GBM

Many signalling pathways are deregulated in GBM, of which the four major pathways are receptor tyrosine kinase (RTK), p53, retinoblastoma (RB) and TERT (Ricard et al., 2012; Killela et al., 2013). EGFR, a tyrosine kinase receptor, is deregulated in 57.4% of primary GBM patients (H. S. Phillips et al., 2006; Verhaak et al., 2010), of which 40% cases have EGFRvIII, a mutant form of EGFR lacking the ligand-binding domain (Brennan et al., 2013). EGFR amplification and mutation has proven to promote angiogenesis, tumorigenesis, invasion and resistance to chemotherapy and radiotherapy (Chakravarti et al., 2004; P. H. Huang et al., 2009; Katanasaka et al., 2013; Feng et al., 2014). Therefore, EGFR has been considered an ideal target for GBM, and EGFR inhibitors, such as Gefitinib (Iressa), Erlotinib (Tarceva), Lapatinib (Tykerb) and monoclonal antibodies, such as Cetuximab (Erbitux), Panitumumab (Vectibix) have been tested on patients, however, they did not show any significant effect on patient survival (Neyns et al., 2009; van den Bent et al., 2009; Thiessen et al., 2010; Uhm et al., 2011). Glioblastoma is a highly vascularised tumour and is characterised by leaky blood vasculature. It has been demonstrated that nitric oxide (NO) released by the tumour and the endothelial cells are also responsible for the leakiness (Hira et al., 2018), which leads to hypoxia. During hypoxia, the cells respond to the hypoxic environment and eventually secrete pro-angiogenic factors, the most important is VEGF-A (Tate & Aghi, 2009), by inducing transcription factor HIF-1-alpha (Hypoxia inducible factor-1-alpha) (C. Lin et al., 2004). Bevacizumab (Avastin) is a monoclonal anti-VEGF antibody that prevents the binding of VEGF-A to VEGFR2, thus blocking angiogenesis. Even though, phase III clinical trial increased the progression

free survival (PFS) of patients, the overall survival (OS) of the patients did not improve with Bevacizumab (Chinot et al., 2014; Gilbert et al., 2014). Besides targeted therapies, there are also immunotherapies evolving as treatment options for GBM. Blocking the immune checkpoints, such as cytotoxic T-lymphocyte antigen (CTLA-4) and programmed cell death protein (PD-1) or programmed cell death ligand 1 (PD-L1) are promising in recruiting, activating and increasing the efficiency of T cells against cancer. The first immune checkpoint inhibitor was approved in 2011 against melanoma, since then, there have been many studies involved in improving this treatment mechanism against several cancers. Nivolumab, a PD-1 inhibitor, was compared with Bevacizumab in phase III clinical trial in recurrent GBM, yet it did not improve the OS (Reardon et al., 2020). Currently, there is a clinical study (NCT02667587) going on with TMZ plus RT with Nivolumab. Even though there are multiple therapeutic strategies with promising approaches against GBM under development, there are several factors such as GBM heterogeneity, GBM treatment resistance, and the blood-brain barrier, contributing to poor survival. The poor treatment response and GBM's aggressive nature are the reasons for GBM to have the lowest five-year survival of 6.8% in comparison to other brain tumours (Ostrom et al., 2019). Thus, GBM is one of the deadliest diseases and there is an urgent need to find new remedies.

1.2 Apoptosis

1.2.1 Discovery of apoptosis

Apoptosis, a programmed cell death, plays an essential role in growth, development and maintaining cellular homeostasis of the organisms. The process of cell death was first noticed by Carl Vogt in 1842 when he observed cell death in the notochord of toad embryos developing into vertebrae (Vogt & Vogt, 1842). In 1964, Lockshin and Williams observed the regulated loss of muscles in silk moths during development and defined the process as "programmed cell death" (Lockshin & Williams, 1964). In 1972, Kerr and colleagues published a landmark study, where they used electron microscopy to describe the morphological characteristics of apoptosis in hepatocytes and coined the term apoptosis (Kerr et al., 1972). The term apoptosis is a Greek word, which

means leaves falling of trees, describing that this process is essential to maintain the balance during development. Apoptosis is characterised by morphological alterations, such as rounding up of cells and shrinkage, chromatin condensation (pyknosis) and nuclear fragmentation (karyorrhexis) (Kerr et al., 1972; Elmore, 2007). Unlike necrosis, where the cell membrane ruptures and causes inflammation, in apoptosis the cell membrane integrity is maintained and the surrounding cells and tissues are not harmed. During this process, the cell membrane blebs and the cells are separated into apoptotic bodies, which are taken up and eliminated by phagocytes or other cells, such as macrophages (Kerr et al., 1972; Wyllie et al., 1980; Fadok et al., 1998; D'Arcy, 2019). The apoptotic cells are recognised by the phagocytes based on eat-me signals, including phosphotidylserine (PS), lysophosphatidylcholine (LCP) (Lauber et al., 2003), sphingosine-1-phosphate (S1P) (Gude et al., 2008) and more (Segawa & Nagata, 2015; Medina & Ravichandran, 2016). The apoptosis pathway can be classified into the intrinsic and extrinsic pathway. The extrinsic pathway is activated by ligands, such as TNF-related apoptosis-inducing ligand (TRAIL), tumour necrosis factor (TNF), and Fas ligand (FasL), binding to their receptors, TRAIL receptor (TRAILR1/2), TNF receptor 1 (TNFR1) and Fas, respectively, whereas intrinsic apoptosis is induced by intrinsic stimuli, such as DNA damage, irradiation, cellular stress leading to mitochondria outer membrane permeabilisation (MOMP).

1.2.2 Caspases

Caspases, cysteine-dependent aspartate-specific proteases, play a key role in apoptosis regulation and execution in both the extrinsic and intrinsic pathways. In 1977, Sulston and Horvitz, in their cell-lineage study, observed the programmed death of 113 cells in *Caenorhabditis elegans* (*C.elegans*) during development (Sulston & Horvitz, 1977; Sulston et al., 1983). After this discovery, Ellis and Horvitz, used *C.elegans* as a cell death model system and identified two cell death genes, CED-3 and CED-4, determining the fate of the cell (Ellis & Horvitz, 1986). In addition, CED-9, was shown to protect the cells from apoptosis (Hengartner et al., 1992). These studies on *C.elegans* led to the identification of first caspase, interleukin-1β converting enzyme (ICE), a mammalian gene homologous to CED-3, renamed later as caspase-1 (Yuan et al., 1993). To avoid confusion in naming the new members of this family, a universal

name, *caspases*, was given to them. Upon discovery of every additional caspase family member, an Arabic number was added at the end (Alnemri et al., 1996). Besides caspases, other key apoptotic factors, such as B-cell lymphoma 2 (BCL2), a mammalian homolog of CED-9 (Hengartner & Horvitz, 1994) and apoptotic peptidase-activating factor 1 (APAF1), a mammalian homolog of CED-4 (Zou et al., 1997) were also identified. Caspases are synthesised as inactive precursors or zymogens and consist of N-terminal prodomain with a large subunit of 20 kDa and a small subunit of 10 kDa. Caspases in general are classified as pro-inflammatory caspases (caspase-1, -4, -5, -11, -12, -13), initiator caspases (caspase-2, -8, -9, -10) and effector caspases (caspase-3, -6, -7) (T.-J. Fan et al., 2005; Shalini et al., 2015). The initiator caspases have a long prodomain containing protein-protein interaction motifs that regulate their activation; including the death effector domains (DEDs) in caspases-8 and -10 and caspase activation and recruitment domain (CARD) in caspases-2 and -9. On the other hand, the effector caspases have a short prodomain with no motifs (Van Opdenbosch & Lamkanfi, 2019). Initiator procaspases are monomeric and are recruited to activation platforms for dimerisation, activation and autocatalytic cleavage. Effector procaspases are dimeric and are activated upon cleavage by initiator caspases and so the prodomain and subunits are separated which leads to the formation of the active heterotetramer (Lavrik et al., 2005). All the caspases share a conservative pentapeptide active site QACXG, in which X is R, Q or G (Cohen, 1997). Caspases recognise four amino acid sequence P4-P3-P2-P1 and have specificity to cleave after P1, which is usually Aspartic acid, however, it can also be glutamic acid, but with less specificity (Stennicke et al., 2000; Julien & Wells, 2017).

1.3 TNF-related apoptosis-inducing ligand (TRAIL)

1.3.1 TRAIL and its receptors

The concept of treating cancer with TNF family ligands was unintentionally identified in 1891 when William Coley cured his sarcoma patient by administering gram-negative bacteria to activate the immune system (Coley, 1891; Cann et al., 2003; McCarthy, 2006). However, it took a century to discover that the anti-tumour effect was not due to bacteria but due to lipopolysaccharide (LPS)-induced TNF production by the human

body (Carswell et al., 1975). Even though anti-tumour effect was notable, later studies revealed that TNF administration was toxic and induced lethal inflammatory shock syndrome (Kimura et al., 1987; Tracey et al., 1988). Therefore, many research groups started to search for the sequence homology to TNF and discovered Fas or CD95L, which also induced toxicity in mice (Ogasawara et al., 1993). Finally, in 1995, TRAIL was discovered as a part of TNF superfamily ligands by two independent groups using expressed sequence tag (EST) library (Wiley et al., 1995; Pitti et al., 1996). Interestingly, they showed selective cytotoxicity in transformed cell lines but not in normal cells, thus can be beneficial for the treatment of cancer (Ashkenazi et al., 1999; Walczak et al., 1999). Since then, numerous studies emerged with the focus on using TRAIL as an anti-cancer agent for several types of cancers. TRAIL, a type II transmembrane protein consisting of 281 amino acids, is produced by activated human T cells in response to type I interferons (IFNs) (Kayagaki et al., 1999). In addition, they are expressed on the surface of immune effector cells, such as B cells (Kemp et al., 2004), natural killer (NK) cells (Zamai et al., 1998), dendritic cells (Fanger et al., 1999), and monocytes (Griffith et al., 1999). Similar to other TNF family members, TRAIL has an N-terminal cytoplasmic domain and a conserved C-terminal extracellular domain, which is proteolytically processed to form a homotrimeric molecule (LeBlanc & Ashkenazi, 2003). A TRAIL crystal structure study by Cha and colleagues revealed that like other TNF super family members, each TRAIL monomer includes a jelly roll structure with two flat β-sheets and interact with other nearby TRAIL monomer in a head-to-tail fashion forming a bell-shaped homotrimer (Cha et al., 1999). Unlike other TNF family members, cysteine coordination of a zinc atom is required to maintain the stability and activity of TRAIL monomers (J.-L. Bodmer et al., 2000; Hymowitz et al., 2000).

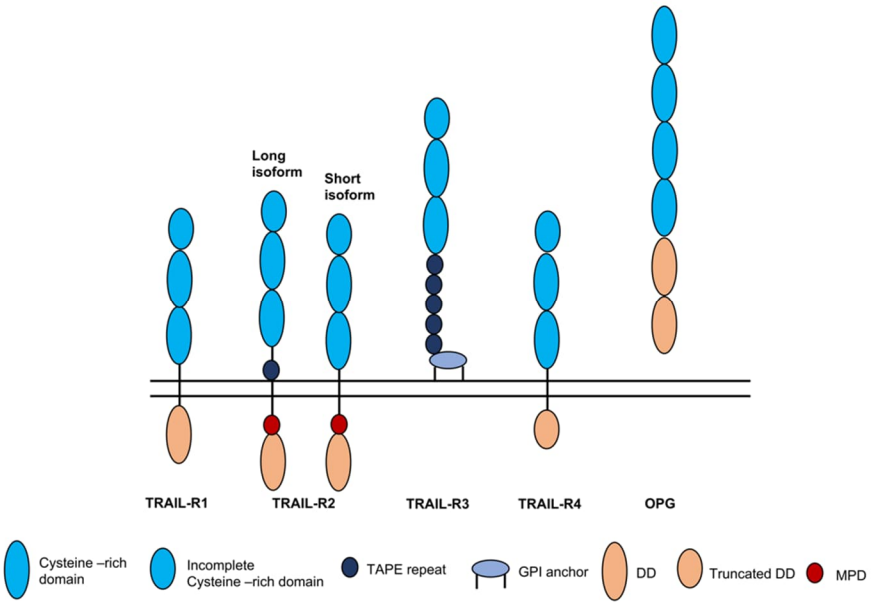

Figure 2: Structure of TRAIL receptors. The TRAIL receptors contain CRD that are responsible for ligand binding leading to apoptosis induction. TRAILR1/2 contain incomplete CRD, whereas TRAILR2 long isoform contains TAPE repeat close to the membrane. TRAILR3 lacks DD and is linked to the plasma membrane with glycosylphosphatidylinositol (GPI), whereas TRAILR4 has a truncated non-functional DD. Figure adapted from (von Karstedt et al., 2017).

In contrast to other TNF family ligands, TRAIL receptors are type 1 transmembrane proteins with an N-terminal extracellular ligand binding domain and C-terminal intracellular domain. Similar to other TNF family receptors, TRAIL receptors contain cysteine-rich domains (CRD), which are responsible for ligand binding leading to apoptosis induction (J.-L. Bodmer et al., 2000; Guicciardi & Gores, 2009). They contain an intracellular cytoplasmic death domain (DD) that are approximately 80 amino acids (aa) and are essential for initiating apoptosis (Ashkenazi & Dixit, 1998). Apoptosis induction in cancer cells is achieved by the binding of TRAIL to the TRAIL death receptors TRAILR1/DR4 (G. Pan, O'Rourke, et al., 1997) and TRAILR2/DR5/TRICK2/KILLER (MacFarlane et al., 1997; G. Pan, Ni, et al., 1997; P. Schneider, Bodmer, et al., 1997; Walczak, 1997).

The first TRAIL receptor, TRAILR1, was identified by Pan and colleagues by an EST database search. TRAILR1 is a 468 aa receptor with intracellular DD that are responsible for inducing apoptosis (G. Pan, O'Rourke, et al., 1997). The second TRAIL receptor, TRAILR2, was identified independently by different groups by searching for a homologous sequence to TRAILR1. Human TRAILR2 can exist as two isoforms, the short form, TRAILR2-s, is similar to TRAILR1 and has 411 aa, whereas, the long

isoform, TRAILR2-l has an extra 29 aa and one TAPE (threonine, alanine, proline and glutamine) repeat close to the membrane (P. Schneider, Bodmer, et al., 1997; Screaton et al., 1997; Kimberley & Screaton, 2004; von Karstedt et al., 2017). In addition to death receptors, two decoy receptors, TRAILR3/DcR1/TRID (Degli-Esposti, Smolak, et al., 1997; Mongkolsapaya et al., 1999; G. Pan, Ni, et al., 1997; P. Schneider, Bodmer, et al., 1997; Sheridan et al., 1997) and TRAILR4/DcR2/TRUNDD (Degli-Esposti, Dougall, et al., 1997; Marsters et al., 1997; G. Pan et al., 1998) were identified. TRAILR3 lacks an intracellular domain, including DD and is linked to the plasma membrane with glycosylphosphatidylinositol (GPI), whereas TRAILR4, has a truncated non-functional DD (Figure 2). These two decoy receptors cannot trigger apoptosis, however, their overexpression makes the cells resistant to TRAIL-TRAILR1/2-mediated apoptosis (Degli-Esposti, Dougall, et al., 1997; Riccioni et al., 2005; Clancy et al., 2005). Osteoprotegerin, a fifth TRAIL receptor, is a soluble receptor and has low binding affinity to TRAIL (Emery et al., 1998).

1.3.2 TRAIL-mediated signalling pathways

TRAIL-mediated extrinsic apoptosis is initiated by binding of TRAIL ligand to its receptors (TRAIL1/2) (Ashkenazi & Dixit, 1998). The TRAIL receptors are pre-assembled on the surface of the cell membrane in an inactive form (Clancy et al., 2005). Upon binding of TRAIL to its receptors, the receptors oligomerise and undergo conformational changes leading to the formation of death inducing signalling complex (DISC) (Kischkel et al., 1995). The clustered or aggregated receptors recruit an adaptor molecule FAS-associated death domain (FADD), also called as Mort-1. FADD contains a DD in its C-terminus and binds to the DD of the TRAIL receptors by homotypic interactions (Boldin et al., 1995; Chinnaiyan et al., 1995; L. R. Thomas et al., 2004). The N-terminus of FADD contains a DED, which aids in the recruitment of procaspase 8 through its DED1 (J. L. Bodmer et al., 2000; Kischkel et al., 2000; Sprick et al., 2000). Once they are recruited in DISC, several other procaspase-8 monomers are recruited via their DED, thus forming a large filament (Dickens et al., 2012; Schleich et al., 2012; Fu et al., 2016; Fox et al., 2021). This brings procaspase 8 monomers in close proximity to undergo dimerisation and activation by auto catalytic cleavage (Muzio et al., 1998; Chang et al., 2003; Hughes et al., 2009). The caspase 8 activation

occurs by a two-step mechanism (Medema et al., 1997; Scaffidi et al., 1997) giving rise to fully processed and cleaved caspase intermediates. The first cleavage at aspartate residue between the linker and small subunit generates a large p43/41 subunit and a small p10 subunit. A subsequent second cleavage step occurs at another aspartate residue between the DED prodomain and larger subunit, therefore cleaving the p43/41 subunit into p26/24 and p18 (Medema et al., 1997; Scaffidi et al., 1997). As a result of this, an active caspase 8 heterotetramer, $p18_2/p10_2$, is formed and released into the cytosol (Chang et al., 2003; Lavrik et al., 2005). The cytosolic active caspase 8 cleaves and activates effector caspase 3 and other substrates (Chang et al., 2003; Tummers & Green, 2017). Later studies have shown that procaspase-10 is also recruited to and activated at the DISC complex via their DED (Kischkel et al., 2001), but caspase 8 remains the main mediator of apoptosis. A cellular FLICE-like inhibitory protein (cFLIP) that has a sequence homology to caspase 8 or caspase 10 is also recruited to the DISC complex. Initially, it was believed that cFLIP competes with caspase 8 to bind to FADD via DED, however, recent studies have shown that procaspase 8 binding to FADD is a key responsible factor for cFLIP recruitment to DISC (Hughes et al., 2016; Humphreys et al., 2020). cFLIP has several splice forms at mRNA level, but only three forms, cFLIP long ($cFLIP_L$), cFLIP short ($cFLIP_S$), and cFLIP short ($cFLIP_R$) exist at protein level. All these variants contain two death effector domains which allows for recruitment into the DISC complex. $cFLIP_S$ and $cFLIP_R$ have been shown to inhibit caspase 8 activation at the DISC. $cFLIP_L$ contains two DED and a caspase-like domain, however, it lacks the cysteine of the catalytic centre that is required for caspase cascade signalling. It has been shown that $cFLIP_L$ does not block the recruitment of caspase 8 to the DISC complex, but leads to only partial processing of caspase 8, whereas, $cFLIP_S$ totally prevents the processing of caspase 8 (Krueger, Baumann, et al., 2001; Krueger, Schmitz, et al., 2001). $cFLIP_L$ has been shown to inhibit apoptosis at higher concentrations, however, some studies have shown that at physiological concentrations, $cFLIP_L$ enhances caspase 8 activation thus promoting apoptosis (Chang et al., 2002; Micheau et al., 2002).

In type I cells, caspase 8 activation of caspase 3 is sufficient to induce apoptosis, whereas type II cells require amplification to achieve apoptosis by connecting the extrinsic and intrinsic apoptotic pathways (Scaffidi et al., 1998). In addition to other cytotoxic stimuli and stress, active caspase 8 can induce mitochondrial outer

membrane permeabilisation (MOMP), a key event of intrinsic apoptosis. Induction of MOMP is highly regulated by the Bcl-2 family members (Chao & Korsmeyer, 1998; Kale et al., 2018). The anti-apoptotic Bcl-2 members include Bcl-2 itself, anti-apoptotic B-cell lymphoma-extra-large protein (BCL-XL), BCL-2-like protein 2 (BCL-W), myeloid cell leukaemia 1 (MCL-1) and BCL-2 related gene A1 (A1/BFL-1). The pro-apoptotic proteins include BH3-only proteins, such as BH3-interacting domain death agonist (Bid), Bcl-2 associated death promoter (Bad), Bcl-2 interacting mediator of cell death (Bim), Bcl-2 modifying factor (Bmf), Harakiri (Hrk), Noxa (Damage protein), and p53-upregulated modulator of apoptosis (Puma). The pore-forming pro-apoptotic multidomain proteins include BCL-2 associated X protein (BAX), BCL-2 homologous killer (BAK) and BCL-2 related ovarian killer (BOK). In type II cells, active caspase 8 cleaves BID into truncated Bid (tBID), which translocates to the mitochondria and activates pro-apoptotic proteins Bax and Bak. They undergo oligomerisation and form pores causing MOMP that leads to cytochrome c, Omi/HtrA2 and second mitochondria-derived activator of caspases (Smac) release into the cytosol (Saelens et al., 2004; Elmore, 2007; Moldoveanu et al., 2013). The released cytochrome c binds to apoptotic protease activating factor-1 (Apaf-1) that has an N-terminal CARD domain. In the presence of (deoxy) adenosine triphosphate (dATP/ATP), Apaf-1 undergoes conformational change and oligomerises into a heptameric complex called the apoptosome (Srinivasula et al., 1998; Acehan et al., 2002). The apoptosome recruits procaspase 9 through their CARD domains. At the apoptosome procaspase 9 is activated and is cleaved into caspase 9 p35/p12 fragment. Caspase 9 activation cleaves and activates effector caspases 3 and 7. These active effector caspases cleave several downstream targets to induce typical molecular and biochemical features of apoptosis like cell blebbing, chromatin condensation, nuclear fragmentation, proteolysis of proteins resulting in cell death. For example, caspase 3 cleaves the inhibitor of caspase activated DNase (ICAD) leading to the activation of CAD, which results in DNA fragmentation. In addition, caspase 3 also cleaves poly (ADP-ribose) polymerases (PARP), which prevents their ability to repair the DNA. However, anti-apoptotic Bcl2 family members like Bcl-2, Bcl-xl and Mcl-1 can prevent BAX and BAK pore formation. On the other hand, these anti-apoptotic proteins can be blocked by the binding of pro-apoptotic proteins like BIM, BAD, PUMA, NOXA to them. Besides Bcl2 family members, inhibitor of apoptosis (IAPs) family members are also involved in regulating intrinsic apoptosis. The well-characterised cellular IAP1 (cIAP1),

cIAP2, X-chromosome-linked IAP (XIAP) proteins can block apoptosis by inhibiting the caspases 3, 7 and 9 (Deveraux & Reed, 1999; Silke & Meier, 2013). But this effect of IAPs is inhibited by SMAC release in the cytosol, when they directly bind as homodimers to IAPs (Du et al., 2000) (Figure 3).

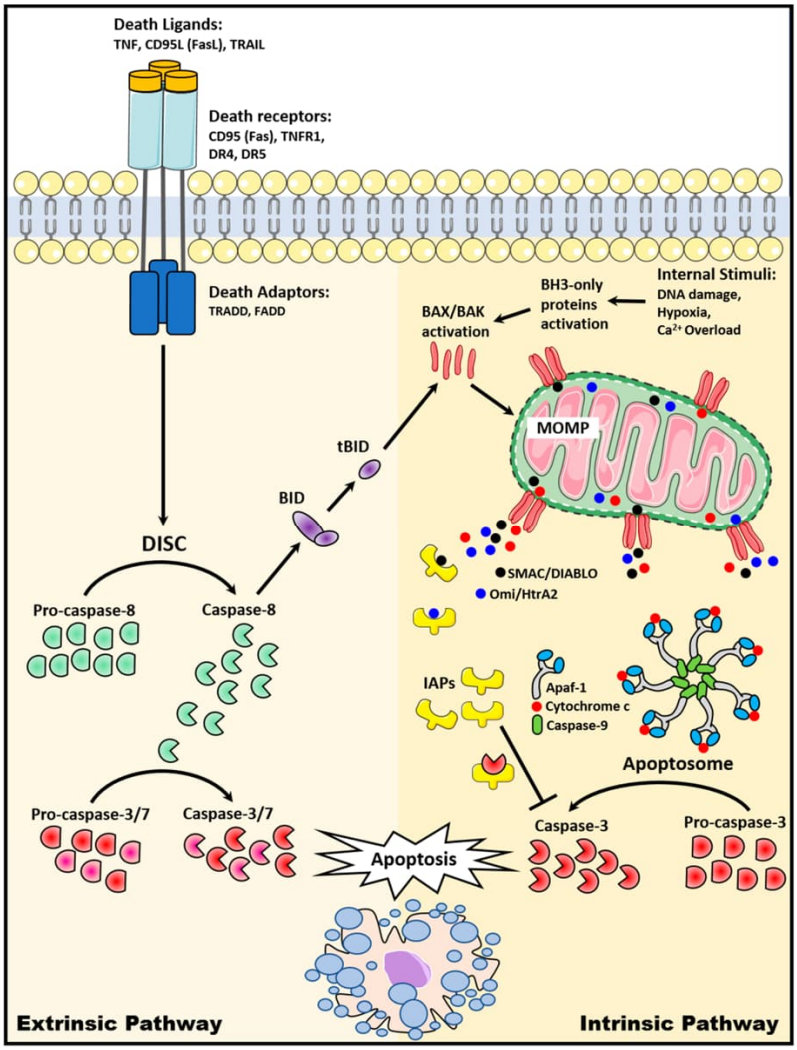

Figure 3: Extrinsic and intrinsic apoptosis signalling. Extrinsic pathway is initiated by binding of TRAIL ligand to its receptors (TRAIL1/2). The receptors trimerise and form DISC complex recruiting initiator and effector caspases. In type II cells, active caspase 8 induce mitochondrial outer membrane permeabilisation (MOMP) leading to cytochrome c release. The released cytochrome binds to Apaf-1, which undergoes conformational change and oligomerises into a heptameric complex called apoptosome. It recruits and activates caspase 9 leading to effector caspases 3, 6 and 7 activation and cell death. Figure adapted from (Choo et al., 2019).

Besides classical apoptosis signalling, TRAIL can induce receptor-interacting serine/threonine protein kinase 1 (RIPK1)-dependent apoptosis, necroptosis, or pro-survival signalling. Under specific conditions, such as depletion of cIAPs, acidic pH,

and TRAIL-R clustering outside lipid rafts, TRAIL can form a secondary complex (complex IIa) (Meurette et al., 2007; Song et al., 2007). This secondary complex lacks TRAILR but contains FADD, procaspase 8, RIPK1, TNF receptor-associated factor 2 (TRAF2), and the NF-κB essential modulator (NEMO). This complex activates caspase 8, leading to RIPK1-dependent apoptosis. However, in the case of caspase 8 inactivation, receptor-interacting serine/threonine-protein kinase 3 (RIPK3) is recruited to the complex (complex IIb). Phosphorylated RIPK3 binds to mixed lineage kinase domain like protein (MLKL) resulting in its oligomerisation. Oligomeric MLKL translocates to the plasma membrane where it forms pores, thus leading to necroptosis (Jouan-Lanhouet et al., 2012; von Karstedt et al., 2017). Moreover, TRAIL upon binding with TRAILR1, TRAILR2, and TRAILR4 can also trigger the NF-*κ*B signalling pathway (Degli-Esposti, Dougall, et al., 1997; P. Schneider, Thome, et al., 1997). Harper and colleagues demonstrated that RIPK1 in the DISC complex activates NF-*κ*B in the presence of caspase inhibition (Harper et al., 2001). Besides NF-*κ*B, the secondary complex can activate other pro-survival signalling pathways, such as c-jun N-terminal kinases (JNK), p38 mitogen-activated protein kinase (MAPK), and phosphatidylinositide 3-kinases (PI3K)/Akt (Azijli et al., 2013; von Karstedt et al., 2017). Recently, it has been demonstrated that the linear ubiquitin chain assembly complex (LUBAC) regulates the outcome of TRAIL signalling. This is mediated by the addition of linear ubiquitination chains to RIPK1 and caspase 8, thus limiting apoptosis and necroptosis. It has also been demonstrated that it promotes the recruitment of the IKK complex, which promotes the pro-survival NF-*κ*B signalling (Lafont et al., 2017).

1.3.3 TRAIL as an anti-cancer agent

Cancer is the transformation of normal cells into malignant cells. It is known that mutations in oncogenes and tumour suppressor genes are involved in the transformation. Cancer is the second leading cause of mortality worldwide (Nagai & Kim, 2017), accounting for 10 million death in 2020 (Sung et al., 2021). Apoptosis is a natural cell death mechanism observed in the human body and therefore utilising a cell's own mechanism to eliminate the abnormal cancer cells has been considered as an essential tool to treat cancer (Kasibhatla & Tseng, 2003). On the other hand, dysregulation, inactivation and suppression of the apoptosis pathway has been shown

to play a role in carcinogenesis and cancer treatment resistance (Lowe & Lin, 2000). Therefore, since its discovery, cancer therapies were developed by targeting the apoptotic pathway (Carneiro & El-Deiry, 2020). Cytotoxic chemotherapeutic drugs mostly induce cell death in cancer cells by apoptosis, by inducing DNA damage or cell cycle arrest. Several drugs such as etoposide, cisplatin, 5′-Flourouracil, paclitaxel have been developed in the past (Hannun, 1997). However, the insensitivity and resistance of cancer cells to chemotherapeutic agents and treatment toxicity to normal cells led to necessity of developing more innovative apoptosis-targeted therapies for cancer treatment (Pommier et al., 2004; S.-T. Pan et al., 2016). For example, Bcl-2 family members have been shown to be upregulated in several cancer types, including colorectal, glioma, lung, breast, thus protecting the tumour cells from apoptosis. Therefore, therapies were developed by targeting the anti-apoptotic Bcl-2 family members (Yip & Reed, 2008; Pfeffer & Singh, 2018). One fine example is Venetoclax (ABT-199), the first FDA approved BH3 mimetic Bcl-2 inhibitor developed by Abbvie (Souers et al., 2013). It has been approved for chronic lymphocytic leukaemia and is currently in several clinical trials against multiple myeloma (NCT03539744), T cell lymphoma (NCT03552692), acute myelogenous leukaemia (NCT02203773) alone or as a combinational therapy. On the other hand, Bcl-2 pro-apoptotic proteins are downregulated in cancer (Burz et al., 2009) and studies also have shown that the genomic loss of these proteins was observed in cancer. In addition, other targets like, SMAC mimetics have been developed, such as Birinapant (NCT03803774), Debio1143 (NCT03270176, NCT04122625). Another apoptotic pathway target for cancer therapy is the development of TRAIL receptor agonists to enhance the clustering of death receptors and processing of caspases leading to cell death only in malignant cells without affecting normal cells. Availability of broad range of apoptotic pathway targets makes apoptosis a mechanism of interest for the development of cancer therapeutics. In the following part of the thesis, TRAIL receptor agonists development and efficacy are explained.

Two categories of TRAIL therapeutics have been developed, one being recombinant TRAIL and the other being agonistic antibodies against TRAILR1 and TRAILR2 (von Karstedt et al., 2017). TRAIL receptor agonists, upon TRAILR1/R2 receptor aggregation, induce the extrinsic pathway of apoptosis exclusively in cancer cells whilst leaving normal cells intact (Walczak et al., 1999; S. Wang & El-Deiry, 2003;

Johnstone et al., 2008). The initial TRAIL recombinant proteins were produced with N-terminal poly-Histidine tag (His) or FLAG epitope tag (FLAG) (Wiley et al., 1995; Pitti et al., 1996) for the purification purpose. They showed encouraging results (Ashkenazi et al., 1999; Walczak et al., 1999), however, they also showed cytotoxicity in normal hepatocytes due to the presence of aggregates (Jo et al., 2000; Lawrence et al., 2001; Ganten et al., 2006). Dulanermin, includes 114–281 amino acids of the extracellular domain of human TRAIL, is the first recombinant TRAIL that reached clinical trial (Herbst et al., 2010). Even with the successful preclinical trials and phase I trial of this recombinant protein, the randomised phase II clinical trial failed due to its short half-life of 30 minutes (Kelley et al., 2001; Soria et al., 2011; Graves et al., 2014). On the other hand, TRAIL receptor agonists such as mapatumumab (Tolcher et al., 2007; Trarbach et al., 2010), conatumumab (Herbst et al., 2010) entered clinical phase II level, but failed in showing efficient therapeutic benefit. The main reason for their failure was due to poor clustering and activation of TRAIL receptors which are required to drive downstream signalling and induce apoptosis.

In the early 2000s, studies have demonstrated that TRAILR1 and TRAILR2 has different crosslinking requirements to induce apoptosis. It was shown that TRAILR1 induces apoptosis by binding to membrane-bound or soluble TRAIL, however, TRAILR2 induced apoptosis only in response to membrane TRAIL or when the soluble TRAIL molecule was crosslinked by antibodies. Thus, the efficient activation of both TRAIL receptors by the antibody cross-linked TRAIL protein was considered important to increase the cytotoxicity of cancer cells (Mühlenbeck et al., 2000; Wajant et al., 2001). The signalling efficiency of sTRAIL (soluble TRAIL) to TRAILR2 was improved when single-chain fragment of variable regions (scFv) that recognizes the tumour stroma marker fibroblast activation protein (FAP) was fused to sTRAIL (Wajant et al., 2001). Following this study Bremer and colleagues developed scFVC54:TRAIL that targets the epithelial cell adhesion molecule (EpCAM) expressed at high level in cancers. When the fusion protein bound to the cancer cells, the sTRAIL mimicked as membrane TRAIL to the neighbouring cancer cells. This increased the apoptotic induction through TRAILR2 and this approach was called bystander apoptotic effect (Bremer et al., 2004). Overall, these studies indicated the importance of TRAILR2 crosslinking, therefore, several approaches have been taken to increase the efficiency of TRAIL. Recently, in 2019, Pan and colleagues showed that the TRAILR2

transmembrane helix is involved in oligomerisation and higher order clustering to activate the downstream signalling and not the extracellular domain. They also highlighted that ligand binding primarily prevents pre-ligand assembly mediated autoinhibition of the transmembrane helix from oligomerisation (L. Pan et al., 2019).

There were also steps carried out to improve the TRAIL efficiency by adding homotrimerisation motifs, including a leucine zipper motif (Walczak et al., 1999), an isoleucine zipper (Ganten et al., 2006), trimerisation motif tenascin-C (TNC) oligomerisation domain (Berg et al., 2007) and human adenovirus type 5 fiber protein (Yan et al., 2016). All these stabilise the trimeric TRAIL conformation (de Miguel et al., 2016). Moreover, addition of a leucine zipper increased the pharmacokinetic profile in rodents with extended elimination half-life of 4.8 h (Walczak et al., 1999). In an attempt to improve TRAIL stability, three TRAIL monomers were linked to form a single chain TRAIL (scTRAIL) format (B. Schneider et al., 2010). Similarly, Siegemund and colleagues developed a fully bioactive scTRAIL trimer by performing N- or C-terminal deletions of TRAIL monomers in single chain format and the resulting optimised scTRAIL showed increased thermal stability, solubility and production rate (Siegemund et al., 2016). In a previous study by the same group, they showed that improving TRAIL valency improves cytotoxicity, their dimeric molecules Db-scTRAIL (Siegemund et al., 2012) and scFv-EHD2-scTRAIL (Seifert, Plappert, et al., 2014) containing six TRAIL molecules engaging TRAIL receptors showed enhanced effect on cancer cells. Therefore, subsequently, stabilized scTRAIL trimer and hexavalent concepts were combined and the Fc-scTRAIL molecule was developed (Hutt et al., 2017). Fc-scTRAIL is a second-generation TRAIL-receptor agonist, produced by fusion of a single-chain TRAIL (scTRAIL) trimer to the Fc region of an IgG, resulting in an overall hexavalent TRAIL-receptor agonist that potently engages TRAIL receptor-mediated apoptosis in a wide range of cancer cells (Hutt et al., 2017; D. C. Phillips et al., 2021; Ratain et al., 2019; Siegemund et al., 2012; Vetma et al., 2020). Importantly, hexavalent TRAIL receptor agonists based on a similar format, ABBV-621, are currently undergoing clinical trials for advanced solid tumours and hematologic malignancies (NCT03082209). Even though first-generation TRAIL formats did not show expected clinical output, continuous efforts and innovative approaches on second-generation TRAIL format development are highly promising.

Besides TRAIL being a promising candidate in inducing apoptosis in tumour cells in general, TRAIL-based therapeutics have also shown great potential in pre-clinical studies as a novel approach for treatment of GBM. For example, a study was performed in 2016 using nanoparticles containing TRAIL expressing stem cell targets to eliminate GBM. Due to limited CNS delivery, the nanoparticles were delivered at the target site intracranially (Jiang et al., 2016). Furthermore, novel treatment combinations have been considered by different groups to sensitize the tumour cells to TRAIL treatment (Boccellato et al., 2021; Dorsey et al., 2009). For example, Fulda and colleagues administered SMAC peptides and TRAIL locally in a glioma xenograft model which led to complete elimination of tumours (Fulda et al., 2002). In another study, Lincoln and colleagues performed mathematical modelling and in vitro experiments in a panel of GBM cell lines. They have shown that GBM cells can be sensitized to TRAIL-mediated apoptosis by using IAP and Bcl2 antagonists (Lincoln et al., 2018). Therefore, TRAIL is a promising drug candidate and has notable potential in treating GBM alone or in combination with sensitizers. Of note, these TRAIL combination studies were either performed on cell lines or xenograft models with tumours injected on the flank region or with local invasive administration of drugs. In these studies, CNS delivery of TRAIL has not been addressed and so there is a need to identify the possibilities of bringing them into the CNS non-invasively.

1.4 Structure and components of BBB

The penetration of large biologics, such as TRAIL, into the CNS is generally controlled and prevented by the presence of the blood brain barrier (BBB), with approximately 0.1% of injected antibody doses reaching the brain parenchyma (W. M. Pardridge, 2005; Boado et al., 2012; W. M. Pardridge, 2020). The presence of this barrier in the central nervous system (CNS) came to light in 1855, when Paul Ehrlich, a German scientist, performed staining on animal organs. He observed that trypan blue dye injected intravenously stained all the organs except brain and spinal cord, he concluded that it was because of lack of binding affinity of the dye to CNS (Ehrlich, 1885). In 1913, Paul Ehrlich’s student, Edwin Goldman, proved that injecting water soluble dye into the cerebrospinal fluid could stain the brain and spinal cord, but not the organs in the peripheral nervous system (PNS). This study showed the existence

of a physical barrier between the periphery and the CNS. However, detailed information on BBB came only after the invention of electron microscopy in 1960's that showed that the cerebral endothelial cells are the central cells in the BBB (Clawson et al., 1966; Goldstein & Betz, 1986; S. Wagner et al., 2012). A study by Reese and Karnovsky identified the presence of tights junctions (TJ) in between the cerebral endothelium preventing the passage of HRP peroxidase into the rodent brain (Reese & Karnovsky, 1967). Additionally, the BBB is composed of pericytes, basement membrane, astrocytes, neurons and they are altogether referred to as the neurovascular unit (NVU) (Daneman & Prat, 2015). Astrocytes wrap around the capillary endothelial cells through their end-feet protrusion, and serve as a mode of interaction between neurons and blood vessels (Abbott, 2002; Abbott et al., 2006). It has also been demonstrated that astrocyte secreted factors are involved in the enhancement of the TJ formation and increased TJ protein expression (Wosik, Cayrol, et al., 2007; Alvarez et al., 2013). Pericytes sit on the abluminal side of the endothelial cells and they share the basement membrane (BM) with endothelial cells. The CNS has the highest pericyte to endothelial cell ratio of 3:1 as in the other tissues they are present in the ratio of 1:100 (Shepro & Morel, 1993; Wong et al., 2013) (Figure 4). The BBB endothelial cells are connected to each other with TJ and adherens junction (AJ) that prevent the paracellular transport of molecules. It is shown that they are formed after the disappearance of fenestrations or gaps during embryonic development in rodent brain (Wolburg & Lippoldt, 2002).

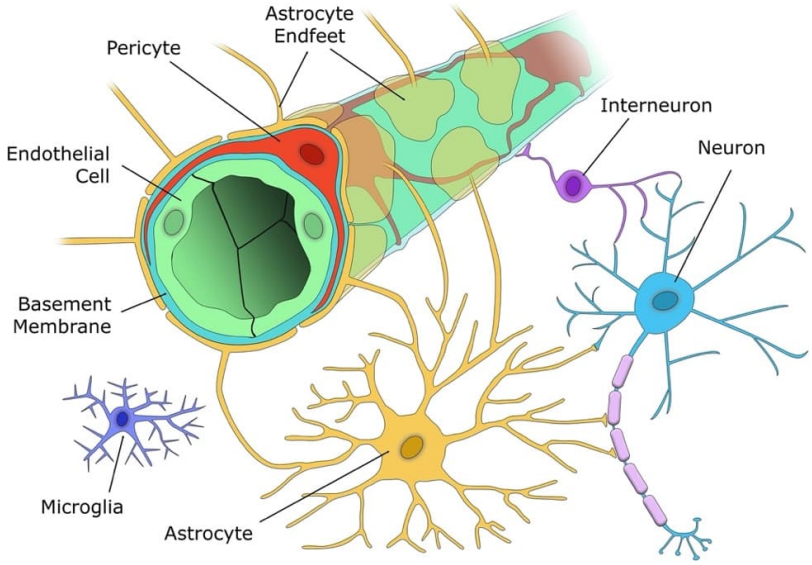

Figure 4: Composition of Neurovascular unit. The NVU is composed of endothelial cells, pericytes, astrocytes, neurons and the basement membrane. The capillary endothelial cells are interconnected by tight and adherens junctions to prevent paracellular transport. Pericytes and astrocytes wrap around the capillaries and play an important role in BBB maintenance and function. Figure obtained from (X. Yu et al., 2020).

In general, the cerebral endothelium is structurally and functionally different from the peripheral endothelial cells: (1) they have TJ that are tighter than in the periphery to prevent the transport (2) the endothelial cells are non-fenestrated (3) cerebral endothelium has less pinocytotic vesicles that are usually used by the peripheral endothelium for the transport of nutrients. TJs being an important part of the BBB, consist of occludin, claudin, junctional adhesion molecules (JAMs) and accessory proteins (Furuse, 2010). Occludin was the first identified integral membrane protein (Furuse et al., 1993; Saitou et al., 2000). Due to alternative splicing, there are occludin variants with molecular weights ranging from 60 to 65 kDa (Cummins, 2011). They are expressed at a higher level in the cerebral endothelium in a continuous cell-cell contact manner, whereas they are expressed at very low level in non-neuronal tissues in a discontinuous pattern, highlighting their specific role in the maintenance and function of the cerebral endothelium (Hirase et al., 1997). Claudins are proteins with a molecular weight of 20 to 24 kDa, have more than 25 family members but no sequence homology to occludins (Furuse et al., 1998; Morita et al., 1999). Studies have shown that they have an impact on paracellular ion transport and are essential for the formation of tight junctions (Van Itallie et al., 2001; Nitta et al., 2003). The zona occluden accessory proteins, such as ZO-1, ZO-2, and ZO-3 link to claudin and occludin through their N-terminal PDZ (postsynaptic density protein) domain (Itoh et

al., 1999; Hawkins & Davis, 2005). In addition, ZO-1 connects the transmembrane TJ to the actin cytoskeleton through its C-terminal domain. This connection is important for the stability and the functioning of the TJ (Fanning et al., 1998; Schneeberger & Lynch, 2004). JAMs are immunoglobulin family proteins. They interact with accessory proteins with their C-terminal PDZ domain in intracellular loops (W. Liu et al., 2012; Greene & Campbell, 2016). They can form homophilic and heterophilic interaction on opposing cells and other JAM family proteins, respectively (Mandell & Parkos, 2005; Weber et al., 2007). The TJs provide the BBB with high trans endothelial electrical resistance (TEER). It has been observed that rats have a TEER value of 1500-2000 Ω cm^2, which is very high in comparison to the TEER in peripheral endothelial cells (Butt et al., 1990; Huber et al., 2001). Overall, the BBB acts as a physical barrier through a combination of TJs and lack of fenestrations and this impermeable barrier is regulated by nearby supporting cells like endothelial cells, pericytes and astrocytes.

1.4.1 Transport at the BBB

The transport across the BBB to reach the CNS is a highly selective and complex process involving various cells, molecules and signalling pathways. But, this protective BBB limits the drug therapeutics for any CNS diseases as it prevents the entry of approximately 100% of large molecules and 98% of small molecules (W. M. Pardridge, 2012). Despite the limited permeability of the BBB, there are some naturally existing transport mechanisms supporting the highly selective entry of molecules. In recent years, these mechanisms have been adapted and used for drug delivery purposes. The following includes the types of transport mechanisms.

Passive diffusion: Small molecules are mostly transported across the BBB through passive diffusion. The factors determining the passive diffusion permeability are predominantly molecular weight, lipophilicity and charge (Lipinski et al., 2001). The molecular weight of the molecules should be below 400 or 500 Da to cross the BBB, but the permeability reduces 100-fold with an increase of molecular weight from 200 Da to 450 Da (Fischer et al., 1998; Mikitsh & Chacko, 2014). Another factor to undergo passive diffusion is lipophilicity. Lipophilic molecules can go across the hydrophobic phospholipid bilayer, and the lipophilicity is measured as logD (octanol/water partition coefficient) (Comer & Tam, 2001). Additionally, molecules with more than eight

hydrogen bonds cannot achieve passive diffusion (Clark, 2003). Moreover, the BBB expresses ATP-binding cassette (ABC) efflux transporters like P-glycoprotein (P-gp), breast-cancer resistance protein (BCRP) and the multi-drug resistance-associated proteins-1 and -2 (MRP-1, -2) (Löscher & Potschka, 2005). In general, these efflux transporters expressed on the apical side prevent the entry of toxic substances into the CNS, including the penetration of CNS drugs (Begley, 2004).

Carrier-mediated transport (CMT): The transport of small polar molecules is facilitated by the transporters at the luminal and abluminal side of the barrier (L. Lin et al., 2015). The CMT is bi-directional based on the concentration gradient and molecules that are required for metabolism are transported, such as, glucose, amino acids, vitamins (Jones & Shusta, 2007).

Adsorptive-mediated transcytosis (AMT): AMT is a non-specific vesicular transport-based mechanism where cationic proteins electrostatically interact with the negatively charged cell membrane and undergo transcytosis (Hervé et al., 2008; Gabathuler, 2010). Therefore, to facilitate the transport mechanism of AMT, the molecules are modified by cationization, such as IgG, albumin (Kumagai et al., 1987; Triguero et al., 1989).

Receptor-mediated transcytosis (RMT): Larger proteins and molecules are generally prevented from transport across the BBB, however, RMT selectively transports larger proteins and lipids across the BBB (W. M. Pardridge et al., 1987; Duffy et al., 1988). Like AMT, RMT is also vesicle-based transport system, but it is achieved through specific binding of a ligand to its receptor (Kadry et al., 2020). RMT is initiated by binding of endogenous proteins to their specific receptors on the luminal side of the BBB. At the binding site the cell membrane invaginates resulting in the formation of coated vesicle with the bound ligand and receptors. Once the vesicle enters the cytoplasm, it loses the coating and fuses with the endosome. Inside the endosomal compartment, the ligand and receptors are sorted and the receptors recycle back to the plasma membrane. The ligand in the endosomal compartment undergoes exocytosis at the abluminal side of the BBB and is released into the CNS parenchyma (Tuma & Hubbard, 2003; W. M. Pardridge, 2006, 2020). In some cases, the endosomal compartment fuses with lysosome and undergoes degradation, which is seen as a limiting step in achieving successful transcytosis (Figure 5) (Abdul Razzak

et al., 2019). The transport across the cell can be clathrin-dependent, caveolin-dependent or clathrin and caveolin-independent (Mayor et al., 2014; Mayor & Pagano, 2007). Among these, clathrin-mediated endocytosis is observed in transcytosis, including the well-known transferrin receptor (Pulgar, 2019). The major advantage in using RMT-mediated transport is that it is well suited for long term treatments, for example, in case of repeated therapy due to tumour recurrence. In addition, it delivers the larger molecules non-invasively unlike the invasive techniques like intraparenchymal, intraventricular and intrathecal delivery. There are several identified target receptors present on the luminal side of the BBB to achieve RMT, such as the insulin receptor (Pardridge et al., 1985; Duffy et al., 1988; Boado et al., 2012), the transferrin receptor (Jefferies et al., 1984; Fishman et al., 1987; Lee et al., 2000) and the low-density lipoprotein (LDL) receptor related protein (Lrp1) (Demeule et al., 2008, 2014; F. C. Thomas et al., 2009).

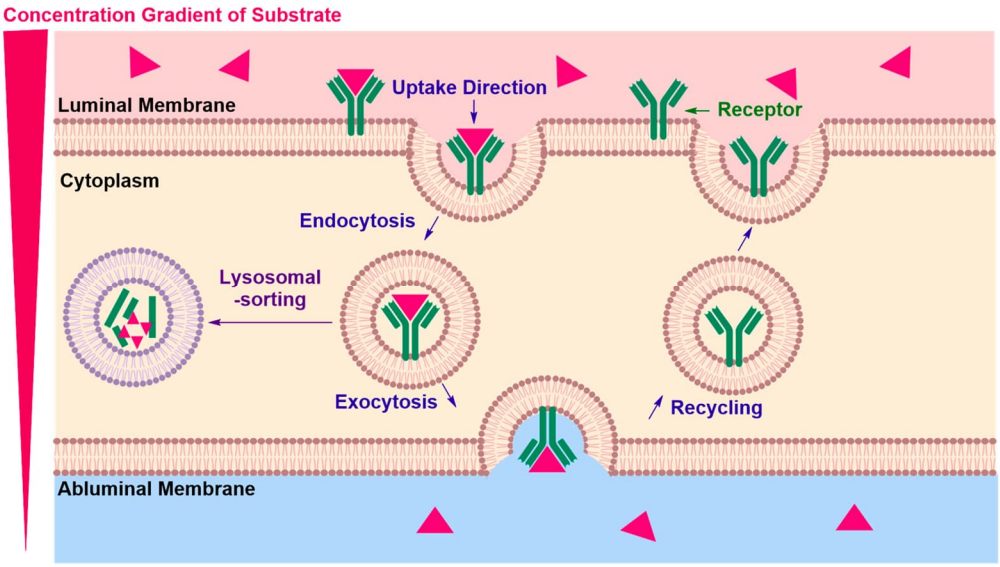

Figure 5: Receptor-mediated transcytosis. Ligands bind to the receptor of interest expressed on the luminal side of the BBB. Once bound, the cell membrane invaginates and pinches off into a vesicle. The endocytosed complex moves through the cytoplasm of the cell. During this process, the receptors are recycled back to the surface of the cell. The ligand is then exocytosed at the abluminal side of the BBB and released into the CNS parenchyma. In some cases, the endosomal compartment fuses with lysosome and undergoes degradation. Figure obtained from (Abdul Razzak et al., 2019).

1.4.2 RMT-mediated protein delivery approaches

Since the identification of the RMT mechanism in the 1980's, an increasing number of studies to improve transcytosis have been conducted. The RMT mechanism has been adapted for the delivery of proteins, peptides, nanoparticles, liposomes and antibodies across the BBB, of which, antibody-based fusion proteins have been often studied. Currently, there are a variety of RMT ligands and receptors investigated and different approaches have been considered for the development of efficient antibody-based RMT drugs. Initially, monoclonal antibodies targeting the transferrin receptor on the BBB were developed for the RMT. However, the in vivo studies were not successful as the endogenous transferrin competed with the transferrin antibody. Therefore, monoclonal antibodies targeting the binding site different from transferrin binding site of the transferrin receptor (TfR) have been developed. Even though there are reports showing the efficient binding and endocytosis of therapeutic antibodies (H. J. Lee et al., 2000; W. Pardridge et al., 1991), the amount of protein reaching the CNS at the end was not at therapeutical level.

Initial studies on RMT-mediated antibody development were based on high affinity proteins to ensure strong binding to the BBB and successful transport. To understand the influence of affinity on the transport efficiency, Yu and colleagues compared the transcytosis of high and low affinity antibodies. They observed that the high affinity antibodies were mostly trapped at the brain endothelium and the lower affinity antibodies showed increased brain uptake and distribution in the mouse parenchyma (Y. J. Yu et al., 2011). They stated that the high affinity antibodies were strictly bound to the BBB cells and were not able to detach from the receptor and therefore were not released into the brain parenchyma. They also developed bispecific antibodies for Alzheimer's disease by using enzyme b-secretase (BACE1) as a drug target. BACE1 is necessary for the processing of amyloid precursor into amyloid-β (Aβ) peptides, thus blocking BACE1 reduces the accumulation of Aβ peptides in the brain. For that, they designed a bispecific antibody with a high affinity anti-TfR on one arm and high affinity anti-BACE1 on the other arm. They reasoned that switching from bivalent to monovalent antibody format reduced the overall affinity and have shown that this bispecific antibody reduced the Aβ accumulation more than the monospecific anti-BACE1. In their follow up study, they also showed that this method was also suitable

for the delivery of TfR mediated drugs in non-human primates (Y. J. Yu et al., 2014). Their research work was ground-breaking in the field of RMT-mediated transport studies and stayed as a crucial factor for the improvement of RMT-mediated delivery. Subsequently, the same group in another study demonstrated in vitro and in vivo that the high affinity bispecific antibodies resulted in the degradation of antibody, by redirecting the ligand and receptor from endosomal to lysosomal compartment. This additionally reduced the level of receptors available on the BBB surface, thus limiting the antibody uptake (Bien-Ly et al., 2014). Similar results were obtained when high and low affinity bivalent rat transferrin binding antibodies were compared for the transcytosis efficiency. It has been shown that lowering the affinity resulted in more than 50-fold increase in the brain uptake, whereas increasing the affinity resulted in lysosomal degradation (Haqqani, Thom, et al., 2018). In another study, Niewoehner and colleagues from Roche fused the Fab fragment of anti-TfR antibody to one or both the C termini of an IgG heavy chain targeted against Aβ and compared between monovalent and bivalent formats (Niewoehner et al., 2014). Their in vivo and in vitro findings showed that the mode of interaction with the TfR determines the intracellular trafficking process of the antibodies. The bivalent antibody was trapped in the lysosome compartment and was not transported, whereas the monovalent antibody successfully achieved 50-fold more uptake into the CNS in preclinical models.

Until now, in the field of antibody-based RMT therapeutics, the target ligands that facilitate RMT were always fused to the standard Fab arm of an antibody. For example, in these formats, one arm binds to the transport peptide and the other arm binds to the therapeutic target in the CNS. This especially limited the use of bispecific or bivalent therapeutic drugs. Therefore, an interesting approach was taken by Kariolis and Ullman from Denali therapeutics, in which they engineered an Fc domain to contain a transferrin receptor binding site. This allowed them to incorporate bivalent or bispecific therapeutic targets as well as other proteins such as lysosomal enzymes into this transport vehicle (Kariolis et al., 2020; Ullman et al., 2020). In their study, BACE1 Fabs were fused to this transferrin transport vehicle, which resulted in 40-fold increase of the antibody uptake in brain when compared to native anti-BACE1 antibody. In addition, this fusion maintained the pharmacodynamic response by reducing amyloid β production in mice and non-human primates (Kariolis et al., 2020). Another study by the same group revealed that this BBB transport vehicle can be used for enzyme

replacement therapy, they fused iduronate 2-sulfatase (IDS) to reduce the accumulation of glycosaminoglycans (GAGs), for the treatment of lysosomal storage disorder Hunter syndrome. This fusion resulted in the reduction of GAG accumulation in the peripheral tissues and the brain, which was not achievable in earlier studies (Ullman et al., 2020). Overall, all the approaches and findings highlight that efficient transcytosis is inversely proportional to affinity and ultimately it has a huge impact on the drug transport across the BBB and it also emerges as one of the many challenging factors in developing optimal RMT-mediating protein therapeutics.

1.4.3 Lrp1 and Angiopep-2 in RMT

Lrp1, also known as α2-macroglobulin receptor or CD91, is a member of low-density lipoprotein receptor family. This type I transmembrane protein is synthesized as a 600 kDa precursor in the endoplasmic reticulum. Furin cleavage in the trans-Golgi compartment leads to the generation of two subunits, where the extracellular 515 kDa α-chain remains non-covalently linked to the transmembrane 85 kDa β-chain (Herz et al., 1988, 1990). The α-subunit, which plays a primary role in Lrp1 ligand binding, consists of four ligand binding domains and the β-subunit contains one tetra amino acid YxxL motif and two intracellular NPxY motifs, which are responsible for endocytosis (Figure 6) (Herz & Strickland, 2001; Potere et al., 2019). Lrp1 is a multiligand receptor known to play major roles in endocytosis, lipoprotein transport, migration, lipid metabolism, degradation of proteases, activation of lysosomal enzymes, entry of toxins and viruses and protects against atherosclerosis (Herz & Bock, 2002; Lillis et al., 2008; Boucher & Herz, 2011). Lrp1 receptor is widely expressed in the body, including hepatocytes, neurons, vascular smooth muscle cells (SMC) and macrophages (Makarova et al., 2003; Kanekiyo et al., 2012; Auderset et al., 2016). Moreover, reverse transcription polymerase chain reaction (RT-PCR) and western blot analysis indicated that Lrp1 receptors are expressed in brain capillaries and they play a major role BBB integrity (Storck et al., 2021; Zhao et al., 2016). The first identified ligands for Lrp1 were apolipoprotein E (ApoE) and α2-macroglobulin (Kowal et al., 1989; Strickland et al., 1990). Currently, there are several known ligands that bind to Lrp1, including receptor-associated protein (RAP), aprotinin, fibronectin, Matrix metallopeptidase 9 (MMP-9), Platelet-derived growth factor (PDGF) and beta-

very low density lipoproteins (β-VLDL) (Bres & Faissner, 2019; Lillis et al., 2008). In particular, studies have shown that Lrp1 mediates the bidirectional transport of amyloid-β, a protein implicated in Alzheimer's disease, across the blood-brain barrier (Pflanzner et al., 2011; Kanekiyo et al., 2012, 2013). For example, increasing the Lrp1 expression in adult mice resulted in active and increased elimination of amyloid-β plaques (Storck & Pietrzik, 2017). Studies have also shown that primary brain endothelial cells lacking functional NPxYxxL showed lower transcytosis than WT cells, highlighting the importance of this endocytosis motif (Bremer et al., 2004; Reekmans et al., 2010; Storck et al., 2016). Moreover, it has been shown that Lrp1 helps in the transport of receptor-associated protein (RAP) and tissue type plasminogen activator (tPA) (Benchenane et al., 2005; W. Pan et al., 2004) from the blood into the brain.

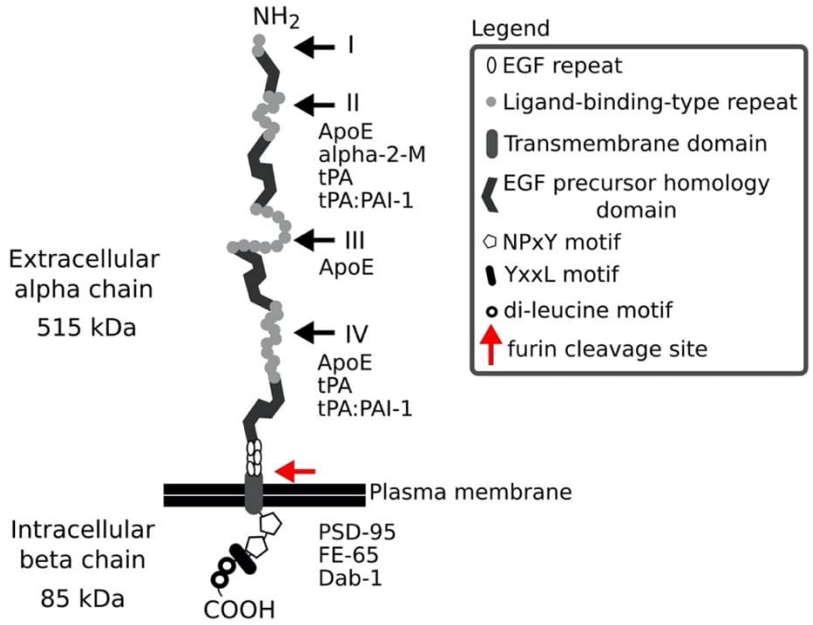

Figure 6: Structure of the Lrp1 receptor. Lrp1 is synthesized as a 600 kDa protein and furin cleavage gives rise two subunits, α and β. The extracellular α-unit has four ligand binding domains to which different ligands bind and the β-subunit consists of YxxL two intracellular NPxY motifs, which are responsible for endocytosis. Figure obtained from (Bres & Faissner, 2019).

In 2008, Demeule and his colleagues performed in vitro and in situ perfusion studies to identify and improve a group of peptides that achieve higher transcytosis through Lrp1 receptor. The kunitz protease inhibitor (KPI) domain is an important substrate for Lrp1 transcytosis. Therefore, they analysed a well-known Lrp1 ligand, aprotinin, with a KPI domain. They aligned the amino acid sequence of aprotinin with other kunitz domain containing proteins. From this alignment, they identified a set of 96 peptides

called Angiopeps. Among this family of identified peptides, Angiopep-2 (ANG2), a small 19 amino acid peptide, showed higher transcytosis rates than the original aprotinin protein (Demeule, Régina, et al., 2008).

In their follow up study, competitive transport experiments have revealed that Lrp1 is involved in the transport of ANG2, however, ANG2 transport was not completely inhibited by the known Lrp1 ligands, indicating that there could be other transport mechanisms involved in its transport (Demeule, Currie, et al., 2008). This Lrp1-ANG2-mediated transcytosis mechanism has been used to increase CNS-penetrance of various cargo from small drugs to proteins to nanoparticle-based systems (S. Huang et al., 2011; Shao et al., 2010; Wei et al., 2014). For example, ANG2 was used as shuttle peptide for the transport of anti-HER2 monoclonal antibodies. This was achieved by conjugating ANG2 to anti-HER2 antibody by copper-free click chemistry resulting in ANG4043. It showed increased in vivo accumulation and efficacy in mice bearing BT-474 brain tumours (Regina et al., 2015). Recently, ANG2-based constructs have entered clinical trials, showing low toxicity. ANG1005, a paclitaxel-ANG2 conjugate, showed better delivery than free paclitaxel for breast cancer patients with recurrent brain metastasis and is currently in clinical phase II, NCT02048059 (F. C. Thomas et al., 2009). NCT01967810 is another clinical trial phase II using ANG1005 for patients with recurrent high-grade glioma. GRN1005, previously mentioned as ANG1005, was also employed for the treatment of patients with solid tumours and is currently in phase II trial alone or in combination with Trastuzumab in breast cancer patients with brain metastases, NCT01480583 (Kurzrock et al., 2012). Currently, there is an ANG1005 clinical phase III study ongoing with patients to be recruited for the treatment of leptomeningeal carcinomatosis or leptomeningeal metastases or brain metastases or HER2-negative breast cancer (NCT03613181). These clinical studies and other preclinical research on Lrp1-ANG2-mediated transcytosis highlights the importance and benefits of using this system to bring therapeutics inside the brain. Of note, developing ANG2 peptide in the fusion protein format was less explored as most of the preclinical and clinical studies were conducted with ANG2 as a nanoparticle or conjugated to drugs like paclitaxel (ANG1005) (Kumthekar et al., 2016) or anti-HER2 mAb (ANG4043) (Regina et al., 2015). Therefore, in this thesis work, studies were performed to produce them as a fusion protein and utilise them as a BBB shuttle for the transport of large molecules into the CNS.

1.4.4 Aim of the thesis

GBM is one of the most aggressive tumours with very limited treatment options and patients have median survival time of 14-15 months. Therefore, novel therapies are required to treat GBM and to improve the survival rate of the patients. Due to its specificity in killing only the cancer cells, TRAIL has been considered a promising candidate for cancer treatment. Recently developed second generation hexavalent TRAIL receptor agonists alone or in combination with sensitizers have shown encouraging results on improving the GBM treatment strategy. Hence, second generation TRAIL receptor agonists were utilised in this project. As the BBB prevents the transport of drugs, ANG2 was employed as a shuttle peptide to undergo RMT and to deliver the TRAIL molecules into the CNS. Lrp1-ANG2 based constructs have entered early phase I/II/III clinical trials for the treatment of breast cancer metastasis, leptomeningeal carcinomatosis, and high-grade glioma. Due to its efficacy and patient safety, in this project, ANG2 peptide was used as a transport shuttle to bring TRAIL biologics into the CNS. The overall objective of the project was to design, produce and validate CNS-targeted TRAIL receptor agonists.

To briefly summarise, the aims of the thesis were:

- To generate CNS-targeted TRAIL receptor agonists to induce apoptosis in GBM cells and transcytosis across the BBB.
- To assess the TRAIL apoptosis efficiency in GBM and BBB endothelial cells by investigating the caspase cascade signalling pathway.
- To produce ANG2 positive control proteins and TRAIL-blocking constructs to characterize the binding of ANG2 to BBB cells.
- To establish an in vitro BBB model to evaluate the transport of CNS-targeted fusion proteins for the treatment of GBM.

2 Materials

2.1 Peptides

The following peptides were purchased from Peptides & Elephants (Brandenburg, Germany).

FITC-ANG2	FITC-Ahx-TFFYGGSRGKRNNFKTTEEY
FITC-scrANG2	FITC-Ahx-NSFEGTGGEYFTYRKRNFK
FLAG-ANG2	DYKDDDDKGGSGGTFFYGGSRGKRNNFK TTEEY

2.2 General consumables

Bolt 4-12% Bis-Tris Plus Gel 1.0 mm x 10 well	Thermo Fisher Scientific Inc., Waltham, USA
Bolt 4-12% Bis-Tris Plus Gel 1.0 mm x 15 well	Thermo Fisher Scientific Inc., Waltham, USA
Bolt 4-12% Bis-Tris Plus Gel 1.0 mm x 17 well	Thermo Fisher Scientific Inc., Waltham, USA
cell culture flasks	Greiner bio-one, Frickenhausen, Germany
cell culture plates	Greiner bio-one, Frickenhausen, Germany
coverslips	Carl Roth GmbH & Co. KG, Karlsruhe, Germany
cryobox	Cryo 1°C Freezing Containers, NALGENE, Thermo Fisher Scientific, Ulm, Germany
cryovial	CELLSTAR, Greiner bio-one, Frickenhausen, Germany
eppendorf tubes	Eppendorf AG, Hamburg, Germany

falcons	Greiner bio-one, Frickenhausen, Germany
iBlot 2 NC Mini Stacks	Thermo Fisher Scientific Inc., Waltham, USA
iBlot 2 NC Regular Stacks	Thermo Fisher Scientific Inc., Waltham, USA
neubauer counting chamber	Paul Marienfeld, GmbH & Co. KK, LaudaKönigshofen, Germany
Page ruler Prestained Protein Ladder	Thermo Fisher Scientific Inc., Waltham, USA
pipettes	Eppendorf Research Family, Eppendorf AG, Hamburg, Germany, BRAND GmbH & CO. KG, Wertheim am Main, Germany
polysine Microscope Adhesion Slides	Thermo Fisher Scientific Inc., Waltham, USA
transwell 24 well plates, 0.4 µm pore polyester membrane and 6.5 mm inserts	Sigma-Aldrich, St. Luis, USA

2.3 Eukaryotic cell lines

A172	Human glioblastoma cell line from ATCC, Manassas, USA
bEnd.3	Mouse brain endothelial cells from ATCC, Manassas, USA
HCT116	Human colorectal carcinoma cell line purchased from Banca Biologica e Cell Factory-IST Genova, IRCCS Azienda Ospedaliera Universitaria, San Martino
hCMEC/D3	Human cerebromicrovascular endothelial cells from Merk Millipore, Burlington, USA

HEK293-6E	National Research Council of Canada (Ottawa, Canada)
HeLa	Royal College of Surgeons in Ireland, Dublin
MEF WT	Institute of Cell Biology and Immunology (kindly provided by Dr. rer. nat. Kornelia Ellwanger).

2.4 Kits

BD OptEIA™ human TRAIL ELISA Set	BD Biosciences, Heidelberg Germany
Dako QIFIKIT$_{TM}$ Kit	Dako, Agilent Technologies, Santa Clara, USA
NucleoBond® Xtra Midi	Machery-Nagel, Düren, Germany
NucleoBond® Gel and PCR Clean-up	Machery-Nagel, Düren, Germany
Nucleospin® RNA kit	Machery-Nagel, Düren, Germany

2.5 Buffers and solutions

0.1% Triton X-100	0.1% (v/v) Triton X-100 in PBS
10 × trypsin/ ethylenediaminetetraacetic acid (EDTA)	Life technologies, Gibco, Karlsruhe, Germany
4% paraformaldehyde (PFA)	4% (w/v) PFA in PBS (pH 7.4); Merck, Darmstadt, Germany

5 x loading buffer	312.5 nM Tris-HCl pH 6.8, 25% (v/v) glycerine, 10% (w/v) SDS, 500 mM DTT, 0.05% (w/v)
Annexin V binding buffer (10 x concentrated)	BD Pharmingen, BD Biosciences, San Diego, USA
Bolt MES SDS Running Buffer (20X)	Thermo Fisher Scientific Inc., Waltham, USA
coomassie staining solution	0.008 % (w/w) Coomassie Brilliant Blue G-250, 35 mM HCl in H2O
collagen, Type I solution from rat tail	Merck KGaA, Darmstadt, Germany
crystal violet solution	0.5% (w/v) crystal violet powder, 20% (v/v) methanol in dd$H_2$0
DMEM (1X)	Life Technologies, Gibco, Karlsruhe, Germany
DNA loading buffer (5x)	25 % (v/v) glycerol, 0.02 % (w/v) bromphenol blue in 5x TAE buffer
eosin solution	Carl Roth GmbH & Co. KG, Karlsruhe, Germany
ELISA TMB substrate set	Biolegend, Inc, California, USA
ELISA stop solution	1 M H_2SO_4
ELISA washing solution	0.05 % (v/v) Tween20 in 1x PBS
fetal calf serum (FCS) (P30-3309)	PAN-Biotech GmbH, Aidenbach, Germany
FreeStyle™ F17 Expression Medium	Life Technologies, Gibco, Karlsruhe, Germany
freezing medium	10% (v/v) DMSO in FCS

LB-medium	1 % (w/v) peptone, 0.5 % (w/v) yeast extract, 0.5 % (w/v) NaCl in H2O
PBA	PBS + 0.05% (w/v) BSA + 0.02% (w/v) NaN_3 in ddH_20
phosphate buffered saline (PBS)	2.67 mM KCl, 1.47 mM KH_2PO_4, 137.9 mM NaCl, 8.06 mM Na_2HPO_4, pH 7.4
protein A – elution buffer	100 mM glycine, pH 3.5
protein A – neutralization buffer	1 M Tris-HCl, pH 9.0
protein A – washing buffer	PBS, pH 7.0
RPMI 1640 medium (+ 2 mM L-glutamine, 21875-034)	Life Technologies, Gibco, Karlsruhe, Germany
TBS with Tween-20 (TBST)	0.1% (v/v) Tween-20 in TBS
tris buffered saline (TBS)	20 mM Tris-HCl, 150 mM NaCl in ddH_20, pH 7.4

2.6 Chemicals and reagents

agarose	Carl Roth GmbH & Co. KG, Karlsruhe, Germany
Annexin V-EGFP	Manufactured by Dr. Fabian Richter, Institute of Cell Biology and Immunology, University of Stuttgart
blocking reagent	Roche Diagnostics, Mannheim, Germany
bond-Breaker® TCEP	0.5 M, Thermo Scientific, Rockford, USA
bovine serum albumin (BSA)	Sigma-Aldrich, Munich, Germany

bovine serum albumin (BSA) standard	Paesel + Lorei GmbH & Co. KG, Rheinberg, Germany
Bradford reagent	Carl Roth GmbH & Co. KG, Karlsruhe, Germany
crystal violet powder	Carl Roth GmbH & Co. KG, Karlsruhe, Germany
4’, 6-diamidin-2-phenylindol (DAPI)	Thermo Fisher Scientific, Ulm, Germany
dimethyl sulfoxide (DMSO)	Carl Roth GmbH & Co. KG, Karlsruhe, Germany
ethanol	Carl Roth GmbH & Co. KG, Karlsruhe, Germany
fluoromount-G Slide Mounting Medium	Southern Biotechnology Associates Inc., Birmingham, USA
glycerol	Carl Roth GmbH & Co. KG, Karlsruhe, Germany
Hoechst 33342	Thermo Fisher Scientific, Ulm, Germany
KCl	Carl Roth GmbH & Co. KG, Karlsruhe, Germany
KH_2PO_4	Carl Roth GmbH & Co. KG, Karlsruhe, Germany
Koliphor P 188	10% (w/v), Sigma Aldrich, Merck KGaA, Darmstadt, Germany
L-cysteine	1 mM L-cysteine in dH2O, pH 5.5
methanol	Carl Roth GmbH & Co. KG, Karlsruhe, Germany

Na_2HPO_4	Carl Roth GmbH & Co. KG, Karlsruhe, Germany
NaCl	Carl Roth GmbH & Co. KG, Karlsruhe, Germany
Power SYBR™ Green PCR-Master-Mix	Thermo Fisher Scientific Inc., USA
protease inhibitor cocktail complete, EDTA free	Roche Diagnostics AG, Basel, Switzerland
puromycin	Sigma Aldrich, Merck KGaA, Darmstadt, Germany
QVD-Oph (QVD)	Sigma-Aldrich, Munich, Germany
RNase-free water	QIAGEN, Hilden, Germany
sodium azide (NaN_3)	Carl Roth GmbH & Co. KG, Karlsruhe, Germany
$ZnCl_2$	100 mM in H2O, sterile filtered

2.7 Instruments

-20°C freezer	Comfort NoFrost, Liebherr, Bulle, Switzerland
-80°C freezer	HT5786-A, Hettich lab technologies, Tuttlingen, Germany
centrifuge	Eppendorf centrifuge 5415R, Hettich lab technologies, Tuttlingen Germany
centrifuge	Heraeus Multifuge 3-LR, Hettich lab technologies, Tuttlingen, Germany
centrifuge	Eppendorf centrifuge 5810R, Hettich lab technologies, Tuttlingen, Germany

centrifuge	J2-MC with rotors JA10, JA14, JA20, JA30.5, Beckman Coulter, Krefled, Germany
centrifuge	Avanti J-30I, Beckman Coulter, Krefeld, Germany
centrifuge	Optima™ TL with rotor TLA 100.3, Beckman Coulter, Krefeld, Germany
ECL imager	Amersham Imager 600, GE Healthcare Europe GmbH, Freiburg, Germany
electrophoresis power supply	EPS 601, Amersham Pharmacia Biotech; GE Healthcare Europe GmbH, Freiburg, Germany
electrophoresis power supply	EPS 301, Amersham Pharmacia Biotech; GE Healthcare Europe GmbH, Freiburg, Germany
EVOM epithelial Voltmeter	World Precision Instruments, Hitchin, UK
flow cytometer	MACSQuant Analyser 10, Militneyi Biotec, Bergisch Gladbach, Germany
gel documentation	Transilluminator, Gel documentation system Felix, Biostep, Jahnsdorf, Germany
heat block	HBT-1-131, Haep Labor Consult, Bovenden, Germany
heat block	Eppendorf Thermomixer compact, Merck KGaA, Darmstadt, Germany
heat block	Eppendorf Thermomixer F1.5, Merck KGaA, Darmstadt, Germany
HPLC systems	Waters 2695 Separation Module, Waters 2489 UV/Visible detector, Waters Cooperation, Milford, USA
iBlot 2 Dry Blotting System	Thermo Fisher Scientific Inc., Waltham, USA
incubator for cell culture	Varocell, Varolab GmbH, Giesen, Germany
incubator for cell culture	Forma Reach-In CO_2 Incubator, Thermo Fisher Scientific Inc., Waltham, USA

incubator for cell culture	BD 53, Binder, Stuttgart, Germany
inverted digital microscope	EVOS FL Imaging System, Thermo Fisher Scientific, Ulm, Germany
laser scanning microscope	LSM 710, Carl Zeiss MicroImaging GmbH, Jena, Germany
microplate reader	SPARK, Tecan, Meannedorf, Switzerland
mini–Gel Tank	Thermo Fisher Scientific Inc., Waltham, USA
nitrogen tank	K SERIES cryostorage system, tec-lab GmbH, Taunusstein, Germany
PCR Cycler	RoboCycler 96, Stratagene, La Jolla, USA
qPCR device	qPCR Cfx96 device, Biorad, Munich, Germany
spectrophotometer	NanoDrop Spectrophotometer ND-1000, Thermo Fisher Scientific, Ulm, Germany

2.8 Special implements

anti-FLAG® M2 affinity gel	Sigma-Aldrich, St. Louis, MO, USA
bottle Top Filter	CA Low Protein binding, 500 mL, 0.2 µm/0.45 µm, Corning Incorporated, Tewksbury, MA, USA
chromatography columns	Poly-Prep® (Bio-Rad, Munich, Germany)
dialysis membrane	High retention seamless cellulose tubing, 23 mm, MWCO 12.400, Sigma-Aldrich, St. Louis, MO, USA
FLAG peptide	5 mg/ml, peptides&elephants, Brandenburg, Germany

FPLC column	Superdex 200 10/300 GL, GE Healthcare, Little Chalfont, Buckinghamshire, UK
HPLC column	Yarra™ 3 µm SEC-2000, Yarra™ 3 µm SEC-3000, Phenomenex, Torrance, CA, USA
syringe filter	Acrodisc® 13 mm, 0.2 µm, HT Tuffryn® Membrane, Pall Corporation, Port Washington, NY, USA
ultrafiltration spin columns	Vivaspin 500, 30,000 MWCO PES (Sartorius, Göttingen, Germany)

2.9 Plasmids

pAB1	Vector for prokaryotic protein expression and secretion into the periplasm of *E. coli* (Kontermann *et al.*, 1997)
pSecTagA	Vector for eukaryotic protein expression and secretion, Thermo Fisher Scientific, Waltham, MA, USA
pSecTagAL1	Modification of pSecTagAHis with an additional AgeI restriction site in the Igκ chain leader sequence (Julia Seitter, 2007, Institute of Cell Biology and Immunology)

2.10 Primers

No	Name	Sequence	Purpose
89	pET-Seq1-for	TAATACGACTCACTATAGG	pSecTagA
91	pSec-Seq2-back	TAGAAGGCACAGTCGAGG	pSecTagA
1	EcoRI-Stopp-Angiopep-(G4S)2-Fc-for	CCCTGTCTCCGGGTAAAGGAGGTGGCGGATCAGGTGGAGGAGGCGGTTCTACTTTTTTCTACGGTGGGTCTAGGGGCAAGAGGAACAATTTTAAGACGGAAGAATACTGAGAATTCAAA	scTRAIL-Fc-ANG2

2	EcoRI-Stopp-Angiopep-(G2SG2)2-for	GGCGGATCTGGCGGCACTTTTTTCTACGGTGG GTCTAGGGGCAAGAGGAACAATTTTAAGACGG AAGAATACTGAGAATTCAAA	scTRAIL-ANG2
3	AgeI-Flag-back	AAAACCGGTGACTACAAAGACG	scTRAIL-Fc-ANG2 and scTRAIL-ANG2
4	AgeI-FcΔab-back	AAAAAACCGGTGACAAGACCCACACCTGTC	$Fc^{\Delta ab}$-ANG2
5	EcoRI-Stopp-Angiopep-(G4S)2-FcΔab-for	GCCTGTCCCCCGGCAAAGGAGGTGGCGGATC AGGTGGCGGTGGATCTACTTTTTTCTACGGTG GGTCTAGGGGCAAGAGGAACAATTTTAAGACG GAAGAATACTGAGAATTCAAAAA	$Fc^{\Delta ab}$-ANG2
6	AgeI-Angiopep-FcΔab-back	AAAAAACCGGTACTTTTTTCTACGGTGGGTCTA GGGGCAAGAGGAACAATTTTAAGACGGAAGAA TACGGAGGTGGCGGATCAGGTGGCGGTGGAT CTGACAAGACCCACACCTGTC	ANG2- $Fc^{\Delta ab}$
7	EcoRI-Stopp-FcΔab-for	CCCCCGGCAAATAAGAATTCAAAAATTTTTGAA TTCTTATTTGCCGGGGGG	ANG2- $Fc^{\Delta ab}$

2.11 Enzymes

BshTI (AgeI)	10 U/µl, Thermo Fisher Scientific, Waltham, MA, USA
DreamTaq™ Green PCR Master Mix	2.5 U/µl (Thermo Fisher Scientific, Waltham, MA, USA)
EcoRI	10 U/µl, Thermo Fisher Scientific, Waltham, MA, USA
T4 DNA Ligase	5 U/µl, Thermo Fisher Scientific, Waltham, MA, USA

2.12 Antibodies

2.12.1 Antibodies for western blot

Antibody	species	dilution/ concentration	manufacturer
anti-caspase 8 (IC12)	mouse	1:1000	Cell Signaling Technology, Danvers, USA
anti-caspase 8 (D35G2)	rabbit	1:1000	Cell Signaling Technology, Danvers, USA
anti-Lrp1 (ab92544)	rabbit	1:50000	Abcam, Cambridge, UK

anti-PARP (4C10-5)	mouse	1:500	BioLegend, San Diego, USA
anti-PARP (9542)	rabbit	1:1000	Cell Signaling Technology, Danvers, USA
anti-procaspase 3 (9662)	rabbit	1:1000	Cell Signaling Technology, Danvers, USA
anti-α-tubulin	mouse IgG1	1:1000	Cell Signaling Technology, Danvers, USA
anti-β-actin (4967)	rabbit	1:1000	Cell Signaling Technology, Danvers, USA
horse radish peroxidase (HRP)-conjugated goat anti-mouse IgG+IgM	goat	1:10000	Dianova, Hamburg, Germany
horse radish peroxidase (HRP)-conjugated goat anti-rabbit IgG+IgM	goat	1:10000	Dianova, Hamburg, Germany

2.12.2 Antibodies for flow cytometry

Antibody	species	dilution/ concentration	manufacturer
anti-DYKDDDDK-PE	human	1:200	Miltenyi Biotec, Bergisch Gladbach, Germany
anti- Lrp1 (8G1)	mouse	1:1000	Santa Cruz Biotechnology Inc., Santa Cruz, USA
anti-TRAILR1 (MAB347)	mouse IgG1	4 µg/ml	R&D Systems, Wiesbaden-Nordenstadt, Germany
anti-TRAILR2 (MAB6311)	mouse IgG2b	4 µg/ml	R&D Systems, Wiesbaden-Nordenstadt, Germany
anti-TRAILR3 (MAB6302)	mouse IgG1	4 µg/ml	R&D Systems, Wiesbaden-Nordenstadt, Germany
anti-TRAILR4 (MAB633)	mouse IgG1	4 µg/ml	R&D Systems, Wiesbaden-Nordenstadt, Germany

isotype control	mouse IgG1	1:100	BD Pharmingen, Heidelberg, Germany
isotype control	mouse IgG2b	1:100	BD Pharmingen, Heidelberg, Germany
isotype control	mouse IgG2b	1:100	R&D Systems, Wiesbaden-Nordenstadt, Germany
isotype control	mouse IgG2a	1:100	BD Pharmingen, Heidelberg,
isotype control	rabbit	1:100	Cell Signaling Technology, Danvers, MA, USA
Alexa Fluor 488 conjugated goat anti- mouse IgG (H+L)	goat	10 µg/ml	Thermo Fisher Scientific Inc., Waltham, USA

2.12.3 Antibodies for ELISA

Antibody	species	dilution/ concentration	manufacturer
anti-FLAG® M2-HRP	mouse IgG1	1:15,000	Sigma-Aldrich, Germany
anti- human IgG (Fc) specific- alkaline phosphatase antibody	goat	1:1000	Sigma-Aldrich, Germany
anti- human IgG (Fc) CH2 Domain:HRP	mouse	1:500	Bio-Rad Antibodies, Germany

2.13 Softwares and online tools

Clone Manager Professional 7	Scientific & Educational software, Carey, USA
ExPASy Prot Param Tool	http://web.expasy.org/protparam/
fiji	distribution of ImageJ (Schindelin et al., 2012)
Flowing software 2.5.1	Cell Imaging Core, Turku Centre for Biotechnology, University of Turku and Åbo Akademi University

FlowJo 7.6.1	Tree Star Inc., Ashland, Oregon, USA
GraphPad Prism 7	GraphPad Software Inc., San Diego, CA, USA
MACSQuantify	MACS Miltenyi Biotec, Bergisch Gladbach, Germany
RCSB protein databank	http://www.pdb.org/pdb/home/home.do
BLAST	http://blast.ncbi.nlm.nih.gov/Blast.cgi
Zen Lite 2011 (black edition)	Carl Zeiss MicroImaging GmbH, Jena
Flex Control and Flex Analysis	Bruker Daltronics, Massachusetts, United States

3 Methods

3.1 Cell culture

All the cell lines used were grown in their respective medium with supplements, as mentioned below. The cells lines were cultured in a T75 flask and maintained at 37°C with 5% CO_2 in a humidified atmosphere. Once the cells reached 90% confluency, they were prepared for cell passaging. For which, cells were washed with phosphate-buffered saline (PBS) of pH 7.4 to deactivate the medium followed by detaching the cells with 2 ml of 1x trypsin/ ethylenediaminetetraacetic acid (EDTA) (15400054, Life technologies, Gibco, Karlsruhe, Germany) for 5 min in the incubator. Later, the cells were resuspended in medium to stop the trypsin reaction. The cell suspension was transferred to a 15 ml falcon tube and centrifuged at 300 x *g* for 5 min (Eppendorf centrifuge 5810R, Hettich lab technologies, Tuttlingen, Germany). The supernatant was removed, and the cell pellet was resuspended in medium to have 1:5 dilution in T75 flask. For cell seeding, the cell pellet was resuspended in 2 ml of medium, and 10 µl of it was mixed with 10 µl of trypan blue solution, and 10 µl of the mixture was added to the Neubauer counting chamber (Paul Marienfeld, GmbH & Co. KK, LaudaKönigshofen, Germany). The cell number was obtained by taking the mean of unstained cells multiplied by the volume of cell suspension loaded, multiplied by 10^4. For permanent storage, the cell pellet was resuspended in 500 µl of respective growth medium and 500 µl freezing medium (10 % dimethyl sulfoxide (DMSO) in FCS) and added to a cryovial (CELLSTAR, Greiner bio-one, Frickenhausen, Germany), which was then transferred to -80°C (HT5786-A, Hettich lab technologies, Tuttlingen, Germany).

Table 1: Cell lines

Cell line	Medium	Supplement
HCT116	RPMI 1640 medium (+ 2 mM L-glutamine)	10 % FCS
Hela	RPMI 1640 medium (+ 2 mM L-glutamine)	10 % FCS
hCMEC/D3	EndoGRO™ - MV Complete Media Kit	1 ng/mL Fibroblast growth factor 2 (FGF-2).
bEnd.3	DMEM medium (+4.5g/L L-glutamine, L-glucose)	10 % FCS
A172	DMEM medium (+4.5g/L L-glutamine, L-glucose)	10 % FCS
MEF	DMEM medium (+4.5g/L L-glutamine, L-glucose)	10 % FCS
HEK293	FreeStyle™ F17 Expression Medium	4 mM GlutaMAX, 0.1% Koliphor P188

3.2 Cloning steps

3.2.1 Polymerase chain reaction

Polymerase chain reaction (PCR) was performed to amplify the required DNA fragments with specifically designed primers. The composition of the PCR mixture was included as in Table 2. The standard PCR program includes five steps and during the steps, temperature, cycles and time were modified depending on the factors mentioned. The PCR program consisted of an initial denaturation step (94°C for 5 min), 35 cycles of denaturation (94 °C for 1 min), annealing (temperature based on the primers, 1 min), elongation (72 °C for time based on the length of the PCR fragment) and final elongation step (72 °C for 5 min). Subsequently, the amplified DNA fragments were loaded on agarose gel and extracted.

Table 2: PCR mixture content

DNA template (10 ng/µl to 100 ng/µl)	1 µl
DNA polymerase	1 µl
dNTPs (5 mM each)	1 µl
Forward primer (10 µM	1 µl
Reverse primer (10 µM)	1 µl
DNA Polymerase buffer	10 µl
dH_2O	35 µl

3.2.2 Agarose gel electrophoresis and DNA extraction

The amplified or the digested DNA fragments after PCR and restriction digestion, respectively were run through horizontal agarose gel electrophoresis. Based on the size of the DNA, 0.7 to 1 % of agarose (Carl Roth GmbH & Co. KG, Karlsruhe, Germany) was dissolved in TAE buffer by heating. 6X DNA loading buffer was added to the DNA samples and loaded on agarose gel containing 1 µg/µl of ethidium bromide for visualization under UV light source. The gel was run at 100 V for 30 min. Then, the DNA fragments of respective size were cut out from the gel and purified by Nucleospin® Gel and PCR Clean- up kit (740588.50, Machery-Nagel, Düren, Germany) according to the manufacturer's protocol.

3.2.3 Restriction digestion and ligation

For the restriction digestion, total PCR product or 3 µg of vector DNA were used. The sample volume was made up to 50 µl with 1 µl of each restriction enzymes, buffer and dH_2O. The mixture was incubated for 2 h. 1 µl of FastAP was added to the vector DNA to prevent religation. After the restriction digestion, the digested products were run through agarose gel electrophoresis and extracted by Nucleospin® Gel and PCR Clean- up kit according to the manufacturer's protocol. Ligation was performed with T4 DNA ligase enzyme. The digested and purified vector (100 ng to 200 ng) and insert

were usually ligated in the molar ratio of 1:3 to 1:5 with 1 µl of T4 DNA ligase, 5 µl ligase buffer in a total volume of 40 µl for 1 h at RT. The whole was performed with Thermo Fisher Scientific products (Waltham, MA, USA)

3.2.4 Transformation of *E. coli* cells

DH5 alpha competent *E. coli* cells were thawed on ice prior to transformation. 10 ng of ligated plasmid was diluted in 20 µl of H_2O. To which, 40 µL of TCM buffer (10 mM Tris-HCI, pH=8.0, 10 mM CaCl2 and 10 mM MgCl2) was added. For the transformation, 100 µl of competent cells were added to the mixture and incubated for 10 min on ice, followed by 1 min of heat shock at 42 °C and then 1 min incubation on ice. To the bacteria, 1 ml of LB medium was added and incubated in a shaker (Eppendorf Thermomixer F1.5, Merck KGaA, Darmstadt, Germany) at 37 °C for 1 h. The mixture was centrifuged, and the cell pellet was resuspended in 50 µl of LB medium and streaked on LB agar plates with 100 µg/ml of Ampicillin. The plates were incubated overnight at 37 °C. The next day, one colony was picked and added to 150 ml of LB medium containing 100 µg/ml of Ampicillin and incubated in orbital shaker overnight at 37 °C.

3.2.5 Plasmid-DNA preparation

After the incubation, the plasmid DNA was prepared utilizing DNA Midi kits. One clone from the LB_{AMP} plate was picked and used as an overnight culture in 150 ml LB medium containing Ampicillin. Plasmid DNA was purified with NucleoBond® Xtra Midi kit (740410.50, Machery-Nagel, Düren, Germany) for Midi preparation according to manufacturer's protocol. The same protocol was followed for re-transformation of plasmid DNA but with 1 µl of DNA sample.

3.2.6 DNA concentration determination and sequence analysis

The DNA concentration was estimated by measuring the absorbance at 260 nm using NanoDrop™ ND-1000. Respective primers were added to the produced DNA and sent

to GATC Biotech AG (Constance, Germany) for sequence analysis. The obtained sequencing data were compared with BLAST analysis data using online program ‘nucleotide BLAST’ from NCBI to check for mismatches.

3.3 Eukaryotic protein production

3.3.1 Maintenance of suspension HEK cells for production

HEK293-6E cells with DR5 knockout were generated by Dr. Martin Siegemund (Institute of Cell Biology and Immunology, University of Stuttgart, Germany). The constructs with TRAIL were produced using HEK293-6E with DR5 KO cells and the rest were produced using HEK293-6E cells. The HEK293-6E cells are suspension cells and were grown in Erlenmeyer flasks and maintained in F17 expression style medium (A13835-02, Life Technologies, Gibco, Karlsruhe, Germany) supplemented with 4 mM GlutaMAX (35050-038, Life Technologies, Gibco, Karlsruhe, Germany), 0.1% Koliphor P188 (K4894-500G, Sigma Aldrich, Germany) and with 4 µg/mL Puromycin (for HEK293-6E cells with DR5 KO) on orbital shaker at 115 rpm, 37°C, 5% CO_2. For the production, the cells were centrifuged, counted using CASY cell counter (Omni Life Sciences, Germany) and expanded until their exponential growth phase (1.5 to 2 x 10^6 cells/ml). One day prior to transfection, 1.2 x 10^6 cells/ml were collected and added to 360 ml of F17 Expression Style Medium supplemented with 4 mM GlutaMAX, 0.1% Koliphor P188, without Puromycin.

3.3.2 Transfection with polyethyleneimine (PEI) and protein harvesting

On the day of transfection, the cells were counted and checked for their viability. For the transfection, 20 ml of F17 medium were vortexed with 400 µg plasmid DNA and 20 ml of F17 medium was vortexed with 1200 µL (1mg/mL) PEI separately and incubated for 2 min. Later, the PEI mixture was added to the DNA mixture and incubated in RT for 15 min. The 40 ml mixture was added to the 360 ml cell suspension and maintained on orbital shaker. After 24 h, 0.5% tryptone N1 (TN1, Organotechnie S.A.S, France)

and 10 µM $ZnCl_2$ (only for the production of TRAIL constructs) were added to the cell suspension. The cells were maintained on orbital shaker for 96 h at 115 rpm, 37°C, 5% CO_2. After 96 h, the cell suspension was centrifuged at 2000 x g for 30 min at 4°C. The supernatant containing protein was collected and sterile filtered followed by purification.

3.4 Purification of proteins

3.4.1 FLAG affinity chromatography

The constructs with TRAIL moieties were purified through anti-FLAG antibody agarose. The anti-FLAG M2 affinity resin (A2220, Sigma Aldrich, Germany) was equilibrated by washing with 100 mM Glycin-HCl, pH 3.5 followed by five washing steps with DPBS. After that, to the sterile filtered supernatant, the M2 FLAG affinity resin was added and incubated rolling overnight at 4°C. The next day, the affinity resin along with target protein was collected by centrifuging at 1000 g for 10 min and transferred to a chromatography column. The resins were washed with DPBS and the bound protein was eluted with DPBS containing 100 µg/ml FLAG peptide. The wash and elution steps were analysed by Bradford assay (10 µl of wash or protein sample was added to 90 µl of Bradford reagent (K015.3, Carl Roth GmbH & Co. KG, Karlsruhe, Germany)). The proteins were carefully eluted and dialyzed against 5 l PBS overnight at 4°C.

3.4.2 Protein A affinity chromatography

TRAIL-R2-Fc, TRAIL-R2-mFc^{LALA}, Fc$^{\Delta ab}$-ANG2 and ANG2-Fc$^{\Delta ab}$ fusion proteins were purified through protein A affinity chromatography. 3 ml of protein A Sepharose (50 % slurry) were added to the column and equilibrated with 30 ml H_2O and 30 ml binding buffer (PBS). The protein A Sepharose were collected carefully with a Pasteur pipette from the column and added to the sterile filtered supernatant and incubated rolling overnight at 4°C. The next day, supernatant with beads was centrifuged at 700 g at 4°C for 5 min (Heraeus Multifuge 3-LR, Hettich lab technologies, Tuttlingen, Germany). The beads were loaded on to the column with a small volume of supernatant and

washed with 5-10 SV binding buffer. The proteins were eluted with 8.5 ml of 100 mM Glycin-HCl pH 3.0. The wash and elution steps were analysed by Bradford assay as in 3.5.1. The protein A Sepharose beads were regenerated with 10 ml of elution buffer and 10 ml of H_2O and stored in 20% EtOH at 4°C.

3.5 Biochemical characterisation of proteins

3.5.1 Determination of protein concentration

Protein concentration c (µg/µL) was determined by measuring the absorption (A) at 280 nm with a NanoDropTM ND-1000 spectrophotometer using the molecular mass MW (g/mol) and the molar extinction coefficient ε ($M^{-1}cm^{-1}$) of the respective protein. Molecular weight and extinction coefficient was determined by using the online tool 'Expasy ProtParam'. The Beer-Lambert equation was used to calculate the concentration of protein:

$$C = \frac{A}{\varepsilon} . MW$$

3.5.2 Size exclusion chromatography

The purified proteins were analysed through size exclusion chromatography. 35 to 40 µl of 0.3 µg/ml protein was collected and applied on a Superdex 200 10/300 GL column using PBS as mobile phase and a flow rate of 0.5 ml/min. The fractions were collected and the fractions with targeted protein molecular weight were pooled. Proteins with aggregates, multimers or cleavage products were further purified by size exclusion FPLC. Size exclusion was performed by Doris Göttsch (Institute of Cell Biology and Immunology, University of Stuttgart, Germany).

3.5.3 SDS-PAGE

2 µg of protein samples were mixed with Laemmli loading buffer (reducing and non-reducing conditions) and incubated for 5 min at 95°C. They were loaded into Bolt 4-12% Bis-Tris Plus Gel along with PageRuler^{TM} prestained protein ladder. The gel was boiled in ddH_2O and incubated in Coomassie solution for 1 h at RT. The incubated gel was destained with Coomassie destaining solution. The gel was visualized using the photo scanner Epson Perfection V200 (Saiko Epson Corporation, Amsterdam, Netherlands).

3.5.4 Crystal violet cell viability assay

To test the cell death efficacy of TRAIL treatments, crystal violet assay was performed on HCT116 cells. 10,000 HCT116 cells/ well were seeded in 100 µl medium in 96-well plate (F bottom) and incubated for 24 h at 37°C, 5 % CO2. 200 µl of serial diluted proteins were added to the cells and were incubated for 16 h at 37 °C, 5 % CO2. After incubation for 16 h, the cells were washed with PBS and 50 µl/well of crystal violet staining solution was added and incubated for 15 min at RT. Staining was removed and the cells were left to dry overnight at RT. 100 µL of methanol was added per well and the absorption was measured at 570 nm on a microplate reader (SPARK, Tecan, Männedorf, Switzerland).

3.6 Mass spectrometry - MALDI

scTRAIL-Fc-ANG2 and Fc-scTRAIL were loaded on Bolt 4-12% Bis-Tris Plus pre-cast gel with Bolt MES SDS running buffer (20X) placed on Bolt Mini Gel Tank chamber (Thermo Fisher Scientific). The gel was washed with Milli-Q water to remove the buffer and then stained with instant Coomassie blue (11022018, Expedeon). After staining, the gel was again washed with Milli-Q water. The stained protein bands were cut, washed with Milli-Q water and then centrifuged for 1 min at 11,000 rpm. To the gel pieces, 200 µl of 50 mM NH_4HCO_3 (09830-500G, Sigma Aldrich, Germany) and 100% acetonitrile (4722.1, Carl Roth, Germany) 1+1 (v/v) was added and incubated in the

shaker for 15 min. The solution was discarded and the gel was incubated with 50 µl of 100% acetonitrile for 5 min for dehydration. Once the gel was shrunk, acetonitrile was removed and 50 mM of NH_4HCO_3 was added to the gel and incubated for 5 min for rehydration. Then an equal volume of acetonitrile was added and incubated for 15 min while shaking. The remaining solution was removed and the gel was air dried in a vacuum centrifuge. For the in-gel digestion, the air-dried gel particle was digested with a solution of 5 ng/ml Trypsin (sequencing grade modified Trypsin, Promega, Germany), 50 mM NH_4HCO_3 and 100% acetonitrile and incubated overnight at 37°C. The supernatant was removed and 25 µl of TA20 (20% acetonitrile and 0.1% of Trifluoroacetic acid, TFA (P088.2, Roth) was added. The gel particles were ultrasonicated (USR32H, Merck eurolab, Germany) for 5 min and incubated for 30 min. The supernatant was collected and the steps were repeated with TA50 (50% acetonitrile and 0.1% of TFA). The supernatants were combined and dried for 1 h in a vacuum centrifuge (Eppendorf, concentrator plus, Germany). The dried pellet was dissolved in 10 µl of 0.1% TFA. 1 µl of the sample was added to the MALDI target plate (MTP Anchor Chip 384TF, Bruker Daltronics, Germany). After drying, 1µl of Matrix solution (0,7mg/ml a-Cyano-4-hydroxycinnamic acid (39468-10x10MG, Sigma Aldrich, Germany) was dissolved in a solvent mixture containing 85% acetonitrile, 15% H_2O, 0,1% TFA and 1mM $NH_4H_2PO_4$ (17842, Fluka, Germany) was spotted above the sample. For peptide calibration 0.5 µl Peptide Calibration Standard II (222570, Bruker Daltronics, Germany) was spotted on the same target plate. The plate was inserted in the MALDI-TOF machine (Bruker™ Autoflex Speed MALDI TOF, Germany) and the samples were analysed using Flex Control and Flex Analysis software.

3.7 Flow cytometry

3.7.1 Flow cytometric measurement of surface death receptors

The cells were cultivated in T75 flasks until they reached 90% confluency. For the flow experiment, the cells were washed with PBS and harvested by incubating with 1 x trypsin for 5 min at 37°C. Later, the medium was added to stop the trypsin reaction and cells were centrifuged at 300 x *g* for 5 min. Then, cells were counted and 1 x 10^5 cells per well were added to a 96-well plate (V bottom) and spun down with 300 g for 5 min

at 4 °C. The pellet was resuspended in ice-cold PBA (0.05% (w/v) bovine serum albumin (BSA) + 0.02% (w/v) NaN3 in PBS) and spun again to remove the leftover medium. The supernatant was removed, and the pellet was resuspended in 100 µL ice-cold PBA containing the primary antibody (dilution 1:100) and incubated on ice for 1 h. Afterwards, 100 µL calibration beads were added to an empty well. The cells were washed again with PBA and resuspended in 50 µL of secondary antibody (dilution 1:50) in PBA. The cells were left to incubate for 45 min on ice and in the dark. The cells were spun down and washed with 100 µL PBA and then transferred to a 96-well plate (U bottom). The fluorescence was measured by flow cytometry (MACSQuant Analyser 10, Miltenyi Biotec). The number of cell surface receptors were measured against DAKO QIFIKIT (Dako, Agilent Technologies, Santa Clara, USA) beads as per manufacturer's instructions. IgG1 (anti-TRAILR1, anti-TRAILR3, anti-TRAILR4) and IgG2b (anti-TRAILR2) were used as isotype controls.

Table 3: QIFI Kit calibration beads with its respective number of receptors

Calibration	Number of antibody molecules per bead
B	1700
C	9800
D	50000
E	220000
F	723000

3.7.2 Annexin V/PI cell death measurement

A172 and hCMEC/D3 cells were seeded in a 96-well plate (F bottom) and let to attach and grow for two days. Then, the cells were treated with scTRAIL-Fc-ANG2, scTRAIL-ANG2 and IZI1551 in serial dilution for 24 h. After the incubation of cells with the constructs, the supernatant was transferred to a 96-well plate (U bottom) and the cells were washed with PBS, which was transferred to the plate with supernatant. The supernatant was spun down at 300 x *g* for 5 min and the cells from the 96-well plate (F bottom) were detached by incubating with 1 x trypsin for 5 min. The detached cells were harvested with 90 µL from the supernatant that was centrifuged and was

transferred to the V bottom plate followed by centrifugation at 300 x *g* for 5 min. The supernatant was removed, and pellets were resuspended in Annexin V binding buffer (BD Pharmingen, BD Biosciences) containing Propidium Iodide (Biolegend, Germany or Sigma Aldrich, Germany) (2 µg/ml) and Annexin V-GFP (produced in-house) (1:200) and incubated in the dark for 10 min. Measurements were done on a MacsQuant flow cytometer (MACSQuant Analyser 10, Miltenyi Biotec)

3.7.3 Cell binding assays

The produced proteins were tested for their binding efficiency to different cell lines. Cells were cultured in their respective medium at 37°C in a humidified incubator. hCMEC/D3, bEnd.3 and Jurkat cells were washed with PBS and detached using 1x trypsin/ ethylenediaminetetraacetic acid (EDTA) and washed in cold PBA (1xPBS, 0.05% BSA and 0.02% Sodium Azide). The cell number was determined (50,000 cells per well) and the cells were centrifuged. Firstly, the cell pellets were washed with PBA. The cells were incubated with the protein constructs in a total volume of 100 µl. For blocking TRAIL moieties in the constructs, the TRAIL constructs were incubated with blocking construct TRAIL-R2-Fc (200-fold molar excess) for 30 min at 4°C. The cells were incubated with different constructs in serial dilution for 2 h on ice. After incubation, cells were washed with PBA and incubated for 2 h with the secondary antibody depending on the detection moiety of the constructs. The binding was measured by flow cytometry and the median fluorescence intensities were obtained for each construct.

3.7.4 Analysis of flow cytometric data

To analyse the data generated by flow cytometry the software FlowJo 7.6.1 (Tree Star Inc.), MACSQuantify (MACS Miltenyi Biotec) and flowing software 2.5.1 (Cell Imaging Core, Turku Centre for Biotechnology, University of Turku and Åbo Akademi University) were used.

3.8 MTT assay

bEnd.3 cells were seeded in a 96-well plate (F bottom) and left to attach and grow for 24 h. Then, the cells were treated with scTRAIL-Fc-ANG2, scTRAIL-ANG2 and IZI1551 in serial dilution for 24 h. After the treatment, 20 µl of MTT solution (5 mg/ml) were added to each well including the wells without cells. The plate was incubated for 3-4 h in the incubator at 37°C. Later, the medium was aspirated and 200 µl of methanol was added to each well and incubated for 10 min in the incubator. The absorbance was measured at a wavelength of 570 nm with a Tecan plate reader (Infinite M200 or SPARK, Tecan, Meannedorf, Switzerland).

3.9 Western Blotting

3.9.1 Protein extraction for western blotting

The cells were cultivated in 10 cm petri dishes and on the day of protein extraction, the cells were harvested by trypsinization. The medium with dead cells was collected and the cells were washed with PBS followed by trypsinization. The cells were spun down at 300 g for 5 min at 4°C. Thereafter, the cells were resuspended in cold PBS and centrifuged again. The supernatant was removed and cell pellets were stored at -20°C.

For protein extraction, the cell pellets were resuspended in lysis buffer and incubated for 15 min on ice, then the samples were centrifuged for 15 min at 16000 g and the supernatant was transferred to new reaction tubes. To determine the protein concentration in the lysates, a Bradford assay was performed. The protein lysates were diluted to 1:10, 1:20 in ddH2O and 10 µl of these dilutions were pipetted into a 96 well plate in duplicates. At the same time, Bovine serum albumin (BSA) standard (Paesel + Lorei GmbH & Co; 0.0, 0.125, 0.25, 0.5, 0.75, 1.0, 1.5, 2.0 mg/ml BSA diluted in ddH2O) were used to generate a standard curve and a 1:10, 1:20 lysis buffer dissolved in ddH2O was used as a blank. The Bradford Reagent (Carl Roth GmbH & Co) was diluted 1:5 in water and 200 µl of this dilution were added to every well and incubated for 5 min at RT and the absorbance was measured at a wavelength of 595 nm with a microplate reader (Infinite M200 or SPARK, Tecan, Meannedorf, Switzerland). The

protein concentration was calculated and then prepared with ddH2O and 5x loading buffer with a final concentration of 1 µg/µl - 2 µg/µl protein. The samples were incubated for 5 min at 95°C on a heat block (HBT-1-131, Haep Labor Consult, Bovenden, Germany) and frozen at -20°C. For the SDS PAGE, the samples and the molecular weight marker were loaded into Bolt 4-12% Bis-Tris Plus Gel1.0 mm x 15 well or Bolt 4-12% Bis-Tris Plus Gel 1.0 mm x 17 well with Bolt MES SDS Running Buffer (20X) placed on Bolt Mini Gel Tank chamber (Thermo Fisher Scientific). The proteins were separated in the gel at 150 V for about 40 min.

3.9.2 Protein transfer and western Blot

The separated proteins were transferred to a nitrocellulose membrane using the iBlot 2 Dry Blotting System (transfer settings: 20 V; 7 min, Thermo Fisher Scientific Inc.). The transfer was visualized by incubating with Ponceau S staining for 30 min. Then, the membranes were washed and incubated for at least 1 h with blocking reagent (diluted 1:10 in TBST, Roche Diagnostics) washed three times with TBST for 10 min and incubated with the primary antibody (diluted in TBST with blocking reagent (1:20) and 0.02% (w/v) NaN3)) overnight at 4°C or for 1h at RT. After three more washing steps with TBST, membranes were incubated with a horseradish peroxidase (HRP) coupled secondary antibody (diluted in TBST with blocking reagent (1:20) 1 h at RT. The membranes were washed and prepared for detection. For the detection process, the membranes were incubated with an HRP substrate (SuperSignal West Pico ECL Substrate/SuperSignal West Dura Extended, Pierce Protein Research Products; Luminata Forte Western HRP Substrate, Merck Millipore) and detected with the Amersham™ Imager 600 (GE Healthcare Bio-Sciences, Pittsburgh, USA).

3.10 Binding of the constructs to bEnd.3 cells

3.10.1 Immunocytochemistry

Cells were grown on coverslips coated with 2.5 µg/ml Collagen R solution (08-115, Sigma-Aldrich). Once the cells were confluent, they were incubated with the constructs

for 15 and 30 min at 37°C. After the incubation, cells were washed with PBS and fixed with 4% paraformaldehyde (sc-281692, Santa Cruz) for 30 min. Thereafter, cells were permeabilized with Triton X-100 in PBS for 10 min and blocked with 4% BSA. The cells were incubated with primary antibodies for 1 h at RT and diluted in PBS followed by washing and incubation with 4 µg/ml secondary antibodies for 45 min at RT. After washing, cells were mounted with Fluoromount-G. Images were acquired on a confocal laser scanning microscope (LSM 710, Carl Zeiss, Oberkochen, Germany) equipped with a Plan-Apochromat 63x/1.4 Oil objective. DAPI was excited with a 405 nm diode laser, its emission was detected from 410-490 nm. PE was excited with a 561 nm DPSS laser, its emission was detected from 553-660 nm. Linear adjustments to brightness and contrast, as well as maximum intensity projections were made using the ZEN black software version 2.1 (Carl Zeiss). Images were quantified using CellProfiler version 3.1.8 (McQuin et al., 2018). In brief, cells were segmented and speckles in the PE channel under the cell mask were counted. Additionally, the mean intensity in the red channel was measured for each cell.

3.11 Blood brain barrier transwell setup and transport assay

The bEnd.3 cells (30,000 cells/well), were seeded in 24-well transwell plates (0.33 cm^2 surface area, 0.4 µm pore size) with their respective medium. Transendothelial electrical resistance (TEER) was measured every day for 6-7 days using an EVOM 2 / STX2 electrode to check the integrity of barrier cells. The medium was changed once in two days. Two negative controls without the cells were maintained to subtract from the resistance of the samples. To establish BBB barrier with hCMEC/D3 cells, the cells were seeded on the wells coated with type I rat tail collagen (10 µg/cm^2 diluted in PBS).

Once the stable TEER value was reached, the cells were prepared for the transport experiment. The cells were preincubated cells for 1 h with 50 µM QVD with medium. After that, the medium was removed, and the cells were washed with sterile PBS. BSA (2%) with 20 nM of $Fc^{\Delta ab}$-ANG2, ANG2-$Fc^{\Delta ab}$, scTRAIL-Fc-ANG2 and Fc-scTRAIL (IZI1551) were added to the wells with cells and incubated at 37°C. After 1 h, the sample from the top and bottom were taken and measured using ELISA. The top well samples were diluted 1:20 for the measurement.

3.12 ELISA for the transport measurement

To measure the constructs transported across the Blood brain barrier transport setup, ELISA was performed. The ELISA plates were coated with anti-human IgG (Fc) diluted (1:1000) in ELISA coating buffer and left overnight at 4°C. The next day, ELISA plates were washed with ELISA washing buffer three times and blocked with 2% BSA in PBS for 1 h. Plates were rinsed with washing buffer five times. 100 µl of the samples from the transwell and also the samples for the standard were added to the ELISA plate and incubated for 2 h at RT. The plates were again washed with washing buffer for five times. The plates were incubated with the detection antibody anti-human IgG (Fc) CH2 Domain: HRP diluted (1:500) in 2% BSA for 2 h at RT. The plates were washed seven times with washing buffer and then incubated with TMB substrate for 5 to 10 min. After that, to stop the reaction, the ELISA stop solution was added. A standard curve was established for each construct and the transported proteins in the transwell were determined by interpolation from the standard curve and under consideration of the dilution factor. The absorbance was measured at a wavelength of 450 nm with a Tecan plate reader (Infinite M200 or SPARK, Tecan, Meannedorf, Switzerland).

3.13 Statistical analysis

GraphPad Prism 7 (GraphPad Software, San Diego) was used to analyse all data. Data are shown as mean values plus and minus the standard deviation (SD) or standard error of the mean (SEM). Statistical significance of difference between groups was performed by indicated significance test. Parametric tests were performed only after confirming normal distribution of the data using the D'Agostino & Pearson omnibus normality test. Significance levels were denoted with asterisks: * = $p \leq 0.05$; ** = $p \leq 0.01$; *** = $p \leq 0.001$ **** = $p \leq 0.0001$.

4 RESULTS

4.1 Production and characterisation of apoptosis and transcytosis inducing CNS-targeted fusion proteins

Second-generation hexavalent TRAIL fusion proteins have evolved as a potential treatment strategy against GBM (Hutt et al., 2017; Boccellato et al., 2021). Therefore, in the first part of this study, CNS-targeted TRAIL fusion proteins were generated to render both apoptosis in GBM cells and transcytosis across the BBB. The produced fusion proteins required biochemical characterisation and quality controls to verify their robust apoptosis and efficient transcytosis.

4.1.1 Designing, production and purification of CNS-targeted TRAIL fusion proteins

Three functional units were included in the CNS-targeted fusion proteins, the crystallisable fragment (Fc) domain of a human IgG including the hinge region, a single chain format of trimeric TRAIL (scTRAIL) and ANG2. These units were used to yield the final construct with dimerisation (Fc; Figure 7A), apoptosis induction (scTRAIL; Figure 7B) and CNS-targeting (ANG2; Figure 7C) properties.

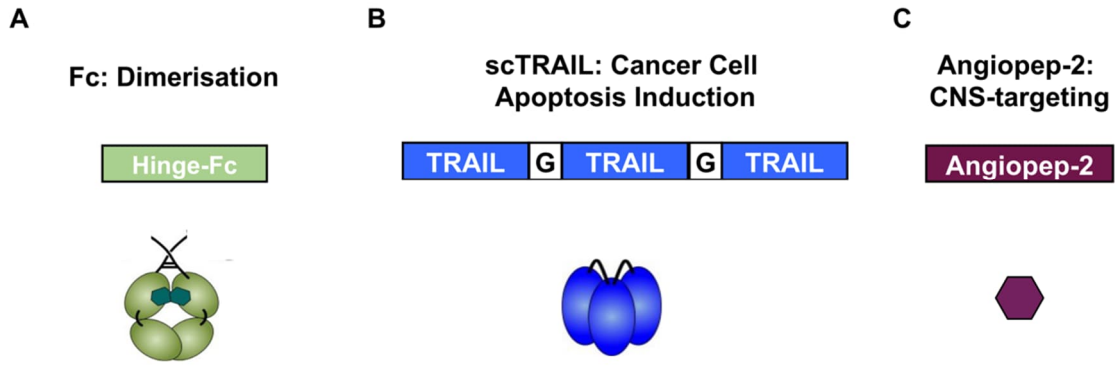

Figure 7: Functional units of a CNS-targeted TRAIL-receptor agonist. (A) Fc part of IgG for dimerisation (B) scTRAIL for apoptosis and (C) Angiopep-2 for transcytosis.

scTRAIL consists of three copies of the extracellular domain, amino acid residues 118 to 281 of TRAIL interspaced by single glycine residues forming a single chain soluble trimer. Angiopep-2, a synthetic peptide derived from the kunitz domain of aprotinin, was used to target Lrp1-receptors on the blood-brain-barrier cells (Demeule, Régina,

et al., 2008; Demeule, Currie, et al., 2008). Fc-scTRAIL, consisting of two trivalent scTRAIL units dimerised via their fusion to the C-terminus of an IgG1 Fc and previously demonstrated to induce highly efficient apoptosis, was used as a base model to generate the TRAIL fusion proteins (Siegemund et al., 2016; Hutt, 2017).

To render apoptosis and transcytosis simultaneously, TRAIL and ANG2 moieties were fused together. To combine the superior apoptosis induction of Fc-scTRAIL with ANG2, scTRAIL was fused to the N-terminus of human IgG1 Fc with a flexible glycine-serine linker $(GGSGG)_2$ and ANG2 was fused to the C-terminus of the Fc interspaced with a $(G_4S)_2$ linker (Figure 8A ii, Figure 8B ii). The resulting hexavalent TRAIL construct included two ANG2 moieties per molecule. The trivalent construct was generated by fusing scTRAIL to the N-terminus of ANG2 with a flexible glycine-serine linker $(GGSGG)_2$. The resulting trivalent construct included one ANG2 moiety per molecule. Notably, TRAIL-ANG2 fusion proteins were created (Figure 8b ii and iii) with ANG2 on the C-terminus in accordance with previous studies (Böckenhoff et al., 2014; Ji et al., 2019).

The constructs were designed, cloned and produced in stably transfected HEK293-6E cells with DR5 KO to eliminate the binding of TRAIL molecule to DR5 receptors in the cells. The leader peptide from Igκ light chain was fused to the N-terminus of the protein of interest and that enables secretion of the protein into the supernatant and the cleavage of the Igκ light chain leader peptide during export as described in previous studies (Siegemund et al., 2014). The FLAG-tag was included at the N-terminus for the purification through FLAG affinity chromatography. The scTRAIL-Fc-ANG2 and scTRAIL-ANG2 were produced with the yield of 10 mg/l and 2.7 mg/l of cell culture supernatant respectively and were ready for purification.

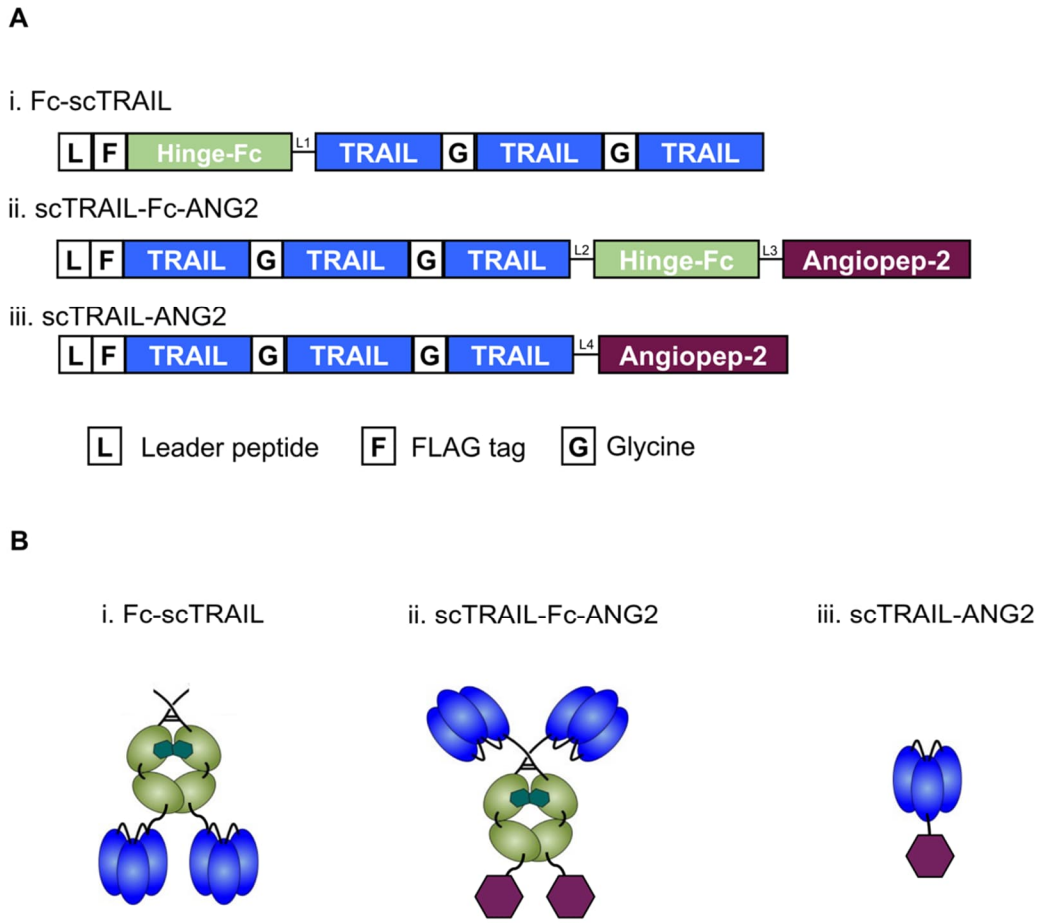

Figure 8: Designing CNS-targeted TRAIL-receptor agonists. (A) Composition and (B) schematic assembly of scTRAIL variants. L1, $(GGSGG)_2$ linker. L2, $(GGSGG)_4$ linker. L3, $(G4S)_2$ linker. L4, $(GGSGG)_2$ linker.

4.1.2 Biochemical characterisation of CNS-targeted TRAIL fusion proteins

In order to eliminate any aggregates, fast protein liquid chromatography-size exclusion chromatography (FPLC-SEC) was performed for scTRAIL-Fc-ANG2 and scTRAIL-ANG2 fusion proteins. SDS-PAGE was performed to check the purity, oligomerisation status and the quality of the CNS-targeted TRAIL fusion proteins. For the hexavalent scTRAIL-Fc-ANG2, β-mercaptoethanol was used to reduce the disulfide bonds in the Fc part of IgG. Under reducing conditions, scTRAIL-Fc-ANG2 ran corresponding to its predicted monomeric molecular weight as a clear single band at approximately 88.3 kDa (Figure 9A). Under non-reducing conditions, the dimeric scTRAIL-Fc-ANG2 was observed as a single band at 176.6 kDa (Figure 9A). The monomeric protein, scTRAIL-

ANG2 was observed at the predicted molecular weight of 61.43 kDa under non-reducing conditions (Figure 9B). Correlating with purity shown by SDS PAGE, in size-exclusion chromatography (SEC), both the proteins were eluted as one clear peak with no aggregates (Figure 9C and Figure 9D). Overall, the biochemical characterisation proved that the CNS-targeted TRAIL fusion proteins are pure, intact and correctly oligomerised. Fusion proteins were designed and successfully purified to confer the specific GBM killing of hexavalent TRAIL-receptor agonists with enhanced CNS delivery properties of ANG2.

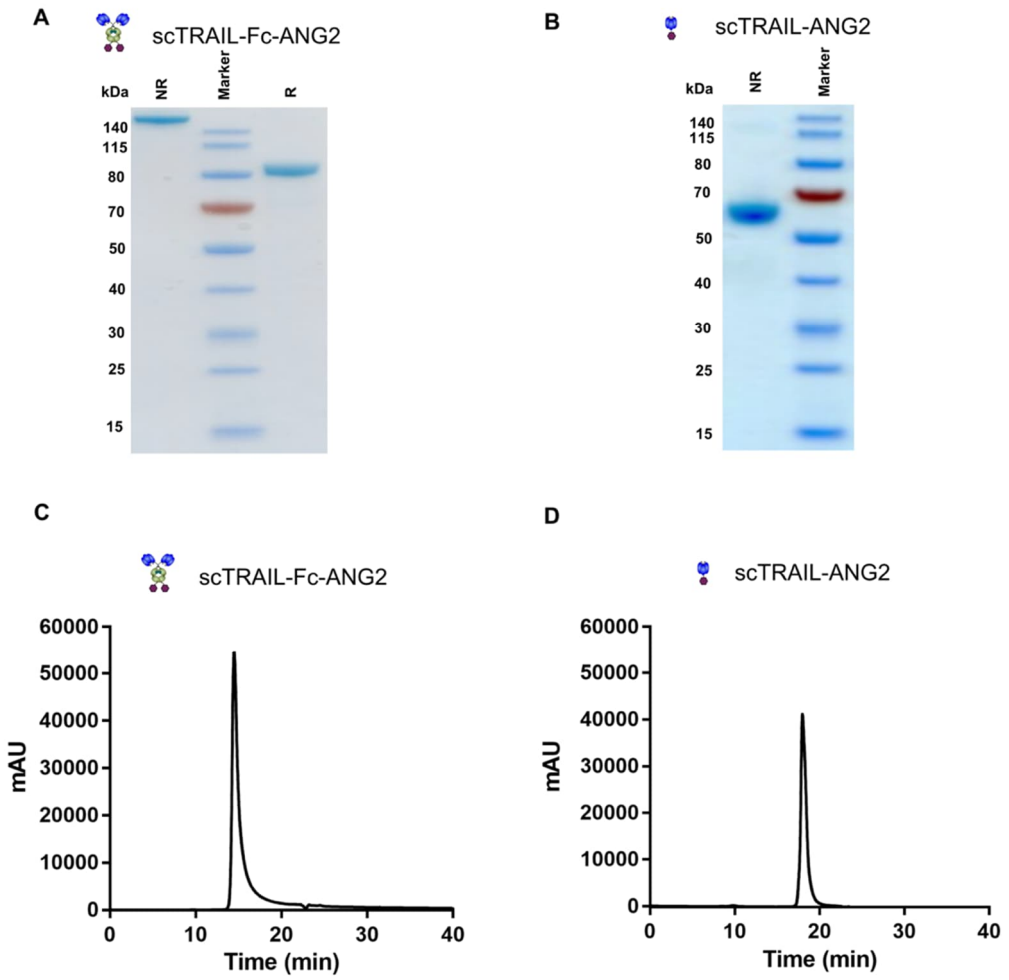

Figure 9: Biochemical characterisation of CNS-targeted TRAIL fusion proteins. (A) SDS PAGE of indicated constructs was performed with (R) or without the reducing agent (NR) β-mercaptoethanol and stained with coomassie blue. 2 µg of the protein was loaded. **(B)** Size exclusion HPLC chromatogram of indicated constructs with elution time. kDa, kilodalton. MW, molecular weight. mAU, milli absorbance unit.

4.1.3 Validation of apoptotic functionality of scTRAIL-Fc-ANG2 and scTRAIL-ANG2 in TRAIL sensitive HCT116 cells

After successful production of pure CNS-targeted TRAIL fusion proteins and prior to in depth apoptosis analysis, a rapid cell viability assay was performed to ascertain basic apoptosis functionality of the constructs. The human colon cancer cell line HCT116, a well-established TRAIL responsive cell line, was used for this analysis in a crystal violet assay. The HCT116 cells were treated with scTRAIL-Fc-ANG2, scTRAIL-ANG2 and Fc-scTRAIL in a serial dilution for 16 h. Fc-scTRAIL was used as a positive control in this test. During this assay, the dead cells detach and are washed away and the remaining live attached cells are stained with crystal violet dye, which binds to protein and DNA of the cells allowing measurement by absorbance at 570 nm. A time-dependent reduction of viable cells was observed after scTRAIL-Fc-ANG2 treatment, with a loss of 80% of cells at maximal concentration (Figure 10A). As expected from previous studies, trivalent TRAIL showed reduced apoptotic efficiency than hexavalent Fc-scTRAIL (Siegemund et al., 2016). Only 20% of viable cells were lost at the maximal concentration with the trivalent scTRAIL-ANG2 (Figure 10B).

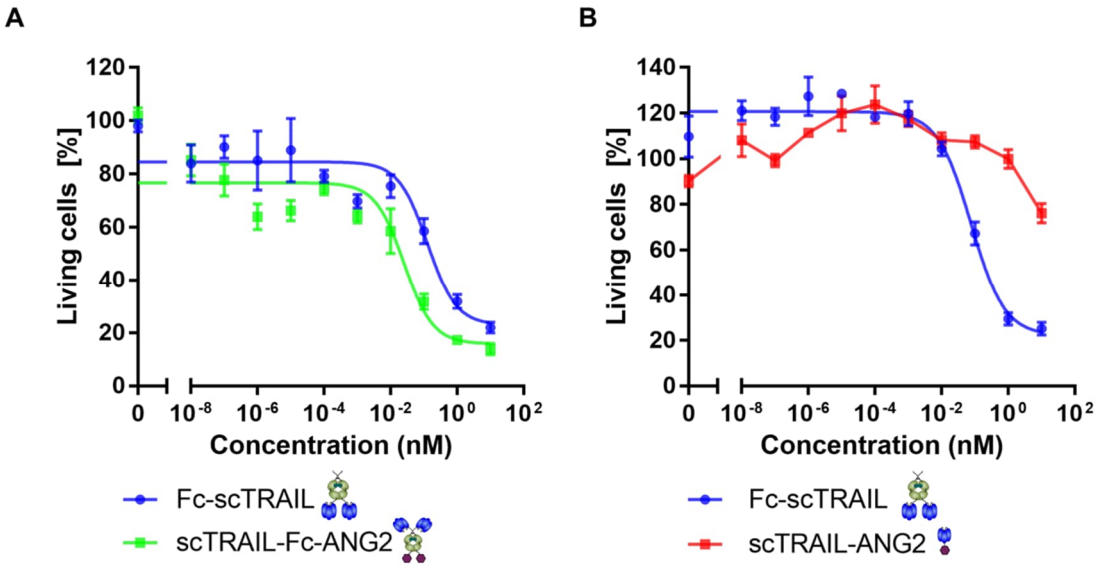

Figure 10: Validation of apoptosis functionality of CNS-targeted TRAIL fusion proteins. Dose dependent response of HCT116 colon cancer cells to **(A)** Fc-scTRAIL or scTRAIL-Fc-ANG2 **(B)** Fc-scTRAIL or scTRAIL-ANG2 after 16 h stimulation with different concentrations of the constructs. Cell viability was measured by crystal violet assay from one experiment.

4.1.4 Mass spectrometry identification of Angiopep-2 in CNS-targeted TRAIL fusion protein

As a part of quality control, MALDI-TOF (matrix assisted laser desorption ionization - time of flight) mass spectrometry was performed to verify the presence of ANG2 in the CNS-targeted fusion protein. For that, scTRAIL-Fc-ANG2 was compared with ANG2 lacking Fc-scTRAIL. In MALDI-TOF, the sample protein is reduced, trypsinised and placed on a matrix, which is an energy absorbent. Once the laser is applied to the sample-matrix mixture, the matrix absorbs the laser and releases the heat to the sample. This leads to desorption and ionization of the sample to generate singly charged ions. The charged analytes are measured by Time of Flight (TOF) mass analyser. At the end, the detected peptide sequence is compared with the actual peptide of interest and therefore this technique helps in identification of the ANG2 part of the fusion protein.

For the analysis, the fusion proteins were run on SDS PAGE and collected. They were digested with 5 ng/ml, 10 ng/ml and 20 ng/ml of trypsin. The samples were analysed using MALDI-TOF Bruker machine and the peaks were fitted using Flex analysis software. Figure 11 shows the generated mass spectrum of analytes in which mass-to-charge is plotted against intensity. The Fc-scTRAIL spectrum showed peaks at (m/z = 1138), (m/z = 1367), (m/z = 1607), (m/z = 1873), (m/z = 2066), (m/z = 2580) similar to scTRAIL-Fc-ANG2 spectrum as shown in Figure 11B. Importantly, an additional peak, (m/z = 1621.8), was observed in scTRAIL-Fc-ANG2 spectrum and it indicated the presence of the sequence GGGGSGGGGSTFFYGGSR. This detected sequence is a part of the linker and ANG2 and it confirmed the presence of Angiopep-2 in the scTRAIL-Fc-ANG2 fusion protein.

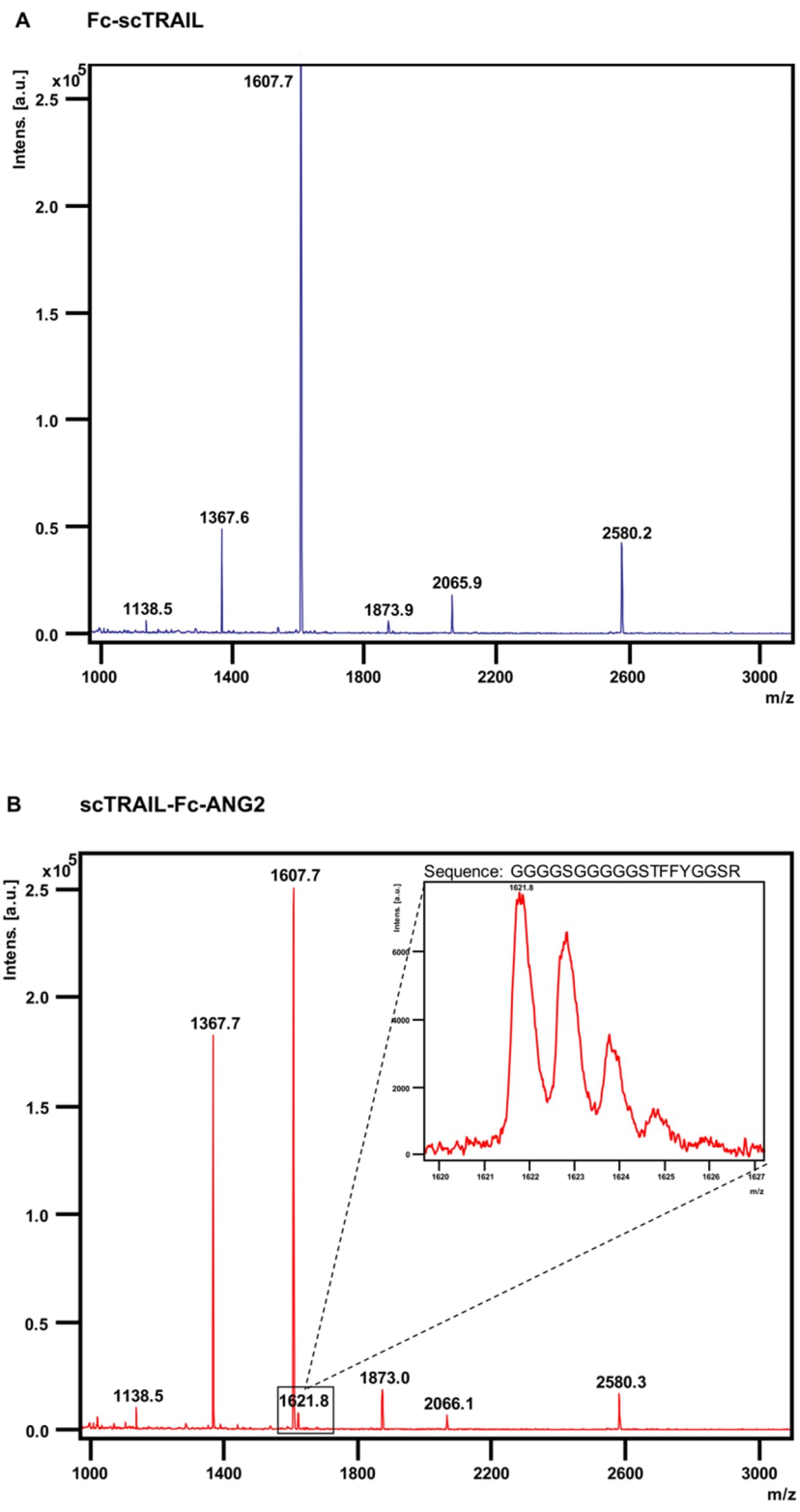

Figure 11: Presence of Angiopep-2 in the CNS-targeted TRAIL fusion protein. MALDI-TOF spectrum of **(A)** Fc-scTRAIL and **(B)** scTRAIL-Fc-ANG2. The intensities of ions are shown on the Y axis and the masses of the ions are shown on the x axis. m/z, mass-to-charge ratio. Data shown from one mass spectrometry analysis. The experiment was performed with the Dr. Sarah Weirich from the Institute of Biochemistry and Technical Biochemistry.

4.1.5 Designing and production of transcytosis inducing fusion proteins: $Fc^{\Delta ab}$-ANG2 and ANG2- $Fc^{\Delta ab}$

In order to understand the transcytotic potential of Angiopep-2 on its own in a fusion protein format and also to serve as a positive control for this study, two separate ANG2-positive control proteins were generated. The proteins were designed by fusing ANG2 to the C- or N- terminal end of an Fcγ receptor binding (FcγR)-deficient mutant Fc ($Fc^{\Delta ab}$), interspaced with a glycine-serine linker $(G_4S)_2$ (Armour et al., 1999) (Figure 12 A and B). The resulting proteins had two Angiopep-2 moieties per molecule. These fusion proteins were produced by using stable transfected HEK293T suspension cells. They were tag free proteins and were purified by protein A affinity chromatography. In protein A affinity chromatography, the proteins are purified by protein A Sepharose beads that bind to the Fc region of IgG. The $Fc^{\Delta ab}$-ANG2 and ANG2-$Fc^{\Delta ab}$ fusion proteins were produced with the yield of 2.2 mg/l and 6.4 mg/l of cell supernatant, respectively.

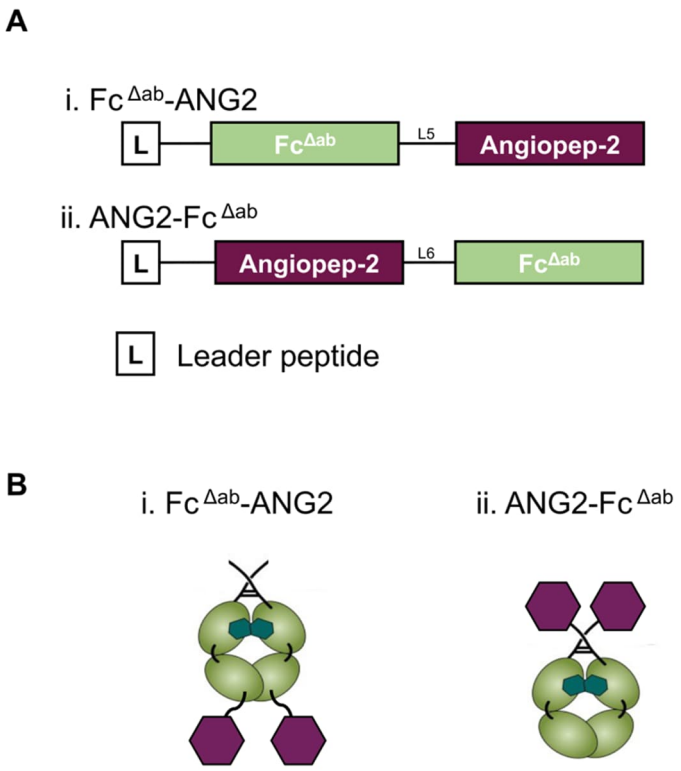

Figure 12: Designing transcytosis inducing Angiopep-2 fusion proteins. (A) Composition and (B) schematic assembly of $Fc^{\Delta ab}$-ANG2 and ANG2- $Fc^{\Delta ab}$. L5, $(GGGGS)_2$ linker. L6, $(GGGGS)_2$ linker.

4.1.6 Biochemical characterisation of $Fc^{\Delta ab}$-ANG2 and ANG2- $Fc^{\Delta ab}$

Size exclusion chromatography (FPLC-SEC) was performed for both the fusion proteins to eliminate aggregates. SDS PAGE was performed to check the purity and the quality of the fusion proteins. For both the proteins, β-mercaptoethanol was used to reduce the disulfide bonds in the Fc part of IgG. The SDS PAGE shows that $Fc^{\Delta ab}$-ANG2 and ANG2- $Fc^{\Delta ab}$ appears at higher molecular weight than expected in reducing (33 kDa, monomeric) and non-reducing (66 kDa, dimeric) conditions (Figure 13 A and B).

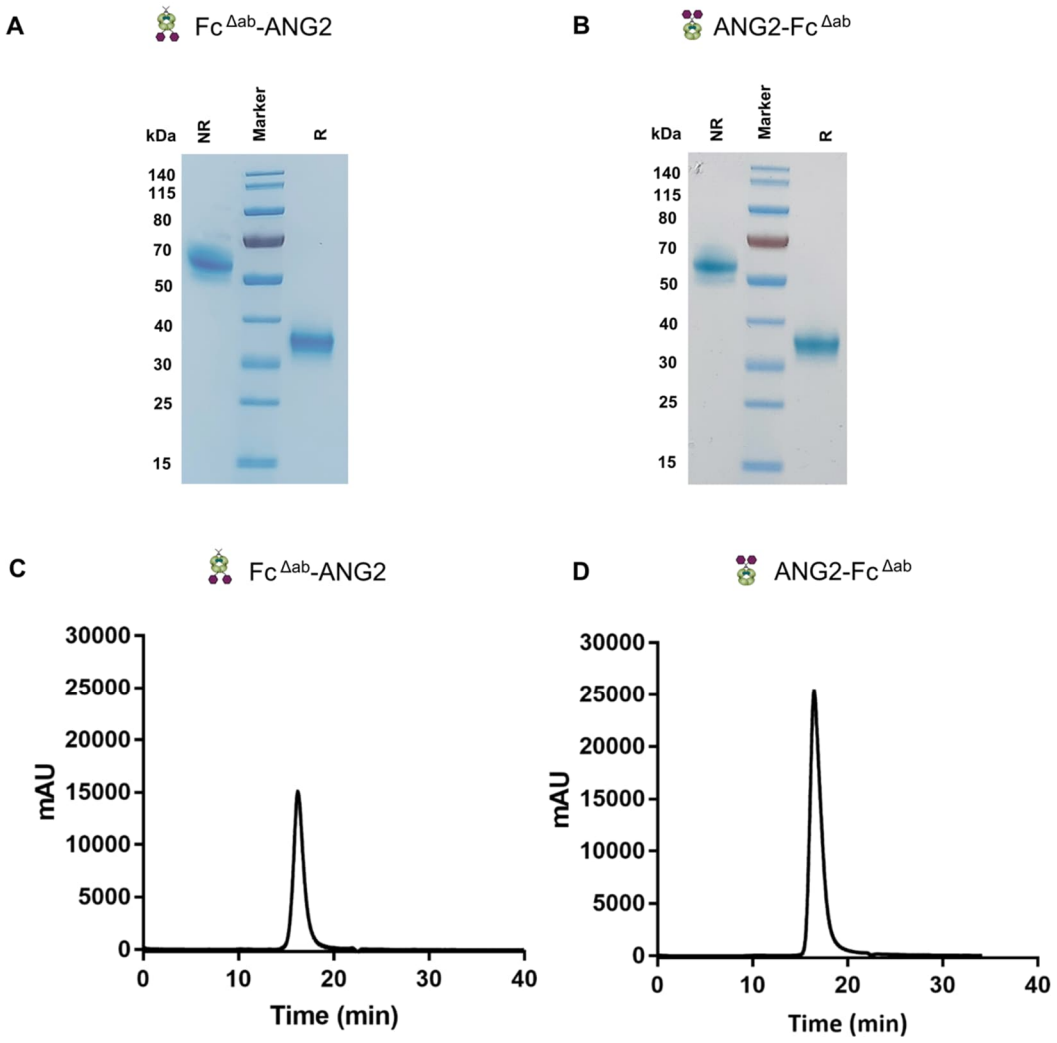

Figure 13: Biochemical characterisation of transcytosis inducing Angiopep-2 fusion proteins. (A) SDS PAGE of indicated constructs was performed with (R) or without the reducing agent (NR) β-mercaptoethanol and stained with coomassie blue. 2 µg of the protein was loaded. **(B)** Size exclusion HPLC chromatogram of indicated constructs with elution time. kDa, molecular weight. mAU, milli absorbance unit.

The $Fc^{\Delta ab}$ part has one N-glycosylation position, therefore, it affected the molecular weight of the molecules. In HPLC, both the proteins eluted as one clear peak with no unexpected aggregates (Figure 13 C and D). Altogether, the biochemical characterisation proved that the ANG2 fusion proteins are pure and intact.

4.1.7 Production, purification and characterisation of soluble TRAIL receptor proteins

To understand the nature of binding, soluble TRAIL receptor proteins were added to this project. The soluble TRAIL receptors were created by fusing the extracellular domain of TRAIL receptor to the human Fc region, to block TRAIL-mediated binding to target cells. The fusion protein was produced in stably transfected HEK293 cells. As it has an Fc region, the fusion protein was purified by protein A affinity chromatography. The fusion proteins were produced with the yield of 18 mg/l of cell supernatant.

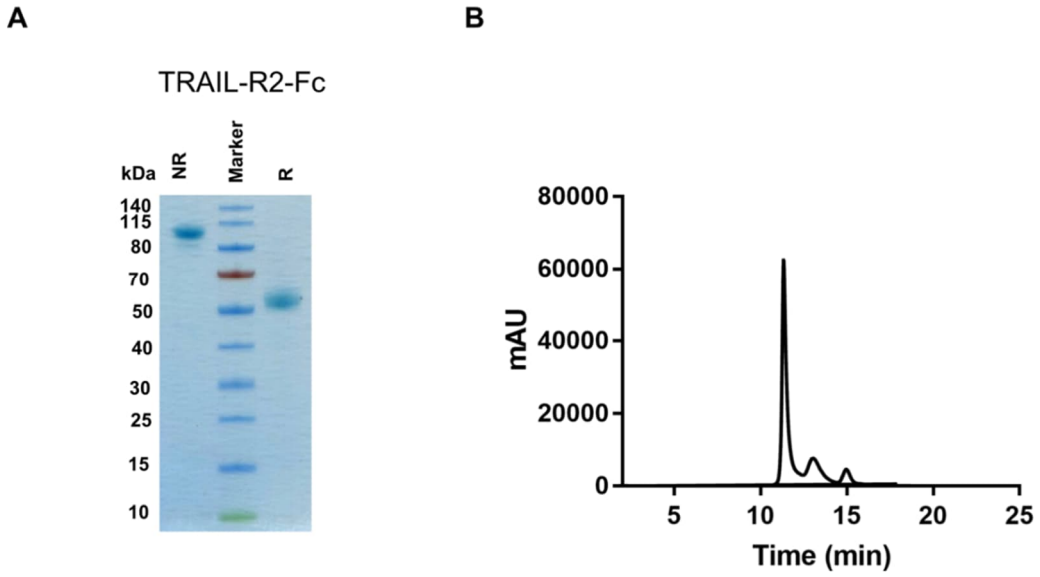

Figure 14: Biochemical characterisation of TRAIL-R2-Fc. (A) SDS PAGE of TRAIL-R2-Fc was performed with (R) or without the reducing agent (NR) β-mercaptoethanol and stained with coomassie blue. 2 µg of the protein was loaded. **(B)** Size exclusion HPLC chromatogram of the construct with elution time. kDa, molecular weight. mAU, milli absorbance unit.

SDS PAGE was performed to determine the purity and integrity of the construct. The protein ran approximately at 105 kDa in non-reducing condition and at 53 kDa under reducing condition, which is higher than the calculated molecular weight of the protein.

It could be due to the N-glycosylation position at the Fc-region of these fusion protein. Under native conditions examined by size exclusion HPLC, TRAIL-R2-Fc eluted as one major peak with a small fraction of aggregates.

The proteins were later checked for their binding ability to TRAIL moieties. For this purpose, 200 ng of TRAIL-R2-Fc were coated on ELISA plates and increasing concentration of Fc-scTRAIL were added to it. As the Fc-scTRAIL fusion protein is FLAG tagged, the bound molecules were detected with anti-FLAG-HRP. Figure 15 indicates the binding of TRAIL-R2-Fc to TRAIL subunits. Therefore, the produced soluble TRAIL-R2-Fc fusion protein is functional.

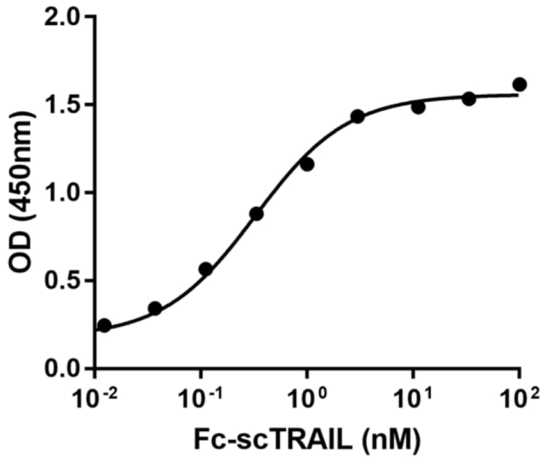

Figure 15: Binding of TRAIL-R2-Fc to TRAIL moiety in Fc-scTRAIL fusion protein through ELISA. TRAIL-R2-Fc (200 ng/well) was coated and the binding was tested by adding increasing concentration of Fc-scTRAIL. Bound molecules were detected with an anti-FLAG-HRP. OD (450nm), OD of sample measured at 450 nm divided by OD of coating control. Data shown as a representative of one experiment.

Since the binding of produced soluble TRAIL-R2-Fc was proven by ELISA, they could be used later in this thesis for binding and transport studies, which helps in understanding the contribution of ANG2 in binding to the BBB cells.

In later immunostaining studies, TRAIL-R2-mFc^{LALA} was used to prevent non-specific signal from anti-human Fc-based detection and engagement of Fc-receptors. The TRAIL-R2-mFc^{LALA} was cloned using the extracellular domain of human TRAIL-R2 and fused with the primers to a murine Fc part containing the PGLALA-mutation vector. The fusion protein was produced in stably transfected HEK293 cells and was purified by protein A affinity chromatography. The protein ran approximately at 95 kDa in non-

reducing condition and at 55 kDa under reducing condition, which is higher than the calculated molecular weight of the protein. It could be due to the N-glycosylation position at the Fc-region of these fusion proteins.

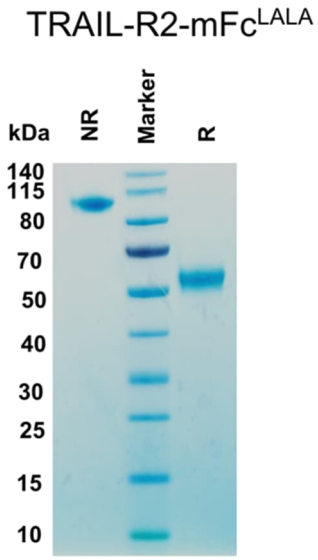

Figure 16: Biochemical characterisation of TRAIL-R2- mFc^{LALA} . SDS PAGE of TRAIL-R2-mFc^{LALA} was performed with (R) or without the reducing agent (NR) β-mercaptoethanol and stained with coomassie blue. 2 µg of the protein was loaded.

Overall, in this part of the thesis, apoptosis and transport inducing TRAIL fusion proteins, ANG2 positive controls and TRAIL blocking peptides have been successfully produced and purified for later apoptosis and transport studies.

Summary of the constructs and their functions:

Constructs	Moieties	Functions
scTRAIL-Fc-ANG2 scTRAIL-ANG2	scTRAIL, Fc, ANG2	Apoptosis and transcytosis
Fc$^{\Delta ab}$-ANG2 ANG2-Fc$^{\Delta ab}$	Fc$^{\Delta ab}$ (Fc moiety lacking FcγRs receptor binding), ANG2	Transcytosis
TRAIL-R2-Fc	TRAIL-R2, Fc	TRAIL blocking
TRAIL-R2-mFc^{LALA}	TRAIL-R2, mFc^{LALA} (mouse Fc with reduced binding to FcγRs)	TRAIL blocking

4.2 Responsiveness of cancer cells to TRAIL treatment

4.2.1 Fusion of ANG2 to hexavalent TRAIL maintains its potency in inducing apoptosis in cancer cells

In the previous section 4.1.3, it was demonstrated that CNS-targeted TRAIL fusion proteins are able to reduce cell viability as shown by a crystal violet assay. To analyse apoptosis induction itself, the cells were treated with TRAIL constructs and stained for Annexin V-PI to identify apoptotic cells. HCT116 cells are positive controls whereas A172 cells are cells of interest in GBM therapy design. Therefore, in this part, the cell death induction was validated on A172 cells by Annexin V-PI assay.

The glioblastoma cell line A172 was treated with increasing concentrations of scTRAIL-Fc-ANG2, scTRAIL-ANG2 and Fc-scTRAIL for 24 h and were stained for Annexin V-GFP and PI. Annexin V is an intracellular protein that has high affinity for phosphatidylserine (PS), which is present on the cytoplasmic surface of the plasma membrane. During apoptosis, PS translocates to the extracellular side of the plasma membrane and there can be detected by fluorescently labelled Annexin V (Annexin V-GFP). To distinguish between dead and alive cells, Propidium Iodide (PI), that crosses the membrane and binds between the bases of the DNA and RNA of dead cells, was used. The gating for the analysis was performed as shown in Figure 17, lower left quadrant, Q4, showing alive cells (AnV- PI-), the lower right, Q3, indicating early apoptotic cells (AnV+ PI-), the upper right, Q2, indicating late apoptotic cells (AnV+ PI+) and the upper left, Q1, showing other dead cells (AnV- PI+). In the untreated condition, 97% of the A172 cell population stayed in the lower left Annexin V-GFP$^-$ PI$^-$ (Q4) quadrant, indicating that the cells are alive. Upon treatment with 0.1 nM of Fc-scTRAIL and scTRAIL-Fc-ANG2, the cell population shifted to either early (Annexin V-GFP$^+$ PI$^-$) or late apoptosis (Annexin V-GFP$^+$ PI$^+$) quadrant.

A strong response of cells to both hexavalent TRAIL constructs scTRAIL-Fc-ANG2 and Fc-scTRAIL in a dose-dependent manner was observed (Figure 17). Moreover, the EC_{50} values of Fc-scTRAIL (0.15 nM) and scTRAIL-Fc-ANG2 (0.11 nM) stayed in a similar range. Similar to the crystal violet assay in Figure 10, the treatment with 0.2 nM trivalent scTRAIL-ANG2 did not induce significant cell death and most of the cell

population stayed in Annexin V-GFP$^-$ PI$^-$ (Q4) quadrant. The overall cell death analysis experiment demonstrated that the addition of ANG2 did not affect the TRAIL potency and the hexavalent TRAIL induced robust apoptosis in GBM cells.

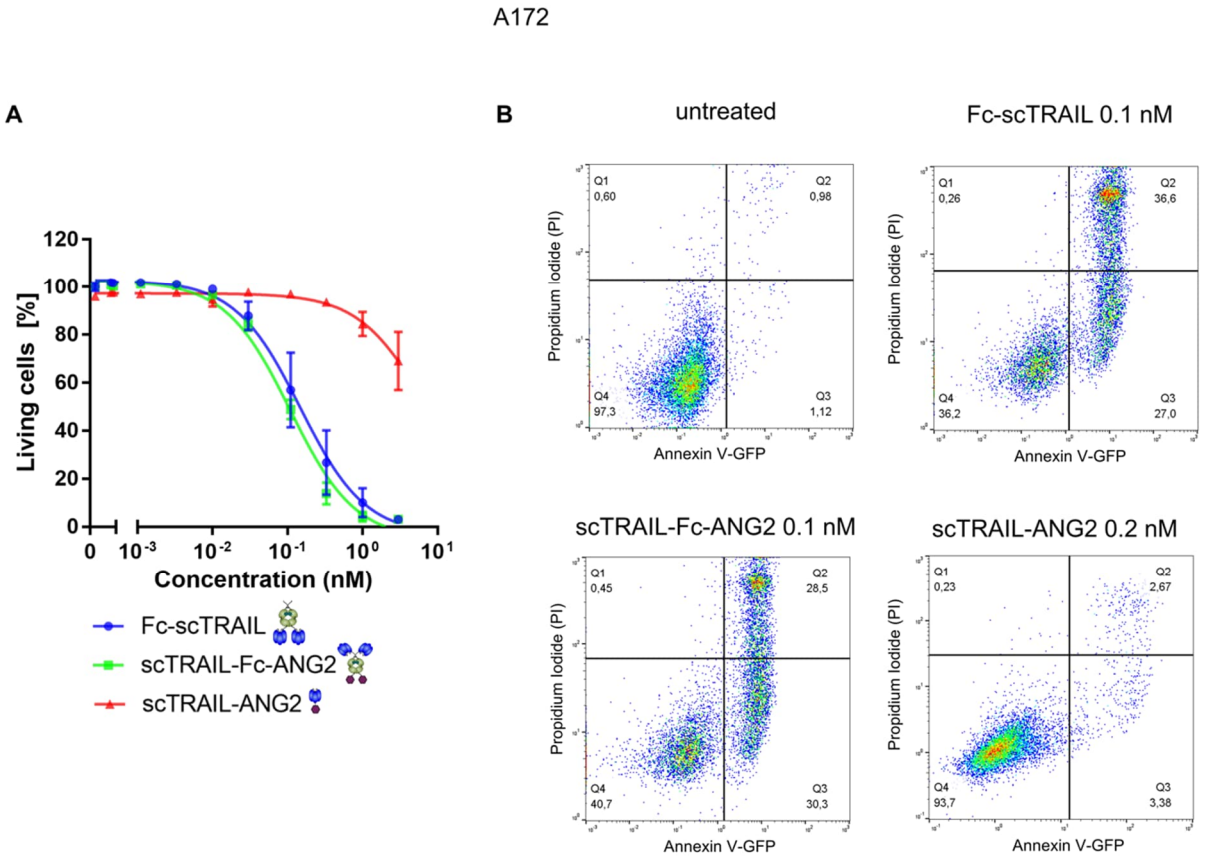

Figure 17: ANG2 fusion does not affect the hexavalent TRAIL potency against cancer cells. (A) A172 glioblastoma cells were treated with varying concentrations of indicated construct for 24 h and viable cells were determined by Annexin V-PI negativity using flow cytometry. Equimolar amounts of the TRAIL trimer were added i.e., 0.1 nM hexavalent scTRAIL-Fc-ANG2 or 0.2 nM trivalent scTRAIL-ANG2. Data are shown as mean ± SEM from three independent experiments. **(B)** The quadrant Q4 - alive cells (Annexin V-GFP$^-$ PI$^-$), Q3 - early apoptotic cells (Annexin V-GFP$^+$ PI$^-$), Q2 - late apoptotic cells (Annexin V-GFP$^+$ PI$^+$), Q1 - other dead cells (Annexin V-GFP$^-$ PI$^+$). Data shown is a representative of three independent experiments.

4.2.2 Hexavalent TRAIL induces the processing of pro-caspase 8, pro-caspase 3 and PARP in A172 and HCT116 cells

TRAIL is known to induce apoptosis by a very well-defined signalling cascade. Therefore, to confirm the TRAIL-mediated apoptosis induction, caspase cascade signalling was analysed using western blotting. TRAIL sensitive HCT116 cells and

A172 Glioblastoma cells were stimulated with equimolar amounts of the TRAIL trimer i.e., 1 nM hexavalent scTRAIL-Fc-ANG2 or 2 nM trivalent scTRAIL-ANG2, for 6h with or without the pre-incubation of QVD. After 6 h the cells were lysed and detected for procaspase 8, cleaved caspase 8 (p18), procaspase 3, cleaved caspase 3 (p21/p19/p17), poly-[ADP]-ribose polymerase (PARP) and cleaved PARP (cPARP)

Following TRAIL binding, the oligomerised TRAIL receptors cluster together and form the DISC complex for the recruitment and activation of procaspase 8. Within the DISC, procaspase 8 monomers dimerise and are activated by auto catalytic cleavage to produce fully processed and cleavage intermediates by a two-step mechanism (Medema et al., 1997; Scaffidi et al., 1997). As shown in Figure 18, upon treatment with hexavalent TRAIL (scTRAIL-Fc-ANG2), robust processing of procaspase 8 was observed in both the cell lines. Particularly, strong reduction of procaspase 8 signal and increase in cleaved caspase fragments (p41/p43 and p18) was detected. As expected from the lower level of cell death induction from the previous Annexin V-PI cell death assay, only minor processing of procaspase 8 was observed with the trivalent scTRAIL-ANG2. Fully processed caspase 8 is the main mediator of downstream apoptosis signalling. The activated caspase 8 activates downstream effector caspase 3 or caspase 7, either by direct cleavage or via the Bid-MOMP-caspase 9 axis, to induce apoptosis. It can be seen in Figure 18 that the hexavalent TRAIL induced the procaspase 3 processing into its cleaved fragments p21/p19/p17 with a strong reduction in its pro-form, whereas the trivalent TRAIL induced only mild processing. The lysates were also probed for PARP, an enzyme involved in DNA repair mechanism and an established substrate for caspase 3 (Satoh & Lindahl, 1992; Simbulan-Rosenthal et al., 1999). The hexavalent TRAIL treatment resulted in reduction of full-length PARP (113 kDa) and processing into its cleaved form p89. Furthermore, the processing of the caspases and PARP was inhibited by the pan-caspase inhibitor Q-VD-Oph in A172 and HCT116 cells. This demonstrated that the enhanced clustering from hexavalent TRAIL-receptor agonists led to stronger apoptosis signalling as seen from Figure 18 and that is the reason for stronger apoptosis induction.

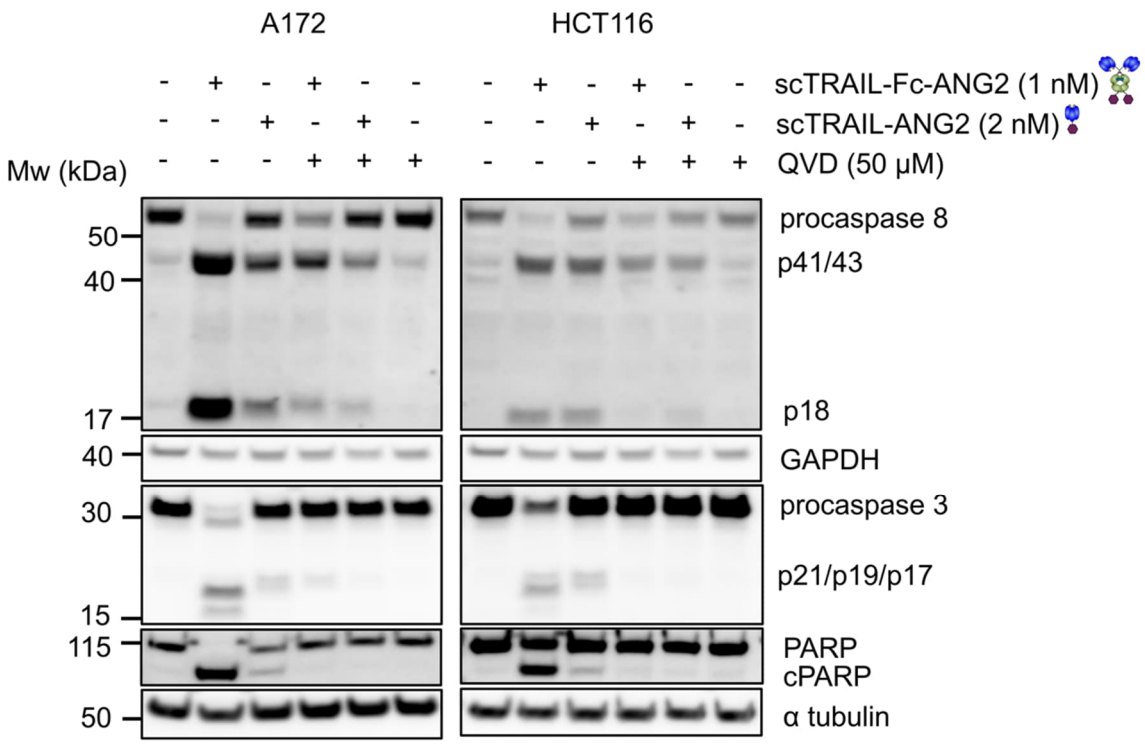

Figure 18: Hexavalent TRAIL treatment leads to caspase 8 and 3 processing: A172 and HCT116 cells were treated with 1 nM of scTRAIL-Fc-ANG2 or 2 nM of scTRAIL-ANG2 for 6 h with or without 50 µM QVD and blotted for procaspase 8, cleaved caspase 8 (p18), procaspase 3, cleaved caspase 3 (p21/p19/p17), PARP and cleaved PARP (cPARP). GAPDH and α tubulin served as loading controls. Representative western blots from two independent experiments are shown. Mw, molecular weight. KDa, kilodalton.

4.3 Blood brain barrier cells are resistant to TRAIL treatment

In the previous section, it was shown that TRAIL can induce apoptosis in cancer cells, in particular, GBM cells. In this section, experiments were performed to examine if TRAIL treatment affects BBB endothelial cells.

4.3.1 hCMEC/D3 cell express less surface TRAIL receptors: TRAIL-R1 and TRAIL-R2 than HCT116 and HeLa cells

TRAIL induces apoptosis by engaging with TRAIL-R1 and TRAIL-R2 on the cell surface. Besides TRAIL-R1 and TRAIL-R2, TRAIL can also bind to the decoy receptors TRAIL-R3 (DcR1) and TRAIL-R4 (DcR2), but this does not lead to activation of the

apoptosis pathway. Therefore, the number of surface TRAIL receptors TRAIL-R1, TRAIL-R2, TRAIL-R3 and TRAIL-R4 were quantified and were compared to TRAIL-sensitive HCT116 and HeLa cells. The QIFIKIT, consisting of a series of five population of calibration beads each with a pre-defined number of receptors, was used to quantitatively determine the number of cell surface receptors.

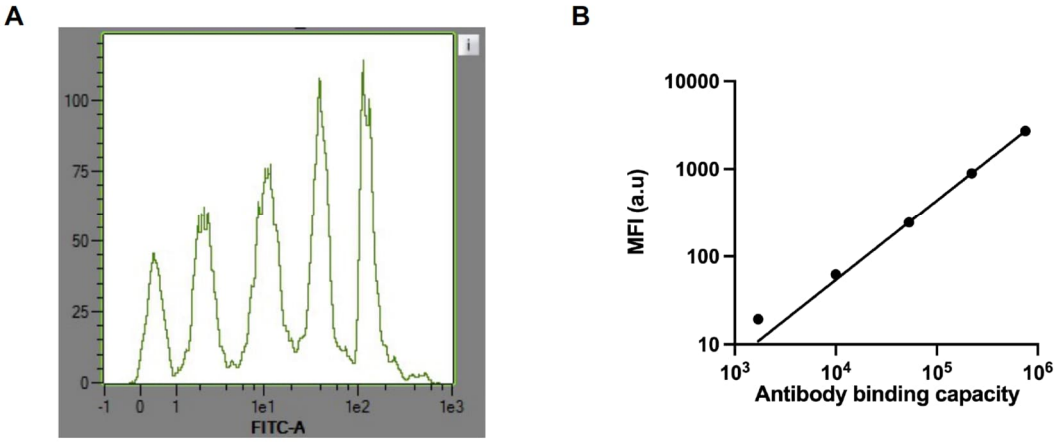

Figure 19: Histogram of QIFIKIT calibration beads and calibration curve. (A) The histogram of five peaks obtained from the calibration beads from the provider **(B)** The calibration curve was generated by plotting the number of receptors against the obtained FITC signal. MFI, Mean Fluorescence Intensity. a.u, arbitrary unit.

The number of receptors on each bead ranges from 1700 to 723 000. With the utilisation of these beads, a calibration curve was generated by plotting the fluorescence intensity of the beads against their specified number of receptors. Then, the number of receptors on the cell surface was determined by interpolation. In hCMEC/D3 cells, a strong reduction in TRAIL-R1 was observed compared to HCT116 and HeLa cells, whereas significantly lower expression of TRAIL-R2 was observed compared to HCT116 cells. Importantly, these two receptors are the key mediators of downstream apoptosis signalling in response to TRAIL (G. Pan, Ni, et al., 1997; G. Pan, O'Rourke, et al., 1997; Walczak, 1997). The decoy receptor, TRAIL-R3, was expressed at low levels in all cell lines. There was a marginal decrease in TRAIL-R4 expression in hCMEC/D3 and HeLa cells compared to HCT116 cells (Figure 20A). As for later drug transport studies hCMEC/D3 cells will be cultured on a transwell system, TRAIL receptor expression was also analysed in hCMEC/D3 cells grown in this setup. The cells were grown in a transwell for approximately 7 days and checked for their transendothelial electrical resistance (TEER) every day. Once the cells reached stable

TEER value for 3 days, the setup was used for further experiments. Therefore, to check if the different growing conditions will have an impact TRAIL receptor expression, the cells from a T75 flask and the transwell system were collected and probed for the TRAIL receptors. No significant differences were observed in TRAIL receptor expression, demonstrating that the TRAIL receptor expression in hCMEC/D3 cells is not altered by different growing conditions as shown in Figure 20B. Taken together, hCMEC/D3 cells have low numbers of TRAIL-R1 and TRAIL-R2 available for binding and so they could be resistant or less able to activate TRAIL-mediated apoptosis than HCT116 or HeLa cells.

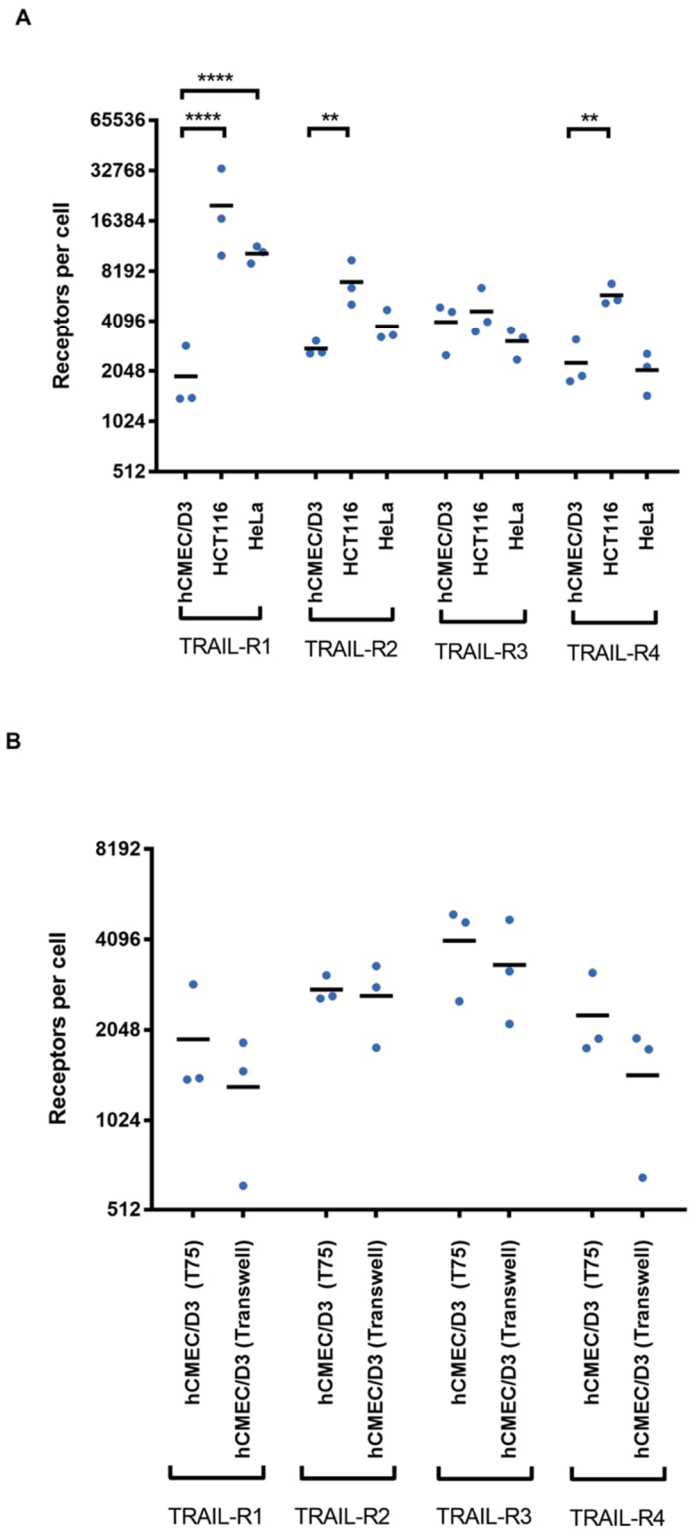

Figure 20: hCMEC/D3 cells express less TRAIL-R1 and TRAIL-R2. (A) Surface expression of TRAIL-R1, TRAIL-R2, TRAIL-R3, TRAIL-R4 receptors in hCMEC/D3, HCT116 and HeLa. **(B)** hCMEC/D3 (T75 and transwell) cells were quantified by the QIFIKIT and flow cytometry. The mean ± SD of three independent experiments is shown here. Statistical significance was tested by Tukey's two-way ANOVA: **** =p<0.0001, **=p<0.01 on log-transformed receptor values.

4.3.2 Hexavalent TRAIL does not induce efficient cell death in hCMEC/D3 and bEnd.3 cells

It was shown in the previous section that the blood-brain barrier cells express less amount of TRAIL receptors compared to cancer cells. Since reduced expression of TRAIL receptors does not prove the resistance of hCMEC/D3 cells to TRAIL treatment, apoptosis induction was analysed by Annexin V-GFP PI. The cells were treated with increasing concentrations of scTRAIL-Fc-ANG2, scTRAIL-ANG2 and Fc-scTRAIL for 24 h and were stained for Annexin V-GFP and PI as shown in section 4.2.1.

The gating was performed as shown in Figure 21B. In the untreated condition, 96% of the cell population stayed in the lower left Annexin V-GFP$^-$ PI$^-$ (Q4) quadrant, demonstrating that the cells are alive. However, upon treatment with 0.1 nM Fc-scTRAIL, scTRAIL-Fc-ANG2 and 0.2 nM of scTRAIL-ANG2 the cell population stayed in the same lower left quadrant and remain unaffected. This demonstrates that the hCMEC\D3 cells are resistant to TRAIL treatment. As expected, the maximum cell death of approximately 20% was achieved with only higher concentration (3 nM) of hexavalent constructs, which is 30 times more than the EC_{50} concentration required for A172 and HCT116 cells. Therefore, the flow cytometry analysis indicates that the hCMEC/D3 cells are resistant to TRAIL treatment.

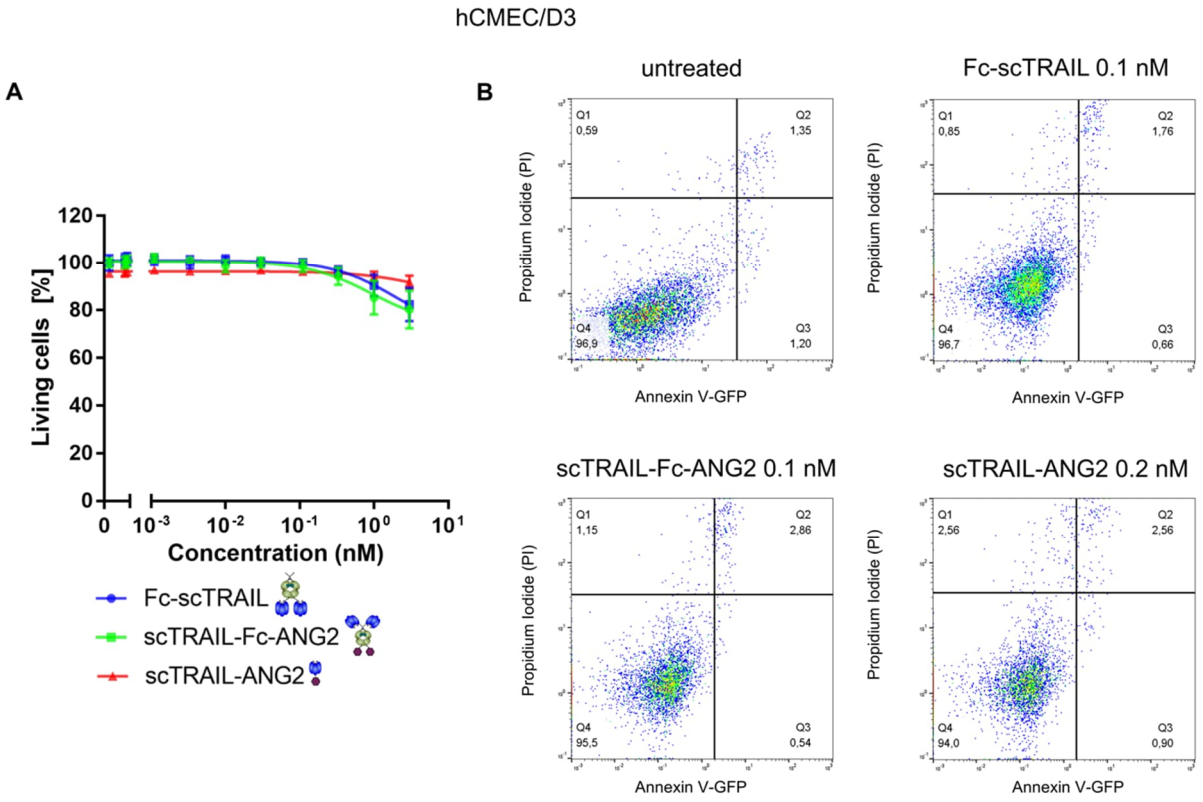

Figure 21: hCMEC/D3 cells are non-responsive to TRAIL treatment. (A) hCMEC/D3 cells were treated with varying concentrations of indicated construct for 24 h and viable cells were determined by Annexin V-PI negativity using flow cytometry. Equimolar amounts of the TRAIL trimer were added i.e., 0.1 nM hexavalent scTRAIL-Fc-ANG2 or 0.2 nM trivalent scTRAIL-ANG2. Data are shown as mean ± SEM from three independent experiments. **(B)** The quadrant Q4 - alive cells (Annexin V-GFP$^-$ PI$^-$), Q3 - early apoptotic cells (Annexin V-GFP$^+$ PI$^-$), Q2 - late apoptotic cells (Annexin V-GFP$^+$ PI$^+$), Q1 - other dead cells (Annexin V-GFP$^-$ PI$^+$). Data shown is a representative of three independent experiments.

In previous ANG2 transport studies, bovine cells and mice were used, not human (Demeule, Régina, et al., 2008; Demeule, Currie, et al., 2008). Therefore, in this project, an additional blood-brain barrier cell line, a mouse cell line, bEnd.3, was utilised. They were also tested for the responsiveness to the TRAIL treatment. Due to their strong adherent nature to the cell culture plate, they required aggressive trypsinisation for detachment leading to some loss of cell membrane integrity. Therefore, to analyse cell viability in the absence of trypsinisation, an MTT assay was performed. The bEnd.3 cells were treated with increasing concentrations of scTRAIL-Fc-ANG2, scTRAIL-ANG2 and Fc-scTRAIL for 24 h and the cells were incubated with MTT (3-(4,5-dimethylthiazol-2-yl)-2,5-diphenyltetrazolium bromide) for 4 h.

Unlike Annexin V/PI, this assay determines the cell viability and not cell death. In this assay, NAD(P)H-dependent oxidoreductase enzymes in the viable cells reduces MTT

to formazan crystals and the absorbance is measured at a wavelength of 570 nm. The cell viability was measured and the treated cells were normalised to untreated control cells. Figure 22A shows that the cells are very resistant even to the highest concentration of the TRAIL fusion proteins. This is in agreement with the previous studies that the non-cancerous cells are resistant to TRAIL-mediated apoptosis (Ashkenazi et al., 1999; Walczak et al., 1999).

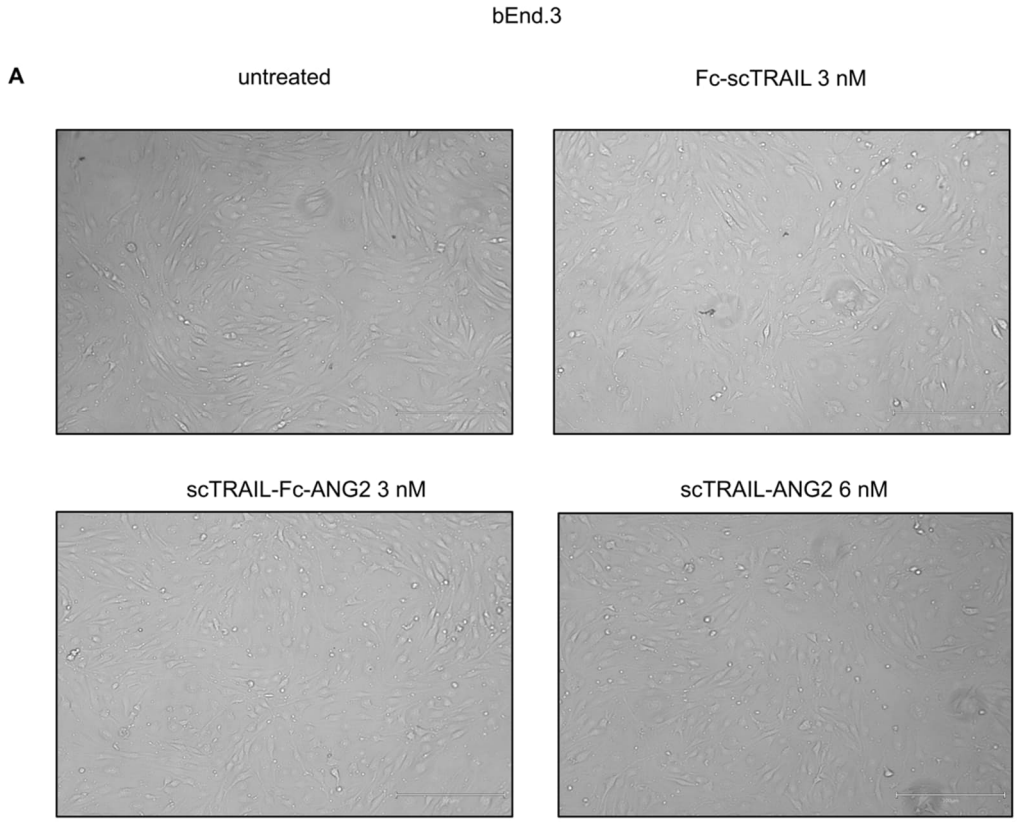

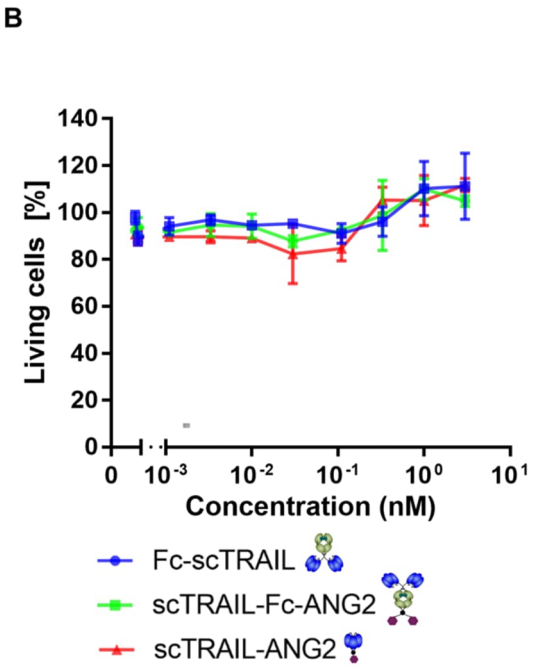

Figure 22: bEnd.3 cells are resistant to TRAIL treatment determined by MTT assay. bEnd.3 cells were treated with indicated construct for 24 h. Equimolar amounts of the TRAIL trimer were added i.e., 3 nM hexavalent scTRAIL-Fc-ANG2, 3 nM hexavalent Fc-scTRAIL or 6 nM trivalent scTRAIL-ANG2. **(A)** Representative images obtained from EVOS microscope. Scale bar 300 µm **(B)** Viable cells were determined by MTT assay. Data are shown as mean ± range from two independent experiments.

4.3.3 Only high concentration of TRAIL treatment induces processing of key apoptotic proteins in hCMEC/D3 cells

The caspase cascade signalling pathway was next analysed in hCMEC/D3 and bEnd.3 cells for responses to hexavalent TRAIL. The cells were treated with a low (0.1 nM) and a high (4 nM) concentration of Fc-scTRAIL for 6 h and then probed for caspase-3, caspase-8 and poly-[ADP]-ribose polymerase (PARP).

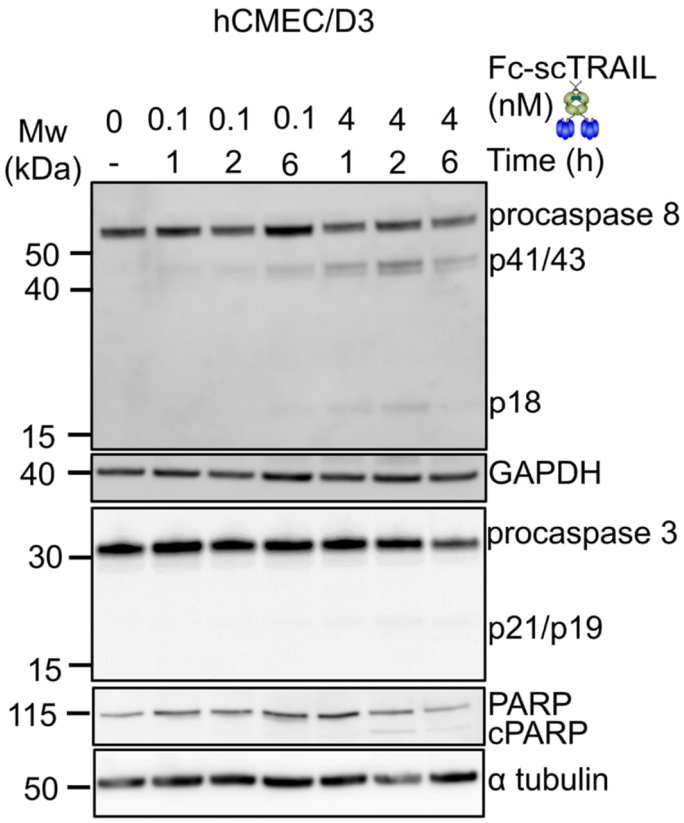

Figure 23: Treatment with high concentration of hexavalent TRAIL leads to the processing of key apoptotic proteins. hCMEC/D3 were treated with the indicated concentration of Fc-scTRAIL 1, 2 or 6 hours and then analysed for procaspase 8, cleaved caspase 8 (p18), procaspase 3 and cleaved caspase 3 (p21/p19/p17) by western blotting. GAPDH and α tubulin served as loading controls. Representative image from two independently experiments are shown. Mw, molecular weight. KDa, kilodalton.

Figure 23 shows that in the hCMEC/D3 cells treated with a low concentration of hexavalent Fc-scTRAIL, the intermediate caspase 8 fragment, p41/43 appeared after 2 h. However, p18 fragment was barely detectable at this concentration. Upon treatment with higher concentration, strong detection of p41/p43 fragments was observed, which correlated with low processing to p18 fragment. The p18 fragment at 6 h in the last lane was lost, this could be due to the instability of cleaved small fragments. Similar to caspase 8, caspase 3 processing was not observed at the lower concentration. However, at high concentration, a time-dependent reduction of procaspase-3 was seen, but the accumulation of p21/p19 fragments appeared to be very minimal. Cleavage of PARP was only observed at later time point with the high concentration. Therefore, as expected, even at the higher concentration of Fc-scTRAIL only residual accumulation of cleaved subunits was observed in hCMEC/D3 cells.

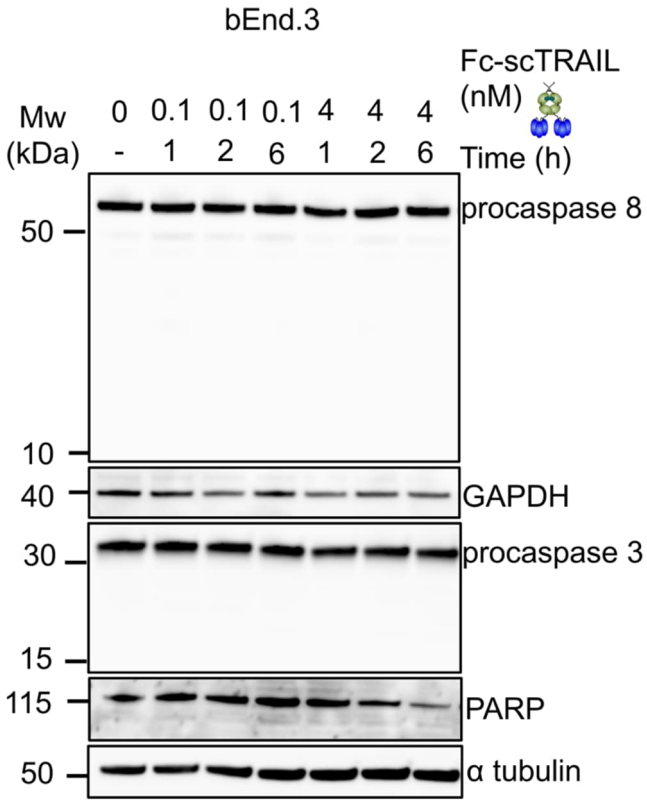

Figure 24: bEnd.3 cells are extremely resistant even at high concentration of hexavalent TRAIL. bEnd.3 cells were treated with the indicated concentration of Fc-scTRAIL 1, 2 or 6 hours and then analysed for procaspase 8, cleaved caspase 8 (p10), procaspase 3 and cleaved caspase 3 (p19/p17) by western blotting. GAPDH and α tubulin served as loading controls. Mw, molecular weight. KDa, kilodalton. Representative image from two independently experiments are shown.

Similar to MTT assay results, the bEnd.3 cells were non-responsive to hexavalent TRAIL treatment. Probing for key apoptotic proteins through western blot showed no evidence of processing of them as shown in Figure 24. Unlike the caspase detection in TRAIL induced hCMEC/D3 cells, the intermediate caspase fragments in bEnd.3 cells were not detectable due to the lack of detection antibodies specific for mouse. Although intermediate fragments could not be detected, no notable decline in full length was observed suggesting that the processing is overall minimal in these cells. Altogether, the data from Annexin V-PI, MTT and western blot demonstrate that blood brain barrier cells are resistant to TRAIL treatment, which corresponds to their low expression of the death receptors TRAIL-R1 and TRAIL-R2.

4.4 Investigating the binding of TRAIL-ANG2 fusion proteins to blood-brain barrier cells

4.4.1 Detection of Lrp1 receptor expression through flow cytometry, western blot and immunostaining

As it was shown in section 4.3.1 that the TRAIL receptors are expressed at low level at blood-brain barrier cells, in this section, the expression of the ANG2-target receptor Lrp1 on human and mouse BBB cells was determined. Initially, the Lrp1 expression was determined with QIFIKIT as shown in (Figure 25). For that, the hCMEC/D3 cells grown in T75 flask were collected and stained for Lrp1 antibody. Surprisingly, Lrp1 expression was not detectable above isotype control levels in these cells as seen in Figure 25A. Therefore, western blot was performed with hCMEC/D3, bEnd.3 and mouse embryonic fibroblast (MEF) cells.

As shown in Figure 25B, the hCMEC/D3 cells express very low levels of Lrp1. Altogether, western blot analysis and flow cytometry measurements demonstrated that hCMEC/D3 cells express very low levels of Lrp1 compared to the known Lrp1-expressing mouse embryonic fibroblasts (MEFs) (Storck et al. 2016) or bEnd.3 cells. Additionally, immunostaining was performed on bEnd.3 cells for Lrp1 expression and the expression was spatially distributed in the perinuclear region in line with previous studies (Figure 25C) (Tian et al., 2020).

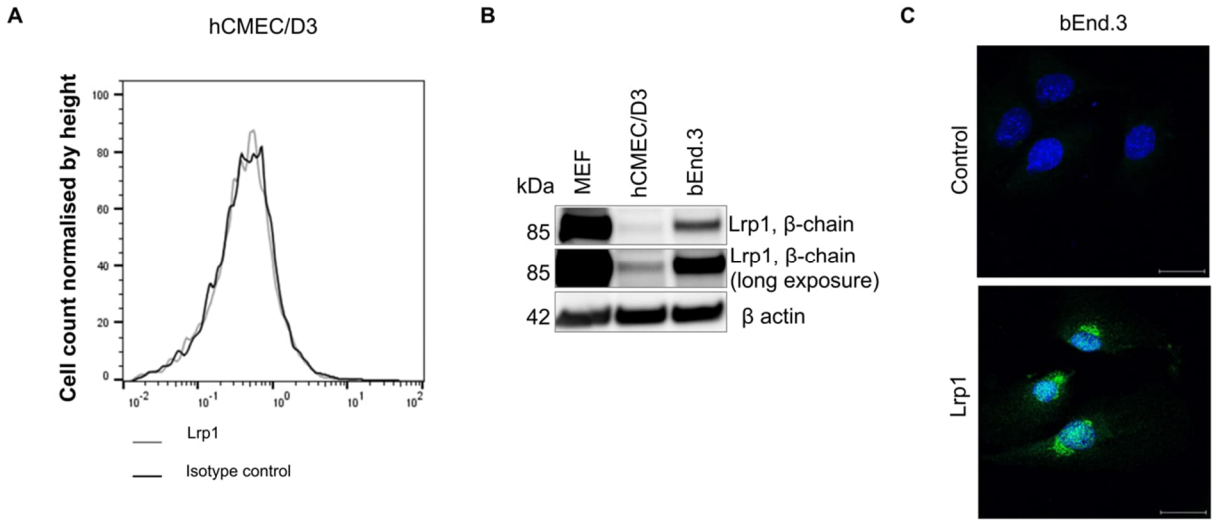

Figure 25: Lrp1 expression characterisation by flow cytometry, western blot and immunostaining. (A) The surface expression of Lrp1 in hCMEC/D3 cells as quantified by the QIFIKIT and flow cytometry. **(B)** Lysates of MEF, hCMEC/D3 and bEnd.3 were analysed for the expression of Lrp1 receptors by western blot analysis. β actin served as a loading control. Western blot was performed once **(C)** Immunofluorescence staining of Lrp1 on bEnd.3 cells, nuclei were stained in blue with Hoechst. Scale bar 20 µm.

4.4.2 Dose-dependent binding of the fusion proteins to blood-brain barrier cells

Given that blood-brain barrier cells express TRAIL-receptors, albeit at low levels, the binding of the TRAIL-ANG2 fusion proteins to the blood brain barrier cells was analysed. Initially, the hCMEC/D3 cells were incubated with Fc-scTRAIL or scTRAIL-Fc-ANG2 or scTRAIL-ANG2 for 2 h. The fusion proteins can bind to the surface receptors on the cells and internalise at 37ºC, therefore, to prevent the internalisation the binding assay was performed at 4ºC. All the fusion proteins used here were FLAG tagged and were detected with anti-FLAG-PE antibody. Figure 26A shows that the constructs were able to bind to the cells in a dose-dependent manner. Importantly, Fc-scTRAIL and scTRAIL-ANG2 fusion proteins were binding better to the cells than the hexavalent scTRAIL-Fc-ANG2, even though, scTRAIL-Fc-ANG2 was expected to bind better because of its bivalent ANG2 moiety. Figure 26B shows that the peaks shifted from right to left with increasing concentration. Despite the lack of TRAIL receptors in hCMEC/D3 cells, dose-dependent binding of the constructs to the cells was observed suggesting that the constructs were binding via TRAIL.

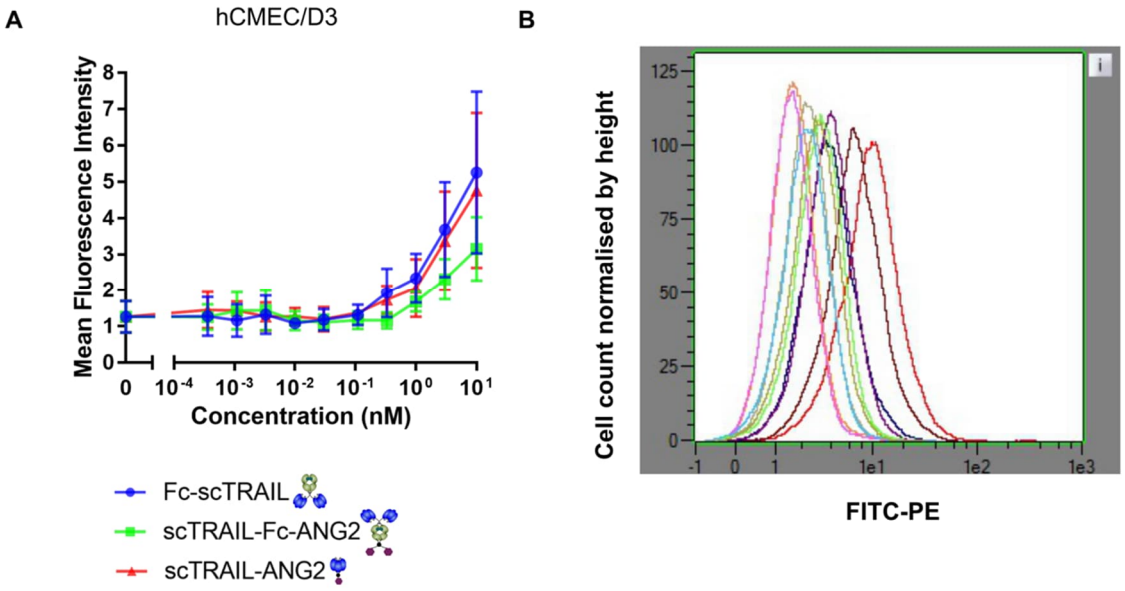

Figure 26: The fusion proteins bind to the hCMEC/D3 cells in a dose-dependent manner. (A) hCMEC/D3 cells were incubated with indicated constructs for 1 h and then binding of fusion proteins was detected by anti-FLAG-PE. Data are shown as mean ± SEM from three independent experiments. **(B)** The binding to the cells is showed as histogram. Pink indicates the lowest concentration and red indicates the highest concentration. Histogram of representative of three independent experiments.

4.4.3 Binding of TRAIL-ANG2 fusion proteins to the blood-brain barrier cells is TRAIL-mediated

Due to the high expression of Lrp1 receptors in bEnd.3 cells, subsequent binding and transport studies were conducted in bEnd.3 cells. The bEnd.3 cells were collected and incubated in a 96-well plate with increasing concentration of Fc-scTRAIL or scTRAIL-Fc-ANG2 or scTRAIL-ANG2 for 2 h. Similar to hCMEC/D3 cells, dose-dependent binding of fusion proteins to the cells was observed. However, the binding of Fc-scTRAIL that lacks an Angiopep-2 moiety was higher in comparison to scTRAIL-Fc-ANG2 and scTRAIL-ANG2. Although, BBB cells express lower amount of TRAIL receptors, it could be that the TRAIL moiety can also bind to TRAIL receptors on these cells. Therefore, TRAIL blocking studies were performed with soluble TRAIL receptors.

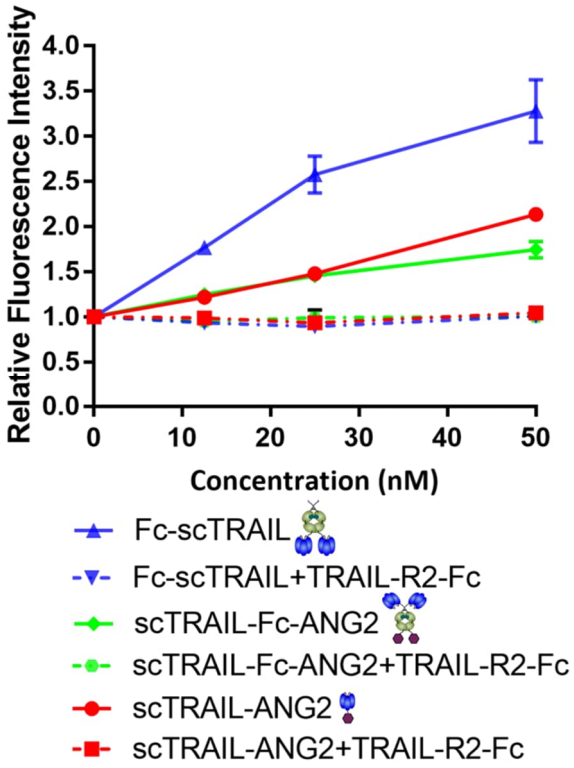

Figure 27: Binding of TRAIL-ANG2 fusion proteins to bEnd.3 cells is TRAIL-mediated. bEnd.3 cells were incubated with Fc-scTRAIL, scTRAIL-Fc-ANG2 and scTRAIL-ANG2 constructs for 1 h with or without the presence of 100-fold molar excess of TRAL-R2-Fc soluble receptor. The binding of fusion proteins was determined by anti-FLAG-PE. Data are shown as mean ± SEM from three independent experiments.

For the blocking study, 50 nM, 25 nM and 12.5 nM of Fc-scTRAIL, scTRAIL-Fc-ANG2 and scTRAIL-ANG2 fusion proteins were incubated with 100-fold molar excess of TRAIL-R2-Fc for 30 min. Then the mixture of TRAIL fusion protein and TRAIL-R2-Fc soluble receptors was added to the cells and incubated for 2 h on ice. The binding was detected with FLAG-PE antibody. Figure 27 shows that the dose-dependent binding of the fusion proteins to bEnd.3 cells, however, the binding was strongly inhibited when blocking TRAIL.

To verify further, two positive control peptides, FLAG-ANG2 and FITC-ANG2 were introduced. The peptides were purchased from Peptides & Elephants (Brandenburg, Germany). Given the reported low affinity (313 nM) of ANG2 for Lrp1 (Bertrand et al., 2010), it is reasoned that ANG2-binding to the cells at 4ºC may be too low for specific robust detection of surface binding. Indeed, as expected, the binding of various ANG2 positive controls proteins, FLAG-ANG2, FITC-ANG2 or FITC-scrambled ANG2 (FITC-scrANG2) to bEnd.3 cells at 4ºC was not detectable (Figure 28).

Moreover, binding of FITC-ANG2 was not increased compared to scrambled control, suggesting the signal was predominantly due to non-specific interaction with the FITC-label. Therefore, in this section, it could not be demonstrated that ANG2 was functional by flow cytometry at + 4 degrees.

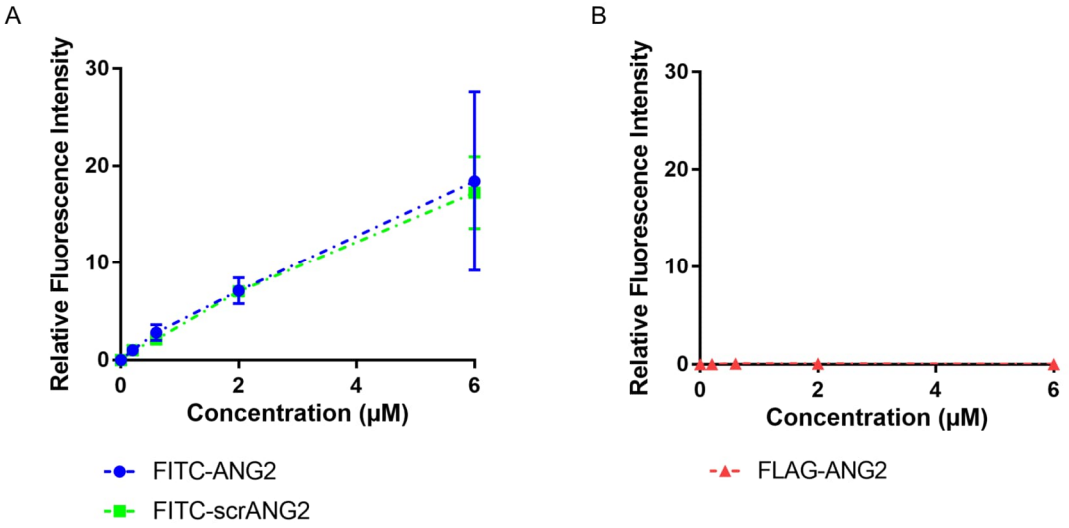

Figure 28: Binding of positive control peptides to bEnd.3 cells in flow cytometry. bEnd.3 cells were incubated with **(A)** FITC-labelled ANG2, scrambled ANG2 (scrANG2) or **(B)** FLAG-tagged ANG2. Data points are mean ± SEM of three independent experiments.

4.5 Examining the binding and transcytotic efficiency of ANG-2 in the presence and absence of TRAIL

4.5.1 Successful binding of ANG2 control peptides to the blood-brain barrier cells

As binding of ANG2 was not observed at 4 ºC, immunostaining-based analysis was utilised where one could observe both cell surface binding and uptake of constructs at 37ºC. Immunostaining was performed to verify the binding of ANG2 fusion proteins to bEnd.3 cells. The cells were incubated with 50 nM of $Fc^{\Delta ab}$-ANG2, ANG2-$Fc^{\Delta ab}$ for 15 min or 30 min. After incubation of the constructs, the cells were fixed, stained and imaged with confocal microscope. In comparison to the control condition, a specific signal was observed from positive control proteins $Fc^{\Delta ab}$-ANG2 and ANG2-$Fc^{\Delta ab}$ after 15 min or 30 min incubation (Figure 29A). The cells were segmented and puncta under the cell mask were counted (Figure 29B). Notably, binding was independent of whether ANG2 was fused to the N- or C-terminus of the protein. The number of puncta was significantly more in the cells with fusion proteins incubation than the cells in the control condition. The immunostaining assay at 37ºC allowed binding and internalisation of ANG2, it could be conclusively demonstrated that ANG2 was indeed active within the constructs and could be specifically bound and internalised.

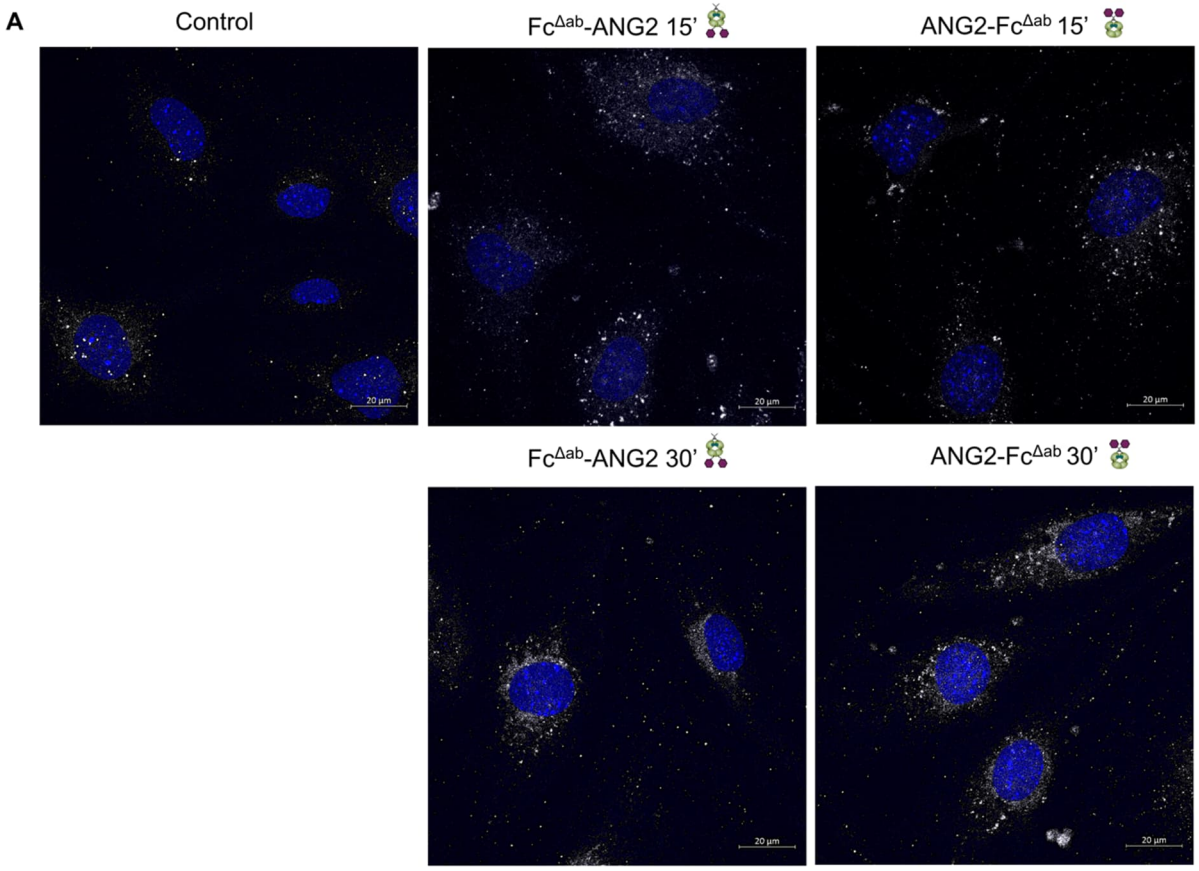
A
Control
Fc$^{\Delta ab}$-ANG2 15'
ANG2-Fc$^{\Delta ab}$ 15'
Fc$^{\Delta ab}$-ANG2 30'
ANG2-Fc$^{\Delta ab}$ 30'
20 µm

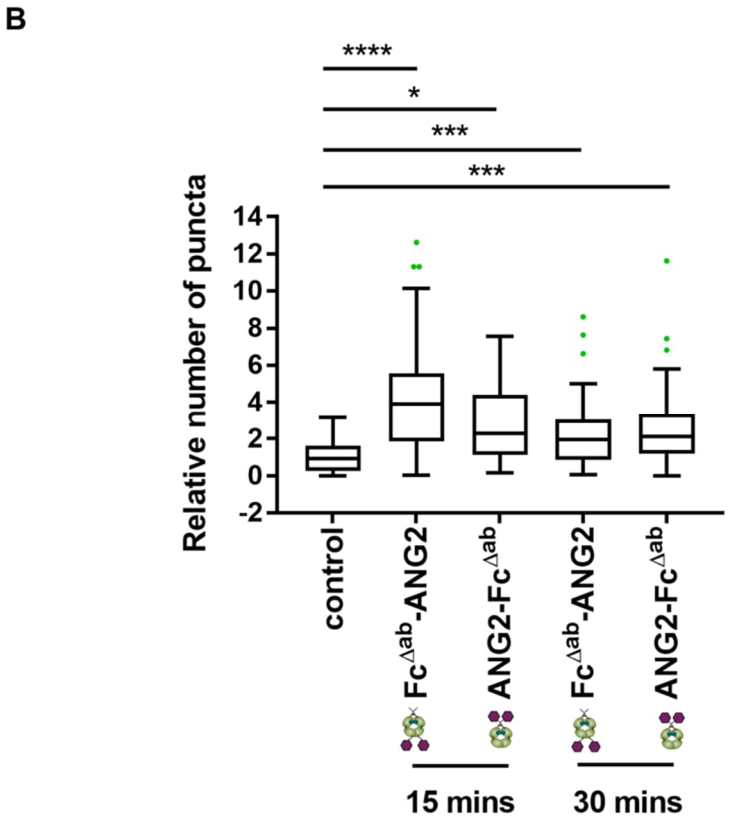

Figure 29: Binding of $Fc^{\Delta ab}$-ANG2, ANG2-$Fc^{\Delta ab}$ to bEnd.3 cells. (A) bEnd.3 cells were incubated with 50 nM of indicated ANG2-control protein for 30 min. Nuclei were stained in blue with Hoechst. White signal indicates the binding of the constructs. Scale bar 20 µm. **(B)** The number of vesicles from A were quantified at 15 min and 30 min and compared between control and ANG2-control protein conditions. Data was plotted as a Tukey boxplot with outliers represented as individual points, minimum 44 cells per group pooled from three independent experiments. Statistical significance was tested by Tukey's two-way ANOVA: * = $p \leq 0.05$; *** = $p \leq 0.001$ **** = $p \leq 0.0001$.

4.5.2 TRAIL binds stronger to BBB cells than ANG2

Having demonstrated that ANG2 binding could be detected in an immunostaining binding assay, it was applied to the other constructs. TRAIL-R2-mFc^{LALA}, a fusion of the extracellular domain of the human TRAIL-R2 and the Fc-receptor binding mutant murine Fc (mFc^{LALA}), was used to prevent non-specific signal from anti-human Fc-based detection and engagement of Fc-receptors. Hereby, the cells were incubated with 50 nM of Fc-scTRAIL or scTRAIL-Fc-ANG2 with or without 100-fold molar excess of soluble TRAIL-R2-mFc^{LALA} for 15 min or 30 min and imaged using confocal microscopy. The total cell fluorescence intensity was measured for each cell.

Strikingly, a marked fold increase of between 2.9 and 4.5 in the intensity of binding of TRAIL-based constructs, Fc-scTRAIL and scTRAIL-Fc-ANG2, as compared to the ANG2-only positive controls was observed (Figure 30B), in line with the flow cytometry experiments in 4.4.3. Moreover, signals from the TRAIL-based constructs were highly diffuse across the entire cell, whilst ANG2-only constructs were predominantly localised to the perinuclear region (Figure 30A), in line with the spatial expression pattern of its target receptor, Lrp1 as shown in 4.4.1. Blocking of TRAIL with 100-fold molar excess of TRAIL-R2-mFc^{LALA}, brought the binding back to the level of ANG2-only control proteins and returned the spatial distribution to the perinuclear region (Figure 30A).

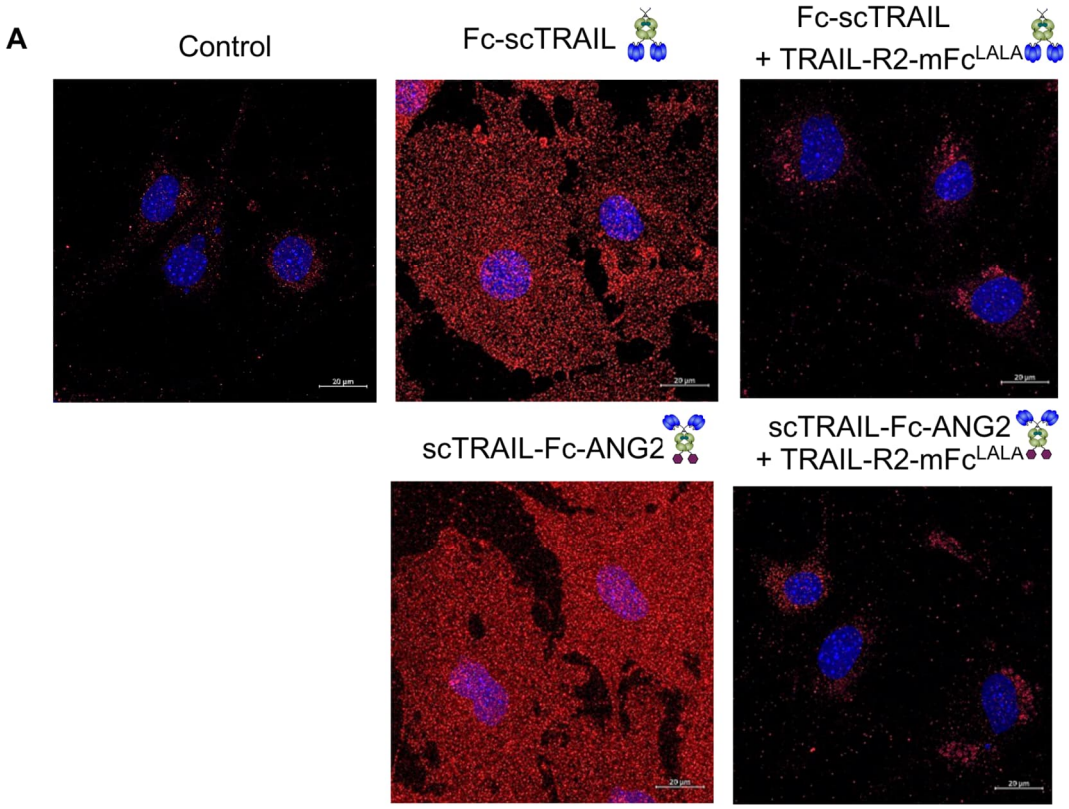

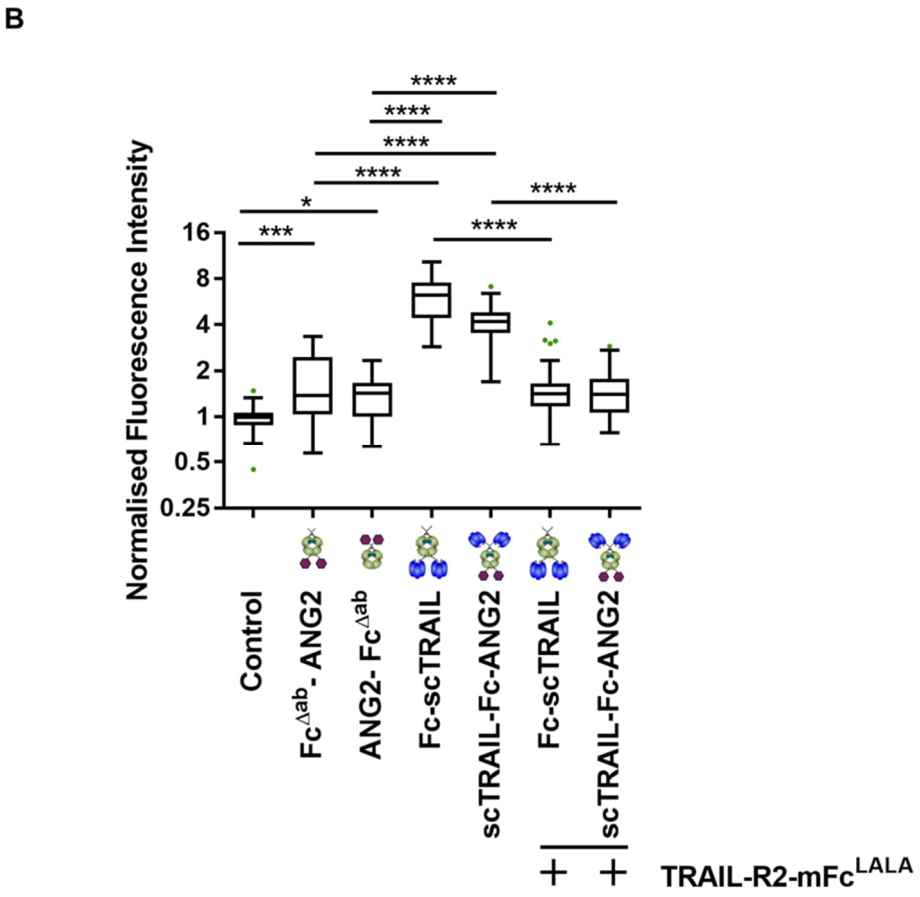

Figure 30: Binding to blood-brain barrier cells is predominantly TRAIL-mediated. (A) bEnd.3 cells were incubated with 50 nM of indicated construct for 15 min with or without 30 min pre-incubation of 100-fold molar excess of TRAIL-R2-mFcLALA. nuclei were stained in blue with Hoechst. Red signal indicates binding of the constructs. Secondary antibody, anti-Fc-PE was used as a control for non-specific signal. Scale bar 20 µm. **(B)** The fluorescence intensity of the cells in A was quantified and compared between control and construct condition. Data was plotted as a Tukey boxplot with outliers represented as individual points, minimum 43 cells per group pooled from three independent experiments. Statistical significance was tested by non-parametric one-way ANOVA, Kruskal-Wallis test with Dunn's correction: * = $p \leq 0.05$; *** = $p \leq 0.001$ **** = $p \leq 0.0001$.

Taken together, these data demonstrated that ANG2 is functional within fusion proteins, but that despite low expression of TRAIL receptors on blood brain barrier cell lines, masking or absence of TRAIL or TRAIL receptors is required for effective detection of ANG2-mediated binding.

4.5.3 CNS transport of TRAIL-fusion proteins

Having established that scTRAIL-Fc-ANG2 binds both via ANG2 and TRAIL moieties to BBB cells, transcytosis of this fusion protein across the BBB was characterised. An in vitro BBB model by growing bEnd.3 cells to a confluent layer on a transwell was established (Figure 31B) and a steady barrier with a transendothelial electrical resistance (TEER) of 17 Ω×cm^2 was obtained. 20 nM of Fc$^{\Delta ab}$-ANG2, ANG2-Fc$^{\Delta ab}$, scTRAIL-Fc-ANG2 and Fc-scTRAIL was placed in the apical compartment with or without 30 min pre-incubation with 100-fold molar excess of soluble TRAIL-R2-mFc^{LALA}.

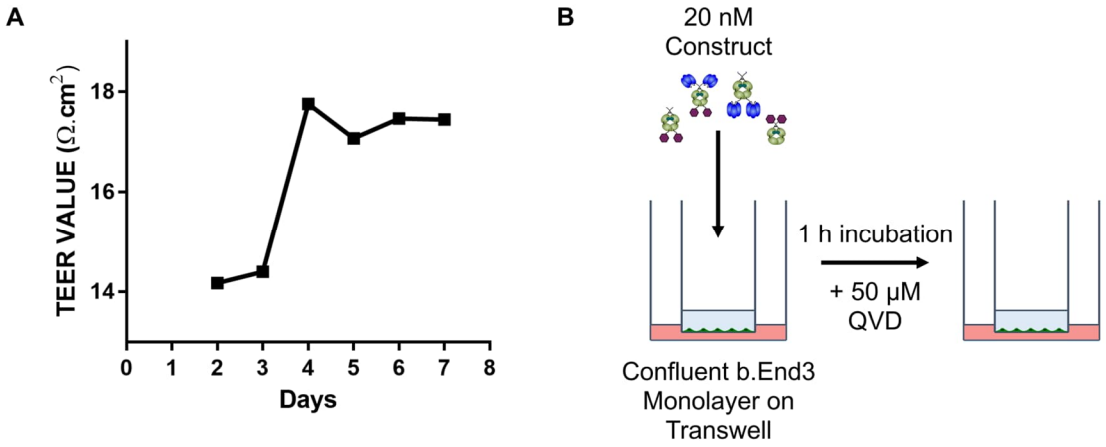

Figure 31: Transport assay setup using transwell. (A) TEER value was measured every day for 7 days with the help of STX2 electrode**. (B)** bEnd.3 cells were grown to a confluent monolayer on a transwell insert and then 20 nM of indicated construct, with or without 30 min pre-incubation of 100-fold molar excess of TRAIL-R2-mFc^{LALA}, was added to the apical compartment.

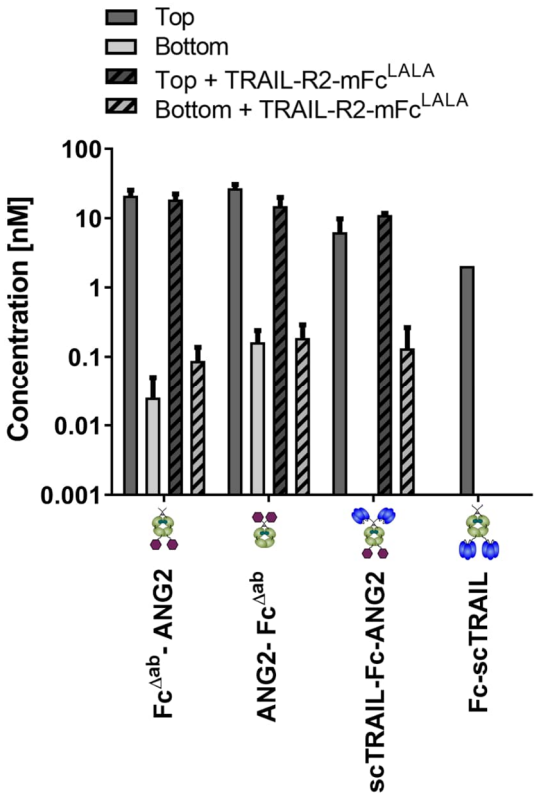

Figure 32: ELISA for determination of CNS-transport efficiency. After 60 min incubation with proteins at 37°C, the samples were taken from the top and bottom compartment of the transwell and the concentration was determined through quantitative sandwich ELISA. Data points are mean + range from two independent experiments. Fc-scTRAIL is the result of one experiment performed in duplicate.

After 1 h incubation at 37ºC, the concentration of fusion proteins in the apical and basolateral compartments was determined using quantitative sandwich ELISA. ANG2-only positive control proteins, ANG2-Fc$^{\Delta ab}$ and Fc$^{\Delta ab}$-ANG2, were both detected after 1 h in the basolateral compartment (Figure 32). Additionally, ANG2 binding was independent of whether ANG2 was fused to the N- or C- terminus of the protein, successful transport was also observed for both conformations of the ANG2-controls. On the contrary, scTRAIL-Fc-ANG2 was only detectable in the basolateral compartment after blocking of TRAIL through TRAIL-R2-mFc^{LALA}. As expected, Fc-scTRAIL was not transported to the basolateral compartment, confirming that the ability to be transported is strictly ANG2-dependent. Overall, the transport study indicated that binding to TRAIL receptors interferes with ANG2-mediated transport of scTRAIL-Fc-ANG2 across the BBB, but that TRAIL-based biologics can be transported by interfering with TRAIL/TRAIL-R interactions on the apical side.

5 Discussion

GBM is the deadliest tumour worldwide with a 5 year survival rate of less than 10% (Stupp et al., 2009). Despite the available GBM golden standard of care, patients suffer with GBM recurrence and poor prognosis with a very low median survival rate of approximately 14 months. Studies have shown that there are several factors, such as extreme proliferative nature, diffusive infiltration, recurrence after resection, heterogeneity influencing the GBM treatment resistance and failure (Claes et al., 2007; Patel et al., 2014; Xie et al., 2014). The extent of tumour resection plays an important role in GBM, as these extremely proliferative and diffusive infiltrated tumours can escape the first surgical resection and lead to recurrence (Lara-Velazquez et al., 2017). Therefore, new treatment strategies are required to actively prevent the recurrence in GBM patients.

Since its discovery, the TRAIL molecule has been produced in several formats to utilize as an anti-cancer agent. The initial TRAIL constructs were not efficient in inducing apoptosis for various reasons. For example, the constructs with tags resulted in apoptosis in hepatocytes. This effect was attributed to cross-linking or poor zinc coordination (Ganten et al., 2006). This highlighted the importance of producing stable TRAIL molecules without aggregates. Despite their efficient apoptosis induction in preclinical tumour models (Kelley et al., 2001; Lawrence et al., 2001) and safety profile in human clinical trials (Lemke et al., 2014), recombinant TRAIL molecules failed to induce strong antitumour effects in patients. This was reasoned to be due to their short half-life period and due to the low molecular weight of the rather unstable non-covalently linked trimers. The monoclonal antibodies against DR4 and DR5 failed in inducing efficient apoptosis despite their longer half-lives. This was likely due to the poor clustering of the death receptors. Therefore, in later studies, all the fore-mentioned issues have been addressed to create a TRAIL receptor agonist with increased stability, longer half-life, and increased apoptosis induction (Hutt et al., 2017). This successful hexavalent TRAIL receptor agonist was used in this thesis work for better apoptosis induction in cancer cells.

TRAIL-based therapeutics have shown great potential in pre-clinical studies as a novel approach for the treatment of GBM (Fulda et al., 2002; Hetschko et al., 2008; Opel et

al., 2008). Beyond GBM, the CNS is also a frequent secondary site for many cancer metastases, including lung cancer, breast cancer and melanoma, consequently leading to lower treatment responses and poor patient outcomes (Bagci-Onder et al., 2015; J. Wagner et al., 2018). It has also been reported that the patient death rate is higher due to metastasis than the actual primary cancer (Dillekås et al., 2019). Once the primary tumour cells are in the vasculature, they extravasate and metastasize to the distal organs and impair their functions leading to multiple organ failures. Therefore, a CNS-targeted therapeutic variant of TRAIL, which shows broad anti-cancer efficacy in various cancer types (Polanski et al., 2015; Khawaja et al., 2020; Vetma et al., 2020; D. C. Phillips et al., 2021) would be of considerable clinical interest as an anti-cancer agent. Recent studies have suggested that endogenous TRAIL plays an important role in immune modulation in multiple sclerosis (Sanmarco et al., 2021). It has been shown in an animal model of multiple sclerosis that the TRAIL-positive astrocytes limit inflammation by inducing apoptosis in pro-inflammatory T cells. In another study, it has been demonstrated that TRAIL blocked the cell cycle progression of T cells and prevented their differentiation into effector T cells. These identifications suggest that a CNS-targeted TRAIL variant could also be used in the treatment of multiple sclerosis and other inflammatory CNS disorders (Hilliard et al., 2001; White et al., 1998). Taken together, this demonstrates that a CNS-targeted therapeutic variant of TRAIL would have broad therapeutic potential and is of considerable clinical interest.

The clinical utilisation of TRAIL for CNS diseases is hindered by the poor penetration of large molecules (W. M. Pardridge, 2005). Therefore, a widely exploited mechanism like RMT is studied for bringing large molecules across the BBB. Since the 1980s, many RMT drugs targeting different ligands are under development. However, therapeutics based on RMT have yet to translate into clinically approved drugs. Therefore, several groups were involved in finding new CNS targets for better transcytosis. In search of that, a group of scientists came across the Lrp1 receptor. Lrp1 is known to bind to more than 40 ligands with an endocytosis rate of less than 30 seconds (Y. Li et al., 2000; Lillis et al., 2008). It has also been demonstrated that the Lrp1-mediated transport of aprotinin is at least 8-fold higher than that of the well-known holo-transferrin through TfR (Demeule, Régina, et al., 2008). In addition, the synthetic Lrp1 ligand, ANG2, showed better transcytosis than avidin, transferrin, and lactoferrin. This mechanism has also shown promising results by entering clinical trials for CNS

diseases. Hence, in this thesis work, the Lrp1-ANG2 mechanism was utilised to bring the TRAIL molecules across the BBB.

5.1 Successful production of CNS-targeted TRAIL fusion proteins

Previously, it was demonstrated that TRAIL receptor agonists have broad efficacy against GBM cells alone or in combination with sensitisers (Fulda et al., 2002; Hetschko et al., 2008; Opel et al., 2008; Lincoln et al., 2018; Koessinger et al., 2021; Boccellato et al., 2021), but the BBB prevents the entry of TRAIL-based biologics from effectively reaching GBM tumours. Therefore, in this thesis work, for the purpose of bringing TRAIL into the CNS, the fusion proteins were produced to achieve not only apoptosis but also transcytosis. Among the few naturally existing mechanisms that benefit endogenous substances to go across the BBB, a widely exploited mechanism for the delivery of therapeutics across the blood–brain barrier was utilized in this work named receptor-mediated transcytosis (W. M. Pardridge et al., 1985, 1987; Schwartz et al., 1990). This mode of CNS access is advantageous as this does not disrupt the BBB, does not modify the therapeutic cargo and allows the transport of wide range of therapeutics from smaller peptides to larger antibodies (W. M. Pardridge, 2006, 2022a; Pulgar, 2019). In this project, the small peptide ANG2 was deployed to increase CNS-penetration of TRAIL variants due to the following reasons. Firstly, ANG2 was shown to undergo efficient transport and parenchymal distribution in in vitro and in situ brain perfusion set ups (Bertrand et al., 2010; Demeule, Currie, et al., 2008; Demeule, Régina, et al., 2008). Secondly, in clinical trials, it has been demonstrated that ANG1005, ANG2 covalently linked to three paclitaxel molecules, shows promising anti-tumour effect and patient safety in multiple subset of patients with breast cancer with leptomeningeal carcinomatosis and recurrent brain metastases (Kumthekar et al., 2020). Additionally, there are several ANG2-based clinical trials currently in phase I/II/III for the treatment of CNS specific tumours (NCT01480583, NCT01967810, NCT02048059), these studies highlight that ANG2-Lrp1-mediated RMT transport is clinically relevant, safe and effective for the drug delivery in humans. Finally, broad species specificity and ease of inclusion of a 19 amino acid peptide within fusion proteins, make ANG2 an optimal choice for such an exploratory study. Taken together,

these pre-clinical and clinical studies demonstrate that utilising ANG2 can be an efficient strategy to deliver therapeutics to the CNS.

The TRAIL moiety of the CNS-targeted TRAIL fusion proteins was generated similar to the Fc-scTRAIL construct, as it is potently cytotoxic against cancer cells, has a greater half-life and stability (Figure 8). Three TRAIL monomers fused through their extracellular part via small flexible linkers generate scTRAIL and it was utilised for its known improved stability compared to conventional soluble TRAIL (B. Schneider et al., 2010; Siegemund et al., 2012; Seifert, Plappert, et al., 2014; Siegemund et al., 2016). For several reasons, in the recent past, the Fc part of IgG has been used as a fusion partner for the development of fusion protein therapeutics. This was particularly due to the increased plasma half-life rendered by the interaction of the Fc part with FcRn (Kontermann, 2009; Roopenian & Akilesh, 2007). In physiological conditions, TRAIL, a transmembrane II protein, is connected to the cell membrane via its N-terminus, therefore Fc-scTRAIL was generated by fusing Fc to the N-terminus of TRAIL (Hutt et al., 2017). However, the CNS-targeted TRAIL fusion proteins were created with Fc and ANG2 on the C-terminus of scTRAIL (Figure 8), based on the previous studies, in which ANG2 fusion proteins have been produced with ANG2 on the C-terminus (Böckenhoff et al., 2014; Ji et al., 2019). In addition to the CNS-targeted hexavalent TRAIL fusion protein, a trivalent TRAIL fusion protein was also generated with the aim to understand the transcytotic efficiency in the context of overall avidity, as avidity has been shown to affect the transport (Niewoehner et al., 2014). The production yield was higher for the hexavalent TRAIL fusion protein than the trivalent and this enhanced yield was attributed to the Fc part of IgG, which promotes increased expression or secretion of proteins as described and observed in previous studies (Beck & Reichert, 2011; Hutt, 2017; Levin et al., 2015). After the production, the purity and stability check confirmed the clear dimerisation induced by the Fc module as observed in the development of the Fc-scTRAIL construct (Hutt et al., 2017). Overall, in this section of the thesis it was demonstrated that CNS-targeted TRAIL fusion proteins can indeed be produced and ANG2 fusion does not affect the purity and stability of the fusion protein.

5.2 CNS-targeted hexavalent TRAIL retains its potency in inducing apoptosis in GBM cells, not affecting BBB cells

This part of the project was dedicated to verifying the antitumour activity of CNS-targeted TRAIL fusion proteins in GBM cells. Due to the inclusion of ANG2 and the fusion at the C-terminus in the CNS-targeted hexavalent TRAIL fusion protein, scTRAIL-Fc-ANG2 was compared to Fc-scTRAIL to ascertain the TRAIL potency in the CNS-targeted version. The initial quality control study with crystal violet assay in a well-established cancer line demonstrated efficient apoptotic function of hexavalent CNS TRAIL (Figure 10). Likewise, through Annexin V PI staining it can be seen that a GBM cell line, A172, showed a strong cell death response once treated with an increasing dose of CNS hexavalent TRAIL. This effect was confirmed by a lower EC_{50} value (0.11 nM) (Figure 17), which is similar to the EC_{50} of the hexavalent construct Fc-scTRAIL without ANG2 fusion (0.15 nM) (Hutt et al., 2017), therefore cell viability and Annexin V experiments demonstrated that the ANG2 fusion did not affect the typical potency of hexavalent TRAIL proteins. Moreover, the trivalent TRAIL yielded expected results with no effective cell loss in crystal violet cell viability assay (Figure 10). Similarly, by Annexin V staining it was shown that the trivalent construct achieved a maximum of only 30% cell loss at the highest concentration. These results on distinctive effects of trivalent and hexavalent TRAIL fusion proteins focus demonstrate the requirement of higher order clustering to achieve effective cell loss in cancer cells (Hutt et al., 2017; Siegemund et al., 2012). In addition, western blot analysis was performed to check the well-known caspase cascade signalling showed that scTRAIL-Fc-ANG2 induced efficient cleavage of the key apoptotic regulators in A172 and HCT116 cells. It can be seen that the hexavalent TRAIL treatment induced a strong reduction in the pro form and a more pronounced signal in the cleaved caspase forms, whereas the trivalent TRAIL induced only mild processing (Figure 18). In the caspase cascade signalling, caspase 8 is the first activated caspase as a result of the DISC complex that is initiated by TRAIL. In type II cells, including A172 and HCT116 cells, widescale caspase 3 cleavage occurs only after MOMP which can be induced by caspase 8-mediated cleavage of Bid to tBid. The lack of robust caspase 3 processing and PARP cleavage observed with the trivalent TRAIL suggests that trivalent proteins induce weaker caspase 8 activation in comparison to hexavalent proteins and that the

amount was not sufficient to induce MOMP. Similarly, in a study, it has been shown that the hexavalent TRAIL, APG350, induce higher order clustering resulting in strong activation of caspases 8, 3 and 9 (Gieffers et al., 2013). Overall, in accordance to previous studies, these data highlighted that the higher clustering potential of hexavalent scTRAIL was strictly necessary for efficient apoptosis induction in GBM cells as this is required for efficient engagement of TRAILR2 (Siegemund et al., 2012; de Miguel et al., 2016; Hutt et al., 2017). Importantly, hexavalent TRAIL receptor agonists based on a similar format, ABBV-621 (Eftozanermin Alfa), have been developed and shown to be active on a panel of solid tumour cell lines at sub-nanomolar concentrations. It has been also demonstrated that cynomolgus monkeys tolerated the increasing dose of ABBV-621 every week very well and showed low toxicity (D. C. Phillips et al., 2021). ABBV-621 is currently in clinical trial phase I for the treatment of haematologic malignancies (NCT03082209) and multiple myeloma (NCT04570631). Given this observed potential of TRAIL in GBM and other cancer types, hexavalent TRAIL could serve as a promising therapeutic agent in the treatment of GBM patients. As TRAIL induces apoptosis by engaging TRAILR on the cell surface, the number of TRAIL receptors on hCMEC/D3 cells were quantified. It was shown that levels of TRAIL receptors in the BBB endothelial cell line hCMEC/D3 were considerably reduced compared to cancer cells. Moreover, it was also revealed that different growing conditions do not alter the TRAIL receptor expression (Figure 20). The receptor numbers in these BBB cells were also generally lower than published levels in a wide range of cancer cell lines (D. C. Phillips et al., 2021; Vetma et al., 2020). Since low number of TRAIL receptor expression does not correspond to reduced cell death induction, the BBB endothelial cells were tested for apoptosis induction. In contrast to cancer cells, BBB endothelial cells were largely resistant to hexavalent TRAIL receptor agonists even at high concentrations, in accordance with the concept that TRAIL-mediated apoptosis occurs almost exclusively in cancer cells (Ashkenazi et al., 1999; Walczak et al., 1999). hCMEC/D3 cells achieved their maximum cell death of just 20% at a concentration that is 30 times more than required to induce cell death in tumour cells. The results obtained in this part of the thesis are in line with previous studies that have shown that endothelial cells do express TRAIL receptors but are not sensitive to TRAIL-mediated apoptosis. For example, Zhang and colleagues have shown that the endothelial cell line, human umbilical vein endothelial cells (HUVECs) do express TRAIL receptors and the expression of TRAILR3 was

required to be resistant to TRAIL treatment (Wosik et al., 2007). Moreover, the death to decoy receptor expression ratio is quite high in cancer cells, whereas their expression is similar in case of BBB endothelial cell line hCMEC/D3. However, in this thesis work, TRAILR3 requirement for TRAIL resistance was not observed but there is an indication that decoy receptors are maybe involved as the expression ratio is similar. In particular, Wosik and colleagues showed that primary human brain endothelial cells (HBECs), when treated with 5 nM of human soluble TRAIL, were resistant to TRAIL-mediated cell death despite the presence of TRAIL receptors (Wosik, Biernacki, et al., 2007). Moreover, a study by Li and colleagues revealed that human recombinant TRAIL induced cell death in endothelial cell HUVEC and human dermal microvascular endothelial cell (HDMEC), but 70% of the cell population survived the TRAIL treatment. However, cotreatment with TRAIL and cycloheximide (CHX) induced significant cell death of 80% in these cells (J. H. Li et al., 2003). This result was expected as CHX, a protein synthesis inhibitor, has been reported to enhance caspase activation by depleting anti-apoptotic proteins (L. Wang et al., 2008). Therefore, this indicates that apoptosis in endothelial cells is achieved only under additional treatment conditions. Furthermore, due to the superior antitumour activity of the hexavalent TRAIL, the concentration required to kill the tumour cells is very low as shown in the previous section with EC_{50} value (0.11 nM) of scTRAIL-Fc-ANG2 and at this concentration the BBB endothelial cells are completely resistant.

From MTT assays, it can be seen that there is a slight increase in percentage of living cells with increased concentration of TRAIL treatment (Figure 22). As this was observed in only one of the repeats, it is necessary to repeat the experiments for concrete results. However, this increase could relate to the studies that have shown that TRAIL can promote the survival and proliferation of endothelial cells by activating the Akt and ERK pathways, thus protecting them from apoptosis (Secchiero et al., 2003; Alladina et al., 2005). This non-apoptotic effect of TRAIL on endothelial cells has been studied in the context of angiogenesis. It has been shown that TRAIL induces endothelial cell proliferation and differentiation (Alladina et al., 2005; Di Bartolo et al., 2015; Secchiero et al., 2003). On the contrary, it has been demonstrated that high concentration of TRAIL had no proliferative effect or migration effect on hCMEC/D3 cells (Chen & Easton, 2010). This contradictory result can also be due to different cell type, amount of death receptor expression and experimental techniques employed

(Patil et al., 2020). In this thesis work, no non-apoptotic effect on BBB endothelial cells was reported, however considering these interesting findings, it can be beneficial to investigate this effect in the future. Western blot analysis was performed to analyse the caspase cascade signalling and revealed that only high concentration treatment with TRAIL induced residual accumulation of caspase subunits in hCMEC/D3 cells (Figure 23) with no caspase processing at lower concentrations of TRAIL. This is in line with the report that has shown that only high concentrations of TRAIL induced caspase 3 activity in this cell line (Chen & Easton, 2010). Interestingly, bEnd.3 cells showed no caspase processing along with no decline in the full-length caspases, indicating that these cells are overall resistant to TRAIL treatment (Figure 24). Previous studies have also shown that endothelial cells of the BBB endothelial cells are highly resistant to extrinsic apoptosis, due to the activity of the pro-survival factors TAK1 and NEMO (Ridder et al., 2015). This, together with the findings of low TRAIL-receptor expression, demonstrates that there are multiple factors contributing to high TRAIL resistance in BBB endothelial cells.

5.3 TRAIL-TRAILR binding prevents the transport of CNS-targeted TRAIL fusion proteins

After having investigated the apoptosis inducing effect of CNS hexavalent TRAIL proteins in a GBM cell line, the binding and transport ability was investigated in this section of the thesis. The initial step was detecting the target receptor in the cell lines used, which revealed very low expression of Lrp1 receptors in comparison to the known Lrp1-expressing mouse embryonic fibroblasts (MEFs) (Storck et al. 2016). The Lrp1 expression in bEnd.3 cells was spatially distributed in the perinuclear region similar to previous studies (Figure 25C) (Tian et al., 2020). Later, the binding studies performed on hCMEC/D3 cells revealed dose-dependent binding of CNS fusion proteins. This binding could be TRAIL-mediated as this cell line has very low amount of Lrp1 receptors. But, this was the case also in the Lrp1 positive bEnd.3 cell line, as TRAIL blocking proteins inhibited the binding of fusion proteins to the cells. This suggested that ANG2 may not be present or functional in the construct or that the assay is not able to detect ANG2-LRP1 binding. However, the MALDI-TOF mass spectrometry of scTRAIL-Fc-ANG2 confirmed the presence of the small peptide ANG2

by showing an additional peak at m/z = 1621.8 in comparison to Fc-scTRAIL (Figure 11). As ANG2 was less utilised as a fusion protein in the previous studies (Kurzrock et al., 2012; Regina et al., 2015; Kumthekar et al., 2016), this identification also demonstrates that ANG2 is intact and not degraded during the production process. The lack of binding through ANG2 despite its presence in the fusion proteins led to the first hypothesis that Lrp1 might cleave off during the trypsinisation process that is required to analyse the cells for binding. The main reason for this hypothesis was that the extracellular α-subunit of Lrp1 receptor is non-covalently attached to the intracellular β-subunit and it has been demonstrated that intermembrane proteolysis occurs in Lrp1 (Lillis et al., 2008; May et al., 2002). In line with these studies, Lrp1 expression was not detectable through flow cytometry after trypsinisation (Figure 25). Another hypothesis was that ANG2-binding to the cells at 4ºC may be too low for specific robust detection of surface binding, as a low affinity (313 nM) of ANG2 for Lrp1 has been observed in previous studies (Bertrand et al., 2010). These two hypotheses led to the utilisation of the immunostaining technique to avoid trypsinisation and observe low binding, if there was any, at 37ºC.

Due to the high expression of Lrp1 receptors, subsequent binding and transport studies were conducted in bEnd.3 cells. The binding data from immunostaining demonstrated that ANG2 based positive control constructs bind to BBB cells, which has been observed also by ANG2 and Lrp1 colocalization studies in bovine brain capillary endothelial cell monolayer (Demeule, Currie, et al., 2008). This demonstrates that the ANG2 moiety is active in these constructs. In addition, it was also demonstrated that ANG2 was active within fusion proteins regardless of whether it was fused to the N- or C-terminus of the protein. In other studies ANG2 was always fused to the C-terminus of the proteins (Böckenhoff et al., 2014; Ji et al., 2019), whereas the immunostaining binding data suggest this is not an absolute requirement for ANG2 function. When binding of hexavalent TRAIL proteins to bEnd.3 cells was measured, a remarkable increase in the binding intensity was observed in comparison to ANG2 only proteins. Interestingly, ANG2-only and TRAIL fusion proteins with TRAIL blocking showed a similar perinuclear localization as Lrp1 expression (Figure 25) (Tian et al., 2020), whereas TRAIL constructs alone were diffuse across the cells. Due to these binding data, it was hypothesized that TRAIL binding to TRAIL receptors could interfere with the binding of ANG2 to Lrp1, however, transport assays mimicking the actual BBB was

required to confirm the shown TRAIL interfering effect. The ANG2-function in inducing transport across BBB cells was investigated by using bEnd.3 cells grown on a transwell insert (Figure 31B). The use of bEnd.3 cells has been characterized previously as a BBB model. It has been demonstrated that bEnd.3 cells that are grown in a transwell have mRNA expression of BBB transporters Na^+-independent glucose transporter (GLUT1), monocarboxylic acid transporters (MCT 1 and 2), amino acid transporters (system L and y^+L), P-glycoprotein and multidrug resistance-associated proteins (MRP 1 and 5) (Omidi et al., 2003). They also express tight junctions ZO-1, JAM, occludin, claudin-1 and -5 and clathrin and other vesicle-associated proteins, thus showing expected BBB characteristics (Omidi et al., 2003). The BBB setup in this thesis work was reported to have a TEER value of 17 $\Omega \cdot cm^2$ (Figure 32A), however, previous studies have reported to have a wide range of TEER values from 15–140 $\Omega \cdot cm^2$ (Booth & Kim, 2012; Brown et al., 2007; Yang et al., 2017). Technical reasons may have contributed to the lower TEER value. STX2 Chopstick electrodes were used to measure the TEER of the BBB model. This equipment is commonly used by many researchers, but it is known to show high variability, particularly at low TEER values. The CellZscope is another instrument that is available on the market for automated TEER measurements. Notably, it measures the impedance and capacitance of the cell layer at varying frequencies to determine the properties of the cell layer. Therefore, it could be beneficial in the future to adapt the experimental setup with advanced equipment like cellZscope.

Even though the reported TEER values in this thesis work are on the lower side of this range, they are in line with what was previously reported (Booth & Kim, 2012), and no apparent effect from passive diffusion at the time step chosen was observed. Among many strategies to increase the TEER, co-culturing BBB endothelial cells with astrocytes, pericytes, utilizing induced pluri- and multipotent stem cells have demonstrated to improve the TEER value (Appelt-Menzel et al., 2017; Thomsen et al., 2015). As mentioned earlier and also in the context of BBB integrity, no trace of molecules undergoing passive diffusion was observed, which demonstrates the barrier function of the BBB model. In this BBB setup QVD was added prior to TRAIL treatment to rule out any effect of TRAIL signalling on barrier function. Previously, co-culture of bEnd.3 cells with rat C6 glioma cells increased the permeability of the BBB with 34% reduction of TEER (Yang et al., 2017a). These C6 cells secrete TNF-α (Y. Fan et al.,

2005) and this cytokine has proven to loosen the BBB (Fiala et al., 1997; Mark et al., 2001). Even though, this effect has not been tested due to QVD pre-treatment and apoptosis resistance of BBB endothelial cell, it could be interesting to investigate the TRAIL effect on the BBB integrity in future. The ANG2 function in the positive control proteins was clearly observed in the transport study. From this in vitro BBB model, ANG2 transport rates of 0.1–0.3 pmoles/cm^2/h were achieved (Figure 32). It has been shown that the ANG2 transport rate for crossing bovine brain endothelial cells was approximately 6 pmoles/cm^2/h by the group that first identified and improved the ANG2 peptide (Demeule, Régina, et al., 2008). In their study, they added 250 nM of iodinated ANG2 in the apical membrane of the transwell. Due to the lack of ANG2 detecting antibodies, in this thesis work, antibodies targeting the Fc moieties of the proteins were used to measure the protein level transported. As there was a detection limit in this ELISA assay, a lower amount of protein (20 nM) was added to the top well to be able to measure the protein at both apical and basal side. This added amount was approximately 10 times lower than what was used in the study by Demeule and colleagues. This could explain the lower transport rate observed. Even though studies have shown that increased affinity interferes with efficient transport, no evidence of poor transport of bivalent ANG2 proteins was observed. Avidity studies mostly focused on transferrin receptors and not Lrp1 or other RMT receptors. Notably, in a study by Farrington and colleagues, a novel single domain antibody, FC5 (Abulrob et al., 2005), was fused monovalently and bivalently to the Fc part of IgG. It has been revealed that bivalent FC5 format showed increased transcytosis of 25% in comparison to the monovalent FC5 format (Farrington et al., 2014). Additionally, insulin-mediated transcytosis was utilised in a study for the treatment of Hurler's syndrome, which is caused by a deficiency of α-L-iduronidase (IDUA) enzyme. IDUA was fused to the human insulin receptor monoclonal antibody (AGT-181) resulting in a bivalent fusion protein (Boado et al., 2007, 2008; Boado & Pardridge, 2017). It has been demonstrated that it is rapidly transported across the BBB in rhesus monkey in vivo and a phase II clinical trial was completed for Hurler's syndrome (NCT03071341). This highlights that avidity effect could vary based on proteins targeting different transport receptors or even different binding sites of the same receptor. Overall, one of the important findings from the ANG2 positive control study in this thesis is that reduced affinity binders in a bivalent format can undergo efficient transcytosis. This is important to know because the ANG2 bivalent format targeting the Lrp1 receptor has never been explored in

previous studies and most of the studies as described earlier focused only on the transferrin receptor. Utilization of ELISA for detection has complicated the inclusion of scTRAIL-ANG2, which was nevertheless shown to be insufficient in apoptotic induction (Figure 17). As expected, no transport sign of Fc-sTRAIL, which is without any shuttle peptide, was seen, also describing no leakage of the BBB setup. Interestingly, scTRAIL-Fc-ANG2 was also not transported across the transwell, however, blocking the TRAIL moieties with TRAIL blocking protein, restored the transport. Overall, this data along with immunostaining data indicate that the presence of TRAIL interfered with ANG2-mediated transport, despite the low expression of TRAIL receptors in BBB endothelial cells. Factors, such as, individual affinities, receptor availability and avidity effects have a huge influence on the binding and transport of peptides. Therefore, it can be suggested that either the receptor levels of Lrp1 are lower than for TRAIL receptors or that TRAIL has a significantly higher binding rate for its receptors than ANG2, potentially due to higher individual affinity or overall avidity. Importantly, recent studies have shown that reduced overall affinity binding is beneficial for efficient RMT, whether by lowering the affinity itself or by reducing the avidity of binding (Y. J. Yu et al., 2011; Haqqani, Thom, et al., 2018; Niewoehner et al., 2014; Kariolis et al., 2020; Webster et al., 2017). It has been demonstrated that it is due to the redirection of cargo to lysosomal compartments instead of being trafficked across the cell (Bien-Ly et al., 2014; Niewoehner et al., 2014; Haqqani, Thom, et al., 2018; Villaseñor et al., 2019). Various factors are involved in sorting RMT drugs for lysosome degradation, yet little is known about these factors. For example, it has been shown that endosomal trafficking plays a significant role in successful transport across the BBB (Haqqani, Delaney, et al., 2018; Villaseñor et al., 2019). A recent study showed that sorting tubules formed due to endocytosis is involved in regulating RMT. They demonstrated that the monovalent transferrin antibodies that are localized to intracellular tubules are sorted for transcytosis. On the other hand, the bivalent transferrin antibodies were sorted for lysosomal degradation (Villaseñor et al., 2017). Ras-Associated Binding (Rab) proteins regulate intracellular vesicular transport through different endosomal compartments. They were utilised as a tool to manipulate the trafficking mechanism (Bhuin & Roy, 2014). In fact, overexpressing the Rab17 protein increased bivalent transferrin into tubules, thus promoting transcytosis. Although manipulation of Rab protein expression has not been often investigated in BBB endothelial cells, it could be

an interesting method for exploring the intracellular trafficking of different RMT candidates.

In line with affinity governing the transport of fusion proteins, it has been reported that ANG2 has a low affinity of 330 nM to its target receptor, Lrp1 (Bertrand et al., 2010). Although ANG2 was not purposely engineered as a reduced affinity binder, this function maybe is beneficial. It has been demonstrated by in situ perfusion that the precursor protein, ANG1, has increased brain and parenchymal volume of distribution, however it also has greater accumulation in brain capillary fractions indicating that the lysosomal sorting can also take place in Lrp1-mediated transcytosis (Demeule, Régina, et al., 2008). On the other hand, TRAIL proteins have been demonstrated to bind to cells at sub-nanomolar concentrations (Degli-Esposti, Dougall, et al., 1997; Degli-Esposti, Smolak, et al., 1997). TRAIL binds to TRAIL receptors DR4, DR5, DcR1, DcR2 with affinities of 29 nM, 10 nM, 47 nM and 62 nM, respectively (H.-W. Lee et al., 2005). In addition, hexavalent TRAIL receptor agonists show higher binding to cells due to the combined high affinity and avidity of the hexavalent agonist (Siegemund et al., 2012; Gieffers et al., 2013). This higher affinity of TRAIL in comparison to ANG2, along with the expression of TRAIL receptors at the BBB endothelial cells, can interfere with the binding of ANG2 to Lrp1. This could potentially explain why in this thesis work it has been found that TRAIL-ANG2 fusion proteins bound BBB endothelial cells in a predominantly TRAIL-mediated manner, consequently resulting in poor transport across the BBB. This effect has not been demonstrated in the field of BBB RMT delivery before, whereas similar effects have been demonstrated in bispecific anti-tumour therapeutics in general. For example, it has been revealed that a bispecific antibody consisting of HER2 and EGFR moieties showed enhanced tumour targeting upon reducing EGFR affinity (Mazor et al., 2017). This finding in this thesis work is particularly important for the development of future RMT-based drugs. Therapeutic targets should be deliberately chosen so that they do not interfere with BBB endothelial cell binding and transport. It is important to consider that high affinity (Haqqani, Thom, et al., 2018; Y. J. Yu et al., 2011), avidity (Niewoehner et al., 2014), pH based binding (Sade et al., 2014), and lysosomal degradation effects (Bien-Ly et al., 2014; Haqqani, Thom, et al., 2018; Niewoehner et al., 2014) has been described only using transferrin receptor as a transport model. In particular, it is not clear, if other RMT receptors, including Lrp1, will likely work in a similar manner as transferrin receptor and this is an

area of interest for further studies. Additionally, quantitative protein expression profile in isolated mouse capillaries revealed that Lrp1 (1.02 ± 0.20 fmol/µg protein) is expressed at lower levels in comparison to other RMT targets such as the transferrin receptor (5.16 ± 0.44 fmol/µg protein) (Agarwal et al., 2012). Similar results were obtained for freshly isolated human brain microvessels analysis (Shawahna et al., 2011; Uchida et al., 2011). The greater levels of receptors for other targets may help to balance the reduced affinity of binding. Overall, it has been shown that the ANG2 in this fusion protein is indeed functional, however, TRAIL binding to TRAIL receptors hinders the overall transport.

From a translational perspective, these CNS-targeted TRAIL receptor agonists can still be used, providing the presence of TRAIL or TRAIL-blocking peptides. The transport can be achieved by adding systemic TRAIL-blocking peptides after the TRAIL treatment, so the ANG2 moiety can bind to the BBB cells. For the release of TRAIL-blocking peptides from the drug, esterase-responsive TRAIL-blocking peptides can be designed. Esterases are known to be overexpressed in cancer cells (McGoldrick et al., 2014). They function by hydrolysing the ester bonds in the drugs. Therefore, they have been considered a drug release candidate to deliver the drug to the target site (Dong et al., 2019; Shi et al., 2022). Notably, this approach was used in the RMT-inducing ANG2 drug candidate, ANG1005, to release paclitaxel at the tumour site. Esterase-mediated drug release has also been tested using nanoparticles, particularly in the GBM environment (Ye et al., 2022). Therefore, this can be one possibility in bringing the CNS-targeted TRAIL fusion proteins into the CNS. The complexity of the tumour microenvironment (TME) poses significant challenges for finding suitable drugs for cancer treatment. However, the unique TME features can be utilised for delivering TME-responsive drugs (Bhuin & Roy, 2014). Among many characteristics, TME has a lower pH than healthy tissues. Therefore, pH-responsive TRAIL-blocking peptides can be used. This way, the blocking peptides can be cleaved at the tumour site, and the TRAIL moieties can be exposed for apoptosis induction. TRAIL moieties in the CNS-targeted TRAIL fusion proteins can be modified to achieve transport across the BBB. One possibility is making them a trimer or dimer to reduce their affinity and activate them on site. In previous studies, it has been demonstrated that adding a tumour-targeting moiety like EGFR to the dimeric TRAIL increased its bioactivity (Seifert, Pollak, et al., 2014). Upon binding of EGFR to tumour cells, the dimeric TRAIL was

able to mimic the membrane TRAIL, which led to increased receptor activation. Therefore, adding a GBM or CNS target moiety to the dimeric TRAIL fusion protein will aid in the activation of TRAIL on site without interfering with ANG2 binding. Another possibility is mutation-led affinity reduction of the TRAIL molecule. Indeed, affinity reduction has been performed on several RMT candidates, for example, transferrin. The initial transferrin antibodies were designed to have a higher affinity (W. Pardridge et al., 1991), but later they were modified to have a lower affinity of 76 nM and 108 nM. In order to generate transferrin with lower affinity, alanine mutations were introduced into key positions (Haqqani, Thom, et al., 2018; Y. J. Yu et al., 2011). Although high-affinity TRAIL hinders the transport of CNS-targeted TRAIL fusion proteins, there are promising methods that could be adapted to reduce the affinity and prevent the interference.

In addition to RMT, other methods of bringing large molecules across the BBB have also been considered (W. M. Pardridge, 2022b), including invasive and non-invasive techniques. Surgical resection of the tumour is considered the first line of treatment for GBM. Therefore, alongside surgery, TRAIL can be utilised as an implant placed in the tumour cavity. This approach, in fact, is currently used for the treatment of GBM by using commercially available Gliadel® wafers. They are biodegradable wafers containing a chemotherapy drug, carmustine. They can be safely placed at the tumour site after surgery (Ashby et al., 2016; Chowdhary et al., 2015). Currently, steps are taken to introduce other drugs in this format, so the TRAIL molecules can also be produced as wafers and implanted after surgery (Turek et al., 2020; Yen et al., 2016). However, this approach is not feasible for recurrent GBM, where surgical resection is not recommended due to its infiltrative nature. In such cases, invasive approaches, such as intrathecal, intraventricular, and convection-enhanced delivery, can be applied. Intrathecal delivery directly administers the drugs into the cerebrospinal fluid via the spinal cord. This method allows the delivery of drugs at a low dosage level. In general, the success rate of direct drug injection into the CNS depends mainly on the diffusion rate. Poor diffusion leads to poor penetration of the drugs to the target site. To address the problem of poor diffusion, a group identified a convection-enhanced delivery approach (Bobo et al., 1994). It is a catheter-based delivery, where the catheters are connected to an infusion pump to enhance the delivery of the drugs. The drugs are delivered at the tumour site by the pressure gradient (Lonser et al., 2015).

All these approaches that help in direct drug delivery at the CNS tumour site reduce peripheral organ distribution, thus preventing systemic toxicity (Jahangiri et al., 2017). However, systemic toxicity is not expected with TRAIL treatment due to its safety profile observed in patients. Therefore, these approaches can be adapted to deliver large biomolecules like TRAIL. Moreover, a temporary BBB opening approach has been considered for GBM drug delivery. This was achieved using a Sonocloud-9 device, which applies low-intensity ultrasound to disrupt the BBB temporarily (Idbaih et al., 2019). This device is implanted in a skull window under the skin. Upon activation for a few minutes, the BBB is disrupted for a few hours. In this time window, the drugs can be administered to reach the brain at effective concentrations. After completing phase I/II clinical trials, this device recently received breakthrough device designation by the FDA for treating recurrent GBM (Carpentier et al., 2016). Therefore, this can be an alternative approach for bringing TRAIL molecules across the BBB.

6 Summary and Outlook

Treatment options and survival rate of GBM patients have not improved in the last decade and therefore, in this thesis work, the possibilities of bringing TRAIL molecules inside the CNS utilising the BBB shuttle peptide ANG2 was investigated. The initial biochemical characterisation studies revealed that these antibody-based TRAIL fusion proteins can indeed be developed and produced with high purity and in high yield. Here it was shown that the fusion of ANG2 to the hexavalent TRAIL proteins did not affect the potency of TRAIL-mediated apoptosis, which was confirmed by strong apoptotic induction in GBM cells at a very low concentration. As shown in previous studies, the trivalent construct was not efficient in apoptosis induction and this was likely due to the lack of higher order clustering resulting in poor processing of key apoptotic proteins. Several groups have demonstrated the TRAIL potency in killing GBM cells alone or in combination with sensitisers, such as proteosome inhibitors, phosphatidylinositol 3-kinase (PI3K) inhibition, IAP antagonist (Boccellato et al., 2021; Hetschko et al., 2008; Lincoln et al., 2018; Opel et al., 2008). Therefore, these combinatorial approaches can be employed in the future to address the heterogenous response of GBM to TRAIL treatment. TRAIL receptor expression level measurements revealed that BBB endothelial cells do express TRAIL receptors in general but TRAILR1 and TRAILR2 are expressed at lower levels than in cancer cells. The TRAIL treatment did not affect the cells despite the presence of TRAIL receptors which was in line with previous studies on apoptosis resistance of BBB cells. The subsequent binding and transport studies using an in vitro BBB model revealed that the ANG2 only positive control proteins can undergo transcytosis regardless of the C- or N-terminal fusion. In contrast to previous studies that have shown no transport of bivalent constructs, it has been shown here that low affinity ANG2 constructs can undergo transcytosis despite the bivalent format. However, TRAIL binding to TRAIL receptors on the BBB endothelial cells interfered with the transport of hexavalent TRAIL fusion proteins. It was reasoned that the lower affinity of ANG2 to Lrp1 and higher sub nanomolar level affinity of TRAIL receptors plays a major role in this interference. However, a TRAIL-masking strategy successfully eliminated this interfering effect. Therefore, as an alternative approach, mutation-mediated TRAIL affinity reduction can be performed for future studies or avidity reduction with trimeric TRAIL receptor agonists that are selectively clustered in

situ at cancer cells can be employed. In fact, various mutations that reduce TRAIL affinities have been established in previous studies (Gasparian et al., 2009). In addition, TRAIL or TRAILR blocking strategies could be considered by using systemic blocking peptides, as utilised in this thesis work. Altogether, it has been demonstrated that high affinity cargo can interfere with the overall transport of the fusion protein and it is important to consider when developing fusion proteins with low affinity BBB shuttle peptides like ANG2.

7 References

Abbott, N. J. (2002). Astrocyte-endothelial interactions and blood-brain barrier permeability. *Journal of Anatomy*, *200*(6), 629–638. https://doi.org/10.1046/j.1469-7580.2002.00064.x

Abbott, N. J., Rönnbäck, L., & Hansson, E. (2006). Astrocyte–endothelial interactions at the blood–brain barrier. *Nature Reviews Neuroscience*, *7*(1), 41–53. https://doi.org/10.1038/nrn1824

Abdul Razzak, R., Florence, G. J., & Gunn-Moore, F. J. (2019). Approaches to CNS Drug Delivery with a Focus on Transporter-Mediated Transcytosis. *International Journal of Molecular Sciences*, *20*(12), E3108. https://doi.org/10.3390/ijms20123108

Abulrob, A., Sprong, H., Van Bergen en Henegouwen, P., & Stanimirovic, D. (2005). The blood-brain barrier transmigrating single domain antibody: Mechanisms of transport and antigenic epitopes in human brain endothelial cells. *Journal of Neurochemistry*, *95*(4), 1201–1214. https://doi.org/10.1111/j.1471-4159.2005.03463.x

Acehan, D., Jiang, X., Morgan, D. G., Heuser, J. E., Wang, X., & Akey, C. W. (2002). Three-dimensional structure of the apoptosome: Implications for assembly, procaspase-9 binding, and activation. *Molecular Cell*, *9*(2), 423–432. https://doi.org/10.1016/s1097-2765(02)00442-2

Agarwal, S., Uchida, Y., Mittapalli, R. K., Sane, R., Terasaki, T., & Elmquist, W. F. (2012). Quantitative Proteomics of Transporter Expression in Brain Capillary Endothelial Cells Isolated from P-Glycoprotein (P-gp), Breast Cancer Resistance Protein (Bcrp), and P-gp/Bcrp Knockout Mice. *Drug Metabolism and Disposition*, *40*(6), 1164–1169.

Alladina, S. J., Song, J. H., Davidge, S. T., Hao, C., & Easton, A. S. (2005). TRAIL-Induced Apoptosis in Human Vascular Endothelium Is Regulated by Phosphatidylinositol 3-Kinase/Akt through the Short Form of Cellular FLIP and Bcl-2. *Journal of Vascular Research*, *42*(4), 337–347. https://doi.org/10.1159/000086599

Alnemri, E. S., Livingston, D. J., Nicholson, D. W., Salvesen, G., Thornberry, N. A., Wong, W. W., & Yuan, J. (1996). Human ICE/CED-3 protease nomenclature. *Cell*, *87*(2), 171. https://doi.org/10.1016/s0092-8674(00)81334-3

Alvarez, J. I., Katayama, T., & Prat, A. (2013). Glial influence on the Blood Brain Barrier. *Glia*, *61*(12), 1939–1958. https://doi.org/10.1002/glia.22575

Appelt-Menzel, A., Cubukova, A., Günther, K., Edenhofer, F., Piontek, J., Krause, G., Stüber, T., Walles, H., Neuhaus, W., & Metzger, M. (2017). Establishment of a Human Blood-Brain Barrier Co-culture Model Mimicking the Neurovascular Unit Using Induced Pluri- and Multipotent Stem Cells. *Stem Cell Reports*, *8*(4), 894–906. https://doi.org/10.1016/j.stemcr.2017.02.021

Armour, K. L., Clark, M. R., Hadley, A. G., & Williamson, L. M. (1999). Recombinant human IgG molecules lacking Fcgamma receptor I binding and monocyte triggering activities. *European Journal of Immunology*, *29*(8), 2613–2624. https://doi.org/10.1002/(SICI)1521-4141(199908)29:08<2613::AID-IMMU2613>3.0.CO;2-J

Ashby, L. S., Smith, K. A., & Stea, B. (2016). Gliadel wafer implantation combined with standard radiotherapy and concurrent followed by adjuvant temozolomide for treatment of newly diagnosed high-grade glioma: A systematic literature review. *World Journal of Surgical Oncology*, *14*(1), 225. https://doi.org/10.1186/s12957-016-0975-5

Ashkenazi, A., & Dixit, V. M. (1998). Death Receptors: Signaling and Modulation. *Science*, *281*(5381), 1305–1308. https://doi.org/10.1126/science.281.5381.1305

Ashkenazi, A., Pai, R. C., Fong, S., Leung, S., Lawrence, D. A., Marsters, S. A., Blackie, C., Chang, L., McMurtrey, A. E., Hebert, A., DeForge, L., Koumenis, I. L., Lewis, D., Harris, L., Bussiere, J., Koeppen, H., Shahrokh, Z., & Schwall, R. H. (1999). Safety and antitumor activity of recombinant soluble Apo2 ligand. *The Journal of Clinical Investigation*, *104*(2), 155–162. https://doi.org/10.1172/JCI6926

Auderset, L., Cullen, C. L., & Young, K. M. (2016). Low Density Lipoprotein-Receptor Related Protein 1 Is Differentially Expressed by Neuronal and Glial Populations in the Developing and Mature Mouse Central Nervous System. *PLOS ONE*, *11*(6), e0155878. https://doi.org/10.1371/journal.pone.0155878

Azijli, K., Weyhenmeyer, B., Peters, G. J., de Jong, S., & Kruyt, F. a. E. (2013). Non-canonical kinase signaling by the death ligand TRAIL in cancer cells: Discord in the death receptor family. *Cell Death & Differentiation*, *20*(7), 858–868. https://doi.org/10.1038/cdd.2013.28

Bagci-Onder, T., Du, W., Figueiredo, J.-L., Martinez-Quintanilla, J., & Shah, K. (2015). Targeting breast to brain metastatic tumours with death receptor ligand expressing therapeutic stem cells. *Brain*, *138*(6), 1710–1721. https://doi.org/10.1093/brain/awv094

Batistella, G. N. de R., Santos, A. J., Paiva, M. A. de, Ferrigno, R., Camargo, V. P. de, Stavale, J. N., & Maldaun, M. V. C. (2021). Approaching glioblastoma during COVID-19 pandemic: Current recommendations and considerations in Brazil. *Arquivos de Neuro-Psiquiatria*, *79*, 167–172. https://doi.org/10.1590/0004-282X-anp-2020-0434

Beck, A., & Reichert, J. M. (2011). Therapeutic Fc-fusion proteins and peptides as successful alternatives to antibodies. *MAbs*, *3*(5), 415–416. https://doi.org/10.4161/mabs.3.5.17334

Begley, D. J. (2004). ABC transporters and the blood-brain barrier. *Current Pharmaceutical Design*, *10*(12), 1295–1312. https://doi.org/10.2174/1381612043384844

Benchenane, K., Berezowski, V., Fernández-Monreal, M., Brillault, J., Valable, S., Dehouck, M.-P., Cecchelli, R., Vivien, D., Touzani, O., & Ali, C. (2005). Oxygen glucose deprivation switches the transport of tPA across the blood-brain barrier from an LRP-dependent to an increased LRP-independent process. *Stroke*, *36*(5), 1065–1070. https://doi.org/10.1161/01.STR.0000163050.39122.4f

Berg, D., Lehne, M., Müller, N., Siegmund, D., Münkel, S., Sebald, W., Pfizenmaier, K., & Wajant, H. (2007). Enforced covalent trimerization increases the activity of the TNF ligand family members TRAIL and CD95L. *Cell Death & Differentiation*, *14*(12), 2021–2034. https://doi.org/10.1038/sj.cdd.4402213

Bertrand, Y., Currie, J.-C., Demeule, M., Régina, A., Ché, C., Abulrob, A., Fatehi, D., Sartelet, H., Gabathuler, R., Castaigne, J.-P., Stanimirovic, D., & Béliveau, R. (2010). Transport characteristics of a novel peptide platform for CNS therapeutics. *Journal of Cellular and Molecular Medicine*, *14*(12), 2827–2839. https://doi.org/10.1111/j.1582-4934.2009.00930.x

Bhuin, T., & Roy, J. K. (2014). Rab proteins: The key regulators of intracellular vesicle transport. *Experimental Cell Research*, *328*(1), 1–19. https://doi.org/10.1016/j.yexcr.2014.07.027

Bien-Ly, N., Yu, Y. J., Bumbaca, D., Elstrott, J., Boswell, C. A., Zhang, Y., Luk, W., Lu, Y., Dennis, M. S., Weimer, R. M., Chung, I., & Watts, R. J. (2014). Transferrin receptor (TfR) trafficking determines brain uptake of TfR antibody affinity variants. *The Journal of Experimental Medicine*, *211*(2), 233–244. https://doi.org/10.1084/jem.20131660

Boado, R. J., Hui, E. K.-W., Lu, J. Z., & Pardridge, W. M. (2012). Glycemic Control and Chronic Dosing of Rhesus Monkeys with a Fusion Protein of Iduronidase and a Monoclonal Antibody Against the Human Insulin Receptor. *Drug Metabolism and Disposition*, *40*(10), 2021–2025. https://doi.org/10.1124/dmd.112.046375

Boado, R. J., & Pardridge, W. M. (2017). Brain and Organ Uptake in the Rhesus Monkey in Vivo of Recombinant Iduronidase Compared to an Insulin Receptor Antibody-Iduronidase Fusion Protein. *Molecular Pharmaceutics*, *14*(4), 1271–1277. https://doi.org/10.1021/acs.molpharmaceut.6b01166

Boado, R. J., Zhang, Y., Zhang, Y., & Pardridge, W. M. (2007). Humanization of anti-human insulin receptor antibody for drug targeting across the human blood–brain barrier. *Biotechnology and Bioengineering*, *96*(2), 381–391. https://doi.org/10.1002/bit.21120

Boado, R. J., Zhang, Y., Zhang, Y., Xia, C.-F., Wang, Y., & Pardridge, W. M. (2008). Genetic engineering of a lysosomal enzyme fusion protein for targeted delivery across the human blood-brain barrier. *Biotechnology and Bioengineering*, *99*(2), 475–484. https://doi.org/10.1002/bit.21602

Bobo, R. H., Laske, D. W., Akbasak, A., Morrison, P. F., Dedrick, R. L., & Oldfield, E. H. (1994). Convection-enhanced delivery of macromolecules in the brain. *Proceedings of the National Academy of Sciences of the United States of America*, *91*(6), 2076–2080. https://doi.org/10.1073/pnas.91.6.2076

Boccellato, C., Kolbe, E., Peters, N., Juric, V., Fullstone, G., Verreault, M., Idbaih, A., Lamfers, M. L. M., Murphy, B. M., & Rehm, M. (2021). Marizomib sensitizes primary glioma cells to apoptosis induced by a latest-generation TRAIL receptor agonist. *Cell Death & Disease*, *12*(7), 1–11. https://doi.org/10.1038/s41419-021-03927-x

Böckenhoff, A., Cramer, S., Wölte, P., Knieling, S., Wohlenberg, C., Gieselmann, V., Galla, H.-J., & Matzner, U. (2014). Comparison of five peptide vectors for improved brain delivery of the lysosomal enzyme arylsulfatase A. *The Journal of Neuroscience: The Official Journal of the Society for Neuroscience*, *34*(9), 3122–3129. https://doi.org/10.1523/JNEUROSCI.4785-13.2014

Bodmer, J. L., Holler, N., Reynard, S., Vinciguerra, P., Schneider, P., Juo, P., Blenis, J., & Tschopp, J. (2000). TRAIL receptor-2 signals apoptosis through FADD and caspase-8. *Nature Cell Biology*, *2*(4), 241–243. https://doi.org/10.1038/35008667

Bodmer, J.-L., Meier, P., Tschopp, J., & Schneider, P. (2000). Cysteine 230 Is Essential for the Structure and Activity of the Cytotoxic Ligand TRAIL *. *Journal of Biological Chemistry*, *275*(27), 20632–20637. https://doi.org/10.1074/jbc.M909721199

Boldin, M. P., Mett, I. L., Varfolomeev, E. E., Chumakov, I., Shemer-Avni, Y., Camonis, J. H., & Wallach, D. (1995). Self-association of the "death domains" of the p55 tumor necrosis factor (TNF) receptor and Fas/APO1 prompts signaling for TNF and Fas/APO1 effects. *The Journal of Biological Chemistry*, *270*(1), 387–391. https://doi.org/10.1074/jbc.270.1.387

Booth, R., & Kim, H. (2012). Characterization of a microfluidic in vitro model of the blood-brain barrier (μBBB). *Lab on a Chip*, *12*(10), 1784–1792. https://doi.org/10.1039/C2LC40094D

Boucher, P., & Herz, J. (2011). Signaling through LRP1: Protection from atherosclerosis and beyond. *Biochemical Pharmacology*, *81*(1), 1–5. https://doi.org/10.1016/j.bcp.2010.09.018

Bremer, E., Samplonius, D., Kroesen, B.-J., van Genne, L., de Leij, L., & Helfrich, W. (2004). Exceptionally Potent Anti-Tumor Bystander Activity of an scFv:sTRAIL Fusion Protein with Specificity for EGP2 Toward Target Antigen-Negative Tumor Cells. *Neoplasia*, *6*(5), 636–645. https://doi.org/10.1593/neo.04229

Brennan, C. W., Verhaak, R. G. W., McKenna, A., Campos, B., Noushmehr, H., Salama, S. R., Zheng, S., Chakravarty, D., Sanborn, J. Z., Berman, S. H., Beroukhim, R., Bernard, B., Wu, C.-J., Genovese, G., Shmulevich, I., Barnholtz-Sloan, J., Zou, L., Vegesna, R., Shukla, S. A., … TCGA Research Network. (2013). The somatic genomic landscape of glioblastoma. *Cell*, *155*(2), 462–477. https://doi.org/10.1016/j.cell.2013.09.034

Bres, E. E., & Faissner, A. (2019). Low Density Receptor-Related Protein 1 Interactions With the Extracellular Matrix: More Than Meets the Eye. *Frontiers in Cell and Developmental Biology*, *7*, 31. https://doi.org/10.3389/fcell.2019.00031

Brown, R. C., Morris, A. P., & O'Neil, R. G. (2007). TIGHT JUNCTION PROTEIN EXPRESSION AND BARRIER PROPERTIES OF IMMORTALIZED MOUSE BRAIN MICROVESSEL ENDOTHELIAL CELLS. *Brain Research*, *1130*(1), 17–30. https://doi.org/10.1016/j.brainres.2006.10.083

Burz, C., Berindan-Neagoe, I., Balacescu, O., & Irimie, A. (2009). Apoptosis in cancer: Key molecular signaling pathways and therapy targets. *Acta Oncologica*, *48*(6), 811–821. https://doi.org/10.1080/02841860902974175

Butt, A. M., Jones, H. C., & Abbott, N. J. (1990). Electrical resistance across the blood-brain barrier in anaesthetized rats: A developmental study. *The Journal of Physiology*, *429*, 47–62.

Cann, S. A. H., Netten, J. P. van, & Netten, C. van. (2003). Dr William Coley and tumour regression: A place in history or in the future. *Postgraduate Medical Journal*, *79*(938), 672–680.

Carneiro, B. A., & El-Deiry, W. S. (2020). Targeting apoptosis in cancer therapy. *Nature Reviews Clinical Oncology*, *17*(7), 395–417. https://doi.org/10.1038/s41571-020-0341-y

Carpentier, A., Canney, M., Vignot, A., Reina, V., Beccaria, K., Horodyckid, C., Karachi, C., Leclercq, D., Lafon, C., Chapelon, J.-Y., Capelle, L., Cornu, P., Sanson, M., Hoang-Xuan, K., Delattre, J.-Y., & Idbaih, A. (2016). Clinical trial of blood-brain barrier disruption by pulsed ultrasound. *Science Translational Medicine*, *8*(343), 343re2. https://doi.org/10.1126/scitranslmed.aaf6086

Carswell, E. A., Old, L. J., Kassel, R. L., Green, S., Fiore, N., & Williamson, B. (1975). An endotoxin-induced serum factor that causes necrosis of tumors. *Proceedings of the National Academy of Sciences of the United States of America*, *72*(9), 3666–3670. https://doi.org/10.1073/pnas.72.9.3666

Cha, S.-S., Kim, M.-S., Choi, Y. H., Sung, B.-J., Shin, N. K., Shin, H.-C., Sung, Y. C., & Oh, B.-H. (1999). 2.8 Å Resolution Crystal Structure of Human TRAIL, a Cytokine with Selective Antitumor Activity. *Immunity*, *11*(2), 253–261. https://doi.org/10.1016/S1074-7613(00)80100-4

Chakrabarti, I., Cockburn, M., Cozen, W., Wang, Y.-P., & Preston-Martin, S. (2005). A population-based description of glioblastoma multiforme in Los Angeles County, 1974-1999. *Cancer*, *104*(12), 2798–2806. https://doi.org/10.1002/cncr.21539

Chakravarti, A., Dicker, A., & Mehta, M. (2004). The contribution of epidermal growth factor receptor (EGFR) signaling pathway to radioresistance in human gliomas: A review of preclinical and correlative clinical data. *International Journal of Radiation Oncology, Biology, Physics*, *58*(3), 927–931. https://doi.org/10.1016/j.ijrobp.2003.09.092

Chang, D. W., Xing, Z., Capacio, V. L., Peter, M. E., & Yang, X. (2003). Interdimer processing mechanism of procaspase-8 activation. *The EMBO Journal*, *22*(16), 4132–4142. https://doi.org/10.1093/emboj/cdg414

Chang, D. W., Xing, Z., Pan, Y., Algeciras-Schimnich, A., Barnhart, B. C., Yaish-Ohad, S., Peter, M. E., & Yang, X. (2002). C-FLIP(L) is a dual function regulator for caspase-8 activation and CD95-mediated apoptosis. *The EMBO Journal*, *21*(14), 3704–3714. https://doi.org/10.1093/emboj/cdf356

Chao, D. T., & Korsmeyer, S. J. (1998). BCL-2 FAMILY: Regulators of Cell Death. *Annual Review of Immunology*, *16*(1), 395–419. https://doi.org/10.1146/annurev.immunol.16.1.395

Chen, P.-L., & Easton, A. S. (2010). Evidence that tumor necrosis factor-related apoptosis inducing ligand (TRAIL) inhibits angiogenesis by inducing vascular endothelial cell apoptosis. *Biochemical and Biophysical Research Communications*, *391*(1), 936–941. https://doi.org/10.1016/j.bbrc.2009.11.168

Chinnaiyan, A. M., O'Rourke, K., Tewari, M., & Dixit, V. M. (1995). FADD, a novel death domain-containing protein, interacts with the death domain of Fas and initiates apoptosis. *Cell*, *81*(4), 505–512. https://doi.org/10.1016/0092-8674(95)90071-3

Chinot, O. L., Wick, W., Mason, W., Henriksson, R., Saran, F., Nishikawa, R., Carpentier, A. F., Hoang-Xuan, K., Kavan, P., Cernea, D., Brandes, A. A., Hilton, M., Abrey, L., & Cloughesy, T. (2014). Bevacizumab plus radiotherapy-temozolomide for newly diagnosed glioblastoma. *The New England Journal of Medicine*, *370*(8), 709–722. https://doi.org/10.1056/NEJMoa1308345

Choo, Z., Loh, A. H. P., & Chen, Z. X. (2019). Destined to Die: Apoptosis and Pediatric Cancers. *Cancers*, *11*(11), 1623. https://doi.org/10.3390/cancers11111623

Chowdhary, S. A., Ryken, T., & Newton, H. B. (2015). Survival outcomes and safety of carmustine wafers in the treatment of high-grade gliomas: A meta-analysis. *Journal of Neuro-Oncology*, *122*(2), 367–382. https://doi.org/10.1007/s11060-015-1724-2

Claes, A., Idema, A. J., & Wesseling, P. (2007). Diffuse glioma growth: A guerilla war. *Acta Neuropathologica*, *114*(5), 443–458. https://doi.org/10.1007/s00401-007-0293-7

Clancy, L., Mruk, K., Archer, K., Woelfel, M., Mongkolsapaya, J., Screaton, G., Lenardo, M. J., & Chan, F. K.-M. (2005). Preligand assembly domain-mediated ligand-independent association between TRAIL receptor 4 (TR4) and TR2 regulates TRAIL-induced apoptosis. *Proceedings of the National Academy of Sciences*, *102*(50), 18099–18104. https://doi.org/10.1073/pnas.0507329102

Clark, D. E. (2003). In silico prediction of blood-brain barrier permeation. *Drug Discovery Today*, *8*(20), 927–933. https://doi.org/10.1016/s1359-6446(03)02827-7

Clawson, C. C., Hartmann, J. F., & Vernier, R. L. (1966). Electron microscopy of the effect of gram-negative endotoxin on the blood-brain barrier. *Journal of Comparative Neurology*, *127*(2), 183–197. https://doi.org/10.1002/cne.901270204

Cloughesy, T. F., Cavenee, W. K., & Mischel, P. S. (2014). Glioblastoma: From molecular pathology to targeted treatment. *Annual Review of Pathology*, *9*, 1–25. https://doi.org/10.1146/annurev-pathol-011110-130324

Cohen, G. M. (1997). Caspases: The executioners of apoptosis. *The Biochemical Journal*, *326 (Pt 1)*, 1–16. https://doi.org/10.1042/bj3260001

Coley, W. B. (1891). II. Contribution to the Knowledge of Sarcoma. *Annals of Surgery*, *14*(3), 199–220. https://doi.org/10.1097/00000658-189112000-00015

Comer, J., & Tam, K. (2001). Lipophilicity Profiles: Theory and Measurement. In *Pharmacokinetic Optimization in Drug Research* (pp. 275–304). John Wiley & Sons, Ltd. https://doi.org/10.1002/9783906390437.ch17

Cummins, P. M. (2011). Occludin: One Protein, Many Forms. *Molecular and Cellular Biology*. https://doi.org/10.1128/MCB.06029-11

Daneman, R., & Prat, A. (2015). The Blood–Brain Barrier. *Cold Spring Harbor Perspectives in Biology*, *7*(1), a020412. https://doi.org/10.1101/cshperspect.a020412

D'Arcy, M. S. (2019). Cell death: A review of the major forms of apoptosis, necrosis and autophagy. *Cell Biology International*, *43*(6), 582–592. https://doi.org/10.1002/cbin.11137

de Miguel, D., Lemke, J., Anel, A., Walczak, H., & Martinez-Lostao, L. (2016). Onto better TRAILs for cancer treatment. *Cell Death and Differentiation*, *23*(5), 733–747. https://doi.org/10.1038/cdd.2015.174

Degli-Esposti, M. A., Dougall, W. C., Smolak, P. J., Waugh, J. Y., Smith, C. A., & Goodwin, R. G. (1997). The novel receptor TRAIL-R4 induces NF-kappaB and protects against TRAIL-mediated apoptosis, yet retains an incomplete death domain. *Immunity*, *7*(6), 813–820. https://doi.org/10.1016/s1074-7613(00)80399-4

Degli-Esposti, M. A., Smolak, P. J., Walczak, H., Waugh, J., Huang, C. P., DuBose, R. F., Goodwin, R. G., & Smith, C. A. (1997). Cloning and characterization of TRAIL-R3, a novel member of the emerging TRAIL receptor family. *The Journal of Experimental Medicine*, *186*(7), 1165–1170. https://doi.org/10.1084/jem.186.7.1165

Demeule, M., Currie, J.-C., Bertrand, Y., Ché, C., Nguyen, T., Régina, A., Gabathuler, R., Castaigne, J.-P., & Béliveau, R. (2008). Involvement of the low-density lipoprotein receptor-related protein in the transcytosis of the brain delivery vector angiopep-2. *Journal of Neurochemistry*, *106*(4), 1534–1544. https://doi.org/10.1111/j.1471-4159.2008.05492.x

Demeule, M., Régina, A., Ché, C., Poirier, J., Nguyen, T., Gabathuler, R., Castaigne, J.-P., & Béliveau, R. (2008). Identification and design of peptides as a new drug delivery system for the brain. *The Journal of Pharmacology and Experimental Therapeutics*, *324*(3), 1064–1072. https://doi.org/10.1124/jpet.107.131318

Denny, B. J., Wheelhouse, R. T., Stevens, M. F., Tsang, L. L., & Slack, J. A. (1994). NMR and molecular modeling investigation of the mechanism of activation of the antitumor drug temozolomide and its interaction with DNA. *Biochemistry*, *33*(31), 9045–9051. https://doi.org/10.1021/bi00197a003

Deveraux, Q. L., & Reed, J. C. (1999). IAP family proteins—Suppressors of apoptosis. *Genes & Development*, *13*(3), 239–252.

Di Bartolo, B. A., Cartland, S. P., Prado-Lourenco, L., Griffith, T. S., Gentile, C., Ravindran, J., Azahri, N. S. M., Thai, T., Yeung, A. W. S., Thomas, S. R., & Kavurma, M. M. (2015). Tumor Necrosis Factor-Related Apoptosis-Inducing Ligand (TRAIL) Promotes Angiogenesis and Ischemia-Induced Neovascularization Via NADPH Oxidase 4 (NOX4) and Nitric Oxide-Dependent Mechanisms. *Journal of the American Heart Association*, *4*(11), e002527. https://doi.org/10.1161/JAHA.115.002527

Dickens, L. S., Boyd, R. S., Jukes-Jones, R., Hughes, M. A., Robinson, G. L., Fairall, L., Schwabe, J. W. R., Cain, K., & Macfarlane, M. (2012). A death effector domain chain DISC model reveals a crucial role for caspase-8 chain assembly in mediating apoptotic cell death. *Molecular Cell*, *47*(2), 291–305. https://doi.org/10.1016/j.molcel.2012.05.004

Dillekås, H., Rogers, M. S., & Straume, O. (2019). Are 90% of deaths from cancer caused by metastases? *Cancer Medicine*, *8*(12), 5574–5576. https://doi.org/10.1002/cam4.2474

Dong, H., Pang, L., Cong, H., Shen, Y., & Yu, B. (2019). Application and design of esterase-responsive nanoparticles for cancer therapy. *Drug Delivery*, *26*(1), 416–432. https://doi.org/10.1080/10717544.2019.1588424

Donson, A. M., Addo-Yobo, S. O., Handler, M. H., Gore, L., & Foreman, N. K. (2007). MGMT promoter methylation correlates with survival benefit and sensitivity to temozolomide in pediatric glioblastoma. *Pediatric Blood & Cancer*, *48*(4), 403–407. https://doi.org/10.1002/pbc.20803

Dorsey, J. F., Mintz, A., Tian, X., Dowling, M. L., Plastaras, J. P., Dicker, D. T., Kao, G. D., & El-Deiry, W. S. (2009). Tumor necrosis factor-related apoptosis-inducing ligand (TRAIL) and paclitaxel have cooperative in vivo effects against glioblastoma multiforme cells. *Molecular Cancer Therapeutics*, *8*(12), 3285–3295. https://doi.org/10.1158/1535-7163.MCT-09-0415

Du, C., Fang, M., Li, Y., Li, L., & Wang, X. (2000). Smac, a mitochondrial protein that promotes cytochrome c-dependent caspase activation by eliminating IAP inhibition. *Cell*, *102*(1), 33–42. https://doi.org/10.1016/s0092-8674(00)00008-8

Duffy, K. R., Pardridge, W. M., & Rosenfeld, R. G. (1988). Human blood-brain barrier insulin-like growth factor receptor. *Metabolism: Clinical and Experimental*, *37*(2), 136–140. https://doi.org/10.1016/s0026-0495(98)90007-5

Dunn, G. P., Rinne, M. L., Wykosky, J., Genovese, G., Quayle, S. N., Dunn, I. F., Agarwalla, P. K., Chheda, M. G., Campos, B., Wang, A., Brennan, C., Ligon, K. L., Furnari, F., Cavenee, W. K., Depinho, R. A., Chin, L., & Hahn, W. C. (2012). Emerging insights into the molecular and cellular basis of glioblastoma. *Genes & Development*, *26*(8), 756–784. https://doi.org/10.1101/gad.187922.112

Egaña, L., Auzmendi-Iriarte, J., Andermatten, J., Villanua, J., Ruiz, I., Elua-Pinin, A., Aldaz, P., Querejeta, A., Sarasqueta, C., Zubia, F., Matheu, A., & Samprón, N. (2020). Methylation of MGMT promoter does not predict response to temozolomide in patients with glioblastoma in Donostia Hospital. *Scientific Reports*, *10*(1), 18445. https://doi.org/10.1038/s41598-020-75477-9

Ehrlich, P. (1885). *Das Sauerstoff-Bedürfniss des Organismus: Eine farbenanalytische Studie*. A. Hirschwald.

Eigenbrod, S., Trabold, R., Brucker, D., Erös, C., Egensperger, R., La Fougere, C., Göbel, W., Rühm, A., Kretzschmar, H. A., Tonn, J. C., Herms, J., Giese, A., & Kreth, F. W. (2014). Molecular stereotactic biopsy technique improves diagnostic accuracy and enables personalized treatment strategies in glioma patients. *Acta Neurochirurgica*, *156*(8), 1427–1440. https://doi.org/10.1007/s00701-014-2073-1

Ellingson, B. M., Wen, P. Y., & Cloughesy, T. F. (2017). Modified Criteria for Radiographic Response Assessment in Glioblastoma Clinical Trials. *Neurotherapeutics*, *14*(2), 307–320. https://doi.org/10.1007/s13311-016-0507-6

Ellis, H. M., & Horvitz, H. R. (1986). Genetic control of programmed cell death in the nematode C. elegans. *Cell*, *44*(6), 817–829. https://doi.org/10.1016/0092-8674(86)90004-8

Elmore, S. (2007). Apoptosis: A Review of Programmed Cell Death. *Toxicologic Pathology*, *35*(4), 495–516. https://doi.org/10.1080/01926230701320337

Emery, J. G., McDonnell, P., Burke, M. B., Deen, K. C., Lyn, S., Silverman, C., Dul, E., Appelbaum, E. R., Eichman, C., DiPrinzio, R., Dodds, R. A., James, I. E., Rosenberg, M., Lee, J. C., & Young, P. R. (1998). Osteoprotegerin is a receptor for the cytotoxic ligand TRAIL. *The Journal of Biological Chemistry*, *273*(23), 14363–14367. https://doi.org/10.1074/jbc.273.23.14363

Fadok, V. A., Bratton, D. L., Konowal, A., Freed, P. W., Westcott, J. Y., & Henson, P. M. (1998). Macrophages that have ingested apoptotic cells in vitro inhibit proinflammatory cytokine production through autocrine/paracrine mechanisms involving TGF-beta, PGE2, and PAF. *The Journal of Clinical Investigation*, *101*(4), 890–898. https://doi.org/10.1172/JCI1112

Fan, T.-J., Han, L.-H., Cong, R.-S., & Liang, J. (2005). Caspase Family Proteases and Apoptosis. *Acta Biochimica et Biophysica Sinica*, *37*(11), 719–727. https://doi.org/10.1111/j.1745-7270.2005.00108.x

Fan, Y., Zhang, W., & Mulholland, M. (2005). Thrombin and PAR-1-AP increase proinflammatory cytokine expression in C6 cells. *The Journal of Surgical Research*, *129*(2), 196–201. https://doi.org/10.1016/j.jss.2005.07.041

Fanger, N. A., Maliszewski, C. R., Schooley, K., & Griffith, T. S. (1999). Human Dendritic Cells Mediate Cellular Apoptosis via Tumor Necrosis Factor–Related Apoptosis-Inducing Ligand (Trail). *The Journal of Experimental Medicine*, *190*(8), 1155–1164.

Fanning, A. S., Jameson, B. J., Jesaitis, L. A., & Anderson, J. M. (1998). The tight junction protein ZO-1 establishes a link between the transmembrane protein occludin and the actin cytoskeleton. *The Journal of Biological Chemistry*, *273*(45), 29745–29753. https://doi.org/10.1074/jbc.273.45.29745

Farrington, G. K., Caram-Salas, N., Haqqani, A. S., Brunette, E., Eldredge, J., Pepinsky, B., Antognetti, G., Baumann, E., Ding, W., Garber, E., Jiang, S., Delaney, C., Boileau, E., Sisk, W. P., & Stanimirovic, D. B. (2014). A novel platform for engineering blood-brain barrier-crossing bispecific biologics. *The FASEB Journal*, *28*(11), 4764–4778. https://doi.org/10.1096/fj.14-253369

Feng, H., Hu, B., Vuori, K., Sarkaria, J. N., Furnari, F. B., Cavenee, W. K., & Cheng, S.-Y. (2014). EGFRvIII stimulates glioma growth and invasion through PKA-dependent serine phosphorylation of Dock180. *Oncogene*, *33*(19), 2504–2512. https://doi.org/10.1038/onc.2013.198

Fiala, M., Looney, D. J., Stins, M., Way, D. D., Zhang, L., Gan, X., Chiappelli, F., Schweitzer, E. S., Shapshak, P., Weinand, M., Graves, M. C., Witte, M., & Kim, K. S. (1997). TNF-alpha opens

a paracellular route for HIV-1 invasion across the blood-brain barrier. *Molecular Medicine (Cambridge, Mass.)*, *3*(8), 553–564.

Fischer, H., Gottschlich, R., & Seelig, A. (1998). Blood-brain barrier permeation: Molecular parameters governing passive diffusion. *The Journal of Membrane Biology*, *165*(3), 201–211. https://doi.org/10.1007/s002329900434

Fox, J. L., Hughes, M. A., Meng, X., Sarnowska, N. A., Powley, I. R., Jukes-Jones, R., Dinsdale, D., Ragan, T. J., Fairall, L., Schwabe, J. W. R., Morone, N., Cain, K., & MacFarlane, M. (2021). Cryo-EM structural analysis of FADD:Caspase-8 complexes defines the catalytic dimer architecture for co-ordinated control of cell fate. *Nature Communications*, *12*(1), 819. https://doi.org/10.1038/s41467-020-20806-9

Fu, T.-M., Li, Y., Lu, A., Li, Z., Vajjhala, P. R., Cruz, A. C., Srivastava, D. B., DiMaio, F., Penczek, P. A., Siegel, R. M., Stacey, K. J., Egelman, E. H., & Wu, H. (2016). Cryo-EM Structure of Caspase-8 Tandem DED Filament Reveals Assembly and Regulation Mechanisms of the Death Inducing Signaling Complex. *Molecular Cell*, *64*(2), 236–250. https://doi.org/10.1016/j.molcel.2016.09.009

Fujisawa, H., Reis, R. M., Nakamura, M., Colella, S., Yonekawa, Y., Kleihues, P., & Ohgaki, H. (2000). Loss of heterozygosity on chromosome 10 is more extensive in primary (de novo) than in secondary glioblastomas. *Laboratory Investigation; a Journal of Technical Methods and Pathology*, *80*(1), 65–72. https://doi.org/10.1038/labinvest.3780009

Fulda, S., Wick, W., Weller, M., & Debatin, K.-M. (2002). Smac agonists sensitize for Apo2L/TRAIL- or anticancer drug-induced apoptosis and induce regression of malignant glioma in vivo. *Nature Medicine*, *8*(8), 808–815. https://doi.org/10.1038/nm735

Furuse, M. (2010). Molecular Basis of the Core Structure of Tight Junctions. *Cold Spring Harbor Perspectives in Biology*, *2*(1), a002907. https://doi.org/10.1101/cshperspect.a002907

Furuse, M., Fujita, K., Hiiragi, T., Fujimoto, K., & Tsukita, S. (1998). Claudin-1 and -2: Novel integral membrane proteins localizing at tight junctions with no sequence similarity to occludin. *The Journal of Cell Biology*, *141*(7), 1539–1550. https://doi.org/10.1083/jcb.141.7.1539

Furuse, M., Hirase, T., Itoh, M., Nagafuchi, A., Yonemura, S., Tsukita, S., & Tsukita, S. (1993). Occludin: A novel integral membrane protein localizing at tight junctions. *The Journal of Cell Biology*, *123*(6 Pt 2), 1777–1788. https://doi.org/10.1083/jcb.123.6.1777

Gabathuler, R. (2010). Approaches to transport therapeutic drugs across the blood–brain barrier to treat brain diseases. *Neurobiology of Disease*, *37*(1), 48–57. https://doi.org/10.1016/j.nbd.2009.07.028

Ganten, T. M., Koschny, R., Sykora, J., Schulze-Bergkamen, H., Büchler, P., Haas, T. L., Schader, M. B., Untergasser, A., Stremmel, W., & Walczak, H. (2006). Wng. *Clinical Cancer Research*, *12*(8), 2640–2646. https://doi.org/10.1158/1078-0432.CCR-05-2635

Gasparian, M. E., Chernyak, B. V., Dolgikh, D. A., Yagolovich, A. V., Popova, E. N., Sycheva, A. M., Moshkovskii, S. A., & Kirpichnikov, M. P. (2009). Generation of new TRAIL mutants DR5-A and DR5-B with improved selectivity to death receptor 5. *Apoptosis: An International Journal on Programmed Cell Death*, *14*(6), 778–787. https://doi.org/10.1007/s10495-009-0349-3

Gieffers, C., Kluge, M., Merz, C., Sykora, J., Thiemann, M., Schaal, R., Fischer, C., Branschädel, M., Abhari, B. A., Hohenberger, P., Fulda, S., Fricke, H., & Hill, O. (2013). APG350 induces superior clustering of TRAIL receptors and shows therapeutic antitumor efficacy independent of cross-linking via Fcγ receptors. *Molecular Cancer Therapeutics*, *12*(12), 2735–2747. https://doi.org/10.1158/1535-7163.MCT-13-0323

Gilbert, M. R., Sulman, E. P., & Mehta, M. P. (2014). Bevacizumab for newly diagnosed glioblastoma. *The New England Journal of Medicine*, *370*(21), 2048–2049. https://doi.org/10.1056/NEJMc1403303

Goldstein, G. W., & Betz, A. L. (1986). The Blood-Brain Barrier. *Scientific American*, *255*(3), 74–83.

Graves, J. D., Kordich, J. J., Huang, T.-H., Piasecki, J., Bush, T. L., Sullivan, T., Foltz, I. N., Chang, W., Douangpanya, H., Dang, T., O'Neill, J. W., Mallari, R., Zhao, X., Branstetter, D. G., Rossi, J. M., Long, A. M., Huang, X., & Holland, P. M. (2014). Apo2L/TRAIL and the death receptor 5 agonist antibody AMG 655 cooperate to promote receptor clustering and antitumor activity. *Cancer Cell*, *26*(2), 177–189. https://doi.org/10.1016/j.ccr.2014.04.028

Greene, C., & Campbell, M. (2016). Tight junction modulation of the blood brain barrier: CNS delivery of small molecules. *Tissue Barriers*, *4*(1), e1138017. https://doi.org/10.1080/21688370.2015.1138017

Griffith, T. S., Wiley, S. R., Kubin, M. Z., Sedger, L. M., Maliszewski, C. R., & Fanger, N. A. (1999). Monocyte-mediated tumoricidal activity via the tumor necrosis factor-related cytokine, TRAIL. *The Journal of Experimental Medicine*, *189*(8), 1343–1354. https://doi.org/10.1084/jem.189.8.1343

Gude, D. R., Alvarez, S. E., Paugh, S. W., Mitra, P., Yu, J., Griffiths, R., Barbour, S. E., Milstien, S., & Spiegel, S. (2008). Apoptosis induces expression of sphingosine kinase 1 to release sphingosine-1-phosphate as a "come-and-get-me" signal. *The FASEB Journal*, *22*(8), 2629–2638. https://doi.org/10.1096/fj.08-107169

Guicciardi, M. E., & Gores, G. J. (2009). Life and death by death receptors. *The FASEB Journal*, *23*(6), 1625–1637. https://doi.org/10.1096/fj.08-111005

Hannun, Y. A. (1997). Apoptosis and the dilemma of cancer chemotherapy. *Blood*, *89*(6), 1845–1853.

Haqqani, A. S., Delaney, C. E., Brunette, E., Baumann, E., Farrington, G. K., Sisk, W., Eldredge, J., Ding, W., Tremblay, T.-L., & Stanimirovic, D. B. (2018). Endosomal trafficking regulates receptor-mediated transcytosis of antibodies across the blood brain barrier. *Journal of Cerebral Blood Flow & Metabolism*, *38*(4), 727–740. https://doi.org/10.1177/0271678X17740031

Haqqani, A. S., Thom, G., Burrell, M., Delaney, C. E., Brunette, E., Baumann, E., Sodja, C., Jezierski, A., Webster, C., & Stanimirovic, D. B. (2018). Intracellular sorting and transcytosis of the rat transferrin receptor antibody OX26 across the blood-brain barrier in vitro is dependent on its binding affinity. *Journal of Neurochemistry*, *146*(6), 735–752. https://doi.org/10.1111/jnc.14482

Harper, N., Farrow, S. N., Kaptein, A., Cohen, G. M., & MacFarlane, M. (2001). Modulation of Tumor Necrosis Factor Apoptosis-inducing Ligand- induced NF-κB Activation by Inhibition of Apical Caspases*. *Journal of Biological Chemistry*, *276*(37), 34743–34752. https://doi.org/10.1074/jbc.M105693200

Hawkins, B. T., & Davis, T. P. (2005). The blood-brain barrier/neurovascular unit in health and disease. *Pharmacological Reviews*, *57*(2), 173–185. https://doi.org/10.1124/pr.57.2.4

Hegi, M. E., Diserens, A.-C., Gorlia, T., Hamou, M.-F., de Tribolet, N., Weller, M., Kros, J. M., Hainfellner, J. A., Mason, W., Mariani, L., Bromberg, J. E. C., Hau, P., Mirimanoff, R. O., Cairncross, J. G., Janzer, R. C., & Stupp, R. (2005). MGMT gene silencing and benefit from temozolomide in glioblastoma. *The New England Journal of Medicine*, *352*(10), 997–1003. https://doi.org/10.1056/NEJMoa043331

Hengartner, M. O., Ellis, R., & Horvitz, R. (1992). Caenorhabditis elegans gene ced-9 protects cells from programmed cell death. *Nature*, *356*(6369), 494–499. https://doi.org/10.1038/356494a0

Hengartner, M. O., & Horvitz, H. R. (1994). C. elegans cell survival gene ced-9 encodes a functional homolog of the mammalian proto-oncogene bcl-2. *Cell*, *76*(4), 665–676. https://doi.org/10.1016/0092-8674(94)90506-1

Herbst, R. S., Eckhardt, S. G., Kurzrock, R., Ebbinghaus, S., O'Dwyer, P. J., Gordon, M. S., Novotny, W., Goldwasser, M. A., Tohnya, T. M., Lum, B. L., Ashkenazi, A., Jubb, A. M., & Mendelson, D. S. (2010). Phase I dose-escalation study of recombinant human Apo2L/TRAIL, a dual proapoptotic receptor agonist, in patients with advanced cancer. *Journal of Clinical Oncology: Official Journal of the American Society of Clinical Oncology*, *28*(17), 2839–2846. https://doi.org/10.1200/JCO.2009.25.1991

Hervé, F., Ghinea, N., & Scherrmann, J.-M. (2008). CNS delivery via adsorptive transcytosis. *The AAPS Journal*, *10*(3), 455–472. https://doi.org/10.1208/s12248-008-9055-2

Hervey-Jumper, S. L., & Berger, M. S. (2016). Maximizing safe resection of low- and high-grade glioma. *Journal of Neuro-Oncology*, *130*(2), 269–282. https://doi.org/10.1007/s11060-016-2110-4

Herz, J., & Bock, H. H. (2002). Lipoprotein receptors in the nervous system. *Annual Review of Biochemistry*, *71*, 405–434. https://doi.org/10.1146/annurev.biochem.71.110601.135342

Herz, J., Hamann, U., Rogne, S., Myklebost, O., Gausepohl, H., & Stanley, K. K. (1988). Surface location and high affinity for calcium of a 500-kd liver membrane protein closely related to

the LDL-receptor suggest a physiological role as lipoprotein receptor. *The EMBO Journal*, *7*(13), 4119–4127.

Herz, J., Kowal, R. C., Goldstein, J. L., & Brown, M. S. (1990). Proteolytic processing of the 600 kd low density lipoprotein receptor-related protein (LRP) occurs in a trans-Golgi compartment. *The EMBO Journal*, *9*(6), 1769–1776.

Herz, J., & Strickland, D. K. (2001). LRP: A multifunctional scavenger and signaling receptor. *The Journal of Clinical Investigation*, *108*(6), 779–784. https://doi.org/10.1172/JCI13992

Hetschko, H., Voss, V., Seifert, V., Prehn, J. H. M., & Kögel, D. (2008). Upregulation of DR5 by proteasome inhibitors potently sensitizes glioma cells to TRAIL-induced apoptosis. *The FEBS Journal*, *275*(8), 1925–1936. https://doi.org/10.1111/j.1742-4658.2008.06351.x

Hilliard, B., Wilmen, A., Seidel, C., Liu, T.-S. T., Göke, R., & Chen, Y. (2001). Roles of TNF-Related Apoptosis-Inducing Ligand in Experimental Autoimmune Encephalomyelitis. *The Journal of Immunology*, *166*(2), 1314–1319. https://doi.org/10.4049/jimmunol.166.2.1314

Hira, V. V. V., Aderetti, D. A., & van Noorden, C. J. F. (2018). Glioma Stem Cell Niches in Human Glioblastoma Are Periarteriolar. *Journal of Histochemistry & Cytochemistry*, *66*(5), 349–358. https://doi.org/10.1369/0022155417752676

Hirase, T., Staddon, J. M., Saitou, M., Ando-Akatsuka, Y., Itoh, M., Furuse, M., Fujimoto, K., Tsukita, S., & Rubin, L. L. (1997). Occludin as a possible determinant of tight junction permeability in endothelial cells. *Journal of Cell Science*, *110 (Pt 14)*, 1603–1613.

Huang, P. H., Xu, A. M., & White, F. M. (2009). Oncogenic EGFR Signaling Networks in Glioma. *Science Signaling*, *2*(87), re6–re6. https://doi.org/10.1126/scisignal.287re6

Huang, S., Li, J., Han, L., Liu, S., Ma, H., Huang, R., & Jiang, C. (2011). Dual targeting effect of Angiopep-2-modified, DNA-loaded nanoparticles for glioma. *Biomaterials*, *32*(28), 6832–6838. https://doi.org/10.1016/j.biomaterials.2011.05.064

Huber, J. D., Egleton, R. D., & Davis, T. P. (2001). Molecular physiology and pathophysiology of tight junctions in the blood–brain barrier. *Trends in Neurosciences*, *24*(12), 719–725. https://doi.org/10.1016/S0166-2236(00)02004-X

Hughes, M. A., Harper, N., Butterworth, M., Cain, K., Cohen, G. M., & MacFarlane, M. (2009). Reconstitution of the death-inducing signaling complex reveals a substrate switch that determines CD95-mediated death or survival. *Molecular Cell*, *35*(3), 265–279. https://doi.org/10.1016/j.molcel.2009.06.012

Hughes, M. A., Powley, I. R., Jukes-Jones, R., Horn, S., Feoktistova, M., Fairall, L., Schwabe, J. W. R., Leverkus, M., Cain, K., & MacFarlane, M. (2016). Co-operative and Hierarchical Binding of c-FLIP and Caspase-8: A Unified Model Defines How c-FLIP Isoforms Differentially Control Cell Fate. *Molecular Cell*, *61*(6), 834–849. https://doi.org/10.1016/j.molcel.2016.02.023

Humphreys, L. M., Fox, J. P., Higgins, C. A., Majkut, J., Sessler, T., McLaughlin, K., McCann, C., Roberts, J. Z., Crawford, N. T., McDade, S. S., Scott, C. J., Harrison, T., & Longley, D. B. (2020). A revised model of TRAIL-R2 DISC assembly explains how FLIP(L) can inhibit or promote apoptosis. *EMBO Reports*, *21*(3), e49254. https://doi.org/10.15252/embr.201949254

Hutt, M. (2017). *Multivalent antibody-scTRAIL fusion proteins for tumor therapy: Impact of format and targeting*. https://doi.org/10.18419/opus-9095

Hutt, M., Marquardt, L., Seifert, O., Siegemund, M., Müller, I., Kulms, D., Pfizenmaier, K., & Kontermann, R. E. (2017). Superior Properties of Fc-comprising scTRAIL Fusion Proteins. *Molecular Cancer Therapeutics*, *16*(12), 2792–2802. https://doi.org/10.1158/1535-7163.MCT-17-0551

Hymowitz, S. G., O'Connell, M. P., Ultsch, M. H., Hurst, A., Totpal, K., Ashkenazi, A., de Vos, A. M., & Kelley, R. F. (2000). A unique zinc-binding site revealed by a high-resolution X-ray structure of homotrimeric Apo2L/TRAIL. *Biochemistry*, *39*(4), 633–640. https://doi.org/10.1021/bi992242l

Idbaih, A., Canney, M., Belin, L., Desseaux, C., Vignot, A., Bouchoux, G., Asquier, N., Law-Ye, B., Leclercq, D., Bissery, A., De Rycke, Y., Trosch, C., Capelle, L., Sanson, M., Hoang-Xuan, K., Dehais, C., Houillier, C., Laigle-Donadey, F., Mathon, B., … Carpentier, A. (2019). Safety and Feasibility of Repeated and Transient Blood-Brain Barrier Disruption by Pulsed Ultrasound in Patients with Recurrent Glioblastoma. *Clinical Cancer Research: An Official*

Journal of the American Association for Cancer Research, *25*(13), 3793–3801. https://doi.org/10.1158/1078-0432.CCR-18-3643

Itoh, M., Morita, K., & Tsukita, S. (1999). Characterization of ZO-2 as a MAGUK family member associated with tight as well as adherens junctions with a binding affinity to occludin and alpha catenin. *The Journal of Biological Chemistry*, *274*(9), 5981–5986. https://doi.org/10.1074/jbc.274.9.5981

Jahangiri, A., Chin, A. T., Flanigan, P. M., Chen, R., Bankiewicz, K., & Aghi, M. K. (2017). Convection-enhanced delivery in glioblastoma: A review of preclinical and clinical studies. *Journal of Neurosurgery*, *126*(1), 191–200. https://doi.org/10.3171/2016.1.JNS151591

Ji, X., Wang, H., Chen, Y., Zhou, J., & Liu, Y. (2019). Recombinant expressing angiopep-2 fused anti-VEGF single chain Fab (scFab) could cross blood-brain barrier and target glioma. *AMB Express*, *9*(1), 165. https://doi.org/10.1186/s13568-019-0869-3

Jiang, X., Fitch, S., Wang, C., Wilson, C., Li, J., Grant, G. A., & Yang, F. (2016). Nanoparticle engineered TRAIL-overexpressing adipose-derived stem cells target and eradicate glioblastoma via intracranial delivery. *Proceedings of the National Academy of Sciences of the United States of America*, *113*(48), 13857–13862. https://doi.org/10.1073/pnas.1615396113

Jo, M., Kim, T. H., Seol, D. W., Esplen, J. E., Dorko, K., Billiar, T. R., & Strom, S. C. (2000). Apoptosis induced in normal human hepatocytes by tumor necrosis factor-related apoptosis-inducing ligand. *Nature Medicine*, *6*(5), 564–567. https://doi.org/10.1038/75045

Johnstone, R. W., Frew, A. J., & Smyth, M. J. (2008). The TRAIL apoptotic pathway in cancer onset, progression and therapy. *Nature Reviews. Cancer*, *8*(10), 782–798. https://doi.org/10.1038/nrc2465

Jones, A. R., & Shusta, E. V. (2007). Blood-Brain Barrier Transport of Therapeutics via Receptor-Mediation. *Pharmaceutical Research*, *24*(9), 1759–1771. https://doi.org/10.1007/s11095-007-9379-0

Jouan-Lanhouet, S., Arshad, M. I., Piquet-Pellorce, C., Martin-Chouly, C., Le Moigne-Muller, G., Van Herreweghe, F., Takahashi, N., Sergent, O., Lagadic-Gossmann, D., Vandenabeele, P., Samson, M., & Dimanche-Boitrel, M.-T. (2012). TRAIL induces necroptosis involving RIPK1/RIPK3-dependent PARP-1 activation. *Cell Death and Differentiation*, *19*(12), 2003–2014. https://doi.org/10.1038/cdd.2012.90

JOVČEVSKA, I., KOČEVAR, N., & KOMEL, R. (2013). Glioma and glioblastoma—How much do we (not) know? *Molecular and Clinical Oncology*, *1*(6), 935–941. https://doi.org/10.3892/mco.2013.172

Julien, O., & Wells, J. A. (2017). Caspases and their substrates. *Cell Death and Differentiation*, *24*(8), 1380–1389. https://doi.org/10.1038/cdd.2017.44

Kadry, H., Noorani, B., & Cucullo, L. (2020). A blood–brain barrier overview on structure, function, impairment, and biomarkers of integrity. *Fluids and Barriers of the CNS*, *17*(1), 69. https://doi.org/10.1186/s12987-020-00230-3

Kale, J., Osterlund, E. J., & Andrews, D. W. (2018). BCL-2 family proteins: Changing partners in the dance towards death. *Cell Death & Differentiation*, *25*(1), 65–80. https://doi.org/10.1038/cdd.2017.186

Kanekiyo, T., Cirrito, J. R., Liu, C.-C., Shinohara, M., Li, J., Schuler, D. R., Shinohara, M., Holtzman, D. M., & Bu, G. (2013). Neuronal Clearance of Amyloid-β by Endocytic Receptor LRP1. *The Journal of Neuroscience*, *33*(49), 19276–19283. https://doi.org/10.1523/JNEUROSCI.3487-13.2013

Kanekiyo, T., Liu, C.-C., Shinohara, M., Li, J., & Bu, G. (2012). LRP1 in brain vascular smooth muscle cells mediates local clearance of Alzheimer's amyloid-β. *The Journal of Neuroscience: The Official Journal of the Society for Neuroscience*, *32*(46), 16458–16465. https://doi.org/10.1523/JNEUROSCI.3987-12.2012

Kariolis, M. S., Wells, R. C., Getz, J. A., Kwan, W., Mahon, C. S., Tong, R., Kim, D. J., Srivastava, A., Bedard, C., Henne, K. R., Giese, T., Assimon, V. A., Chen, X., Zhang, Y., Solanoy, H., Jenkins, K., Sanchez, P. E., Kane, L., Miyamoto, T., … Zuchero, Y. J. Y. (2020). Brain delivery of therapeutic proteins using an Fc fragment blood-brain barrier transport vehicle in mice and monkeys. *Science Translational Medicine*, *12*(545). https://doi.org/10.1126/scitranslmed.aay1359

Kasibhatla, S., & Tseng, B. (2003). Why Target Apoptosis in Cancer Treatment? *Molecular Cancer Therapeutics*, *2*(6), 573–580.

Katanasaka, Y., Kodera, Y., Kitamura, Y., Morimoto, T., Tamura, T., & Koizumi, F. (2013). Epidermal growth factor receptor variant type III markedly accelerates angiogenesis and tumor growth via inducing c-myc mediated angiopoietin-like 4 expression in malignant glioma. *Molecular Cancer*, *12*, 31. https://doi.org/10.1186/1476-4598-12-31

Kayagaki, N., Yamaguchi, N., Nakayama, M., Eto, H., Okumura, K., & Yagita, H. (1999). Type I interferons (IFNs) regulate tumor necrosis factor-related apoptosis-inducing ligand (TRAIL) expression on human T cells: A novel mechanism for the antitumor effects of type I IFNs. *The Journal of Experimental Medicine*, *189*(9), 1451–1460. https://doi.org/10.1084/jem.189.9.1451

Kelley, S. K., Harris, L. A., Xie, D., Deforge, L., Totpal, K., Bussiere, J., & Fox, J. A. (2001). Preclinical studies to predict the disposition of Apo2L/tumor necrosis factor-related apoptosis-inducing ligand in humans: Characterization of in vivo efficacy, pharmacokinetics, and safety. *The Journal of Pharmacology and Experimental Therapeutics*, *299*(1), 31–38.

Kemp, T. J., Moore, J. M., & Griffith, T. S. (2004). Human B cells express functional TRAIL/Apo-2 ligand after CpG-containing oligodeoxynucleotide stimulation. *Journal of Immunology (Baltimore, Md.: 1950)*, *173*(2), 892–899. https://doi.org/10.4049/jimmunol.173.2.892

Kerr, J. F. R., Wyllie, A. H., & Currie, A. R. (1972). Apoptosis: A Basic Biological Phenomenon with Wide-ranging Implications in Tissue Kinetics. *British Journal of Cancer*, *26*(4), 239–257.

Khawaja, H., Campbell, A., Roberts, J. Z., Javadi, A., O'Reilly, P., McArt, D., Allen, W. L., Majkut, J., Rehm, M., Bardelli, A., Di Nicolantonio, F., Scott, C. J., Kennedy, R., Vitale, N., Harrison, T., Sansom, O. J., Longley, D. B., Evergren, E., & Van Schaeybroeck, S. (2020). RALB GTPase: A critical regulator of DR5 expression and TRAIL sensitivity in KRAS mutant colorectal cancer. *Cell Death & Disease*, *11*(10). https://doi.org/10.1038/s41419-020-03131-3

Killela, P. J., Reitman, Z. J., Jiao, Y., Bettegowda, C., Agrawal, N., Diaz, L. A., Friedman, A. H., Friedman, H., Gallia, G. L., Giovanella, B. C., Grollman, A. P., He, T.-C., He, Y., Hruban, R. H., Jallo, G. I., Mandahl, N., Meeker, A. K., Mertens, F., Netto, G. J., … Yan, H. (2013). TERT promoter mutations occur frequently in gliomas and a subset of tumors derived from cells with low rates of self-renewal. *Proceedings of the National Academy of Sciences of the United States of America*, *110*(15), 6021–6026. https://doi.org/10.1073/pnas.1303607110

Kimberley, F. C., & Screaton, G. R. (2004). Following a TRAIL: Update on a ligand and its five receptors. *Cell Research*, *14*(5), 359–372. https://doi.org/10.1038/sj.cr.7290236

Kimura, K., Taguchi, T., Urushizaki, I., Ohno, R., Abe, O., Furue, H., Hattori, T., Ichihashi, H., Inoguchi, K., Majima, H., Niitani, H., Ota, K., Saito, T., Suga, S., Suzuoki, Y., Wakui, A., Yamada, K., & The A-TNF Cooperative Study Group. (1987). Phase I study of recombinant human tumor necrosis factor. *Cancer Chemotherapy and Pharmacology*, *20*(3), 223–229. https://doi.org/10.1007/BF00570490

Kischkel, F. C., Hellbardt, S., Behrmann, I., Germer, M., Pawlita, M., Krammer, P. H., & Peter, M. E. (1995). Cytotoxicity-dependent APO-1 (Fas/CD95)-associated proteins form a death-inducing signaling complex (DISC) with the receptor. *The EMBO Journal*, *14*(22), 5579–5588.

Kischkel, F. C., Lawrence, D. A., Chuntharapai, A., Schow, P., Kim, K. J., & Ashkenazi, A. (2000). Apo2L/TRAIL-dependent recruitment of endogenous FADD and caspase-8 to death receptors 4 and 5. *Immunity*, *12*(6), 611–620. https://doi.org/10.1016/s1074-7613(00)80212-5

Kischkel, F. C., Lawrence, D. A., Tinel, A., LeBlanc, H., Virmani, A., Schow, P., Gazdar, A., Blenis, J., Arnott, D., & Ashkenazi, A. (2001). Death receptor recruitment of endogenous caspase-10 and apoptosis initiation in the absence of caspase-8. *The Journal of Biological Chemistry*, *276*(49), 46639–46646. https://doi.org/10.1074/jbc.M105102200

Kleihues, P., Louis, D. N., Scheithauer, B. W., Rorke, L. B., Reifenberger, G., Burger, P. C., & Cavenee, W. K. (2002). The WHO Classification of Tumors of the Nervous System. *Journal of Neuropathology & Experimental Neurology*, *61*(3), 215–225. https://doi.org/10.1093/jnen/61.3.215

Kleihues, P., & Ohgaki, H. (1999). Primary and secondary glioblastomas: From concept to clinical diagnosis. *Neuro-Oncology*, *1*(1), 44–51.

Knobbe, C. B., Merlo, A., & Reifenberger, G. (2002). Pten signaling in gliomas. *Neuro-Oncology*, *4*(3), 196–211.

Koessinger, A. L., Koessinger, D., Kinch, K., Martínez-Escardó, L., Paul, N. R., Elmasry, Y., Malviya, G., Cloix, C., Campbell, K. J., Bock, F. J., O'Prey, J., Stevenson, K., Nixon, C., Jackson, M. R., Ichim, G., Stewart, W., Blyth, K., Ryan, K. M., Chalmers, A. J., … Tait, S. W. (2021). *Increased apoptotic priming of glioblastoma enables therapeutic targeting by BH3-mimetics* [Preprint]. Cancer Biology. https://doi.org/10.1101/2021.06.13.448232

Kontermann, R. E. (2009). Strategies to extend plasma half-lives of recombinant antibodies. *BioDrugs: Clinical Immunotherapeutics, Biopharmaceuticals and Gene Therapy*, *23*(2), 93–109. https://doi.org/10.2165/00063030-200923020-00003

Koshy, M., Villano, J. L., Dolecek, T. A., Howard, A., Mahmood, U., Chmura, S. J., Weichselbaum, R. R., & McCarthy, B. J. (2012). Improved survival time trends for glioblastoma using the SEER 17 population-based registries. *Journal of Neuro-Oncology*, *107*(1), 207–212. https://doi.org/10.1007/s11060-011-0738-7

Kowal, R. C., Herz, J., Goldstein, J. L., Esser, V., & Brown, M. S. (1989). Low density lipoprotein receptor-related protein mediates uptake of cholesteryl esters derived from apoprotein E-enriched lipoproteins. *Proceedings of the National Academy of Sciences of the United States of America*, *86*(15), 5810–5814.

Krueger, A., Baumann, S., Krammer, P. H., & Kirchhoff, S. (2001). FLICE-inhibitory proteins: Regulators of death receptor-mediated apoptosis. *Molecular and Cellular Biology*, *21*(24), 8247–8254. https://doi.org/10.1128/MCB.21.24.8247-8254.2001

Krueger, A., Schmitz, I., Baumann, S., Krammer, P. H., & Kirchhoff, S. (2001). Cellular FLICE-inhibitory protein splice variants inhibit different steps of caspase-8 activation at the CD95 death-inducing signaling complex. *The Journal of Biological Chemistry*, *276*(23), 20633–20640. https://doi.org/10.1074/jbc.M101780200

Kumagai, A. K., Eisenberg, J. B., & Pardridge, W. M. (1987). Absorptive-mediated endocytosis of cationized albumin and a beta-endorphin-cationized albumin chimeric peptide by isolated brain capillaries. Model system of blood-brain barrier transport. *The Journal of Biological Chemistry*, *262*(31), 15214–15219.

Kumthekar, P., Tang, S.-C., Brenner, A. J., Kesari, S., Piccioni, D. E., Anders, C., Carrillo, J., Chalasani, P., Kabos, P., Puhalla, S., Tkaczuk, K., Garcia, A. A., Ahluwalia, M. S., Wefel, J. S., Lakhani, N., & Ibrahim, N. (2020). ANG1005, a Brain-Penetrating Peptide-Drug Conjugate, Shows Activity in Patients with Breast Cancer with Leptomeningeal Carcinomatosis and Recurrent Brain Metastases. *Clinical Cancer Research: An Official Journal of the American Association for Cancer Research*, *26*(12), 2789–2799. https://doi.org/10.1158/1078-0432.CCR-19-3258

Kumthekar, P., Tang, S.-C., Brenner, A. J., Kesari, S., Piccioni, D. E., Anders, C. K., Carrillo, J. A., Chalasani, P., Kabos, P., Puhalla, S., Garcia, A. A., Tkaczuk, K. H., Ahluwalia, M. S., Lakhani, N. J., & Ibrahim, N. K. (2016). ANG1005, a novel brain-penetrant taxane derivative, for the treatment of recurrent brain metastases and leptomeningeal carcinomatosis from breast cancer. *Journal of Clinical Oncology*, *34*(15_suppl), 2004–2004. https://doi.org/10.1200/JCO.2016.34.15_suppl.2004

Kurzrock, R., Gabrail, N., Chandhasin, C., Moulder, S., Smith, C., Brenner, A., Sankhala, K., Mita, A., Elian, K., Bouchard, D., & Sarantopoulos, J. (2012). Safety, pharmacokinetics, and activity of GRN1005, a novel conjugate of angiopep-2, a peptide facilitating brain penetration, and paclitaxel, in patients with advanced solid tumors. *Molecular Cancer Therapeutics*, *11*(2), 308–316. https://doi.org/10.1158/1535-7163.MCT-11-0566

Lafont, E., Kantari-Mimoun, C., Draber, P., De Miguel, D., Hartwig, T., Reichert, M., Kupka, S., Shimizu, Y., Taraborrelli, L., Spit, M., Sprick, M. R., & Walczak, H. (2017). The linear ubiquitin chain assembly complex regulates TRAIL-induced gene activation and cell death. *The EMBO Journal*, *36*(9), 1147–1166. https://doi.org/10.15252/embj.201695699

Lara-Velazquez, M., Al-Kharboosh, R., Jeanneret, S., Vazquez-Ramos, C., Mahato, D., Tavanaiepour, D., Rahmathulla, G., & Quinones-Hinojosa, A. (2017). Advances in Brain Tumor Surgery for Glioblastoma in Adults. *Brain Sciences*, *7*(12), 166. https://doi.org/10.3390/brainsci7120166

Lauber, K., Bohn, E., Kröber, S. M., Xiao, Y., Blumenthal, S. G., Lindemann, R. K., Marini, P., Wiedig, C., Zobywalski, A., Baksh, S., Xu, Y., Autenrieth, I. B., Schulze-Osthoff, K., Belka, C., Stuhler, G., & Wesselborg, S. (2003). Apoptotic Cells Induce Migration of Phagocytes

via Caspase-3-Mediated Release of a Lipid Attraction Signal. *Cell*, *113*(6), 717–730. https://doi.org/10.1016/S0092-8674(03)00422-7

Lavrik, I. N., Golks, A., & Krammer, P. H. (2005). Caspases: Pharmacological manipulation of cell death. *Journal of Clinical Investigation*, *115*(10), 2665–2672. https://doi.org/10.1172/JCI26252

Lawrence, D., Shahrokh, Z., Marsters, S., Achilles, K., Shih, D., Mounho, B., Hillan, K., Totpal, K., DeForge, L., Schow, P., Hooley, J., Sherwood, S., Pai, R., Leung, S., Khan, L., Gliniak, B., Bussiere, J., Smith, C. A., Strom, S. S., … Ashkenazi, A. (2001). Differential hepatocyte toxicity of recombinant Apo2L/TRAIL versions. *Nature Medicine*, *7*(4), 383–385. https://doi.org/10.1038/86397

LeBlanc, H. N., & Ashkenazi, A. (2003). Apo2L/TRAIL and its death and decoy receptors. *Cell Death & Differentiation*, *10*(1), 66–75. https://doi.org/10.1038/sj.cdd.4401187

Lee, H. J., Engelhardt, B., Lesley, J., Bickel, U., & Pardridge, W. M. (2000). Targeting rat anti-mouse transferrin receptor monoclonal antibodies through blood-brain barrier in mouse. *The Journal of Pharmacology and Experimental Therapeutics*, *292*(3), 1048–1052.

Lee, H.-W., Lee, S.-H., Lee, H.-W., Ryu, Y.-W., Kwon, M.-H., & Kim, Y.-S. (2005). Homomeric and heteromeric interactions of the extracellular domains of death receptors and death decoy receptors. *Biochemical and Biophysical Research Communications*, *330*(4), 1205–1212. https://doi.org/10.1016/j.bbrc.2005.03.101

Lee, S. Y. (2016). Temozolomide resistance in glioblastoma multiforme. *Genes & Diseases*, *3*(3), 198–210. https://doi.org/10.1016/j.gendis.2016.04.007

Lemke, J., von Karstedt, S., Zinngrebe, J., & Walczak, H. (2014). Getting TRAIL back on track for cancer therapy. *Cell Death & Differentiation*, *21*(9), 1350–1364. https://doi.org/10.1038/cdd.2014.81

Levin, D., Golding, B., Strome, S. E., & Sauna, Z. E. (2015). Fc fusion as a platform technology: Potential for modulating immunogenicity. *Trends in Biotechnology*, *33*(1), 27–34. https://doi.org/10.1016/j.tibtech.2014.11.001

Li, J. H., Kirkiles-Smith, N. C., McNiff, J. M., & Pober, J. S. (2003). TRAIL induces apoptosis and inflammatory gene expression in human endothelial cells. *Journal of Immunology (Baltimore, Md.: 1950)*, *171*(3), 1526–1533. https://doi.org/10.4049/jimmunol.171.3.1526

Li, Y., Paz Marzolo, M., van Kerkhof, P., Strous, G. J., & Bu, G. (2000). The YXXL Motif, but Not the Two NPXY Motifs, Serves as the Dominant Endocytosis Signal for Low Density Lipoprotein Receptor-related Protein*. *Journal of Biological Chemistry*, *275*(22), 17187–17194. https://doi.org/10.1074/jbc.M000490200

Lillis, A. P., Van Duyn, L. B., Murphy-Ullrich, J. E., & Strickland, D. K. (2008). LDL receptor-related protein 1: Unique tissue-specific functions revealed by selective gene knockout studies. *Physiological Reviews*, *88*(3), 887–918. https://doi.org/10.1152/physrev.00033.2007

Lin, C., McGough, R., Aswad, B., Block, J. A., & Terek, R. (2004). Hypoxia induces HIF-1alpha and VEGF expression in chondrosarcoma cells and chondrocytes. *Journal of Orthopaedic Research: Official Publication of the Orthopaedic Research Society*, *22*(6), 1175–1181. https://doi.org/10.1016/j.orthres.2004.03.002

Lin, L., Yee, S. W., Kim, R. B., & Giacomini, K. M. (2015). SLC transporters as therapeutic targets: Emerging opportunities. *Nature Reviews. Drug Discovery*, *14*(8), 543–560. https://doi.org/10.1038/nrd4626

Lincoln, F. A., Imig, D., Boccellato, C., Juric, V., Noonan, J., Kontermann, R. E., Allgöwer, F., Murphy, B. M., & Rehm, M. (2018). Sensitization of glioblastoma cells to TRAIL-induced apoptosis by IAP- and Bcl-2 antagonism. *Cell Death & Disease*, *9*(11), 1112. https://doi.org/10.1038/s41419-018-1160-2

Lipinski, C. A., Lombardo, F., Dominy, B. W., & Feeney, P. J. (2001). Experimental and computational approaches to estimate solubility and permeability in drug discovery and development settings. *Advanced Drug Delivery Reviews*, *46*(1–3), 3–26. https://doi.org/10.1016/s0169-409x(00)00129-0

Liu, W., Wang, Z., Zhang, L., Wei, X., & Li, L. (2012). Tight Junction in Blood-Brain Barrier: An Overview of Structure, Regulation, and Regulator Substances. *CNS Neuroscience & Therapeutics*, *18*(8), 609–615. https://doi.org/10.1111/j.1755-5949.2012.00340.x

Liu, X.-Y., Gerges, N., Korshunov, A., Sabha, N., Khuong-Quang, D.-A., Fontebasso, A. M., Fleming, A., Hadjadj, D., Schwartzentruber, J., Majewski, J., Dong, Z., Siegel, P., Albrecht,

S., Croul, S., Jones, D. T., Kool, M., Tonjes, M., Reifenberger, G., Faury, D., … Jabado, N. (2012). Frequent ATRX mutations and loss of expression in adult diffuse astrocytic tumors carrying IDH1/IDH2 and TP53 mutations. *Acta Neuropathologica*, *124*(5), 615–625. https://doi.org/10.1007/s00401-012-1031-3

Lockshin, R. A., & Williams, C. M. (1964). Programmed cell death—II. Endocrine potentiation of the breakdown of the intersegmental muscles of silkmoths. *Journal of Insect Physiology*, *10*(4), 643–649. https://doi.org/10.1016/0022-1910(64)90034-4

Lonser, R. R., Sarntinoranont, M., Morrison, P. F., & Oldfield, E. H. (2015). Convection-enhanced delivery to the central nervous system. *Journal of Neurosurgery*, *122*(3), 697–706. https://doi.org/10.3171/2014.10.JNS14229

Löscher, W., & Potschka, H. (2005). Blood-brain barrier active efflux transporters: ATP-binding cassette gene family. *NeuroRx: The Journal of the American Society for Experimental NeuroTherapeutics*, *2*(1), 86–98. https://doi.org/10.1602/neurorx.2.1.86

Louis, D. N., Ohgaki, H., Wiestler, O. D., Cavenee, W. K., Burger, P. C., Jouvet, A., Scheithauer, B. W., & Kleihues, P. (2007). The 2007 WHO Classification of Tumours of the Central Nervous System. *Acta Neuropathologica*, *114*(2), 97–109. https://doi.org/10.1007/s00401-007-0243-4

Louis, D. N., Perry, A., Reifenberger, G., von Deimling, A., Figarella-Branger, D., Cavenee, W. K., Ohgaki, H., Wiestler, O. D., Kleihues, P., & Ellison, D. W. (2016). The 2016 World Health Organization Classification of Tumors of the Central Nervous System: A summary. *Acta Neuropathologica*, *131*(6), 803–820. https://doi.org/10.1007/s00401-016-1545-1

Louis, D. N., Perry, A., Wesseling, P., Brat, D. J., Cree, I. A., Figarella-Branger, D., Hawkins, C., Ng, H. K., Pfister, S. M., Reifenberger, G., Soffietti, R., von Deimling, A., & Ellison, D. W. (2021). The 2021 WHO Classification of Tumors of the Central Nervous System: A summary. *Neuro-Oncology*, *23*(8), 1231–1251. https://doi.org/10.1093/neuonc/noab106

Lowe, S. W., & Lin, A. W. (2000). Apoptosis in cancer. *Carcinogenesis*, *21*(3), 485–495. https://doi.org/10.1093/carcin/21.3.485

MacFarlane, M., Ahmad, M., Srinivasula, S. M., Fernandes-Alnemri, T., Cohen, G. M., & Alnemri, E. S. (1997). Identification and molecular cloning of two novel receptors for the cytotoxic ligand TRAIL. *The Journal of Biological Chemistry*, *272*(41), 25417–25420. https://doi.org/10.1074/jbc.272.41.25417

Makarova, A., Mikhailenko, I., Bugge, T. H., List, K., Lawrence, D. A., & Strickland, D. K. (2003). The Low Density Lipoprotein Receptor-related Protein Modulates Protease Activity in the Brain by Mediating the Cellular Internalization of Both Neuroserpin and Neuroserpin-Tissue-type Plasminogen Activator Complexes*. *Journal of Biological Chemistry*, *278*(50), 50250–50258. https://doi.org/10.1074/jbc.M309150200

Mandell, K. J., & Parkos, C. A. (2005). The JAM family of proteins. *Advanced Drug Delivery Reviews*, *57*(6), 857–867. https://doi.org/10.1016/j.addr.2005.01.005

Mark, K. S., Trickler, W. J., & Miller, D. W. (2001). Tumor necrosis factor-alpha induces cyclooxygenase-2 expression and prostaglandin release in brain microvessel endothelial cells. *The Journal of Pharmacology and Experimental Therapeutics*, *297*(3), 1051–1058.

Marsters, S. A., Sheridan, J. P., Pitti, R. M., Huang, A., Skubatch, M., Baldwin, D., Yuan, J., Gurney, A., Goddard, A. D., Godowski, P., & Ashkenazi, A. (1997). A novel receptor for Apo2L/TRAIL contains a truncated death domain. *Current Biology: CB*, *7*(12), 1003–1006. https://doi.org/10.1016/s0960-9822(06)00422-2

May, P., Reddy, Y. K., & Herz, J. (2002). Proteolytic Processing of Low Density Lipoprotein Receptor-related Protein Mediates Regulated Release of Its Intracellular Domain*. *Journal of Biological Chemistry*, *277*(21), 18736–18743. https://doi.org/10.1074/jbc.M201979200

Mayor, S., & Pagano, R. E. (2007). Pathways of clathrin-independent endocytosis. *Nature Reviews Molecular Cell Biology*, *8*(8), 603–612. https://doi.org/10.1038/nrm2216

Mayor, S., Parton, R. G., & Donaldson, J. G. (2014). Clathrin-Independent Pathways of Endocytosis. *Cold Spring Harbor Perspectives in Biology*, *6*(6), a016758. https://doi.org/10.1101/cshperspect.a016758

Mazor, Y., Sachsenmeier, K. F., Yang, C., Hansen, A., Filderman, J., Mulgrew, K., Wu, H., & Dall'Acqua, W. F. (2017). Enhanced tumor-targeting selectivity by modulating bispecific antibody binding affinity and format valence. *Scientific Reports*, *7*(1), 40098. https://doi.org/10.1038/srep40098

McCarthy, E. F. (2006). The Toxins of William B. Coley and the Treatment of Bone and Soft-Tissue Sarcomas. *The Iowa Orthopaedic Journal*, *26*, 154–158.

McGirt, M. J., Villavicencio, A. T., Bulsara, K. R., & Friedman, A. H. (2003). MRI-guided stereotactic biopsy in the diagnosis of glioma: Comparison of biopsy and surgical resection specimen. *Surgical Neurology*, *59*(4), 277–281; discussion 281-282. https://doi.org/10.1016/s0090-3019(03)00048-x

McGoldrick, C. A., Jiang, Y.-L., Paromov, V., Brannon, M., Krishnan, K., & Stone, W. L. (2014). Identification of oxidized protein hydrolase as a potential prodrug target in prostate cancer. *BMC Cancer*, *14*(1), 77. https://doi.org/10.1186/1471-2407-14-77

McQuin, C., Goodman, A., Chernyshev, V., Kamentsky, L., Cimini, B. A., Karhohs, K. W., Doan, M., Ding, L., Rafelski, S. M., Thirstrup, D., Wiegraebe, W., Singh, S., Becker, T., Caicedo, J. C., & Carpenter, A. E. (2018). CellProfiler 3.0: Next-generation image processing for biology. *PLOS Biology*, *16*(7), e2005970. https://doi.org/10.1371/journal.pbio.2005970

Medema, J. P., Scaffidi, C., Kischkel, F. C., Shevchenko, A., Mann, M., Krammer, P. H., & Peter, M. E. (1997). FLICE is activated by association with the CD95 death-inducing signaling complex (DISC). *The EMBO Journal*, *16*(10), 2794–2804. https://doi.org/10.1093/emboj/16.10.2794

Medina, C. B., & Ravichandran, K. S. (2016). Do not let death do us part: 'find-me' signals in communication between dying cells and the phagocytes. *Cell Death and Differentiation*, *23*(6), 979–989. https://doi.org/10.1038/cdd.2016.13

Meurette, O., Rebillard, A., Huc, L., Le Moigne, G., Merino, D., Micheau, O., Lagadic-Gossmann, D., & Dimanche-Boitrel, M.-T. (2007). TRAIL induces receptor-interacting protein 1-dependent and caspase-dependent necrosis-like cell death under acidic extracellular conditions. *Cancer Research*, *67*(1), 218–226. https://doi.org/10.1158/0008-5472.CAN-06-1610

Micheau, O., Thome, M., Schneider, P., Holler, N., Tschopp, J., Nicholson, D. W., Briand, C., & Grütter, M. G. (2002). The Long Form of FLIP Is an Activator of Caspase-8 at the Fas Death-inducing Signaling Complex *. *Journal of Biological Chemistry*, *277*(47), 45162–45171. https://doi.org/10.1074/jbc.M206882200

Mikitsh, J. L., & Chacko, A.-M. (2014). Pathways for Small Molecule Delivery to the Central Nervous System Across the Blood-Brain Barrier. *Perspectives in Medicinal Chemistry*, *6*, 11–24. https://doi.org/10.4137/PMC.S13384

Moldoveanu, T., Grace, C. R., Llambi, F., Nourse, A., Fitzgerald, P., Gehring, K., Kriwacki, R. W., & Green, D. R. (2013). BID-induced structural changes in BAK promote apoptosis. *Nature Structural & Molecular Biology*, *20*(5), 589–597. https://doi.org/10.1038/nsmb.2563

Mongkolsapaya, J., Grimes, J. M., Chen, N., Xu, X. N., Stuart, D. I., Jones, E. Y., & Screaton, G. R. (1999). Structure of the TRAIL-DR5 complex reveals mechanisms conferring specificity in apoptotic initiation. *Nature Structural Biology*, *6*(11), 1048–1053. https://doi.org/10.1038/14935

Morita, K., Furuse, M., Fujimoto, K., & Tsukita, S. (1999). Claudin multigene family encoding four-transmembrane domain protein components of tight junction strands. *Proceedings of the National Academy of Sciences of the United States of America*, *96*(2), 511–516. https://doi.org/10.1073/pnas.96.2.511

Mühlenbeck, F., Schneider, P., Bodmer, J.-L., Schwenzer, R., Hauser, A., Schubert, G., Scheurich, P., Moosmayer, D., Tschopp, J., & Wajant, H. (2000). The Tumor Necrosis Factor-related Apoptosis-inducing Ligand Receptors TRAIL-R1 and TRAIL-R2 Have Distinct Cross-linking Requirements for Initiation of Apoptosis and Are Non-redundant in JNK Activation *. *Journal of Biological Chemistry*, *275*(41), 32208–32213. https://doi.org/10.1074/jbc.M000482200

Muzio, M., Stockwell, B. R., Stennicke, H. R., Salvesen, G. S., & Dixit, V. M. (1998). An induced proximity model for caspase-8 activation. *The Journal of Biological Chemistry*, *273*(5), 2926–2930. https://doi.org/10.1074/jbc.273.5.2926

Nagai, H., & Kim, Y. H. (2017). Cancer prevention from the perspective of global cancer burden patterns. *Journal of Thoracic Disease*, *9*(3), 448–451. https://doi.org/10.21037/jtd.2017.02.75

Neyns, B., Sadones, J., Joosens, E., Bouttens, F., Verbeke, L., Baurain, J.-F., D'Hondt, L., Strauven, T., Chaskis, C., In't Veld, P., Michotte, A., & De Greve, J. (2009). Stratified phase II trial of cetuximab in patients with recurrent high-grade glioma. *Annals of Oncology:*

Official Journal of the European Society for Medical Oncology, *20*(9), 1596–1603. https://doi.org/10.1093/annonc/mdp032

Niewoehner, J., Bohrmann, B., Collin, L., Urich, E., Sade, H., Maier, P., Rueger, P., Stracke, J. O., Lau, W., Tissot, A. C., Loetscher, H., Ghosh, A., & Freskgård, P.-O. (2014). Increased brain penetration and potency of a therapeutic antibody using a monovalent molecular shuttle. *Neuron*, *81*(1), 49–60. https://doi.org/10.1016/j.neuron.2013.10.061

Nitta, T., Hata, M., Gotoh, S., Seo, Y., Sasaki, H., Hashimoto, N., Furuse, M., & Tsukita, S. (2003). Size-selective loosening of the blood-brain barrier in claudin-5–deficient mice. *The Journal of Cell Biology*, *161*(3), 653–660. https://doi.org/10.1083/jcb.200302070

Nutt, C. L., Mani, D. R., Betensky, R. A., Tamayo, P., Cairncross, J. G., Ladd, C., Pohl, U., Hartmann, C., McLaughlin, M. E., Batchelor, T. T., Black, P. M., Deimling, A. von, Pomeroy, S. L., Golub, T. R., & Louis, D. N. (2003). Gene Expression-based Classification of Malignant Gliomas Correlates Better with Survival than Histological Classification. *Cancer Research*, *63*(7), 1602–1607.

Ogasawara, J., Watanabe-Fukunaga, R., Adachi, M., Matsuzawa, A., Kasugai, T., Kitamura, Y., Itoh, N., Suda, T., & Nagata, S. (1993). Lethal effect of the anti-Fas antibody in mice. *Nature*, *364*(6440), 806–809. https://doi.org/10.1038/364806a0

Ohgaki, H., & Kleihues, P. (2007). Genetic pathways to primary and secondary glioblastoma. *The American Journal of Pathology*, *170*(5), 1445–1453. https://doi.org/10.2353/ajpath.2007.070011

Ohgaki, H., & Kleihues, P. (2013). The definition of primary and secondary glioblastoma. *Clinical Cancer Research: An Official Journal of the American Association for Cancer Research*, *19*(4), 764–772. https://doi.org/10.1158/1078-0432.CCR-12-3002

Omidi, Y., Campbell, L., Barar, J., Connell, D., Akhtar, S., & Gumbleton, M. (2003). Evaluation of the immortalised mouse brain capillary endothelial cell line, b.End3, as an in vitro blood–brain barrier model for drug uptake and transport studies. *Brain Research*, *990*(1), 95–112. https://doi.org/10.1016/S0006-8993(03)03443-7

Opel, D., Westhoff, M.-A., Bender, A., Braun, V., Debatin, K.-M., & Fulda, S. (2008). Phosphatidylinositol 3-kinase inhibition broadly sensitizes glioblastoma cells to death receptor- and drug-induced apoptosis. *Cancer Research*, *68*(15), 6271–6280. https://doi.org/10.1158/0008-5472.CAN-07-6769

Ostrom, Q. T., Cioffi, G., Gittleman, H., Patil, N., Waite, K., Kruchko, C., & Barnholtz-Sloan, J. S. (2019). CBTRUS Statistical Report: Primary Brain and Other Central Nervous System Tumors Diagnosed in the United States in 2012–2016. *Neuro-Oncology*, *21*(Suppl 5), v1–v100. https://doi.org/10.1093/neuonc/noz150

Ostrom, Q. T., Gittleman, H., Fulop, J., Liu, M., Blanda, R., Kromer, C., Wolinsky, Y., Kruchko, C., & Barnholtz-Sloan, J. S. (2015). CBTRUS Statistical Report: Primary Brain and Central Nervous System Tumors Diagnosed in the United States in 2008-2012. *Neuro-Oncology*, *17*(Suppl 4), iv1–iv62. https://doi.org/10.1093/neuonc/nov189

Pan, G., Ni, J., Wei, Y.-F., Yu, G., Gentz, R., & Dixit, V. M. (1997). An Antagonist Decoy Receptor and a Death Domain-Containing Receptor for TRAIL. *Science*, *277*(5327), 815–818. https://doi.org/10.1126/science.277.5327.815

Pan, G., Ni, J., Yu, G., Wei, Y. F., & Dixit, V. M. (1998). TRUNDD, a new member of the TRAIL receptor family that antagonizes TRAIL signalling. *FEBS Letters*, *424*(1–2), 41–45. https://doi.org/10.1016/s0014-5793(98)00135-5

Pan, G., O'Rourke, K., Chinnaiyan, A. M., Gentz, R., Ebner, R., Ni, J., & Dixit, V. M. (1997). The Receptor for the Cytotoxic Ligand TRAIL. *Science, New Series*, *276*(5309), 111–113.

Pan, L., Fu, T.-M., Zhao, W., Zhao, L., Chen, W., Qiu, C., Liu, W., Liu, Z., Piai, A., Fu, Q., Chen, S., Wu, H., & Chou, J. J. (2019). Higher-Order Clustering of the Transmembrane Anchor of DR5 Drives Signaling. *Cell*, *176*(6), 1477-1489.e14. https://doi.org/10.1016/j.cell.2019.02.001

Pan, S.-T., Li, Z.-L., He, Z.-X., Qiu, J.-X., & Zhou, S.-F. (2016). Molecular mechanisms for tumour resistance to chemotherapy. *Clinical and Experimental Pharmacology and Physiology*, *43*(8), 723–737. https://doi.org/10.1111/1440-1681.12581

Pan, W., Kastin, A. J., Zankel, T. C., van Kerkhof, P., Terasaki, T., & Bu, G. (2004). Efficient transfer of receptor-associated protein (RAP) across the blood-brain barrier. *Journal of Cell Science*, *117*(Pt 21), 5071–5078. https://doi.org/10.1242/jcs.01381

Pardridge, W., Buciak, J. L., & Friden, P. (1991). Selective transport of an anti-transferrin receptor antibody through the blood–brain barrier. *The Journal of Pharmacology and Experimental Therapeutics*, *259*, 66–70.

Pardridge, W. M. (2005). The Blood-Brain Barrier: Bottleneck in Brain Drug Development. *NeuroRx*, *2*(1), 3–14.

Pardridge, W. M. (2006). Molecular Trojan horses for blood–brain barrier drug delivery. *Current Opinion in Pharmacology*, *6*(5), 494–500. https://doi.org/10.1016/j.coph.2006.06.001

Pardridge, W. M. (2012). Drug transport across the blood–brain barrier. *Journal of Cerebral Blood Flow & Metabolism*, *32*(11), 1959–1972. https://doi.org/10.1038/jcbfm.2012.126

Pardridge, W. M. (2020). Blood-Brain Barrier and Delivery of Protein and Gene Therapeutics to Brain. *Frontiers in Aging Neuroscience*, *11*. https://doi.org/10.3389/fnagi.2019.00373

Pardridge, W. M. (2022a). Kinetics of Blood–Brain Barrier Transport of Monoclonal Antibodies Targeting the Insulin Receptor and the Transferrin Receptor. *Pharmaceuticals*, *15*(1), 3. https://doi.org/10.3390/ph15010003

Pardridge, W. M. (2022b). A Historical Review of Brain Drug Delivery. *Pharmaceutics*, *14*(6), 1283. https://doi.org/10.3390/pharmaceutics14061283

Pardridge, W. M., Eisenberg, J., & Yang, J. (1985). Human blood-brain barrier insulin receptor. *Journal of Neurochemistry*, *44*(6), 1771–1778. https://doi.org/10.1111/j.1471-4159.1985.tb07167.x

Pardridge, W. M., Eisenberg, J., & Yang, J. (1987). Human blood-brain barrier transferrin receptor. *Metabolism: Clinical and Experimental*, *36*(9), 892–895. https://doi.org/10.1016/0026-0495(87)90099-0

Patel, A. P., Tirosh, I., Trombetta, J. J., Shalek, A. K., Gillespie, S. M., Wakimoto, H., Cahill, D. P., Nahed, B. V., Curry, W. T., Martuza, R. L., Louis, D. N., Rozenblatt-Rosen, O., Suvà, M. L., Regev, A., & Bernstein, B. E. (2014). Single-cell RNA-seq highlights intratumoral heterogeneity in primary glioblastoma. *Science (New York, N.Y.)*, *344*(6190), 1396–1401. https://doi.org/10.1126/science.1254257

Patil, M. S., Cartland, S. P., & Kavurma, M. M. (2020). TRAIL signals, extracellular matrix and vessel remodelling. *Vascular Biology (Bristol, England)*, *2*(1), R73–R84. https://doi.org/10.1530/VB-20-0005

Peiffer, J., & Kleihues, P. (1999). Hans-Joachim Scherer (1906-1945), pioneer in glioma research. *Brain Pathology (Zurich, Switzerland)*, *9*(2), 241–245. https://doi.org/10.1111/j.1750-3639.1999.tb00222.x

Pfeffer, C. M., & Singh, A. T. K. (2018). Apoptosis: A Target for Anticancer Therapy. *International Journal of Molecular Sciences*, *19*(2), 448. https://doi.org/10.3390/ijms19020448

Pflanzner, T., Janko, M. C., André-Dohmen, B., Reuss, S., Weggen, S., Roebroek, A. J. M., Kuhlmann, C. R. W., & Pietrzik, C. U. (2011). LRP1 mediates bidirectional transcytosis of amyloid-β across the blood-brain barrier. *Neurobiology of Aging*, *32*(12), 2323.e1-2323.e11. https://doi.org/10.1016/j.neurobiolaging.2010.05.025

Phillips, D. C., Buchanan, F. G., Cheng, D., Solomon, L. R., Xiao, Y., Xue, J., Tahir, S. K., Smith, M. L., Zhang, H., Widomski, D., Abraham, V. C., Xu, N., Liu, Z., Zhou, L., DiGiammarino, E., Lu, X., Rudra-Ganguly, N., Trela, B., & Morgan-Lappe, S. E. (2021). Hexavalent TRAIL Fusion Protein Eftozanermin Alfa Optimally Clusters Apoptosis-Inducing TRAIL Receptors to Induce On-Target Antitumor Activity in Solid Tumors. *Cancer Research*, *81*(12), 3402–3414.

Phillips, H. S., Kharbanda, S., Chen, R., Forrest, W. F., Soriano, R. H., Wu, T. D., Misra, A., Nigro, J. M., Colman, H., Soroceanu, L., Williams, P. M., Modrusan, Z., Feuerstein, B. G., & Aldape, K. (2006). Molecular subclasses of high-grade glioma predict prognosis, delineate a pattern of disease progression, and resemble stages in neurogenesis. *Cancer Cell*, *9*(3), 157–173. https://doi.org/10.1016/j.ccr.2006.02.019

Philpott, C., Tovell, H., Frayling, I. M., Cooper, D. N., & Upadhyaya, M. (2017). The NF1 somatic mutational landscape in sporadic human cancers. *Human Genomics*, *11*(1), 13. https://doi.org/10.1186/s40246-017-0109-3

Pitti, R. M., Marsters, S. A., Ruppert, S., Donahue, C. J., Moore, A., & Ashkenazi, A. (1996). Induction of apoptosis by Apo-2 ligand, a new member of the tumor necrosis factor cytokine family. *The Journal of Biological Chemistry*, *271*(22), 12687–12690. https://doi.org/10.1074/jbc.271.22.12687

Polanski, R., Vincent, J., Polanska, U. M., Petreus, T., & Tang, E. K. Y. (2015). Caspase-8 activation by TRAIL monotherapy predicts responses to IAPi and TRAIL combination treatment in breast cancer cell lines. *Cell Death & Disease*, *6*(10), e1893–e1893. https://doi.org/10.1038/cddis.2015.234

Pommier, Y., Sordet, O., Antony, S., Hayward, R. L., & Kohn, K. W. (2004). Apoptosis defects and chemotherapy resistance: Molecular interaction maps and networks. *Oncogene*, *23*(16), 2934–2949. https://doi.org/10.1038/sj.onc.1207515

Potere, N., Del Buono, M. G., Mauro, A. G., Abbate, A., & Toldo, S. (2019). Low Density Lipoprotein Receptor-Related Protein-1 in Cardiac Inflammation and Infarct Healing. *Frontiers in Cardiovascular Medicine*, *6*, 51. https://doi.org/10.3389/fcvm.2019.00051

Pulgar, V. M. (2019). Transcytosis to Cross the Blood Brain Barrier, New Advancements and Challenges. *Frontiers in Neuroscience*, *12*. https://doi.org/10.3389/fnins.2018.01019

Ratain, M. J., Doi, T., De Jonge, M. J., LoRusso, P., Dunbar, M., Chiney, M., Motwani, M., Glasgow, J., Petrich, A. M., Rasco, D. W., & Calvo, E. (2019). Phase 1, first-in-human study of TRAIL receptor agonist fusion protein ABBV-621. *Journal of Clinical Oncology*, *37*(15_suppl), 3013–3013. https://doi.org/10.1200/JCO.2019.37.15_suppl.3013

Reardon, D. A., Brandes, A. A., Omuro, A., Mulholland, P., Lim, M., Wick, A., Baehring, J., Ahluwalia, M. S., Roth, P., Bähr, O., Phuphanich, S., Sepulveda, J. M., De Souza, P., Sahebjam, S., Carleton, M., Tatsuoka, K., Taitt, C., Zwirtes, R., Sampson, J., & Weller, M. (2020). Effect of Nivolumab vs Bevacizumab in Patients With Recurrent Glioblastoma: The CheckMate 143 Phase 3 Randomized Clinical Trial. *JAMA Oncology*, *6*(7), 1003–1010. https://doi.org/10.1001/jamaoncol.2020.1024

Reekmans, S. M., Pflanzner, T., Gordts, P. L. S. M., Isbert, S., Zimmermann, P., Annaert, W., Weggen, S., Roebroek, A. J. M., & Pietrzik, C. U. (2010). Inactivation of the proximal NPXY motif impairs early steps in LRP1 biosynthesis. *Cellular and Molecular Life Sciences: CMLS*, *67*(1), 135–145. https://doi.org/10.1007/s00018-009-0171-7

Reese, T. S., & Karnovsky, M. J. (1967). Fine structural localization of a blood-brain barrier to exogenous peroxidase. *The Journal of Cell Biology*, *34*(1), 207–217. https://doi.org/10.1083/jcb.34.1.207

Regina, A., Demeule, M., Tripathy, S., Lord-Dufour, S., Currie, J.-C., Iddir, M., Annabi, B., Castaigne, J.-P., & Lachowicz, J. E. (2015). ANG4043, a novel brain-penetrant peptide-mAb conjugate, is efficacious against HER2-positive intracranial tumors in mice. *Molecular Cancer Therapeutics*, *14*(1), 129–140. https://doi.org/10.1158/1535-7163.MCT-14-0399

Ricard, D., Idbaih, A., Ducray, F., Lahutte, M., Hoang-Xuan, K., & Delattre, J.-Y. (2012). Primary brain tumours in adults. *The Lancet*, *379*(9830), 1984–1996. https://doi.org/10.1016/S0140-6736(11)61346-9

Riccioni, R., Pasquini, L., Mariani, G., Saulle, E., Rossini, A., Diverio, D., Pelosi, E., Vitale, A., Chierichini, A., Cedrone, M., Foà, R., Lo Coco, F., Peschle, C., & Testa, U. (2005). TRAIL decoy receptors mediate resistance of acute myeloid leukemia cells to TRAIL. *Haematologica*, *90*(5), 612–624.

Rickman, D. S., Bobek, M. P., Misek, D. E., Kuick, R., Blaivas, M., Kurnit, D. M., Taylor, J., & Hanash, S. M. (2001). Distinctive Molecular Profiles of High-Grade and Low-Grade Gliomas Based on Oligonucleotide Microarray Analysis. *Cancer Research*, *61*(18), 6885–6891.

Ridder, D. A., Wenzel, J., Müller, K., Töllner, K., Tong, X.-K., Assmann, J. C., Stroobants, S., Weber, T., Niturad, C., Fischer, L., Lembrich, B., Wolburg, H., Grand'Maison, M., Papadopoulos, P., Korpos, E., Truchetet, F., Rades, D., Sorokin, L. M., Schmidt-Supprian, M., … Schwaninger, M. (2015). Brain endothelial TAK1 and NEMO safeguard the neurovascular unit. *The Journal of Experimental Medicine*, *212*(10), 1529–1549. https://doi.org/10.1084/jem.20150165

Roopenian, D. C., & Akilesh, S. (2007). FcRn: The neonatal Fc receptor comes of age. *Nature Reviews. Immunology*, *7*(9), 715–725. https://doi.org/10.1038/nri2155

Sade, H., Baumgartner, C., Hugenmatter, A., Moessner, E., Freskgård, P.-O., & Niewoehner, J. (2014). A Human Blood-Brain Barrier Transcytosis Assay Reveals Antibody Transcytosis Influenced by pH-Dependent Receptor Binding. *PLoS ONE*, *9*(4). https://doi.org/10.1371/journal.pone.0096340

Saelens, X., Festjens, N., Vande Walle, L., van Gurp, M., van Loo, G., & Vandenabeele, P. (2004). Toxic proteins released from mitochondria in cell death. *Oncogene*, *23*(16), 2861–2874. https://doi.org/10.1038/sj.onc.1207523

Saitou, M., Furuse, M., Sasaki, H., Schulzke, J. D., Fromm, M., Takano, H., Noda, T., & Tsukita, S. (2000). Complex phenotype of mice lacking occludin, a component of tight junction strands. *Molecular Biology of the Cell*, *11*(12), 4131–4142. https://doi.org/10.1091/mbc.11.12.4131

Sanmarco, L. M., Wheeler, M. A., Gutiérrez-Vázquez, C., Polonio, C. M., Linnerbauer, M., Pinho-Ribeiro, F. A., Li, Z., Giovannoni, F., Batterman, K. V., Scalisi, G., Zandee, S. E. J., Heck, E. S., Alsuwailm, M., Rosene, D. L., Becher, B., Chiu, I. M., Prat, A., & Quintana, F. J. (2021). Gut-licensed IFNγ+ NK cells drive LAMP1+TRAIL+ anti-inflammatory astrocytes. *Nature*, *590*(7846), 473–479. https://doi.org/10.1038/s41586-020-03116-4

Satoh, M. S., & Lindahl, T. (1992). Role of poly(ADP-ribose) formation in DNA repair. *Nature*, *356*(6367), 356–358. https://doi.org/10.1038/356356a0

Scaffidi, C., Fulda, S., Srinivasan, A., Friesen, C., Li, F., Tomaselli, K. J., Debatin, K. M., Krammer, P. H., & Peter, M. E. (1998). Two CD95 (APO-1/Fas) signaling pathways. *The EMBO Journal*, *17*(6), 1675–1687. https://doi.org/10.1093/emboj/17.6.1675

Scaffidi, C., Medema, J. P., Krammer, P. H., & Peter, M. E. (1997). FLICE is predominantly expressed as two functionally active isoforms, caspase-8/a and caspase-8/b. *The Journal of Biological Chemistry*, *272*(43), 26953–26958. https://doi.org/10.1074/jbc.272.43.26953

Schleich, K., Warnken, U., Fricker, N., Öztürk, S., Richter, P., Kammerer, K., Schnölzer, M., Krammer, P. H., & Lavrik, I. N. (2012). Stoichiometry of the CD95 Death-Inducing Signaling Complex: Experimental and Modeling Evidence for a Death Effector Domain Chain Model. *Molecular Cell*, *47*(2), 306–319. https://doi.org/10.1016/j.molcel.2012.05.006

Schneeberger, E. E., & Lynch, R. D. (2004). The tight junction: A multifunctional complex. *American Journal of Physiology. Cell Physiology*, *286*(6), C1213-1228. https://doi.org/10.1152/ajpcell.00558.2003

Schneider, B., Münkel, S., Krippner-Heidenreich, A., Grunwald, I., Wels, W. S., Wajant, H., Pfizenmaier, K., & Gerspach, J. (2010). Potent antitumoral activity of TRAIL through generation of tumor-targeted single-chain fusion proteins. *Cell Death & Disease*, *1*, e68. https://doi.org/10.1038/cddis.2010.45

Schneider, P., Bodmer, J. L., Thome, M., Hofmann, K., Holler, N., & Tschopp, J. (1997). Characterization of two receptors for TRAIL. *FEBS Letters*, *416*(3), 329–334. https://doi.org/10.1016/s0014-5793(97)01231-3

Schneider, P., Thome, M., Burns, K., Bodmer, J. L., Hofmann, K., Kataoka, T., Holler, N., & Tschopp, J. (1997). TRAIL receptors 1 (DR4) and 2 (DR5) signal FADD-dependent apoptosis and activate NF-kappaB. *Immunity*, *7*(6), 831–836. https://doi.org/10.1016/s1074-7613(00)80401-x

Schwartz, M. W., Sipols, A., Kahn, S. E., Lattemann, D. F., Taborsky, G. J., Bergman, R. N., Woods, S. C., & Porte, D. (1990). Kinetics and specificity of insulin uptake from plasma into cerebrospinal fluid. *American Journal of Physiology-Endocrinology and Metabolism*, *259*(3), E378. https://doi.org/10.1152/ajpendo.1990.259.3.E378

Schwartzbaum, J. A., Fisher, J. L., Aldape, K. D., & Wrensch, M. (2006). Epidemiology and molecular pathology of glioma. *Nature Clinical Practice. Neurology*, *2*(9), 494–503; quiz 1 p following 516. https://doi.org/10.1038/ncpneuro0289

Screaton, G. R., Mongkolsapaya, J., Xu, X. N., Cowper, A. E., McMichael, A. J., & Bell, J. I. (1997). TRICK2, a new alternatively spliced receptor that transduces the cytotoxic signal from TRAIL. *Current Biology: CB*, *7*(9), 693–696. https://doi.org/10.1016/s0960-9822(06)00297-1

Secchiero, P., Gonelli, A., Carnevale, E., Milani, D., Pandolfi, A., Zella, D., & Zauli, G. (2003). TRAIL promotes the survival and proliferation of primary human vascular endothelial cells by activating the Akt and ERK pathways. *Circulation*, *107*(17), 2250–2256. https://doi.org/10.1161/01.CIR.0000062702.60708.C4

Segawa, K., & Nagata, S. (2015). An Apoptotic "Eat Me" Signal: Phosphatidylserine Exposure. *Trends in Cell Biology*, *25*(11), 639–650. https://doi.org/10.1016/j.tcb.2015.08.003

Seifert, O., Plappert, A., Fellermeier, S., Siegemund, M., Pfizenmaier, K., & Kontermann, R. E. (2014). Tetravalent antibody-scTRAIL fusion proteins with improved properties. *Molecular Cancer Therapeutics*, *13*(1), 101–111. https://doi.org/10.1158/1535-7163.MCT-13-0396

Seifert, O., Pollak, N., Nusser, A., Steiniger, F., Rüger, R., Pfizenmaier, K., & Kontermann, R. E. (2014). Immuno-LipoTRAIL: Targeted Delivery of TRAIL-Functionalized Liposomal Nanoparticles. *Bioconjugate Chemistry*, *25*(5), 879–887. https://doi.org/10.1021/bc400517j

Shalini, S., Dorstyn, L., Dawar, S., & Kumar, S. (2015). Old, new and emerging functions of caspases. *Cell Death and Differentiation*, *22*(4), 526–539. https://doi.org/10.1038/cdd.2014.216

Shao, K., Huang, R., Li, J., Han, L., Ye, L., Lou, J., & Jiang, C. (2010). Angiopep-2 modified PE-PEG based polymeric micelles for amphotericin B delivery targeted to the brain. *Journal of Controlled Release: Official Journal of the Controlled Release Society*, *147*(1), 118–126. https://doi.org/10.1016/j.jconrel.2010.06.018

Shawahna, R., Uchida, Y., Declèves, X., Ohtsuki, S., Yousif, S., Dauchy, S., Jacob, A., Chassoux, F., Daumas-Duport, C., Couraud, P.-O., Terasaki, T., & Scherrmann, J.-M. (2011, July 8). *Transcriptomic and Quantitative Proteomic Analysis of Transporters and Drug Metabolizing Enzymes in Freshly Isolated Human Brain Microvessels* (world) [Research-article]. American Chemical Society. https://doi.org/10.1021/mp200129p

Shepro, D., & Morel, N. M. (1993). Pericyte physiology. *FASEB Journal: Official Publication of the Federation of American Societies for Experimental Biology*, *7*(11), 1031–1038. https://doi.org/10.1096/fasebj.7.11.8370472

Sheridan, J. P., Marsters, S. A., Pitti, R. M., Gurney, A., Skubatch, M., Baldwin, D., Ramakrishnan, L., Gray, C. L., Baker, K., Wood, W. I., Goddard, A. D., Godowski, P., & Ashkenazi, A. (1997). Control of TRAIL-induced apoptosis by a family of signaling and decoy receptors. *Science (New York, N.Y.)*, *277*(5327), 818–821. https://doi.org/10.1126/science.277.5327.818

Shi, L., Wu, X., Li, T., Wu, Y., Song, L., Zhang, W., Yin, L., Wu, Y., Han, W., & Yang, Y. (2022). An esterase-activatable prodrug formulated liposome strategy: Potentiating the anticancer therapeutic efficacy and drug safety. *Nanoscale Advances*, *4*(3), 952–966. https://doi.org/10.1039/D1NA00838B

Siegemund, M., Pollak, N., Seifert, O., Wahl, K., Hanak, K., Vogel, A., Nussler, A. K., Göttsch, D., Münkel, S., Bantel, H., Kontermann, R. E., & Pfizenmaier, K. (2012). Superior antitumoral activity of dimerized targeted single-chain TRAIL fusion proteins under retention of tumor selectivity. *Cell Death & Disease*, *3*(4), e295–e295. https://doi.org/10.1038/cddis.2012.29

Siegemund, M., Richter, F., Seifert, O., Unverdorben, F., & Kontermann, R. E. (2014). Expression and purification of recombinant antibody formats and antibody fusion proteins. *Methods in Molecular Biology (Clifton, N.J.)*, *1131*, 273–295. https://doi.org/10.1007/978-1-62703-992-5_18

Siegemund, M., Seifert, O., Zarani, M., Džinić, T., De Leo, V., Göttsch, D., Münkel, S., Hutt, M., Pfizenmaier, K., & Kontermann, R. E. (2016). An optimized antibody-single-chain TRAIL fusion protein for cancer therapy. *MAbs*, *8*(5), 879–891. https://doi.org/10.1080/19420862.2016.1172163

Silke, J., & Meier, P. (2013). Inhibitor of Apoptosis (IAP) Proteins–Modulators of Cell Death and Inflammation. *Cold Spring Harbor Perspectives in Biology*, *5*(2), a008730. https://doi.org/10.1101/cshperspect.a008730

Simbulan-Rosenthal, C. M., Rosenthal, D. S., Iyer, S., Boulares, H., & Smulson, M. E. (1999). Involvement of PARP and poly(ADP-ribosyl)ation in the early stages of apoptosis and DNA replication. *Molecular and Cellular Biochemistry*, *193*(1–2), 137–148.

Song, J. H., Tse, M. C. L., Bellail, A., Phuphanich, S., Khuri, F., Kneteman, N. M., & Hao, C. (2007). Lipid rafts and nonrafts mediate tumor necrosis factor related apoptosis-inducing ligand induced apoptotic and nonapoptotic signals in non small cell lung carcinoma cells. *Cancer Research*, *67*(14), 6946–6955. https://doi.org/10.1158/0008-5472.CAN-06-3896

Soria, J.-C., Márk, Z., Zatloukal, P., Szima, B., Albert, I., Juhász, E., Pujol, J.-L., Kozielski, J., Baker, N., Smethurst, D., Hei, Y., Ashkenazi, A., Stern, H., Amler, L., Pan, Y., & Blackhall, F. (2011). Randomized phase II study of dulanermin in combination with paclitaxel, carboplatin, and bevacizumab in advanced non-small-cell lung cancer. *Journal of Clinical Oncology: Official Journal of the American Society of Clinical Oncology*, *29*(33), 4442–4451. https://doi.org/10.1200/JCO.2011.37.2623

Souers, A. J., Leverson, J. D., Boghaert, E. R., Ackler, S. L., Catron, N. D., Chen, J., Dayton, B. D., Ding, H., Enschede, S. H., Fairbrother, W. J., Huang, D. C. S., Hymowitz, S. G., Jin, S., Khaw, S. L., Kovar, P. J., Lam, L. T., Lee, J., Maecker, H. L., Marsh, K. C., … Elmore, S.

W. (2013). ABT-199, a potent and selective BCL-2 inhibitor, achieves antitumor activity while sparing platelets. *Nature Medicine*, *19*(2), 202–208. https://doi.org/10.1038/nm.3048

Sprick, M. R., Weigand, M. A., Rieser, E., Rauch, C. T., Juo, P., Blenis, J., Krammer, P. H., & Walczak, H. (2000). FADD/MORT1 and caspase-8 are recruited to TRAIL receptors 1 and 2 and are essential for apoptosis mediated by TRAIL receptor 2. *Immunity*, *12*(6), 599–609. https://doi.org/10.1016/s1074-7613(00)80211-3

Srinivasula, S. M., Ahmad, M., Fernandes-Alnemri, T., & Alnemri, E. S. (1998). Autoactivation of procaspase-9 by Apaf-1-mediated oligomerization. *Molecular Cell*, *1*(7), 949–957. https://doi.org/10.1016/s1097-2765(00)80095-7

Stennicke, H. R., Renatus, M., Meldal, M., & Salvesen, G. S. (2000). Internally quenched fluorescent peptide substrates disclose the subsite preferences of human caspases 1, 3, 6, 7 and 8. *The Biochemical Journal*, *350 Pt 2*, 563–568.

Storck, S. E., Kurtyka, M., & Pietrzik, C. U. (2021). Brain endothelial LRP1 maintains blood-brain barrier integrity. *Fluids and Barriers of the CNS*, *18*(1), 27. https://doi.org/10.1186/s12987-021-00260-5

Storck, S. E., Meister, S., Nahrath, J., Meißner, J. N., Schubert, N., Di Spiezio, A., Baches, S., Vandenbroucke, R. E., Bouter, Y., Prikulis, I., Korth, C., Weggen, S., Heimann, A., Schwaninger, M., Bayer, T. A., & Pietrzik, C. U. (2016). Endothelial LRP1 transports amyloid-β(1-42) across the blood-brain barrier. *The Journal of Clinical Investigation*, *126*(1), 123–136. https://doi.org/10.1172/JCI81108

Storck, S. E., & Pietrzik, C. U. (2017). Endothelial LRP1 - A Potential Target for the Treatment of Alzheimer's Disease: Theme: Drug Discovery, Development and Delivery in Alzheimer's Disease Guest Editor: Davide Brambilla. *Pharmaceutical Research*, *34*(12), 2637–2651. https://doi.org/10.1007/s11095-017-2267-3

Strickland, D. K., Ashcom, J. D., Williams, S., Burgess, W. H., Migliorini, M., & Argraves, W. S. (1990). Sequence identity between the alpha 2-macroglobulin receptor and low density lipoprotein receptor-related protein suggests that this molecule is a multifunctional receptor. *The Journal of Biological Chemistry*, *265*(29), 17401–17404.

Stummer, W., Pichlmeier, U., Meinel, T., Wiestler, O. D., Zanella, F., Reulen, H.-J., & ALA-Glioma Study Group. (2006). Fluorescence-guided surgery with 5-aminolevulinic acid for resection of malignant glioma: A randomised controlled multicentre phase III trial. *The Lancet. Oncology*, *7*(5), 392–401. https://doi.org/10.1016/S1470-2045(06)70665-9

Stupp, R., Hegi, M. E., Mason, W. P., van den Bent, M. J., Taphoorn, M. J. B., Janzer, R. C., Ludwin, S. K., Allgeier, A., Fisher, B., Belanger, K., Hau, P., Brandes, A. A., Gijtenbeek, J., Marosi, C., Vecht, C. J., Mokhtari, K., Wesseling, P., Villa, S., Eisenhauer, E., … National Cancer Institute of Canada Clinical Trials Group. (2009). Effects of radiotherapy with concomitant and adjuvant temozolomide versus radiotherapy alone on survival in glioblastoma in a randomised phase III study: 5-year analysis of the EORTC-NCIC trial. *The Lancet. Oncology*, *10*(5), 459–466. https://doi.org/10.1016/S1470-2045(09)70025-7

Stupp, R., Weller, M., Belanger, K., Bogdahn, U., Ludwin, S. K., Lacombe, D., & Mirimanoff, R. O. (2005). Radiotherapy plus Concomitant and Adjuvant Temozolomide for Glioblastoma. *The New England Journal of Medicine*, 10.

Sulston, J. E., & Horvitz, H. R. (1977). Post-embryonic cell lineages of the nematode, Caenorhabditis elegans. *Developmental Biology*, *56*(1), 110–156. https://doi.org/10.1016/0012-1606(77)90158-0

Sulston, J. E., Schierenberg, E., White, J. G., & Thomson, J. N. (1983). The embryonic cell lineage of the nematode Caenorhabditis elegans. *Developmental Biology*, *100*(1), 64–119. https://doi.org/10.1016/0012-1606(83)90201-4

Sung, H., Ferlay, J., Siegel, R. L., Laversanne, M., Soerjomataram, I., Jemal, A., & Bray, F. (2021). Global Cancer Statistics 2020: GLOBOCAN Estimates of Incidence and Mortality Worldwide for 36 Cancers in 185 Countries. *CA: A Cancer Journal for Clinicians*, *71*(3), 209–249. https://doi.org/10.3322/caac.21660

Tan, A. C., Ashley, D. M., López, G. Y., Malinzak, M., Friedman, H. S., & Khasraw, M. (2020). Management of glioblastoma: State of the art and future directions. *CA: A Cancer Journal for Clinicians*, *70*(4), 299–312. https://doi.org/10.3322/caac.21613

Tate, M. C., & Aghi, M. K. (2009). Biology of angiogenesis and invasion in glioma. *Neurotherapeutics*, *6*(3), 447–457. https://doi.org/10.1016/j.nurt.2009.04.001

Thakkar, J. P., Dolecek, T. A., Horbinski, C., Ostrom, Q. T., Lightner, D. D., Barnholtz-Sloan, J. S., & Villano, J. L. (2014). Epidemiologic and Molecular Prognostic Review of Glioblastoma. *Cancer Epidemiology and Prevention Biomarkers*, *23*(10), 1985–1996.

Thiessen, B., Stewart, C., Tsao, M., Kamel-Reid, S., Schaiquevich, P., Mason, W., Easaw, J., Belanger, K., Forsyth, P., McIntosh, L., & Eisenhauer, E. (2010). A phase I/II trial of GW572016 (lapatinib) in recurrent glioblastoma multiforme: Clinical outcomes, pharmacokinetics and molecular correlation. *Cancer Chemotherapy and Pharmacology*, *65*(2), 353–361. https://doi.org/10.1007/s00280-009-1041-6

Thomas, F. C., Taskar, K., Rudraraju, V., Goda, S., Thorsheim, H. R., Gaasch, J. A., Mittapalli, R. K., Palmieri, D., Steeg, P. S., Lockman, P. R., & Smith, Q. R. (2009). Uptake of ANG1005, a novel paclitaxel derivative, through the blood-brain barrier into brain and experimental brain metastases of breast cancer. *Pharmaceutical Research*, *26*(11), 2486–2494. https://doi.org/10.1007/s11095-009-9964-5

Thomas, L. R., Henson, A., Reed, J. C., Salsbury, F. R., & Thorburn, A. (2004). Direct binding of Fas-associated death domain (FADD) to the tumor necrosis factor-related apoptosis-inducing ligand receptor DR5 is regulated by the death effector domain of FADD. *The Journal of Biological Chemistry*, *279*(31), 32780–32785. https://doi.org/10.1074/jbc.M401680200

Thomsen, L. B., Burkhart, A., & Moos, T. (2015). A Triple Culture Model of the Blood-Brain Barrier Using Porcine Brain Endothelial cells, Astrocytes and Pericytes. *PLOS ONE*, *10*(8), e0134765. https://doi.org/10.1371/journal.pone.0134765

Tian, X., Leite, D. M., Scarpa, E., Nyberg, S., Fullstone, G., Forth, J., Matias, D., Apriceno, A., Poma, A., Duro-Castano, A., Vuyyuru, M., Harker-Kirschneck, L., Šarić, A., Zhang, Z., Xiang, P., Fang, B., Tian, Y., Luo, L., Rizzello, L., & Battaglia, G. (2020). On the shuttling across the blood-brain barrier via tubule formation: Mechanism and cargo avidity bias. *Science Advances*, *6*(48), eabc4397. https://doi.org/10.1126/sciadv.abc4397

Tolcher, A. W., Mita, M., Meropol, N. J., von Mehren, M., Patnaik, A., Padavic, K., Hill, M., Mays, T., McCoy, T., Fox, N. L., Halpern, W., Corey, A., & Cohen, R. B. (2007). Phase I pharmacokinetic and biologic correlative study of mapatumumab, a fully human monoclonal antibody with agonist activity to tumor necrosis factor-related apoptosis-inducing ligand receptor-1. *Journal of Clinical Oncology: Official Journal of the American Society of Clinical Oncology*, *25*(11), 1390–1395. https://doi.org/10.1200/JCO.2006.08.8898

Tracey, K. J., Lowry, S. F., & Cerami, A. (1988). Cachetin/TNF-alpha in septic shock and septic adult respiratory distress syndrome. *The American Review of Respiratory Disease*, *138*(6), 1377–1379. https://doi.org/10.1164/ajrccm/138.6.1377

Tran, B., & Rosenthal, M. A. (2010). Survival comparison between glioblastoma multiforme and other incurable cancers. *Journal of Clinical Neuroscience: Official Journal of the Neurosurgical Society of Australasia*, *17*(4), 417–421. https://doi.org/10.1016/j.jocn.2009.09.004

Trarbach, T., Moehler, M., Heinemann, V., Köhne, C.-H., Przyborek, M., Schulz, C., Sneller, V., Gallant, G., & Kanzler, S. (2010). Phase II trial of mapatumumab, a fully human agonistic monoclonal antibody that targets and activates the tumour necrosis factor apoptosis-inducing ligand receptor-1 (TRAIL-R1), in patients with refractory colorectal cancer. *British Journal of Cancer*, *102*(3), 506–512. https://doi.org/10.1038/sj.bjc.6605507

Triguero, D., Buciak, J. B., Yang, J., & Pardridge, W. M. (1989). Blood-brain barrier transport of cationized immunoglobulin G: Enhanced delivery compared to native protein. *Proceedings of the National Academy of Sciences of the United States of America*, *86*(12), 4761–4765. https://doi.org/10.1073/pnas.86.12.4761

Tuma, P. L., & Hubbard, A. L. (2003). Transcytosis: Crossing Cellular Barriers. *Physiological Reviews*, *83*(3), 871–932. https://doi.org/10.1152/physrev.00001.2003

Tummers, B., & Green, D. R. (2017). Caspase-8; regulating life and death. *Immunological Reviews*, *277*(1), 76–89. https://doi.org/10.1111/imr.12541

Turek, A., Stoklosa, K., Borecka, A., Paul-Samojedny, M., Kaczmarczyk, B., Marcinkowski, A., & Kasperczyk, J. (2020). Designing Biodegradable Wafers Based on Poly(L-lactide-co-glycolide) and Poly(glycolide-co-ε-caprolactone) for the Prolonged and Local Release of Idarubicin for the Therapy of Glioblastoma Multiforme. *Pharmaceutical Research*, *37*(5), 90. https://doi.org/10.1007/s11095-020-02810-2

Uchida, Y., Ohtsuki, S., Katsukura, Y., Ikeda, C., Suzuki, T., Kamiie, J., & Terasaki, T. (2011). Quantitative targeted absolute proteomics of human blood–brain barrier transporters and receptors. *Journal of Neurochemistry*, *117*(2), 333–345. https://doi.org/10.1111/j.1471-4159.2011.07208.x

Uhm, J. H., Ballman, K. V., Wu, W., Giannini, C., Krauss, J. C., Buckner, J. C., James, C. D., Scheithauer, B. W., Behrens, R. J., Flynn, P. J., Schaefer, P. L., Dakhill, S. R., & Jaeckle, K. A. (2011). Phase II evaluation of gefitinib in patients with newly diagnosed Grade 4 astrocytoma: Mayo/North Central Cancer Treatment Group Study N0074. *International Journal of Radiation Oncology, Biology, Physics*, *80*(2), 347–353. https://doi.org/10.1016/j.ijrobp.2010.01.070

Ullman, J. C., Arguello, A., Getz, J. A., Bhalla, A., Mahon, C. S., Wang, J., Giese, T., Bedard, C., Kim, D. J., Blumenfeld, J. R., Liang, N., Ravi, R., Nugent, A. A., Davis, S. S., Ha, C., Duque, J., Tran, H. L., Wells, R. C., Lianoglou, S., … Henry, A. G. (2020). Brain delivery and activity of a lysosomal enzyme using a blood-brain barrier transport vehicle in mice. *Science Translational Medicine*, *12*(545). https://doi.org/10.1126/scitranslmed.aay1163

Urbańska, K., Sokołowska, J., Szmidt, M., & Sysa, P. (2014). Glioblastoma multiforme—An overview. *Contemporary Oncology (Poznan, Poland)*, *18*(5), 307–312. https://doi.org/10.5114/wo.2014.40559

van den Bent, M. J., Brandes, A. A., Rampling, R., Kouwenhoven, M. C. M., Kros, J. M., Carpentier, A. F., Clement, P. M., Frenay, M., Campone, M., Baurain, J.-F., Armand, J.-P., Taphoorn, M. J. B., Tosoni, A., Kletzl, H., Klughammer, B., Lacombe, D., & Gorlia, T. (2009). Randomized phase II trial of erlotinib versus temozolomide or carmustine in recurrent glioblastoma: EORTC brain tumor group study 26034. *Journal of Clinical Oncology: Official Journal of the American Society of Clinical Oncology*, *27*(8), 1268–1274. https://doi.org/10.1200/JCO.2008.17.5984

Van Itallie, C., Rahner, C., & Anderson, J. M. (2001). Regulated expression of claudin-4 decreases paracellular conductance through a selective decrease in sodium permeability. *Journal of Clinical Investigation*, *107*(10), 1319–1327.

Van Opdenbosch, N., & Lamkanfi, M. (2019). Caspases in cell death, inflammation and disease. *Immunity*, *50*(6), 1352–1364. https://doi.org/10.1016/j.immuni.2019.05.020

Verhaak, R. G. W., Hoadley, K. A., Purdom, E., Wang, V., Qi, Y., Wilkerson, M. D., Miller, C. R., Ding, L., Golub, T., Mesirov, J. P., Alexe, G., Lawrence, M., O'Kelly, M., Tamayo, P., Weir, B. A., Gabrie, S., Winckler, W., Gupta, S., Jakkula, L., … Hayes, D. N. (2010). An integrated genomic analysis identifies clinically relevant subtypes of glioblastoma characterized by abnormalities in PDGFRA, IDH1, EGFR and NF1. *Cancer Cell*, *17*(1), 98. https://doi.org/10.1016/j.ccr.2009.12.020

Vetma, V., Guttà, C., Peters, N., Praetorius, C., Hutt, M., Seifert, O., Meier, F., Kontermann, R., Kulms, D., & Rehm, M. (2020). Convergence of pathway analysis and pattern recognition predicts sensitization to latest generation TRAIL therapeutics by IAP antagonism. *Cell Death & Differentiation*, *27*(8), 2417–2432. https://doi.org/10.1038/s41418-020-0512-5

Villaseñor, R., Lampe, J., Schwaninger, M., & Collin, L. (2019). Intracellular transport and regulation of transcytosis across the blood–brain barrier. *Cellular and Molecular Life Sciences*, *76*(6), 1081–1092. https://doi.org/10.1007/s00018-018-2982-x

Villaseñor, R., Schilling, M., Sundaresan, J., Lutz, Y., & Collin, L. (2017). Sorting Tubules Regulate Blood-Brain Barrier Transcytosis. *Cell Reports*, *21*(11), 3256–3270. https://doi.org/10.1016/j.celrep.2017.11.055

Vogt, C., & Vogt, K. C. (1842). *Untersuchungen über die Entwicklungsgeschichte der Geburtshelferkrœte (Alytes obstetricans)*. Jent & Gassmann.

von Karstedt, S., Montinaro, A., & Walczak, H. (2017). Exploring the TRAILs less travelled: TRAIL in cancer biology and therapy. *Nature Reviews. Cancer*, *17*(6), 352–366. https://doi.org/10.1038/nrc.2017.28

Wagner, J., Kline, C. L., Zhou, L., Campbell, K. S., MacFarlane, A. W., Olszanski, A. J., Cai, K. Q., Hensley, H. H., Ross, E. A., Ralff, M. D., Zloza, A., Chesson, C. B., Newman, J. H., Kaufman, H., Bertino, J., Stein, M., & El-Deiry, W. S. (2018). Dose intensification of TRAIL-inducing ONC201 inhibits metastasis and promotes intratumoral NK cell recruitment. *The Journal of Clinical Investigation*, *128*(6), 2325–2338. https://doi.org/10.1172/JCI96711

Wagner, S., Zensi, A., Wien, S. L., Tschickardt, S. E., Maier, W., Vogel, T., Worek, F., Pietrzik, C. U., Kreuter, J., & von Briesen, H. (2012). Uptake Mechanism of ApoE-Modified

Nanoparticles on Brain Capillary Endothelial Cells as a Blood-Brain Barrier Model. *PLoS ONE*, *7*(3), e32568. https://doi.org/10.1371/journal.pone.0032568

Wajant, H., Moosmayer, D., Wüest, T., Bartke, T., Gerlach, E., Schönherr, U., Peters, N., Scheurich, P., & Pfizenmaier, K. (2001). Differential activation of TRAIL-R1 and -2 by soluble and membrane TRAIL allows selective surface antigen-directed activation of TRAIL-R2 by a soluble TRAIL derivative. *Oncogene*, *20*(30), 4101–4106. https://doi.org/10.1038/sj.onc.1204558

Walczak, H. (1997). TRAIL-R2: A novel apoptosis-mediating receptor for TRAIL. *The EMBO Journal*, *16*(17), 5386–5397. https://doi.org/10.1093/emboj/16.17.5386

Walczak, H., Miller, R. E., Ariail, K., Gliniak, B., Griffith, T. S., Kubin, M., Chin, W., Jones, J., Woodward, A., Le, T., Smith, C., Smolak, P., Goodwin, R. G., Rauch, C. T., Schuh, J. C. L., & Lynch, D. H. (1999). Tumoricidal activity of tumor necrosis factor–related apoptosis–inducing ligand in vivo. *Nature Medicine*, *5*(2), 157–163. https://doi.org/10.1038/5517

Wang, L., Du, F., & Wang, X. (2008). TNF-α Induces Two Distinct Caspase-8 Activation Pathways. *Cell*, *133*(4), 693–703. https://doi.org/10.1016/j.cell.2008.03.036

Wang, S., & El-Deiry, W. S. (2003). TRAIL and apoptosis induction by TNF-family death receptors. *Oncogene*, *22*(53), 8628–8633. https://doi.org/10.1038/sj.onc.1207232

Watanabe, K., Tachibana, O., Sata, K., Yonekawa, Y., Kleihues, P., & Ohgaki, H. (1996). Overexpression of the EGF receptor and p53 mutations are mutually exclusive in the evolution of primary and secondary glioblastomas. *Brain Pathology (Zurich, Switzerland)*, *6*(3), 217–223; discussion 23-24. https://doi.org/10.1111/j.1750-3639.1996.tb00848.x

Weber, C., Fraemohs, L., & Dejana, E. (2007). The role of junctional adhesion molecules in vascular inflammation. *Nature Reviews. Immunology*, *7*(6), 467–477. https://doi.org/10.1038/nri2096

Webster, C. I., Hatcher, J., Burrell, M., Thom, G., Thornton, P., Gurrell, I., & Chessell, I. (2017). Enhanced delivery of IL-1 receptor antagonist to the central nervous system as a novel anti-transferrin receptor-IL-1RA fusion reverses neuropathic mechanical hypersensitivity. *Pain*, *158*(4), 660–668. https://doi.org/10.1097/j.pain.0000000000000810

Wei, X., Zhan, C., Chen, X., Hou, J., Xie, C., & Lu, W. (2014). Retro-inverso isomer of Angiopep-2: A stable d-peptide ligand inspires brain-targeted drug delivery. *Molecular Pharmaceutics*, *11*(10), 3261–3268. https://doi.org/10.1021/mp500086e

Weller, M., van den Bent, M., Preusser, M., Le Rhun, E., Tonn, J. C., Minniti, G., Bendszus, M., Balana, C., Chinot, O., Dirven, L., French, P., Hegi, M. E., Jakola, A. S., Platten, M., Roth, P., Rudà, R., Short, S., Smits, M., Taphoorn, M. J. B., … Wick, W. (2021). EANO guidelines on the diagnosis and treatment of diffuse gliomas of adulthood. *Nature Reviews Clinical Oncology*, *18*(3), 170–186. https://doi.org/10.1038/s41571-020-00447-z

White, C. A., McCombe, P. A., & Pender, M. P. (1998). The roles of Fas, Fas ligand and Bcl-2 in T cell apoptosis in the central nervous system in experimental autoimmune encephalomyelitis. *Journal of Neuroimmunology*, *82*(1), 47–55. https://doi.org/10.1016/S0165-5728(97)00187-2

Wiley, S. R., Schooley, K., Smolak, P. J., Din, W. S., Huang, C. P., Nicholl, J. K., Sutherland, G. R., Smith, T. D., Rauch, C., & Smith, C. A. (1995). Identification and characterization of a new member of the TNF family that induces apoptosis. *Immunity*, *3*(6), 673–682. https://doi.org/10.1016/1074-7613(95)90057-8

Wilson, T. A., Karajannis, M. A., & Harter, D. H. (2014). Glioblastoma multiforme: State of the art and future therapeutics. *Surgical Neurology International*, *5*, 64. https://doi.org/10.4103/2152-7806.132138

Wolburg, H., & Lippoldt, A. (2002). Tight junctions of the blood-brain barrier: Development, composition and regulation. *Vascular Pharmacology*, *38*(6), 323–337. https://doi.org/10.1016/s1537-1891(02)00200-8

Wong, A., Ye, M., Levy, A., Rothstein, J., Bergles, D., & Searson, P. (2013). The blood-brain barrier: An engineering perspective. *Frontiers in Neuroengineering*, *6*, 7. https://doi.org/10.3389/fneng.2013.00007

Wosik, K., Biernacki, K., Khouzam, M.-P., & Prat, A. (2007). Death receptor expression and function at the human blood brain barrier. *Journal of the Neurological Sciences*, *259*(1), 53–60. https://doi.org/10.1016/j.jns.2006.08.018

Wosik, K., Cayrol, R., Dodelet-Devillers, A., Berthelet, F., Bernard, M., Moumdjian, R., Bouthillier, A., Reudelhuber, T. L., & Prat, A. (2007). Angiotensin II controls occludin function and is

required for blood brain barrier maintenance: Relevance to multiple sclerosis. *The Journal of Neuroscience: The Official Journal of the Society for Neuroscience*, *27*(34), 9032–9042. https://doi.org/10.1523/JNEUROSCI.2088-07.2007

Wyllie, A. H., Kerr, J. F., & Currie, A. R. (1980). Cell death: The significance of apoptosis. *International Review of Cytology*, *68*, 251–306. https://doi.org/10.1016/s0074-7696(08)62312-8

Xie, Q., Mittal, S., & Berens, M. E. (2014). Targeting adaptive glioblastoma: An overview of proliferation and invasion. *Neuro-Oncology*, *16*(12), 1575–1584. https://doi.org/10.1093/neuonc/nou147

Yan, J., Wang, L., Wang, Z., Wang, Z., Wang, B., Zhu, R., Bi, J., Wu, J., Zhang, H., Wu, H., Yu, B., Kong, W., & Yu, X. (2016). Engineered adenovirus fiber shaft fusion homotrimer of soluble TRAIL with enhanced stability and antitumor activity. *Cell Death & Disease*, *7*(6), e2274–e2274. https://doi.org/10.1038/cddis.2016.177

Yang, S., Mei, S., Jin, H., Zhu, B., Tian, Y., Huo, J., Cui, X., Guo, A., & Zhao, Z. (2017). Identification of two immortalized cell lines, ECV304 and bEnd3, for in vitro permeability studies of blood-brain barrier. *PloS One*, *12*(10), e0187017. https://doi.org/10.1371/journal.pone.0187017

Ye, Z., Gao, L., Cai, J., Wang, Y., Li, Y., Tong, S., Yan, T., Sun, Q., Qi, Y., Xu, Y., Jiang, H., Zhang, S., Zhao, L., Zhang, S., & Chen, Q. (2022). Esterase-responsive and size-optimized prodrug nanoparticles for effective intracranial drug delivery and glioblastoma treatment. *Nanomedicine: Nanotechnology, Biology, and Medicine*, *44*, 102581. https://doi.org/10.1016/j.nano.2022.102581

Yen, S.-Y., Chen, S.-R., Hsieh, J., Li, Y.-S., Chuang, S.-E., Chuang, H.-M., Huang, M.-H., Lin, S.-Z., Harn, H.-J., & Chiou, T.-W. (2016). Biodegradable interstitial release polymer loading a novel small molecule targeting Axl receptor tyrosine kinase and reducing brain tumour migration and invasion. *Oncogene*, *35*(17), 2156–2165. https://doi.org/10.1038/onc.2015.277

Yip, K. W., & Reed, J. C. (2008). Bcl-2 family proteins and cancer. *Oncogene*, *27*(50), 6398–6406. https://doi.org/10.1038/onc.2008.307

Yu, X., Ji, C., & Shao, A. (2020). Neurovascular Unit Dysfunction and Neurodegenerative Disorders. *Frontiers in Neuroscience*, *14*, 334. https://doi.org/10.3389/fnins.2020.00334

Yu, Y. J., Atwal, J. K., Zhang, Y., Tong, R. K., Wildsmith, K. R., Tan, C., Bien-Ly, N., Hersom, M., Maloney, J. A., Meilandt, W. J., Bumbaca, D., Gadkar, K., Hoyte, K., Luk, W., Lu, Y., Ernst, J. A., Scearce-Levie, K., Couch, J. A., Dennis, M. S., & Watts, R. J. (2014). Therapeutic bispecific antibodies cross the blood-brain barrier in nonhuman primates. *Science Translational Medicine*, *6*(261), 261ra154-261ra154. https://doi.org/10.1126/scitranslmed.3009835

Yu, Y. J., Zhang, Y., Kenrick, M., Hoyte, K., Luk, W., Lu, Y., Atwal, J., Elliott, J. M., Prabhu, S., Watts, R. J., & Dennis, M. S. (2011). Boosting Brain Uptake of a Therapeutic Antibody by Reducing Its Affinity for a Transcytosis Target. *Science Translational Medicine*, *3*(84), 84ra44-84ra44. https://doi.org/10.1126/scitranslmed.3002230

Yuan, J., Shaham, S., Ledoux, S., Ellis, H. M., & Horvitz, H. R. (1993). The C. elegans cell death gene ced-3 encodes a protein similar to mammalian interleukin-1 beta-converting enzyme. *Cell*, *75*(4), 641–652. https://doi.org/10.1016/0092-8674(93)90485-9

Zamai, L., Ahmad, M., Bennett, I. M., Azzoni, L., Alnemri, E. S., & Perussia, B. (1998). Natural killer (NK) cell-mediated cytotoxicity: Differential use of TRAIL and Fas ligand by immature and mature primary human NK cells. *The Journal of Experimental Medicine*, *188*(12), 2375–2380. https://doi.org/10.1084/jem.188.12.2375

Zhang, J., Stevens, M. F. G., & Bradshaw, T. D. (2012). Temozolomide: Mechanisms of action, repair and resistance. *Current Molecular Pharmacology*, *5*(1), 102–114. https://doi.org/10.2174/1874467211205010102

Zhang, X. D., Nguyen, T., Thomas, W. D., Sanders, J. E., & Hersey, P. (2000). Mechanisms of resistance of normal cells to TRAIL induced apoptosis vary between different cell types. *FEBS Letters*, *482*(3), 193–199. https://doi.org/10.1016/S0014-5793(00)02042-1

Zhang, Y., Dube, C., Gibert, M., Cruickshanks, N., Wang, B., Coughlan, M., Yang, Y., Setiady, I., Deveau, C., Saoud, K., Grello, C., Oxford, M., Yuan, F., & Abounader, R. (2018). The p53 Pathway in Glioblastoma. *Cancers*, *10*(9), 297. https://doi.org/10.3390/cancers10090297

Zhao, Y., Li, D., Zhao, J., Song, J., & Zhao, Y. (2016). The role of the low-density lipoprotein receptor–related protein 1 (LRP-1) in regulating blood-brain barrier integrity. *Reviews in the Neurosciences*, *27*(6), 623–634. https://doi.org/10.1515/revneuro-2015-0069

Zou, H., Henzel, W. J., Liu, X., Lutschg, A., & Wang, X. (1997). Apaf-1, a Human Protein Homologous to C. elegans CED-4, Participates in Cytochrome c–Dependent Activation of Caspase-3. *Cell*, *90*(3), 405–413. https://doi.org/10.1016/S0092-8674(00)80501-2

List of figures and tables

List of figures

List of tables

Acknowledgements

First, I would like to thank Markus for this wonderful opportunity to work on this project and for the GLIOTRAIN consortium. His extraordinary supervision, scientific discussions, motivation during stressful times and his belief in my work have helped a lot in my professional and personal growth. I have learned a lot from him, especially on how to look at everything from a different perspective and take the positives out of it. I am grateful for his endless support and advice throughout my PhD journey and after.

I would also like to thank Brona for taking her time to be my second examiner.

I would like to thank Gavin for his support throughout the PhD duration. He helped me out in every step of the project and motivated me whenever I had challenging situations. I thank him for the great ideas, suggestions and especially for his help with writing.

I thank Roland and Oli for their support in the antibody engineering part. Their ideas have helped a lot for the growth of the project.

I thank Nats for hearing me out whenever I needed someone to talk to. She inspired and motivated me to learn German. Thanks for your time and patience, you are precious to AG Morrison. I would like to thank Dani for her everyday support professionally and personally. She was always there whenever anybody needed help, I never heard no for an answer from her. I thank her for cheering up all of us during the pandemic time.

I would like to thank present and past AG Morrison members Biswa, Cathrin, Chiara, Christian, Cristiano, Gabi, Josip, Nadine, Senait, Tabea, Vesna. It has been a great time with a lot of group activities, lunchtimes, picnics, etc. I thank them for their warm welcome and memories that I will cherish forever. I also would like to thank GLIOTRAIN mates, even though we have not met the last years due to the pandemic, I thank them for the wonderful times.

I also want to thank my friend Dr. Priya, who has been always by my side and still supports me. Thanks to my friends in Stuttgart who made my stay very pleasant and memorable.

Not but not least, I thank my family. I thank my parents Krishna Moorthy, Vasantha, and my sister Indhu. They always have been supportive and understanding. This dissertation would not have been possible without them.

Trainings, conferences and publications

Trainings:

November 2020	Clinical Trials Course, Society of Neuro Oncology	Online
January 2019	Communication and Dissemination	Rotterdam, Netherlands
January 2019	Scientific Writing, Erasmus Medical Centre	Rotterdam, Netherlands
April 2018	Project management and transferrable skills	Dublin, Ireland
April 2018	Patient advocacy mini symposium	Dublin, Ireland
April 2018	Open science and data management	Dublin, Ireland
August 2018	RNA sequencing, VIB Leuven	Leuven, Belgium

Conferences:

November 2020	Oral presentation at UK & Ireland Early Career Blood Brain Barrier Symposium	Online
September 2019	Oral presentation at European Cell Death Organization	Dresden
May 2019	Poster presentation at Barrier and Transport Meeting	Bad Herrenalb

Publications:

Krishna Moorthy, Nivetha, Oliver Seifert, Stephan Eisler, Sara Weirich, Roland E. Kontermann, Markus Rehm, and Gavin Fullstone. 2021. “Low-Level Endothelial TRAIL-Receptor Expression Obstructs the CNS-Delivery of Angiopep-2 Functionalised TRAIL-Receptor Agonists for the Treatment of Glioblastoma.” *Molecules* 26 (24): 7582. https://doi.org/10.3390/molecules26247582.